THE IMPACT OF GEOLOGIC AND GEOMORPHIC CHARACTERISTICS ON DRAINAGE EFFICIENCY AND DISCHARGE; UNCOMPAHGRE, SAN MIGUEL, AND ANIMAS RIVER WATERSHEDS, COLORADO, USA

A Dissertation

by

GARRETT GAMACHE

Submitted to the Office of Graduate and Professional Studies of
Texas A&M University
in partial fulfillment of the requirements for the degree of

DOCTOR OF PHILOSOPHY

Chair of Committee,	John R. Giardino
Co-Chair of Committee,	John D. Vitek
Committee Members,	Steven M. Quiring
	Hongbin Zhan
Head of Department,	John R. Giardino

August 2014

Major Subject: Geology

ABSTRACT

In the western United States, limited availability of fresh water coupled with growing agricultural and urban demands are causing large urban locations to be heavily dependant on montane water resources as supplemental sources of water supply. Unfortunately, montane water resources are delicate and highly dependent upon persistent weather and climatic conditions. With current research indicating dramatic changes resulting from climate warming, water resources in montane areas are approaching excessive liability. The problem of reduced water resources is being accelerated by the decreasing volume of readily available fresh water and population increasing. Thus, predicting the impact of weather trends and variability on water resources is necessary to ensure that demands for water for irrigation and municipal water supply can be met.

Although snowmelt is the primary hydrologic input to montane streams, other first-order controls affect the spatial variability of the hydrologic response linked to weather phenomena. Spatial differences in geologic and geomorphic controls are likely to have equally significant influences on the response of streamflow, as does the spatial relationship associated with snow accumulation and melt. To understand the hydrologic response related to weather phenomena in montane regions, it is necessary to ask: Do weather phenomena and spatial variations in geology and geomorphology reduce or shift the timing and volume of montane streamflow regimes?

This study focuses on the Uncompahgre, San Miguel and Animas River watersheds, located in the San Juan Mountains of southwestern Colorado. General Least Squares and Weighted Least Squares regression techniques were used to identify changes in the timing and volume of montane streamflow, and determine the extent to which such changes are related to weather phenomena and geologic and geomorphic watershed characteristics. This study suggests that for the selected montane watersheds, streamflow is beginning earlier, peaking earlier and in some cases, lasting longer into the year. It was found that the timing of montane streamflow regimes can be explained by average monthly maximum and minimum temperatures and average monthly precipitation. It was also determined that site specific relationships between the timing and volume of flow regimes can be sufficiently explained by subbasin drainage area, average basin slope, average basin elevation, percentage of subbasin area above 2,250 m, dominant basin aspect, lithologic rippability, landcover and average annual precipitation. The selected explanatory variables were more successful at describing low streamflows in the summer rather than describing low streamflows in the spring.

ACKNOWLEDGEMENTS

I would like to thank my advisor and committee chair, Dr. John R. Giardino for guidance, support and encouragement. Throughout the course of this research, Dr. Giardino has inspired me to be a better scientist. His useful advice, constructive criticism and continuous follow-up helped me to push myself to achieve more than I originally intended.

I also want to extend my gratitude to my committee: Dr. John D. Vitek, Dr. Steven M. Quiring, and Dr. Hongbin Zhan for providing guidance, thought provoking discussion, and encouragement.

Thanks also go to my friends and colleagues of the High Alpine and Arctic Research Program (HAARP) for making my time at Texas A&M University a great experience. Special thanks go to Scott Van Winkle for continuous support and friendship. I am also grateful to Kevin Gamache for encouragement and help with field work and Rita Gamache for her support and hospitality throughout my time in Texas. I would also like to thank Anne Goldsmith of the Department of Statistics at Texas A&M University for her help and advice concerning computer programming and statistical modeling.

I would like to express my deepest gratitude to my mother and father for their encouragement and to my fiancé for her unlimited patience and love. With out such support and encouragement, I would not have been able to reach my goal.

Finally, I appreciate the help of all of the professors and administrative staff of the Department of Geology and Geophysics at Texas A&M University, as well as all those involved with the revisions of this dissertation.

TABLE OF CONTENTS

Page

Page

LIST OF FIGURES

Page

Page

Page

LIST OF TABLES

Page

CHAPTER I

INTRODUCTION

Introduction

Mountain river basins, associated reservoirs, and underlying aquifers supply water demands for over sixty million people in the western United States (Barnett, 2005; Viviroli et al., 2011). This dependence has made mountain systems in the US, and worldwide the subject of significant attention with respect to vulnerability and variability associated with climate change (Nolin, 2012). Recent studies conducted by the Intergovernmental Panel on Climate Change (IPCC) suggest that some of the most crucial and already observable impacts of climate change are changes in seasonal stream-flow patterns attributed to earlier seasonal snowmelt and diminishing annual snow accumulation (Bernstein, 2007; Nolin, 2012). Such changes are already prominent in montane regions, such as the Rocky Mountains of western North America, making people dependent on mountain river basins extremely vulnerable (Kundzewicz et al., 2007). Within the context of climate change, vulnerability has been described as "the degree to which [geophysical, biological, and socioeconomic] systems are susceptible to, and unable to cope with adverse impacts" (Arnell, 1996).

When considering the impact of weather on stream-flow, changes in the patterns of stream-flows have typically been attributed to earlier snowmelt and the reduction of snowpack (Tague, 2009; Viviroli et al., 2011). Although snow accumulation and melt are the primary hydrologic inputs from a montane stream-flow perspective, several other

first-order controls affect the spatial variability of the hydrologic response to weather phenomena (Jasper, 2004; Tague, 2008, 2009; Uhlenbrook, 2005, Viviroli et al., 2011). Spatial differences in geologic and geomorphic controls also may have an equally significant influence on the response of stream-flow as does the spatial relationship associated with the accumulation and melt of snow.

Spatial differences in lithology and land cover have the potential to affect the drainage system in a region, thus, affecting the temporal response of the stream-flow (Tague, 2008, 2009). Similarly, topographic and geomorphic controls, such as slope, aspect, elevation, landcover and surface roughness also have the potential to affect the input pathway of runoff to stream-flow. By understanding the affects of such spatial differences on the relationship between drainage systems and streamflow, it may be possible to better understand the hydrologic response to weather phenomena that can occur in montane regions.

Problem Statement

Research (Nolin, 2012; Nydick, 2012; Rangwala, 2011) has been conducted on topics relating to the effects of climate change on stream-flow; however, little attention has been focused on how spatial variations in geology and geomorphology may potentially influence the impact of weather phenomena on stream-flow in montane drainage basins.

The next level of research must focus on this aspect. One can ask: Do weather phenomena and spatial variations in geology and geomorphology reduce or shift the timing and volume of montane streamflow regimes?

This dissertation will focus on determining the influence and significance of weather phenomena, geologic, and geomorphic spatial variations, with respect to the impact on montane drainage systems and streamflow characteristics.

Goals and Objectives

The goal of this study is to determine the extent to which weather phenomena and spatial variations in geology and geomorphology reduce or shift the stream flow regime in montane environments. This goal can be summarized through the following hypotheses:

H_1: A statistical significance exists between montane weather phenomena and the timing and volume of stream flow regimes.

H_2: A statistical significance exists between montane streamflow regimes and subbasin drainage area, average basin slope, average basin elevation, percentage of subbasin area above 2,250 m, dominant basin aspect, lithologic rippability, landcover and average annual precipitation

To fulfill the goal of this research, the following primary objectives have been established:

1. Determine if a link exists between weather phenomena and timing and volume of montane streamflow regimes for the Uncompahgre River, San Miguel River and Animas River Watersheds.

2. Determine if watershed characteristics influence the timing of the onset of the spring pulse, peak streamflow and the summer streamflow subsidence.

3. Determine if watershed characteristics influence the frequency and magnitude of low streamflows.

Description of Dissertation

This dissertation presents new perspectives to evaluate montane hydrology and the effects of weather phenomena and spatial variations in geology and geomorphology. In addition to the introduction, the four chapters have been written to fulfill the objectives of the study.

The composition of this dissertation will vary from the traditional dissertation in that it will be divided into three separate papers of publishable quality. Each paper will focus on one of the three established objectives, all of which are based around the analysis of the Uncompahgre River, San Miguel River and Animas River Watersheds located in the San Juan Mountains of southwestern Colorado, USA. Chapter II will be written in the format of the journal *Environmental Earth Sciences.* Chapter II presents a statistical methodology to determine if a link exists between weather phenomena and timing and volume of montane stream-flow regimes. Chapter III will be written in the format of the journal *Geomorphology.* Chapter III explains the statistical significance of physical watershed characteristics in influencing and regulating montane streamflow. Similarly, Chapter IV will also be written in the format of the journal *Geomorphology*. Chapter IV explains the relationship between physical watershed characteristics and the frequency and magnitude of low streamflows.

CHAPTER II

WEATHER PHENOMENA AND TIMING AND VOLUME OF MONTANE STREAMFLOW REGIMES

Synopsis

In the western United States, limited availability of fresh water coupled with growing agricultural and urban demands are causing large urban locations to be heavily dependant on montane water resources as supplemental sources of water supply. Unfortunately, montane water resources are delicate and highly dependent upon persistent weather and climatic conditions. With current research indicating dramatic changes from climate warming, water resources in montane areas are approaching excessive liability. The problem of reduced water resources is being accelerated by the decreasing volume of readily available fresh water and increasing population. Thus, predicting the impact of weather trends and variability on water resources is necessary to ensure that demands for water for irrigation and municipal water supply can be met.

Changes in the timing and volume of montane streamflow regimes are typically attributed to earlier snowmelt and the reduction of snow pack. Although snow accumulation and melt are the primary hydrologic inputs from a montane streamflow perspective, several other first-order controls affect the spatial variability of the hydrologic response to weather phenomena. Considerable research has shown that hydrographs for montane streams are significantly affected by geologic controls. Such geologic factors, however, are rarely considered first-order controls on spatial variation

in the hydrologic response to weather phenomena. Spatial differences in geologic and geomorphic controls may have an equally significant influence on the response of streamflow as does the spatial relationship associated with the accumulation and melt of snow. To understand the hydrologic response related to weather phenomena in montane regions, it is necessary to ask: Do weather phenomena and spatial variations in geology, and geomorphology reduce or shift the timing and volume of montane streamflow regimes?

The research presented in this paper is focused on determining if the timing of streamflow regimes for the selected montane watersheds has indeed shifted, and if so, to what extent is the shift in timing related to specific weather phenomena. Time series analysis and General Least Squares (GLS) regression were used to determine if a link exists between weather phenomena and the timing and volume of discharge for the Uncompahgre River, San Miguel River and Animas River located in southwestern Colorado. Time series analysis did not reveal any significant ($\alpha = 0.05$) trends in the timing of streamflow for the three observed locations. GLS regression determined with a level of 0.99 significance, that the selected explanatory variables explain 56 percent of the variance associated with the date at which spring pulse onset occurs, 84 percent of the variance associated with the timing of peak streamflow, and 82 percent of the variance associated with the date at which streamflow ends, or substantially subsides. This research provides the necessary foundation to determine how site-specific changes in streamflow regimes may be the product of spatial variations in geology and geomorphology as well as other watershed characteristics. The results from this research

should be used to improve understanding of changing streamflow regimes in an effort to make critical decisions for water resource management more efficient and effective.

Introduction

When considering the impact of weather on stream-flow, changes in the patterns of stream-flows have typically been attributed to earlier snowmelt and the reduction of snowpack (Tague and Grant 2009; Viviroli, Archer et al. 2011). Although snow accumulation and melt are the primary hydrologic inputs from a montane stream-flow perspective, several other first-order controls affect the spatial variability of the hydrologic response to weather phenomena (Jasper 2004; Uhlenbrook, Huber et al. 2005; Tague, Grant et al. 2008; Tague and Grant 2009; Viviroli, Archer et al. 2011). Spatial differences in geologic and geomorphic controls may have an equally significant influence on the response of stream-flow as does the spatial relationship associated with the accumulation and melt of snow.

Spatial differences in lithology and land cover have the potential to affect the drainage system in a region, thus, affecting the temporal response of the stream-flow (Tague, Grant et al. 2008; Tague 2009). Similarly, topographic and geomorphic controls, such as slope, aspect, elevation, landcover and surface roughness also have the potential to affect the input pathway of runoff to stream-flow. By understanding the affects of such spatial differences on the relationship between drainage systems and stream-flow, it may be possible to better understand the hydrologic response to weather phenomena that can occur in montane regions.

The research presented in this paper will focus on three watersheds in the San Juan Mountains of southwestern Colorado. The primary research objectives are to determine if the timing of streamflow regimes has indeed shifted, and if so, to what extent is the shift in timing related to specific weather phenomena. By analyzing three separate watersheds, this research will also demonstrate the extent to which the effects of weather phenomena on streamflow are site-specific. This research provides the necessary foundation for future research, which will determine how site-specific changes in streamflow regimes may be the product of spatial variations in geology and geomorphology as well as other watershed characteristics. The results from this research should be used to improve understanding of changing streamflow regimes in an effort to make critical water resource management decisions more efficient and effective.

As previously mentioned, water resources from montane areas are approaching excessive liability. The problem of reduced water resources is being accelerated by the decreasing volume of readily available freshwater and increasing population. Mountain river basins, associated reservoirs, and underlying aquifers supply water demands for over sixty million people in the western United States (Barnett, 2005; Viviroli, Archer et al. 2011). This dependence has made montane river systems in the U.S., and worldwide the subject of significant research attention with respect to vulnerability and variability associated with climate change (Nolin 2012). Recent studies conducted by the Intergovernmental Panel on Climate Change (IPCC) suggest that some of the most crucial and already observable impacts of climate change are changes in seasonal stream-flow patterns attributed to earlier seasonal snowmelt and diminishing annual

snow accumulation (Bernstein, 2007; Nolin, 2012). Such changes are already prominent in montane regions, such as the Rocky Mountains of western North America, making people dependent on mountain river basins extremely vulnerable (Kundzewicz et al., 2007). Within the context of climate change, vulnerability has been described as "the degree to which [geophysical, biological, and socioeconomic] systems are susceptible to, and unable to cope with adverse impacts" (Arnell, 1996).

When assessing changes in stream-flow, substantial research has focused on changes in seasonal patterns of stream-flow as a result of earlier snowmelt and the reduction of annual snowpack (Tague, 2009; Bales, 2006; Barnett, 2004). Such research is especially relevant to mountainous regions of the western United States, because much of the precipitation is in the form of winter snowfall and results in a strong seasonal pattern of snowmelt dominated stream-flow. Typically in montane regions, stream-flow is lowest in the summer when little, or no recharge occurs, and highest during spring snowmelt and winter precipitation periods (with the exclusion of high elevation streams, which are typically frozen in the winter). During warmer annual conditions, direct changes in precipitation, evapotranspiration, snow accumulation, and rates of snowmelt, can all result in changes in the timing and magnitude of stream-flow (Barnett et al., 2005; Bales et al., 2006; Tague et al., 2009). Recent studies on what some consider to be the impact of climate change in the western U.S. have shown that a warming climate has shifted the timing of peak stream-flow to earlier in spring, and also decreased the proportion of stream-flow occurring during late summer (Cayan et al., 2001; Knowles and Cayan, 2002; Stewart et al., 2004, Knowles et al. 2006). Shifts toward earlier

streamflow are most likely the result of warmer conditions producing relatively earlier snowmelt and more rain, resulting in a more rapid recharge to streams. For this current study weather patterns rather than climate are of primary concern, as interannual changes in temperature and precipitation are significant.

It is logical to assume that increases in surface temperatures will make regions where the supply of water is dominated by the melting of montane snow extremely vulnerable. Even without a change in the intensity of precipitation, a shift in the type of precipitation and timing can lead to earlier discharge peaks, and result in extremely reduced water availability in the late summer and fall (Leung ; Leung 2005; Lins and Slack 2005; Mote, Hamlet et al. 2005). This change can be of major significance to regions in the western U.S., where the majority of the water demand is in the summer and fall (Service 2004). Regions that are most vulnerable are those where capacities for water storage (natural and human-made) are not sufficient. For example, in regions without soil-water storage or aquifer systems, the winter and spring runoff will be immediately lost, unless captured in reservoirs. As mentioned by Nolin (2012), it is necessary to identify the linkages and feedbacks contributing to water scarcity, and how those translate into spatially varying expressions of vulnerability and variability (Nolin, 2012).

With demand continuously exceeding supply, the Upper Colorado River Basin (UCRB), generates approximately 90 percent of the total flow of the Colorado River, which is the principal source of water and hydropower in the southwestern U.S. (Ficklin, 2013; McCabe, 2007). Multiple studies (Ficklin et al., 2013; McCabe et al., 2007;

Timilsena et al., 2008) have shown that water availability in the UCRB could significantly decline as a result of changing weather patterns. Based on General Circulation Model (GCM) predictions of a 3.5 to 5.6 ° C surface temperature increase, median spring stream-flow is projected to decline by 36 percent by the end of the 21st century, for the UCRB (Ficklin, 2013). More importantly, summer stream-flows for the UCRB are projected to decline with median decreases of 46 percent. Further research has shown that stream-flow in the UCRB is also highly sensitive to interannual and interdecadal phenomena (Timilsena et al., 2008). Ficklin (2013) suggests that an increase in stream-flow occurs during El Nino and a decrease in stream-flow occurs during La Nina.

Recent studies (Kunkel, 2007; Diaz, 1997; Eischeid, 1995; Christensen, 2004) have shown that the Rocky Mountain region of the interior southwestern United States has warmed at one of the highest rates in the contiguous U.S., for the first part of the 21st century. Studies (Rangwala, 2010) show that the San Juan Mountains are characterized by a net warming of 1°C between 1895 and 2005. Most of this warming occurred between 1990 and 2005. Any evident hydrologic impact in the San Juan Mountains may serve as a good indicator of what will happen further down stream; the San Juan Mountains contribute significantly to the annual flow in major streams and rivers, such as the Colorado and Rio Grande rivers (Rangwala, 2010).

Although a significant amount of research addresses the UCRB as a whole, little research has focused on specific montane rivers, and changes associated with them. No available research has connected changes in stream-flow and weather phenomena for the

Uncompahgre, San Miguel and Animas rivers. The research presented in this paper will focus on determining if the timing of streamflow, for the selected montane watersheds has shifted, and if so, to what extent is the shift in timing related to specific weather phenomena. As previously mentioned, the results from the research presented in this paper provide the necessary foundation to determine how site-specific changes in streamflow regimes may be the product of spatial variations in geology and geomorphology, which will be discussed in a separate paper. The results from this research should be used to improve understanding of changing streamflow regimes in an effort to make critical water resource management decisions more efficient and effective.

Description of the Study Area

This study will focus on three adjacent watersheds located in the San Juan Mountains of south-western Colorado: the Uncompahgre, San Miguel, and Animas River Watersheds (Figure 1). These watersheds are most suitable for this study because they represent varying hydrologic, geologic and topographic conditions, and have sufficient periods of record. It is likely that the varying geographic orientations and varying topography of each watershed results in variations in weather patterns that may be evident in streamflow regimes.

The Uncompahgre River flows to the north with an average slope of one degree, and in general is much steeper than the Animas River which flows to the south with an average slope of 0.5 degrees. The San Miguel River, which flows to the west, is

characterized by a much more variable profile, with high relief stream channels in the headwaters, and less relief at lower elevations, in comparison to the Uncompahgre and Animas Rivers.

These watersheds are ideal for stream-flow analyses because they are considered by the Hydro-Climate Data Network (HCDN) as having minimum anthropogenic influences (diversions, dams, reservoirs) (Slack & Landwehr, 1994). Thus, stream-flow records can be interpreted as natural flows. The San Miguel River is well known as one of the last free-flowing rivers in the U.S., making it ideal for hydrologic analysis.

To date, the majority of hydrological research focused on the Uncompahgre River, San Miguel River, and Animas River watersheds is concerned with impaired water quality as a result of historic mining activity. In recent years, however, research of the San Juan Mountains (Rangwala, 2010, 2011) has focused on how changing weather phenomena will affect the volume of stream-flow, with the primary concern being the affects on ecological systems. No available research has focused on the reduction of, and shift in peak timing of stream flow with respect to weather phenomena, geologic and geomorphic spatial variations, for this study area.

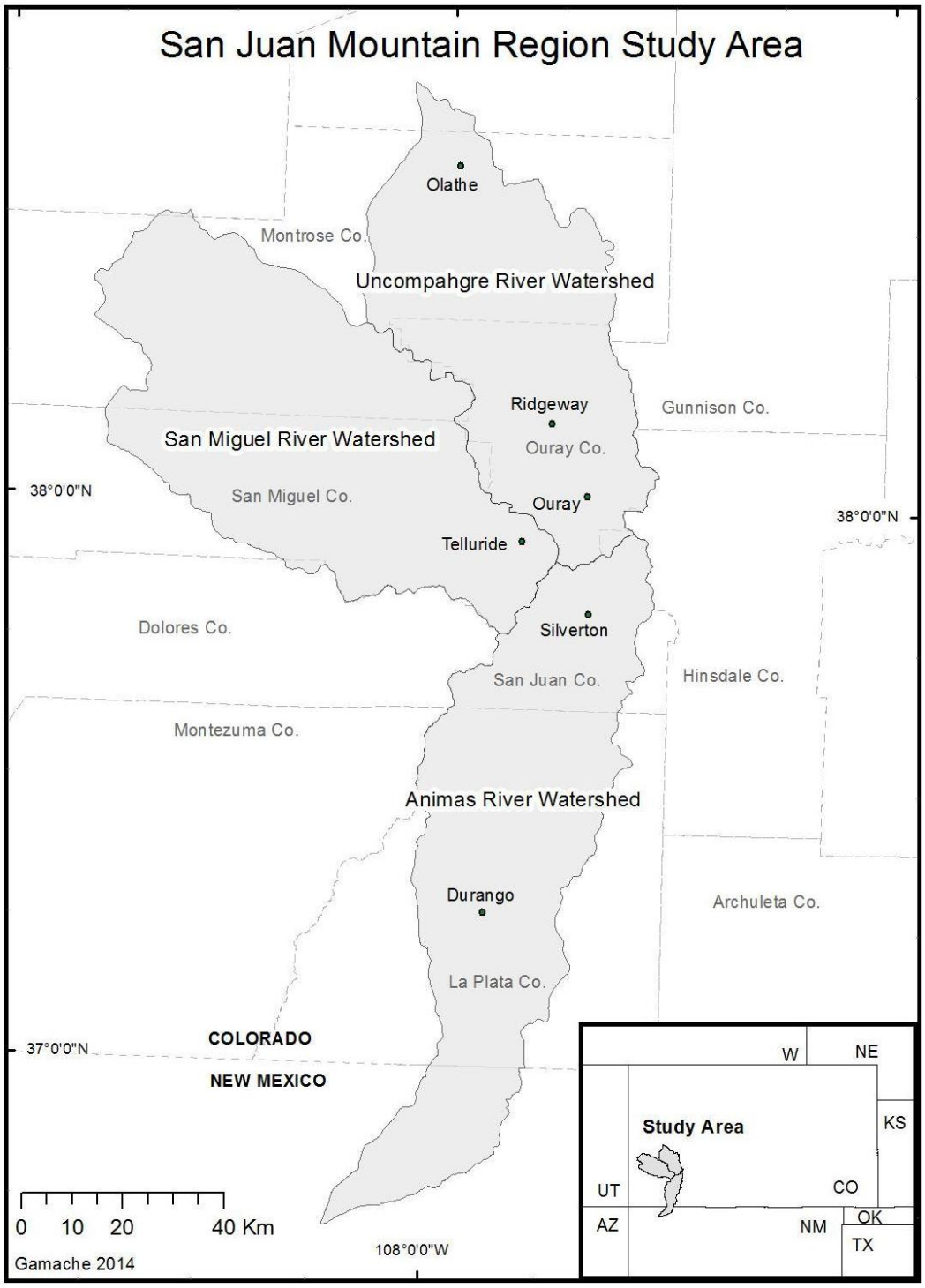

Figure 1: Location of study area for Objective 1.The Uncompahgre (HUC: 14020006), Animas (HUC: 14080104), and San Miguel (HUC: 14030003) River watersheds, located in the San Juan Mountains of southwestern Colorado, USA.

Uncompahgre River Watershed

The Uncompahgre River Watershed (Hydrologic Unit Code (HUC): 14020006) (38° N, 107° W) is located in the San Juan Mountains of south-western Colorado, USA (Figure 2). From north to south, the Uncompahgre River Watershed spans Delta, Montrose and Ouray counties, draining 2,888 km^2 (Nydick, 2012). The Uncompahgre River flows to the north, with the headwaters beginning near Ouray and flowing through Olathe where it joins the Gunnison River. In total, the Uncompahgre River flows approximately 120 km with a total elevation loss of approximately 2,100 m, resulting in a relatively steep gradient. The Uncompahgre River Watershed contains one storage dam and approximately 30 known diversion dams to supply irrigation water to over 26,000 hectares in Delta, Gunnison, and Montrose counties (Uncompahgre Watershed Partnership, 2012). As previously mentioned, according to the Hydro-Climate Data Network (HCDN), the stream-flow for the Uncompahgre River is considered to be representative of natural flows. Natural streamflow is considered as streamflow having less than ten percent of the mean-annual streamflow volume affected by anthropogenic activity (Kircher, 1985).

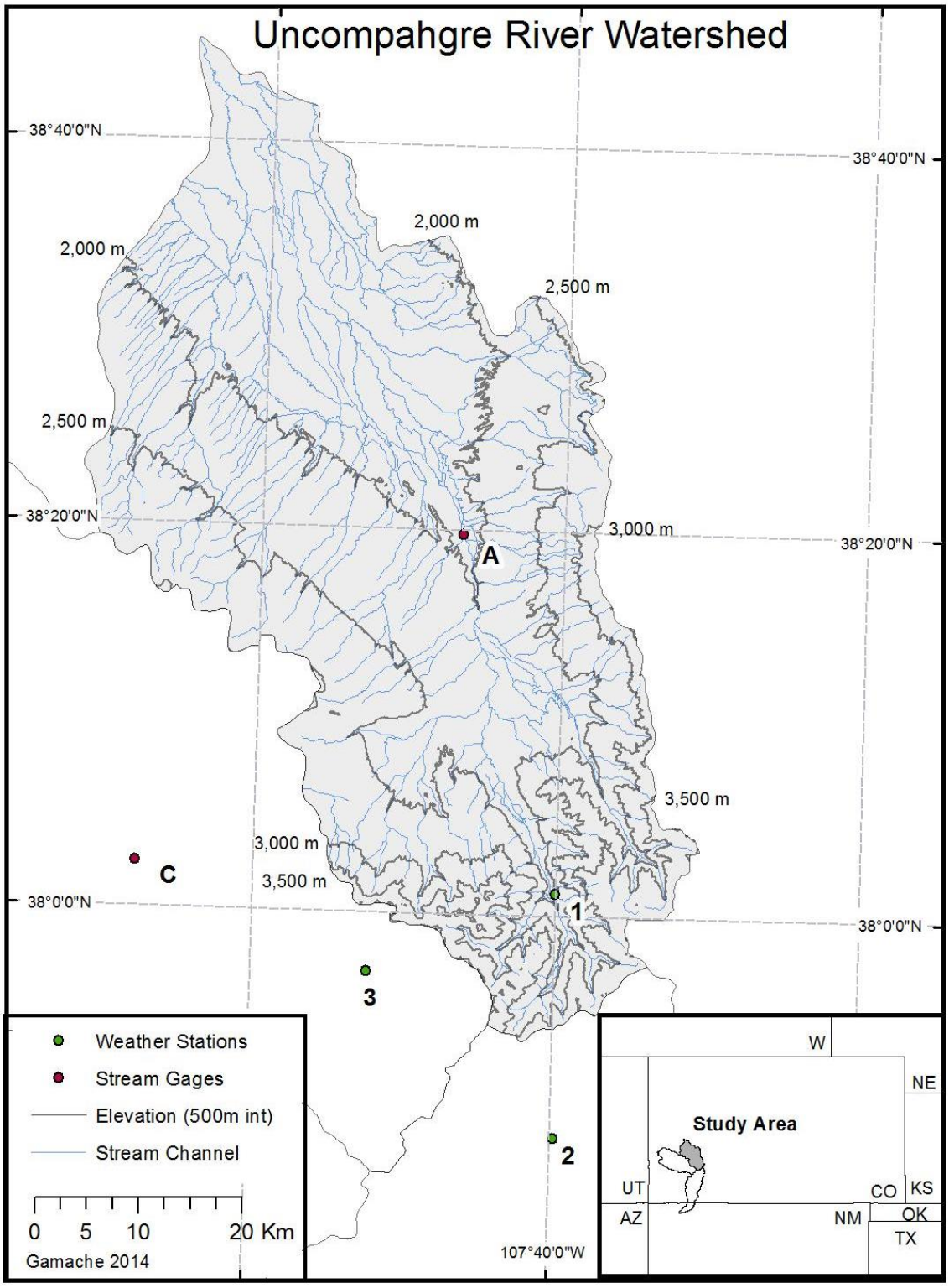

Figure 2: URW weather station and stream gage locations.

The topography of the Uncompahgre watershed is highly varied, ranging from alpine and sub-alpine, to grassland, agricultural land and barren desert (Figure 3). This variable topography results in unique and extremely variable patterns of temperature and precipitation. The weather varies substantially between the southern and northern parts of the watershed because of the significant differences in elevation and landscape features (Nydick, 2012).

Figure 3: High alpine topography typical of high elevations in the URW.

Landscape features are defined as orographic or landcover characteristics that have the potential to influence weather patterns (Nydick, 2012). The climate in the

northern, lower elevation region of the watershed is semi-arid with a low relative humidity. Precipitation is less than 25 cm/yr (Uncompahgre Watershed Partnership, 2013). The maximum monthly rainfall usually occurs in August (28 mm), reflecting the influence of summer, convection thunderstorms (Uncompahgre Watershed Partnership, 2013). Winters at lower elevations are relatively mild when compared to winters at higher elevations, with occasional snowfall, and summers are hot and dry. Average temperatures range from -2°C in the winter to 32°C in the summer (Uncompahgre Watershed Partnership, 2013).

Above 2,250 m, the mountainous conditions result in an increase in precipitation and cooler temperatures. Annual precipitation averages over 76 cm in the high mountains, with 350 cm of snow in Ouray each year (Uncompahgre Watershed Partnership, 2013). Average monthly snowpack is greatest in March and April. Temperatures range from -12°C in the winter to 27°C in the summer (Uncompahgre Watershed Partnership, 2013).

Evidence of the glacial activity that sculpted the Uncompahgre River valley is still visible in the wide valley floor at Ridgeway (Figure 4). When the glaciers melted at the end of the Pleistocene, approximately 10,000 years B.P., valley train deposits filled the U-shaped valley bottom between Ouray and Ridgway, flattening the valley floor (Blair, 1996).

Figure 4: URW glacial evidence. U-shaped valleys filled with glacial deposits are present in all three of the observed watersheds

Groundwater in the Uncompahgre River Watershed is directly related to the local geology. Sedimentary rock aquifers are shallow and have highly variable yields. Hydraulic properties of igneous aquifers vary considerably as the result of differences in type of rock, density and orientation of joints and fractures (Uncompahgre Watershed Partnership, 2013).

The ecological setting of the Uncompahgre River Watershed is a reflection of its diverse geology, topography, climate and landuse (Watershed Partnership, 2013). Landcover in the Uncompahgre River Watershed consists of a mix of range/grassland (44%), forested land (36%), and cropland (13%); approximately 5% of the land is classified as “rock or barren” (NRCS, 2009). Less than one percent of the watershed is

residential/commercial (NRCS, 2009). Landcover is critical in determining the amount of and rate at which surface runoff enters a stream system. Variable landcover results in a significantly different response of streamflow throughout the watershed.

Animas River Watershed

The Animas River Watershed (HUC: 14080104) (37°N, 107°W) is located to the south of the Uncompahgre River Watershed (Figure 5). The Animas River flows from north to south, draining 3,515 km^2. The watershed includes San Juan and La Plata Counties, with the headwaters beginning north of the town of Silverton and passing through the city of Durango, Colorado, flowing as far south as Farmington, New Mexico. Elevations range from more than 4,300 m at the headwaters to less than 1,830 m at the confluence with the San Juan River near Aztec, New Mexico.

The climate is highly variable throughout the watershed, with average annual precipitation ranging from 112 cm at the highest elevations to 33 cm at the lowest elevations (Colorado State University, 2008). The primary sources of precipitation in the watershed are winter snowfall and late summer monsoonal thunderstorms. Approximately 40% of the watershed is above 2,400 m, allowing snowpack to accumulate from late fall to early spring (Colorado State University, 2008).

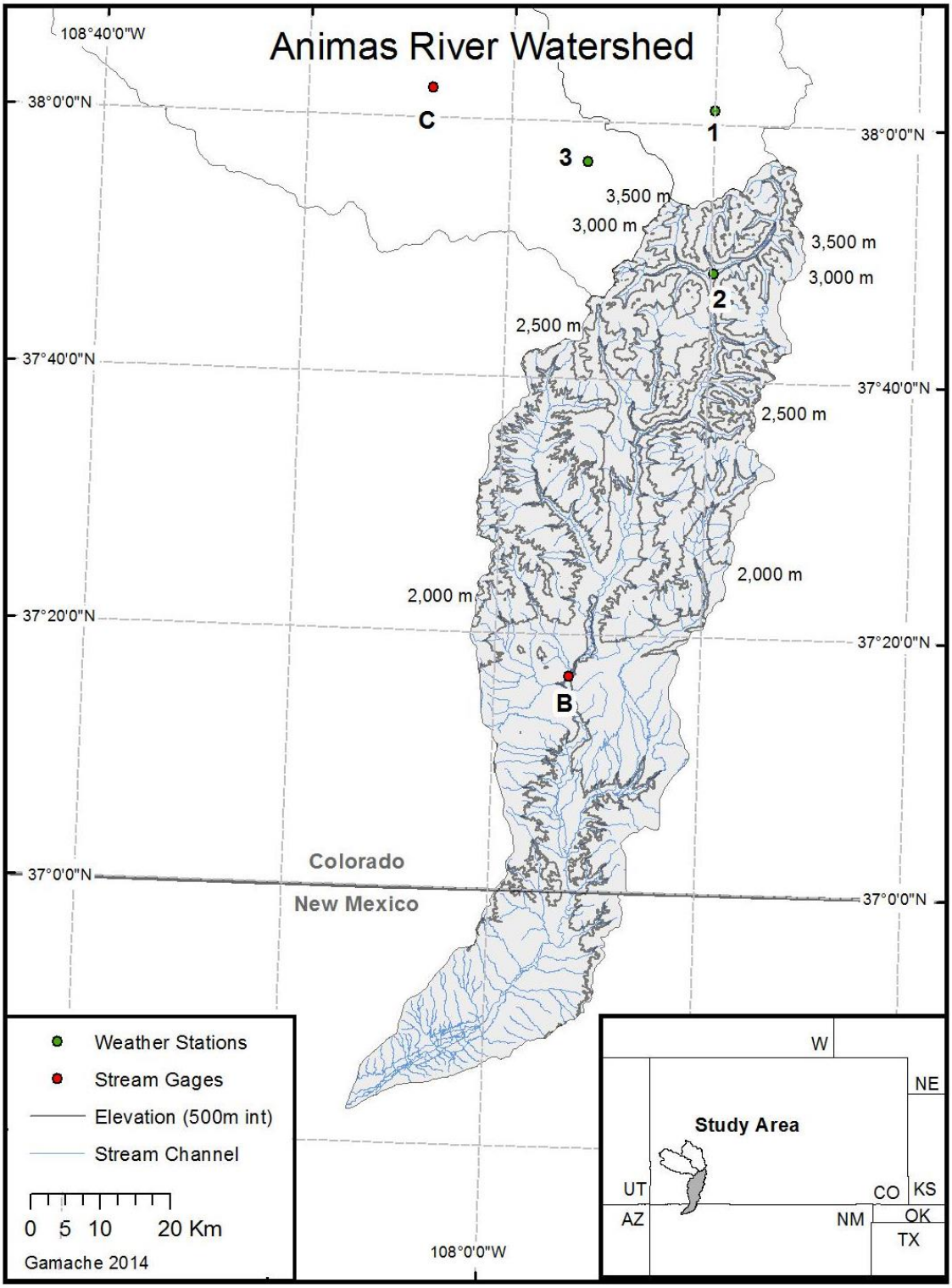

Figure 5: ARW weather station and stream gage locations.

Land use for the Animas River Watershed includes 56% forest, 29 % rangeland, 8% agriculture, 5% developed land, 1% water, and less than 1% wetlands and barren land (NRCS, 2009). As previously mentioned, variable landuse and landcover contribute to varying rates of surface runoff. The rate at which surface runoff enters a stream system has a significant influence on the timing of a stream flow regime.

San Miguel River Watershed

The San Miguel River Watershed (HUC: 14030003) (37°N, 107°W), located to the west of the Animas and Uncompahgre watersheds, drains 4,050 km^2 (Figure 6). The watershed includes portions of San Miguel County and western Montrose County. The headwaters begin above Telluride, at elevations above 4,000 m, with the main river channel traveling 145 km northwest, to the confluence with the Dolores River. The San Miguel River System is considered one of the few remaining intact river systems in the U.S. (Inyan, 2001). With the exception of the affects of acid mine drainage, very little research has focused on the San Miguel Watershed (Inyan, 2001).

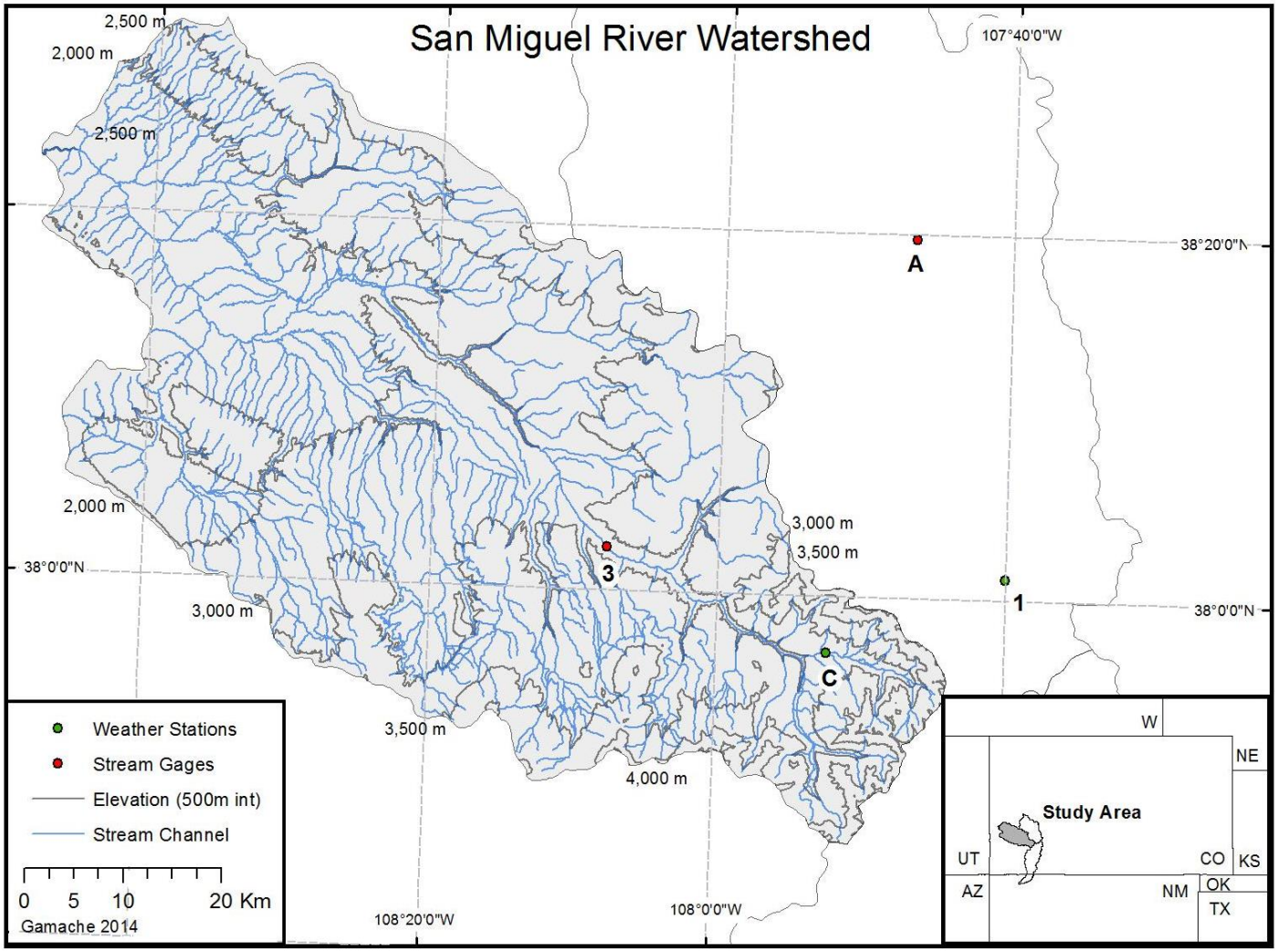

Figure 6: SMRW weather station and stream gage locations.

Methods

Time series analysis was used to identify any significant trends in the timing of montane streamflow regimes for the Uncompahgre River watershed (URW), San Miguel River watershed (SMRW), and Animas River watershed (ARW). The URW has been analyzed from 1937 to 2012, the SMRW has been analyzed from 1943 to 2011 and the ARW has been analyzed from 1914 to 2012. The selected time periods are based on the longest consecutive period of approved data available, to maximize data quantity and increase statistical power.

Daily streamflow data for each watershed was obtained through the USGS, Hydro-Climate Data Network (HCDN) (Slack & Landwehr, 1994). The HCDN includes stream-flow measurements with little or no anthropogenic influences (diversions, dams, reservoirs) and are considered to be representative of natural flows.

Kircher and others (1985) defined natural streamflow as streamflow having less than approximately ten percent of the mean-annual streamflow volume affected by anthropogenic activity. Daily-mean streamflow data for each of the three locations were used to model the annual flow regime for each watershed (Table 1). Flow regimes were modeled using calendar years rather than water years because water years (October, 1 to September, 30) split the streamflow record at a time that did not accurately represent fall precipitation.

Daily temperature and precipitation data were obtained through the National Oceanic and Atmospheric Administration (NOAA). NOAA weather stations were selected based on proximity to watersheds and length of record (Table 2). Daily

temperature and precipitation data were used to compute the monthly-mean precipitation and average-monthly maximum and minimum temperatures. This study defines average monthly maximum temperature as the average of daily maximum temperatures, for each month, over the entire period of record (with the exception of months lacking sufficient data). The same method is used for average monthly minimum temperatures. Similarly, this study defines average monthly precipitation as the average of the daily total precipitation, for each month over the entire period of record.

The timing of flow regimes was described by the beginning, peak and end of annual stream-flows. Beginning of annual streamflow represents the spring pulse onset, which is defined as the date at which the variance of the daily streamflow increases significantly (Stewart, 2004). Spring pulse onset was identified using a moving five-day streamflow variance method. The moving five-day streamflow variance method determines the date at which the variance within any five-day-period exceeds a threshold of 5% of the annual maximum variance. The same moving five-day streamflow variance method was used to determine the end of annual streamflow. This study defines the end of streamflow as the date at which the variance of the daily streamflow decreases significantly. In general, the moving variance method identifies the date, for each annual hydrograph, at which streamflow substantially increases and decreases, for the beginning an end of annual streamflow, respectively.

Table 1: Stream gage locations for the Uncompahgre River, Animas River, and San Miguel River watersheds.

	Station Number	Station Name	Drainage Area (Km^2)	Latitude	Longitude	Data Duration	Source
A	09147500	Uncompahgre River at Colona, CO	1160	38.33	-107.78	1937 -2012	USGS
B	09361500	Animas River at Durango, CO	1792	37.28	-107.88	1914 -2012	USGS
C	09172500	San Miguel River near Placerville CO	803	38.04	-108.13	1943 - 2011	USGS

Table 2: Weather station locations for the Uncompahgre River, Animas River, and San Miguel River watersheds.

	Station	Station Type	Station ID	Data Duration	Latitude	Longitude	Elevation (m)
1	Ouray, CO US	GHCN	GHCND:USC00056203	1937 - 2012	38.02	-107.668	2389.6
2	Silverton, CO US	GHCN	GHCND:USC00057656	1914 - 2012	37.808	-107.663	2830.1
3	Telluride 4 WNW	GHCN	GHCND:USC00058204	1943 - 2011	37.949	-107.873	2635.3

The moving variance method was used to avoid bias created by using the standard percentile method (McCabe et al., 2005), which does not capture the desired information. The standard percentile method describes annual hydrographs by the date at which certain percentages (typically 25%, 50% and 75%) of total streamflow are achieved. This method is not suitable for the current study because the percentages are inherently dependant on total streamflow. This means that substantial precipitation, at any time of the year, can affect the timing of all percentages. For example, substantial precipitation in late-fall could potentially shift the date at which the 10% value is achieved to later in the year. Such occurrences make the standard percentile method inadequate for describing flow regimes for the purpose of this study. The moving variance method determines the timing of flow events (beginning, peak and end) independently of each other. This is crucial when considering montane streamflow because the timing of the onset of the spring pulse is primarily dependant on snowmelt and not summer or fall precipitation.

Similar to other studies, (McCabe et al., 2005; Regonda et al., 2005; Stewart et al., 2004) the peak is characterized by the calendar date at which fifty percent of the annual flow volume was achieved. For simplification, data for February 29th in leap years is averaged with data for February 28th, placed in the record for February 28th, and then the leap day was excluded from the analysis. All data processing was completed using R©, a statistical computing environment capable of processing large data sets (Team, 2005).

For each stream gauge, autocorrelation and partial autocorrelation functions were used to look for dependency within the data. The data showed no sign of autocorrelation warranting further regression analysis. Further analysis involved general least squares (GLS) regression methods to find relationships between weather phenomena and timing and volume of the stream-flow regimes. Average monthly maximum and minimum temperatures and average monthly precipitation were chosen as independent explanatory variables. A least squares regression analysis was developed to model each of the following response variables: the beginning, peak and end of annual stream-flows (according to the previous definitions).

An additional regression analysis was conducted to model correlations between the predictor variables and the total annual streamflow values. This analysis requires streamflow data to be logarithmically transformed prior to the development of the regression model to normalize the distribution. Logarithmic transformation increases the linearity between regression variables and establishes constant variance amongst regression residuals (Cole and King 1968; Geladi and Kowalski 1986; Helsel and Hirsch 2002; Montgomery, Peck et al. 2012).

Results

Time series analysis was used to identify significant trends in the timing of montane streamflow regimes for the Uncompahgre River watershed (URW), San Miguel River watershed (SMRW), and Animas River watershed (ARW). The URW has been

analyzed from 1937 to 2012, the SMRW has been analyzed from 1943 to 2011 and the ARW has been analyzed from 1914 to 2012.

The timing of flow regimes was characterized by the beginning, peak and end of annual streamflows. Beginning of annual streamflow represents the spring pulse onset, which is defined as the date at which the variance of the daily streamflow increases significantly (Stewart, 2004). Similarly, this study defines the end of annual streamflow as the date at which the variance of the daily streamflow decreases significantly. Similar to other studies, (McCabe et al., 2005; Regonda et al., 2005; Stewart et al., 2004) the peak is characterized by the calendar date at which fifty percent of the annual flow volume was achieved.

Study of Table 3 shows that no strong trends in the timing of streamflow were observed for the three selected locations. Luce (2009) explains that the lack of trend is likely a result of the non-linear relationship between snow accumulation and timing of snowmelt. Substantial year-to-year variance is also largely responsible for the poor model fit and low coefficients of determination (R^2). Regardless of poor linear fits, the slope and relative nature of the trends provides valuable insight concerning shifting flow regimes. The time series analysis can be best understood in analyzing plots of the dates of the beginning, the peak and the end of annual streamflows for each individual location.

Table 3: Time series analysis results for the beginning, peak and end of annual streamflow for the URW, SMRW and ARW. Model fit is described by coefficient of determination (R^2).

Model	Coefficient of Determination (R^2)		
	URW	SMRW	ARW
Beginning	0.21	0.26	0.19
Peak	0.52	0.49	0.46
End	> 0.01	> 0.01	> 0.01

Of the three observed watersheds, the URW experienced the most change throughout the period of record (Figure 7). For the URW, spring pulse onset occurs approximately 15 days earlier in 2012 than it did in 1937. This negative trend in spring streamflow is in agreement with most research concerning snow dominated streams. When considering the timing at which fifty percent of annual flow volume is achieved, and the end of annual flow, however, a positive trend was observed. For the URW, in general, the date at which fifty percent of the annual flow volume is achieved occurs approximately ten days later in 2012 than it did in 1937. Streamflow ended approximately 25 days later suggesting that streamflow may be lasting longer into the year.

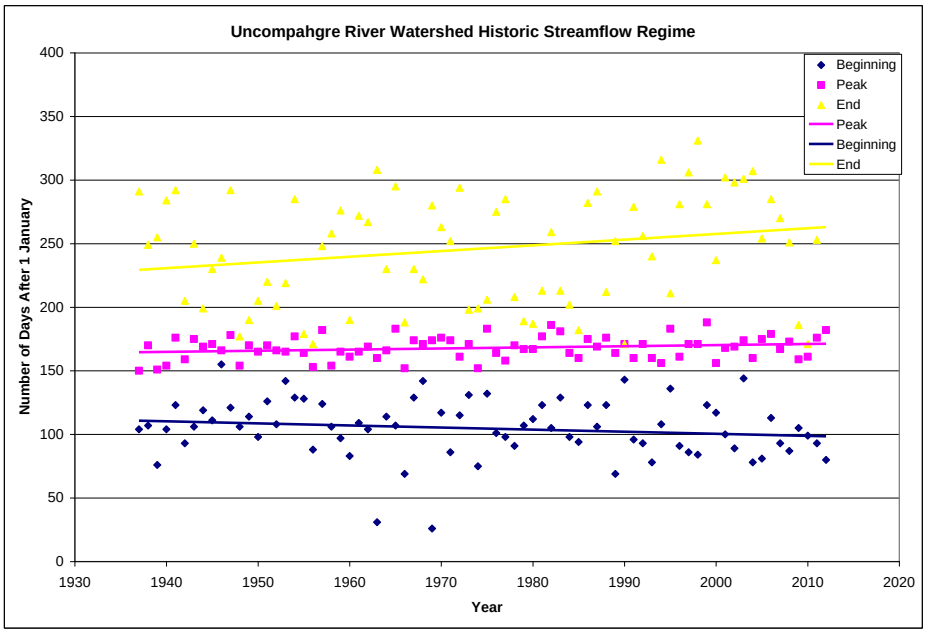

Figure 7: URW historic streamflow regime. URW time series analysis for beginning, peak and end of annual streamflow from 1937 to 2012.

For the SMRW less change was observed, but the pattern in trends is similar to that of the URW (Figure 8). For the SMRW, the onset of the spring pulse and fifty percent of total flow volume occurred approximately ten days earlier in 2011 than in 1943. The end of streamflow, however, showed a positive trend, ending approximately 15 days later in the year.

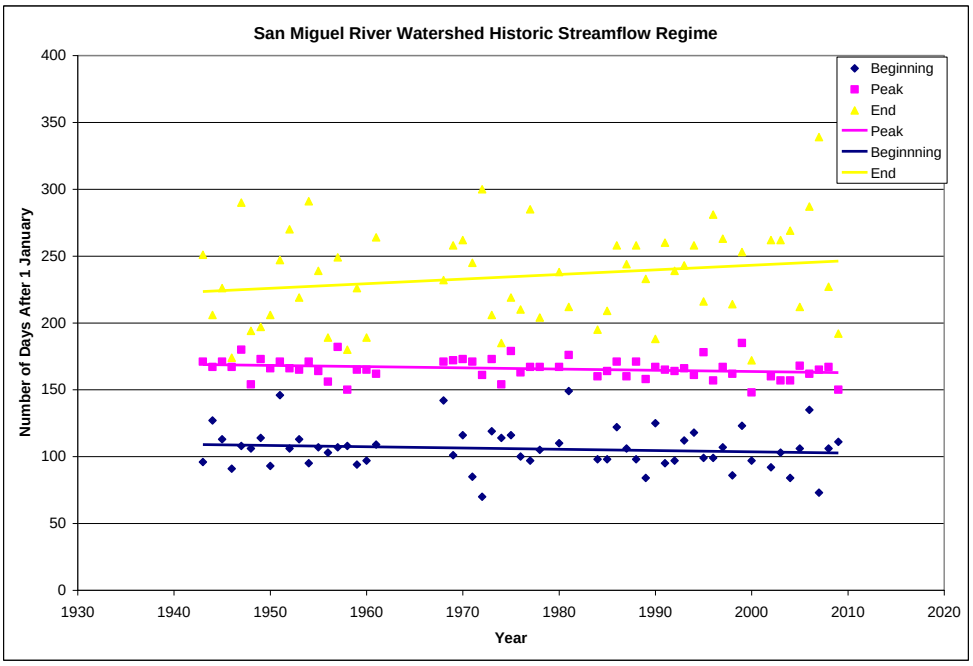

Figure 8: SMRW historic streamflow regime. SMRW time series analysis for beginning, peak and end of annual streamflow from 1943 to 2011.

The ARW observed the least amount of change in flow regime throughout the period of record (Figure 9). A negative trend was observed for the onset of the spring pulse and the date at which fifty percent of total flow volume was achieved; both events occur approximately five days earlier in 2012 than in 1914. No substantial change occurred in the ending dates of annual streamflow.

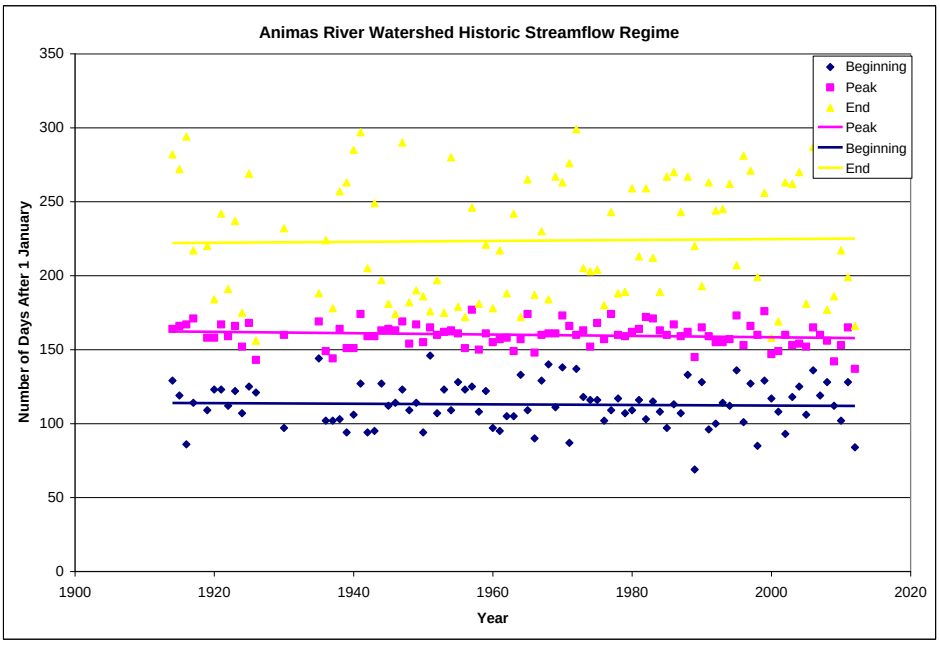

Figure 9: ARW historic streamflow regime. ARW time series analysis for beginning, peak and end of annual streamflow from 1914 to 2012.

Further analysis involved general least squares (GLS) regression to identify more explicit correlations between specific weather phenomena and the timing of montane stream-flow regimes. Average monthly maximum and minimum temperatures and average monthly precipitation were selected as independent explanatory variables, and the beginning, peak and end of annual streamflow were used as response variables. Study of the model determination coefficients in Table 4 shows that, in general, regression analysis is more suitable for modeling the timing of the peak and end of streamflow than the beginning.

Table 4: GLS model results for the beginning, peak and end of streamflows for URW, SMRW and ARW. Model fit is described by coefficient of determination (R^2).

Model	Mean	Coefficients of Determination	
		R^2	Adj. R^2
Beginning	107 (17 April)	0.56	0.35
Peak	165 (14 June)	0.89	0.71
End	234 (22 Aug)	0.82	0.31

GLS regression determined with a level of 0.99 significance, that the selected explanatory variables explain 56 percent of the variance associated with the date at which spring pulse onset occurs (Figure 10). For the beginning of annual streamflow model, the multiple R^2 was 0.56 and an adjusted R^2 was 0.35 (Table 4).

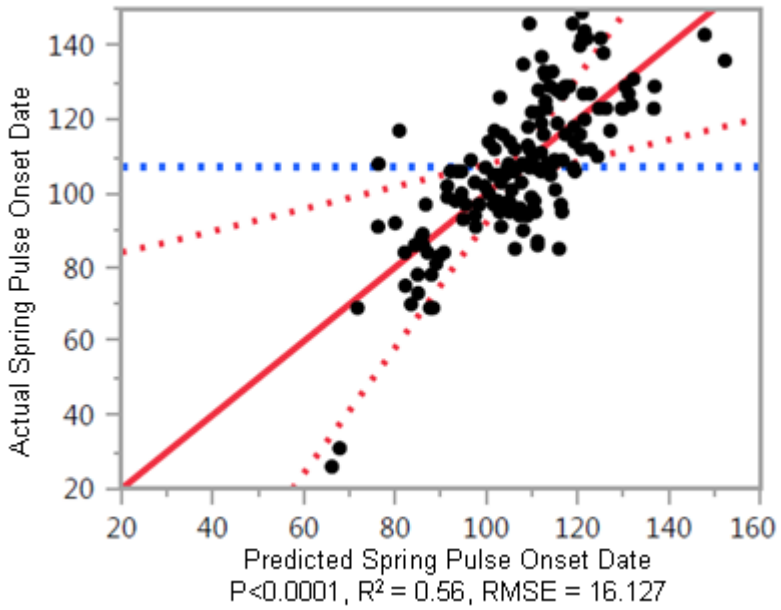

Figure 10: Spring pulse onset model. GLS model fit for the date at which the average onset of the spring pulse occurs (in number of days after 1 Jan), for all three watersheds. The mean of the response is demonstrated by the blue-dotted-line, and the limits of the 0.90 confidence intervals are represented by the red-dotted-lines.

Study of Table 5 shows that the most significant variables in determining the onset of the spring pulse are the average maximum February temperature, and average precipitation in April. These results can be interpreted as follows: on average, an increase of 1°C for the average maximum February temperature will result in the onset of the spring pulse occurring approximately three days later; an average precipitation increase of 0.1 mm for April typically results in the onset of the spring pulse occurring approximately one day later. In general, increases in average maximum temperatures for winter months have the most substantial effect in terms of shifting the onset of the spring pulse later and an increase in average minimum temperatures for spring months have the most substantial effect in terms of shifting the onset of the spring pulse earlier. This is likely because an increase in average winter maximum temperatures prevent precipitation from falling as snow, resulting in less available snowpack come time for spring snowmelt. Conversely, an increase in average minimum temperatures for spring months results in earlier spring snowmelt.

Table 5: GLS beginning of streamflow model. Individual explanatory variable estimates (in days) with corresponding p-values, for all three watersheds.

Month	**Average Tmax.**		**Average Tmin.**		**Average Precipitation**	
	Estimate	**P- value**	**Estimate**	**P- value**	**Estimate**	**P- value**
January	1.67	0.32	1.32	0.33	-0.15	0.60
February	2.82	0.04*	-1.37	0.29	-0.13	0.55
March	-1.64	0.27	1.92	0.17	-0.22	0.22
April	0.32	0.85	-2.32	0.25	0.73	0.001**
May	-0.29	0.85	-3.33	0.14	0.22	0.44

When considering site specific effects on the onset of spring pulse, Table 6 shows that of the three observed watersheds, the San Miguel River watershed was the only site that was seen to have a significant affect ($\alpha < 0.95$) on the timing of the onset of spring pulse. For the evaluated time period, the SMRW, on average experienced the onset of the spring pulse approximately 15 days earlier than the average for the three observed regions. This is likely the result of the SMRW having a larger percentage of lower elevation area; the effects of elevation on the timing of streamflow will be explained in a separate paper.

Table 6: GLS beginning of streamflow model site-specific estimates with corresponding p-values. Estimates in days, for all three watersheds.

Site	Estimate	P- value
URW	16.83	0.10
ARW	-1.56	0.84
SMRW	-15.27	0.02*

In regard to the date at which peak streamflow occurred, GLS regression determined with a level of 0.99 significance, that the selected explanatory variables explain 84 percent of the variance (Figure 11). For the peak streamflow model, the multiple R^2 was 0.84 and an adjusted R^2 was 0.68.

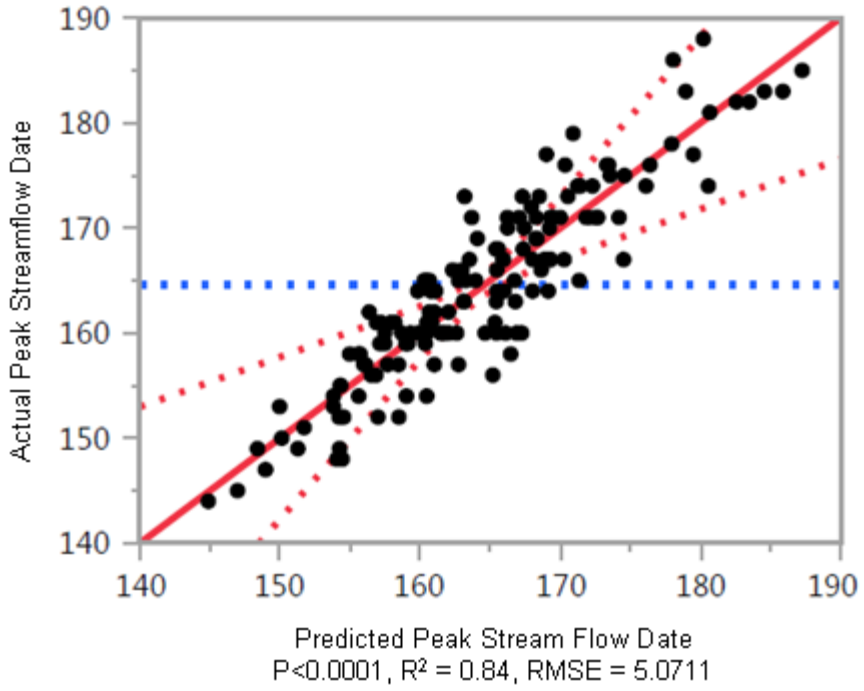

Figure 11: Peak streamflow model. GLS model fit for the date at which the average peak streamflow occurs (in number of days after 1 Jan), for all three watersheds. The mean of the response is demonstrated by the blue-dotted-line, and the limits of the 0.90 confidence intervals are represented by the red-dotted-lines.

Study of Table 7 shows that the most significant explanatory variables for determining the time at which streamflow peaks are the average maximum February temperature and the average maximum and minimum May temperatures. The model suggests that with an average increase in maximum temperature of 1°C for February, peak streamflow shifts, on average, approximately one day later. Similar to the affect on the timing of the onset of the spring pulse, a warmer average maximum February temperature prevents precipitation from falling as snow, resulting in less available snowpack pack come time for spring snowmelt. The average maximum and minimum May temperatures are also seen to have an effect on the timing of peak streamflow; in

general, an increase in average maximum and minimum temperatures causes streamflow to peak approximately two days sooner.

Site was seen to have a significant affect on the timing of peak streamflow for the URW and the ARW (Table 8). Interestingly the shift in timing for the URW and the ARW was opposite, in comparison: the URW, on average experienced peak streamflow approximately ten days later than the average peak streamflow date, and the ARW experienced peak streamflow approximately twelve days earlier than the average peak streamflow date. This could possibly be the result of varying aspects which will also be further explored in a separate paper.

Table 7: GLS peak streamflow model. Individual explanatory variable estimates (in days) with corresponding p-values, for all three watersheds.

Month	Average Tmax.		Average Tmin.		Average Precipitation	
	Estimate	**P- value**	**Estimate**	**P- value**	**Estimate**	**P- value**
January	0.31	0.61	0.67	0.18	0.00	0.93
February	1.25	0.02*	-0.60	0.25	0.02	0.78
March	-0.51	0.33	0.00	0.99	-0.09	0.17
April	-0.03	0.96	0.80	0.28	0.15	0.06
May	-1.55	0.02*	-2.06	0.02*	0.07	0.51
June	-1.41	0.05	-0.27	0.76	0.03	0.73
July	0.03	0.96	0.83	0.30	0.11	0.23
August	0.61	0.35	0.37	0.64	0.16	0.06

Table 8: GLS peak streamflow model site-specific estimates with corresponding p-values. Estimates in number of days, for all three watersheds.

Site	Estimate	P- value
URW	10.06	0.03*
ARW	-11.77	0.002**
SMRW	1.714	0.57

GLS regression determined with a level of 0.99 significance, that the selected explanatory variables explain 82 percent of the variance associated with the date at which streamflow ends, or substantially subsides (Figure 12).

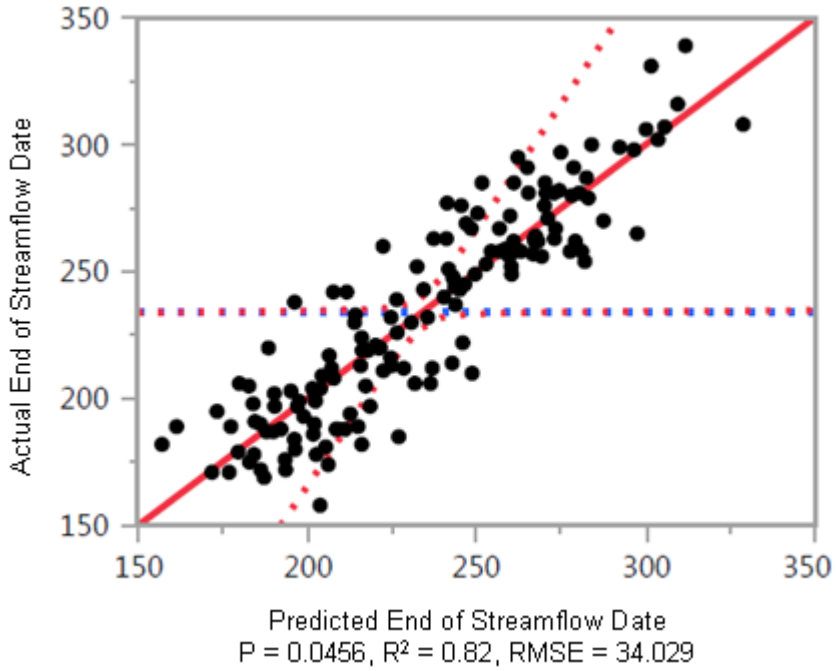

Figure 12: End of streamflow model. GLS model fit for the date at which streamflow ends (in number of days after 1 Jan), for all three watersheds. The mean of the response is demonstrated by the blue-dotted-line, and the limits of the 0.90 confidence intervals are represented by the red-dotted-lines.

The date at which streamflow ends, however, was affected by fewer explanatory variables when compared to the previous two models. The model for the end date suggests that the explanatory variable with the highest confidence level is the average maximum November temperature (Table 9). More specifically, an average increase in maximum temperature of 1°C in November results in streamflow ending on average eleven days later.

Although site did not prove to be a statistically significant explanatory variable for predicting the end of streamflow, the relative magnitude of the estimates should still be taken into account. Study of Table 10 shows that the for the URW and SMRW the timing of the end of streamflow is predicted to shift on average, approximately forty days earlier and forty days later, respectively. In general, it was observed that the most substantial negative affects for the date at which streamflow subsides are associated with increases in the average maximum temperatures during winter and spring months. This is likely because warmer temperatures earlier in the year cause less snow accumulation and earlier snowmelt, so less water is available later in the year.

Table 9: GLS end of streamflow model. Individual explanatory variable estimates (in days) with corresponding p-values, for all three watersheds.

Month	Average Tmax.		Average Tmin.		Average Precipitation	
	Estimate	**P- value**	**Estimate**	**P- value**	**Estimate**	**P- value**
January	3.65	0.49	-3.22	0.44	1.18	0.26
February	-5.9	0.29	6.55	0.15	0.00	0.99
March	-6.1	0.25	0.30	0.95	-1.26	0.06
April	5.89	0.38	-5.29	0.48	-0.17	0.84
May	-7.03	0.28	0.79	0.93	0.09	0.93
June	-1.18	0.84	1.42	0.86	-0.23	0.83
July	1.57	0.81	10.6	0.21	-0.19	0.82
August	2.73	0.69	-12.22	0.15	1.25	0.17
September	-8.73	0.09	7.75	0.30	1.07	0.09
October	-1.75	0.60	6.76	0.22	-0.20	0.72
November	10.56	0.04*	-10.63	0.08	0.84	0.36
December	-9.52	0.05	4.15	0.47	-0.77	0.36

Table 10: GLS end of streamflow model site-specific estimates with corresponding p-values. Estimates in number of days for all three watersheds, individually.

Site	Estimate	P- value
URW	-46.83	0.35
ARW	2.85	0.95
SMRW	43.98	0.20

Discussion and Conclusions

Changes in the timing and accumulation of snowpack are significantly affecting the hydrology of the western United States. In many montane regions, variability in weather phenomena is causing a reduction in snowpack and earlier spring runoff that results in changes in the timing and volume of snowmelt-dominated stream-flow. Shifts in the timing of streamflow have significant implications for water management.

The Upper Colorado River Basin (UCRB) is the principle source of water for much of the southwestern United States. For most years, demand for water form the UCRB exceeds supply (Harding, Wood et al. 2012; Ficklin, Stewart et al., 2013). Recent studies (Kunkel, 2007; Diaz, 1997; Eischeid, 1995; Christensen, 2004) have shown that the mountain region of the interior southwestern United States has warmed at one of the highest rates in the contiguous U.S. for the first part of the 21st Century. It is logical to assume that such warming will affect the timing of montane streamflow; unfortunately, the nature of such effects is not fully understood. Understanding the nature of a potentially shifting flow regime is crucial for the future of water resource management (Luce, 2009).

The San Juan Mountain region of southwestern Colorado encompasses a large portion of the UCRB. Characterizing the nature of changing streamflow in the San Juan Mountain region could possibly help improve water management for the UCRB as a whole. Three watersheds within the San Juan Mountains were analyzed in an attempt to better understand the relationship between weather phenomena and the timing and volume of montane streamflow.

Time series analysis and linear regression models were developed to identify any potential trends in the timing and volume of streamflow as well as the level of correlation between selected weather variables. As a result of the considerable interannual variability in the timing of streamflow, illustrated in Figures 7, 8 and 9, none of the observed trends in shifting flow regimes are significant at the 0.90 significance level. The nature of the observed trends, however, suggests that streamflow is beginning earlier, peaking earlier and in some cases, possibly lasting longer into the year. In comparing the observed trends at each location, it is likely that site specific relationships exist between weather phenomena and flow regimes.

Multiple highly significant correlations occur between specific weather phenomena and streamflow timing, which resulted in positive and negative trends. The general findings of this study suggest that the timing of montane streamflow regimes can be sufficiently explained by average monthly maximum and minimum temperatures and average monthly precipitation. GLS regression determined with a level of 0.99 significance, that the selected explanatory variables explain 56 percent of the variance associated with the date at which the onset of the spring pulse occurs, 84

percent of the variance associated with the timing of peak streamflow, and 82 percent of the variance associated with the date at which streamflow ends, or substantially subsides.

In general, increases in average maximum temperatures for winter months have the most substantial effect in terms of shifting the onset of the spring pulse later and increases in average minimum temperatures for spring months have the most substantial effect in terms of shifting the onset of the spring pulse earlier. This is likely because an increase in average winter maximum temperatures prevent precipitation from falling as snow, resulting in less available snowpack pack come time for spring snowmelt. Conversely, an increase in average minimum temperatures for spring months results in earlier spring snowmelt.

Earlier snowmelt and streamflow are likely to be an increasingly challenging problem for many water resource management systems. With changing weather phenomena, snowmelt dominated streams are becoming less predictable and less reliable (Dettinger and Cayan 1995; Dettinger and Diaz 2000). Although the complex nature of montane hydrologic systems is not fully understood, the ability to characterize which basins are impacted by specific weather phenomena is a crucial step towards understanding future changes and water resource vulnerability.

CHAPTER III

THE INFLUENCE OF SPATIAL VARIATIONS IN EFFICIENCY OF DRAINAGE

Synopsis

In the western United States, limited availability of fresh water coupled with growing agricultural and urban demands are causing large urban locations to be heavily dependant on montane water resources as supplemental sources of water supply. Unfortunately, montane water resources are delicate and highly dependent upon persistent weather and climatic conditions. With current research indicating dramatic changes resulting from climate warming, water resources in montane areas are approaching excessive liability. The problem of reduced water resources is being accelerated by the decreasing volume of readily available fresh water and increasing population. Thus, predicting the impact of weather trends and variability on water resources is necessary to ensure that demands for water for irrigation and municipal water supply can be met.

Changes in the timing and volume of montane streamflow regimes are typically attributed to earlier snowmelt and the reduction of snow pack. Although snow accumulation and melt are the primary hydrologic inputs from a montane streamflow perspective, several other first-order controls affect the spatial variability of the hydrologic response to weather phenomena. Considerable research has shown that hydrographs for montane streams are significantly affected by geologic controls. Such geologic factors, however, are rarely considered first-order controls on spatial variation

in the hydrologic response to weather phenomena. Spatial differences in geologic and geomorphic controls may have an equally significant influence on the response of streamflow as does the spatial relationship associated with the accumulation and melt of snow. To understand the hydrologic response related to weather phenomena in montane regions, it is necessary to ask: Do weather phenomena and spatial variations in geology, and geomorphology reduce or shift the timing and volume of montane streamflow regimes?

Weighted least squares (WLS) regression was used to identify significant relationships between geologic and geomorphic variables and the timing of montane streamflow regimes. The Uncompahgre River watershed (URW), San Miguel River watershed (SMRW) and Animas River watershed (ARW) were each divided into multiple gauged subbasins, which were delineated using USGS stream gauges as pour points. A total of 45 subbasins, within the three watersheds were analyzed. Each subbasin was characterized by eight explanatory variables: drainage area, average basin slope, average basin elevation, percentage of basin area above 2,250 m, dominant basin aspect, lithologic rippability, landcover and average annual precipitation. For each subbasin, the onset of the spring pulse, peak and end of annual streamflow were used as response variables.

For all forty five subbasins, the model suggests with a level of significance greater than 0.99, that 83 percent of the variance of the average onset of the spring pulse can be explained by the eight explanatory variables. 76 percent of the variance of the average date of peak streamflow can be explained by the eight explanatory variables.

And 72 percent of the variance of the date at which streamflow ends, or substantially declines can be explained by the eight explanatory variable. The results from this research suggest that the inclusion of geologic and geomorphic watershed characteristics in hydrologic analyses is beneficial. Such knowledge should be used to improve understanding of changing streamflow regimes in an effort to make critical decisions for water resource management more efficient and effective.

Introduction

When considering the impact of weather on stream-flow, changes in the patterns of stream-flows have typically been attributed to earlier snowmelt and the reduction of snowpack (Tague, 2009; Viviroli et al., 2011). Although snow accumulation and melt are the primary hydrologic inputs from a montane stream-flow perspective, several other first-order controls affect the spatial variability of the hydrologic response to weather phenomena (Jasper, 2004; Tague, 2008, 2009; Uhlenbrook, 2005, Viviroli et al., 2011). Spatial differences in geologic and geomorphic controls also may have an equally significant influence on the response of stream-flow as does the spatial relationship associated with the accumulation and melt of snow (Arnell 1996; Anderton 2002).

Spatial differences in lithology and land cover affect the drainage system in a region, thus, affecting the temporal response of the stream-flow (Tague, 2008, 2009). Similarly, topographic and geomorphic controls, such as slope, aspect, elevation, landcover and surface roughness also have the potential to affect the input pathway of runoff to stream-flow. By understanding the affects of such spatial differences on the

relationship between drainage systems and stream-flow, it may be possible to better understand the hydrologic response to weather phenomena that can occur in montane regions.

Research (Nolin, 2012; Nydick, 2012; Rangwala, 2011) has been conducted on topics relating to the effects of climate change on stream-flow; however, little attention has been focused on how spatial variations in geology and geomorphology may potentially control the impact of weather phenomena on stream-flow in montane drainage basins. The next level of research must focus on this aspect. One can ask: Do weather phenomena and spatial variations in geology, and geomorphology reduce or shift the timing and volume of montane streamflow?

To provide a better overall picture of how the stream-flow in a specific region will be affected by weather phenomena, it is crucial to understand all processes involved. To date, the majority of research concerned with determining future stream-flow has focused primarily on climate-mediated changes in snowpack and regimes of melt (Tague, Grant, 2009). Considerable research (Jasper, 2004; Tague, 2008, 2009; Uhlenbrook, 2005, Viviroli et al., 2011) has shown, however, that hydrographs for montane streams are significantly affected by geologic controls. A better understanding of the impact of relevant geologic controls would help to improve assessment of the impacts of weather phenomena on stream-flow (Stewart, Cayan et al. 2005; Christensen and Lettenmaier 2007).

The effects of weather phenomena are not uniform across all watersheds, thus, it is crucial to have a firm understanding of how surface and sub-surface spatial

heterogeneities occur and operate. Lithology controls which watersheds are surface runoff-dominated and which are groundwater-dominated (Nolin, 2012). Research (Nolin, 2012) has shown that in regions, such as the western U.S. which are typically characterized by dry summers, surface runoff watersheds will consistently experience near-zero late summer discharge; as a result, declining snowpack will have little effect on low flows. This interaction contrasts with groundwater-dominated watersheds, where a shift from snow to rain or a decline in precipitation will reduce recharge, thereby reducing late summer groundwater contributions to stream-flow (Nolin, 2012). Lithology also influences stream patterns, stream spacing, surface roughness and rates of erosion, all of which affect the temporal response of stream-flow.

Geologically determined factors, such as soil, bedrock storage capacity, or hydraulic conductivity, control the subsurface response to precipitation (Bales, 2006). The response time of a watershed can be partially controlled by subsurface soil and geologic properties (i.e., permeability, porosity, transmissivity), which affect the rate of water flux (Hodgkins and Dudley 2006; Hidalgo, Das et al. 2009; Clow 2010). Complex geology and topography typical of the western United States result in significant spatial differences in the rate at which precipitation becomes sheet flow, over-land flow and then into stream-flow. Such geologic factors, however, are rarely considered first-order controls on spatial variation in hydrologic response to the sensitivity of climate change and weather phenomena (Tague, 2008).

In recognizing the lack of research concerning the connection between watershed drainage characteristics and stream-flow sensitivity to weather, Tague (2009) developed

a simple conceptual model, and a process-based hydrologic model that demonstrate how spatial differences in rates of drainage can exacerbate losses in summer stream-flow associated with a diminishing snowpack. Tague (2009) highlighted the importance of geological factors in interpreting the response of hydrology to weather variability by examining multiple drainage basins in the High Cascades and in the Sierra Nevada.

Tague (2009) explained how, in snow-dominated watersheds, stream-flow can be viewed as the product of two filters: the subsurface drainage network and the dynamics of snowpack (Tague, 2009). The combination of both of these filters results in a general smoothing of the time series of precipitation inputs into stream-flow; differences in the efficiency of drainage of a subsurface drainage network might affect spatial patterns of summer stream-flow and its sensitivity to weather phenomena. In this case, efficiency of drainage is not referring to the classical concept of hydraulic conductivity of soil, but instead refers to the rate at which input, either as rain or snowmelt, is transferred to stream-flow.

Tague (2009) used a simple conceptual model to demonstrate how the efficiency of drainage combines with changes in the timing and magnitude of precipitation, or recharge, to control summer stream-flow. The conceptual model is focused on approximating differences in magnitude and timing of snow fall/melt and rates of drainage for sites that differ in terms of geology and snow accumulation and melt regimes (Tague, 2009). Four distinct montane study sites were used. Lookout Creek and McKenzie River at Clear Lake were used to represent the geology of the Western and

High Cascade Mountains, respectively (Tague, 2009). No similar studies have been conducted in the San Juan Mountains.

The results of Tague's conceptual model are supported with physically-based modeling of watersheds. For each of the four study sites, basin-wide estimates of seasonal peak snow and summer stream-flow were compared. Results confirmed that in the slower draining High Cascade watershed compared to the more rapidly draining Western Cascades, a greater change in stream-flow occurred in August, for the same change in the seasonal snowpack (Tague, 2009). In general, it was found that slower draining watersheds are more likely to have more water in summer months, but are also highly vulnerable to summer water losses under a 1.5 ° C warming scenario (Tague, 2009).

Other research (Uhlenbrook, 2005) has suggested that the hydrologic response of montane and high-elevation ecosystems is primarily defined by hillslope processes, making the spatial and temporal variability of hillslope processes in mountain landscapes a critical element for simulating the impact of future changes in land use or weather on hydrology (Uhlenbrook, 2005). Uhlenbrook suggests that the spatial heterogeneity of hillslope processes appears to be closely related to highly variable soil structure overlain by land use and vegetation patterns. Future changes in hydro-climatic inputs (e.g., rainfall, temperature, and snow melt), or land use and vegetation cover, will have a significant influence on the recharge of springs, and consequently, on the runoff components of discharge (Uhlenbrook, 2005). Research by Leibundgut (1998) shows

the vulnerability of springs in mountain regions, which are often used for agricultural and municipal purposes.

Description of the Study Area

This study focuses on three adjacent watersheds located in the San Juan Mountains of south-western Colorado: the Uncompahgre, San Miguel, and Animas River Watersheds (Figure 13). These watersheds are most suitable for this study because they represent varying hydrologic, geologic and geomorphic conditions, and have sufficient periods of record (Figure 14). The geographic orientations of the three watersheds are ideal for making comparisons in terms of how slope, aspect and elevation may control changes in stream-flow. Although all three watersheds are adjacent, the main river reaches of each watershed flow in contrasting directions and have significantly different slopes and surface lithology.

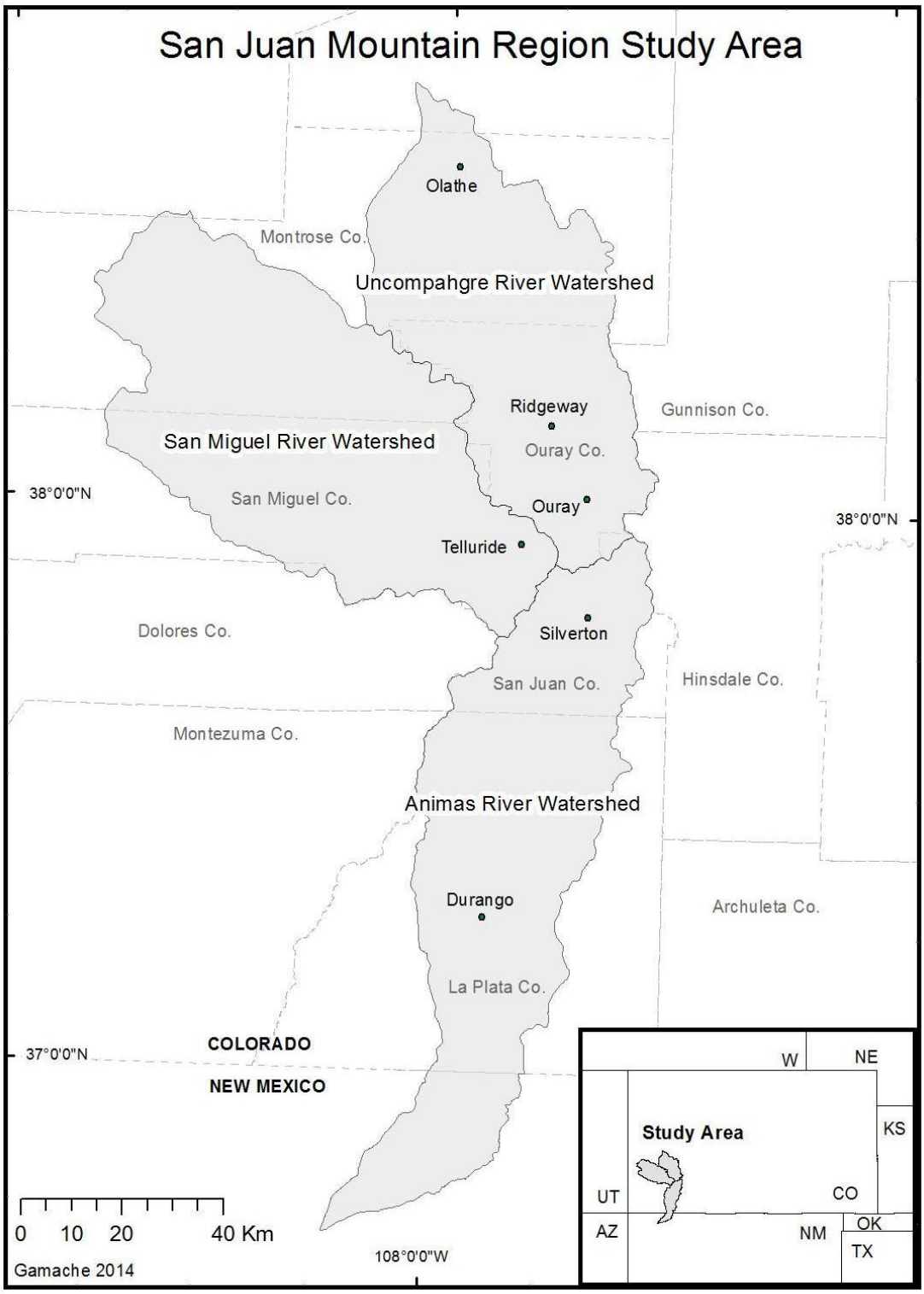

Figure 13: Location of the study area for Objective 2. The Uncompahgre (HUC: 14020006), Animas (HUC: 14080104), and San Miguel (HUC: 14030003) River watersheds, located in the San Juan Mountains of southwestern Colorado, USA.

The Uncompahgre River flows to the north with an average slope of one degree, and in general is much steeper than the Animas River which flows to the south with an average slope of 0.5 degrees. The San Miguel River, which flows to the west, is characterized by a much more variable profile, with high relief stream channels in the headwaters, and a more shallow relief at lower elevations, in comparison to the Uncompahgre and Animas Rivers.

Figure 14: Spatial variations in watershed characteristics. Variations in lithology, landcover, slope and elevation are present in and amongst all three watersheds observed. The picture on the left shows steep, exposed, primarily andesitic slopes, typical of the higher elevations in the URW, compared to gentler, forested slopes in the lower elevations of the SMRW pictured on the right.

These watersheds are ideal for stream-flow analyses because they are considered by the Hydro-Climate Data Network (HCDN) as having minimum anthropogenic influences (diversions, dams, reservoirs) (Slack & Landwehr, 1994). Thus, stream-flow records can be interpreted as natural flows. The San Miguel River is well known as one of the last free-flowing rivers in the U.S., making it ideal for hydrologic analysis.

To date, the majority of hydrological research focused on the Uncompahgre River, San Miguel River, and Animas River watersheds is concerned with impaired water quality as a result of mining activity. In recent years, however, research of the San Juan Mountains (Rangwala, 2010, 2011) has focused on how changing weather phenomena will affect the volume of stream-flow, with the primary concern being the affects on ecological systems. No available research has focused on the reduction of, and shift in peak timing of stream flow with respect to weather phenomena, geologic and geomorphic spatial variations, for this study area.

Uncompahgre River Watershed

The Uncompahgre River Watershed (Hydrologic Unit Code (HUC): 14020006) (38° N, 107° W) is located in the San Juan Mountains of south-western Colorado, USA (Figure 15). From north to south, the Uncompahgre River Watershed spans Delta, Montrose and Ouray counties, draining 2,888 km^2 (Nydick, 2012). The Uncompahgre River flows to the north, with the headwaters beginning near Ouray and flowing through Olathe where it joins the Gunnison River. In total, the Uncompahgre River flows approximately 120 km with a total elevation loss of approximately 2,100 m, resulting in a relatively steep gradient. The Uncompahgre River Watershed contains one storage dam and approximately 30 known diversion dams to supply irrigation water to over 26,000 hectares in Delta, Gunnison, and Montrose counties (Uncompahgre Watershed Partnership, 2012). As previously mentioned, according to the Hydro-Climate Data Network (HCDN), the stream-flow for the Uncompahgre River is considered to be representative of natural flows. Natural streamflow is considered as streamflow having less than ten percent of the mean-annual streamflow volume affected by anthropogenic activity (Kircher, 1985).

The topography of the Uncompahgre watershed is highly varied, ranging from alpine and sub-alpine landscape, to grassland, agricultural land, and barren desert. This variable topography results in unique and extremely variable patterns of temperature and precipitation. The weather varies substantially between the southern and northern parts of the watershed because of the significant differences in elevation and landscape features (Nydick, 2012).

Landscape features are defined as orographic or landcover characteristics that have the potential to influence weather patterns (Nydick, 2012). The climate in the northern, lower elevation region of the watershed is semi-arid with a low relative humidity. Precipitation is less than 25 cm/yr (Uncompahgre Watershed Partnership, 2013). The maximum monthly rainfall usually occurs in August (28 mm) and reflects the influence of summer, convection thunderstorms (Uncompahgre Watershed Partnership, 2013). Winters at lower elevations are relatively mild when compared to winters at higher elevations, with occasional snowfall, and summers are hot and dry. Average temperatures range from -2°C in the winter to 32°C in the summer (Uncompahgre Watershed Partnership, 2013).

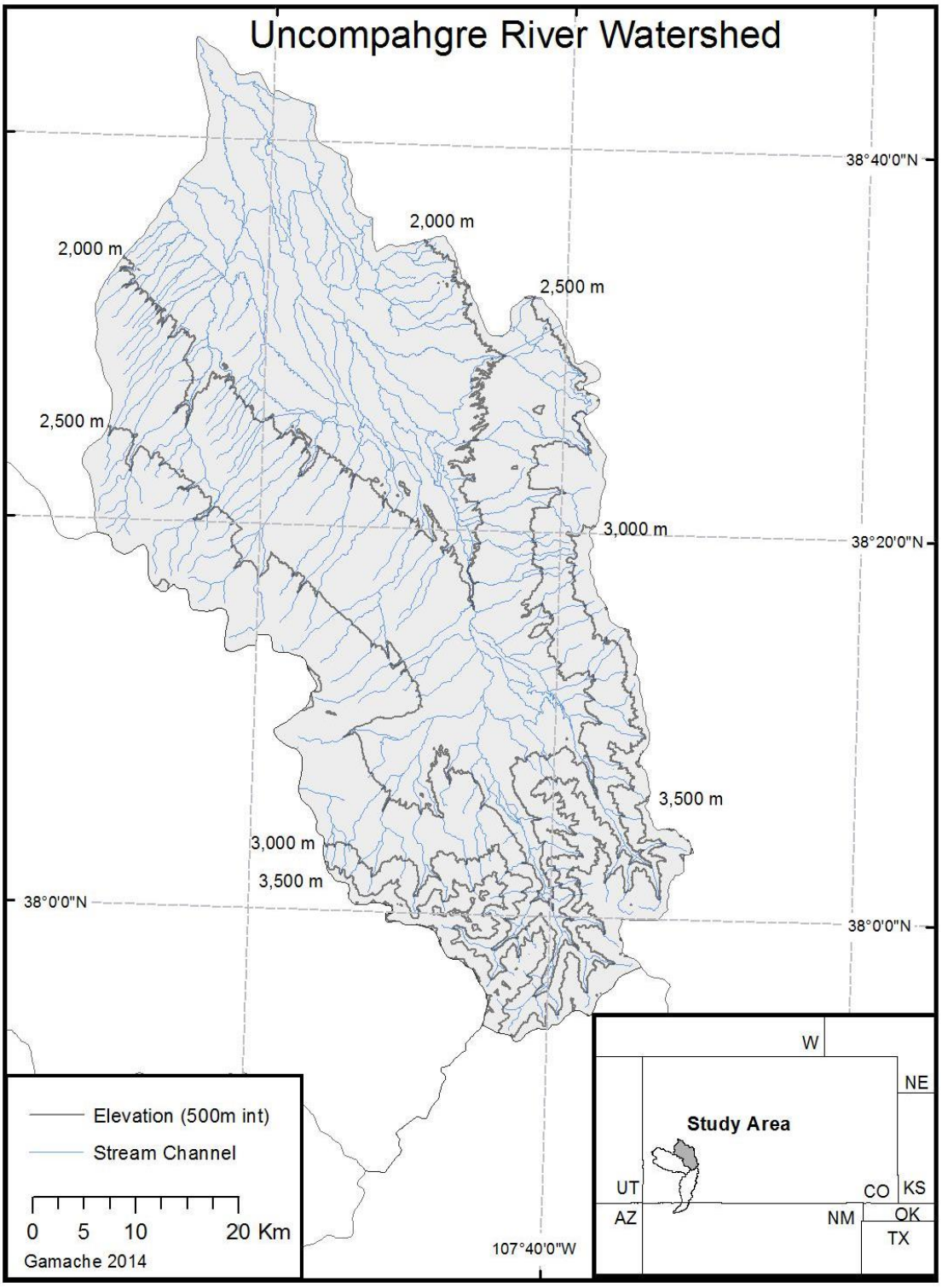

Figure 15: URW topography and stream network for Objective2.

Above 2,250 m, the mountainous conditions result in an increase in precipitation and cooler temperatures. Annual precipitation averages over 76 cm in the high mountains, with 350 cm of snow in Ouray each year (Uncompahgre Watershed Partnership, 2013). Average monthly snowpack is greatest in March and April. Temperatures range from -12°C in the winter to 27°C in the summer (Uncompahgre Watershed Partnership, 2013).

The Uncompahgre Watershed covers portions of two distinct physiographic regions: the Southern Rocky Mountains south of Ridgway and the Colorado Plateau to the north (Blair, 1996). Differences in geology, landscape and climate between the regions create varying hydrologic conditions. The San Juan Mountains are a mixture of pre-Cambrian metamorphics with mid-Tertiary Andesitic volcanic intrusions (Figure 16) (Uncompahgre Watershed Partnership, 2013). Soils of the valley range in age from recent alluvial deposits in the flood plains to the well-weathered soils of higher terraces and benches. The alluvial deposits contain relatively coarse, unconsolidated and stratified soils of poorly graded, well-sorted sand and gravel derived from igneous and sedimentary rock formations (Uncompahgre Watershed Partnership, 2013).

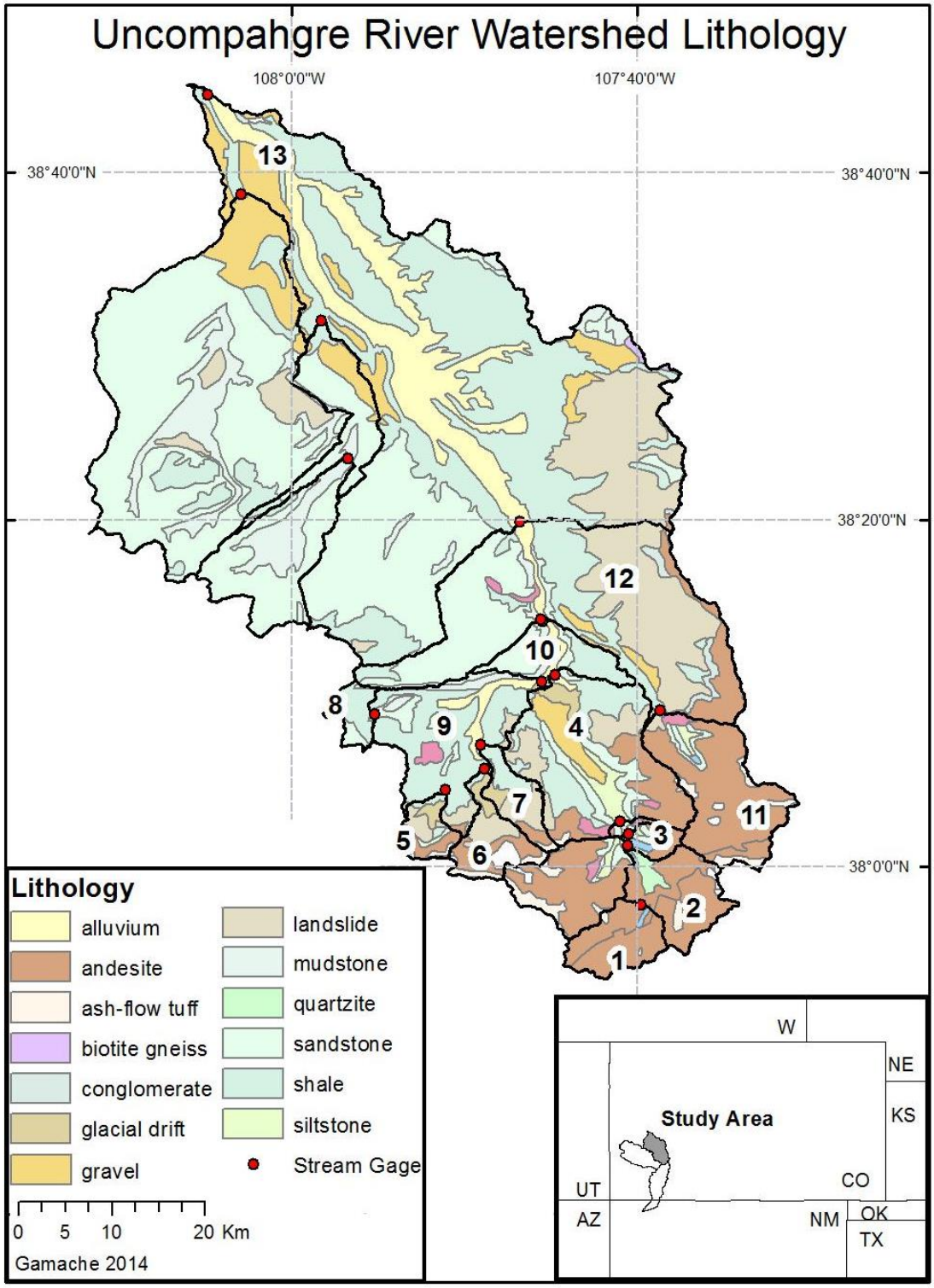

Figure 16: URW surface lithology and subbasin delineations for Objective 2. Numbered subbasins correspond to data in Table 11. Lithologic data provided by USGS.

Evidence of the glacial activity that sculpted the Uncompahgre River valley is still visible in the wide valley floor at Ridgeway (Figure 17). When the glaciers melted at the end of the Pleistocene, approximately 10,000 years B.P., valley train deposits filled the U-shaped valley bottom between Ouray and Ridgway, flattening the valley floor (Blair, 1996).

Figure 17: Topographic and geologic evidence of past glacial activity. Glacial cirques filled with glacial deposits are present in all three of the observed watersheds.

Groundwater in the Uncompahgre River Watershed is directly related to the local geology. Sedimentary rock aquifers are shallow and have highly variable yields. Hydraulic properties of igneous aquifers vary considerably as the result of differences in type of rock, density and orientation of joints and fractures (Uncompahgre Watershed Partnership, 2013).

The ecological setting of the Uncompahgre River Watershed is a reflection of its diverse geology, topography, climate and landuse (Watershed Partnership, 2013). Landcover in the Uncompahgre River Watershed consists of a mix of range/grassland (44%), forested land (36%), and cropland (13%); approximately 5% of the land is classified as "rock or barren" (NRCS, 2009). Less than one percent of the watershed is residential/commercial (NRCS, 2009). Landcover is critical in determining the amount of and rate at which surface runoff enters a stream system. Variable landcover results in significantly different response of streamflow throughout the watershed.

Animas River Watershed

The Animas River Watershed (HUC: 14080104) (37°N, 107°W) is located to the south of the Uncompahgre River Watershed (Figure 18). The Animas River flows from north to south, draining 3,515 km^2. The watershed includes San Juan and La Plata Counties, with the headwaters beginning north of the town of Silverton and passing through the city of Durango, Colorado, flowing as far south as Farmington, New Mexico where it meets the Rio Grande. Elevations range from more than 4,300 m at the headwaters to less than 1,830 m at the confluence with the San Juan River near Aztec, New Mexico.

The climate is highly variable throughout the watershed, with average annual precipitation ranging from 112 cm at the highest elevations to 33 cm at the lowest elevations (Colorado State University, 2008). The primary sources of precipitation in the watershed are winter snowfall and late summer monsoonal thunderstorms. Approximately 40% of the watershed is above 2,400 m, allowing snowpack to accumulate from late fall to early spring (Colorado State University, 2008).

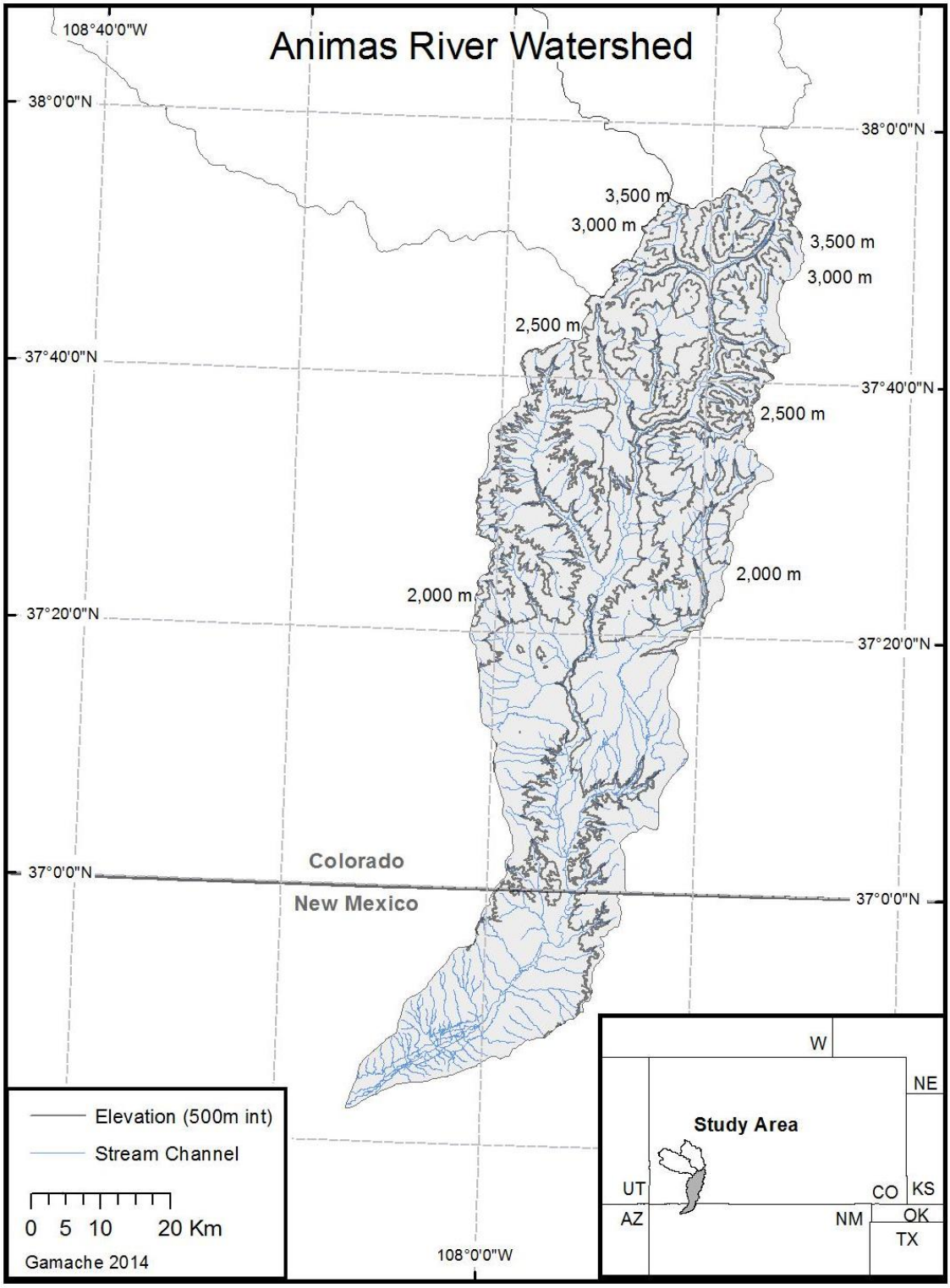

Figure 18: ARW topography and stream network for Objective 2.

The surface lithology is primarily of Precambrian age in the eastern part of the drainage basin, in the Animas Canyon area south of Silverton, with Paleozoic and Mesozoic sedimentary outcrops in the southern part of the drainage basin. The headwaters of the Animas River watershed are underlain by the Tertiary igneous intrusive and volcanic rocks (Figure 19) that formed as a result of late Tertiary episodes of andesitic to dacitic volcanism followed by a later episode of ash-flows, lava flows and intrusions of dacitic to rhyolitic composition (Bush, 1959). This area of the Animas River watershed above Silverton has been extensively fractured, hydrothermally altered, and mineralized by Miocene hydrothermal activity (Casadevall and Ohmoto, 1977).

Similar to landcover, lithology acts as a control to precipitation and runoff. The surface roughness of exposed bedrock determines the rate at which precipitation will be delivered to stream channels, and the degree of fracture of dissection determines the amount of and rate at which precipitation will enter the groundwater system. All of these factors affect the timing of streamflow regimes.

Land use for the Animas River Watershed includes 56% forest, 29 % rangeland, 8% agriculture, 5% developed land, 1% water, and less than 1% wetlands and barren land (NRCS, 2009). As previously mentioned, variable landuse and landcover contribute to varying rates of surface runoff. The rate at which surface runoff enters a stream system has a significant influence on the timing of a stream flow regime.

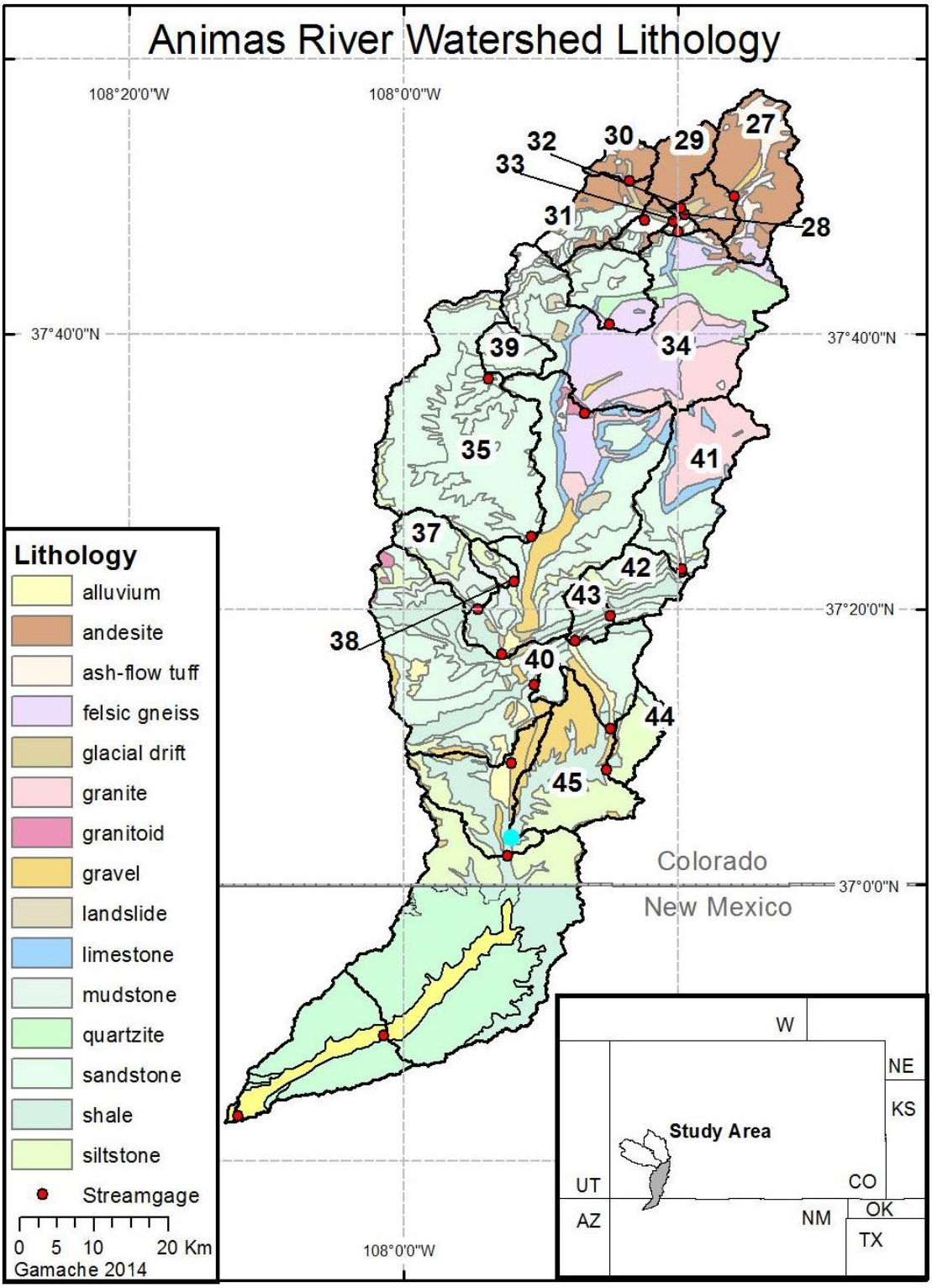

Figure 19: ARW surface lithology and subbasin delineations for Objective 2. Numbered subbasins correspond to data in Table 13. Lithologic data provided by USGS.

San Miguel River Watershed

The San Miguel River Watershed (HUC: 14030003) (37°N, 107°W), located to the west of the Animas and Uncompahgre watersheds, drains 4,050 km^2 (Figure 20). The watershed includes portions of San Miguel County and western Montrose County. The headwaters begin above Telluride, at elevations above 4,000 m, with the main river channel flows 145 km northwest, to the confluence with the Dolores River. The San Miguel River System is considered one of the few remaining intact river systems in the U.S. (Inyan, 2001). With the exception of the affects of acid mine drainage, very little research has focused on the San Miguel Watershed (Inyan, 2001).

San Miguel River watershed is characterized by predominantly sedimentary rocks of late Paleozoic and Mesozoic age (Figure 21) (Atwood, 1932; Bush, 1959). In the southern portion of the watershed the Paleozoic and Mesozoic age sedimentary rocks are covered by younger sedimentary and volcanic rocks, and are intruded by sills and dikes in the Wilson and Dolores Peaks mountain groups, which together form the San Miguel Mountains (Atwood, 1932; Bush, 1959). In the southeast portion of the watershed, a number of andesitic dikes cut the sedimentary rocks of the Cretaceous age (Atwood, 1932; Bush, 1959).

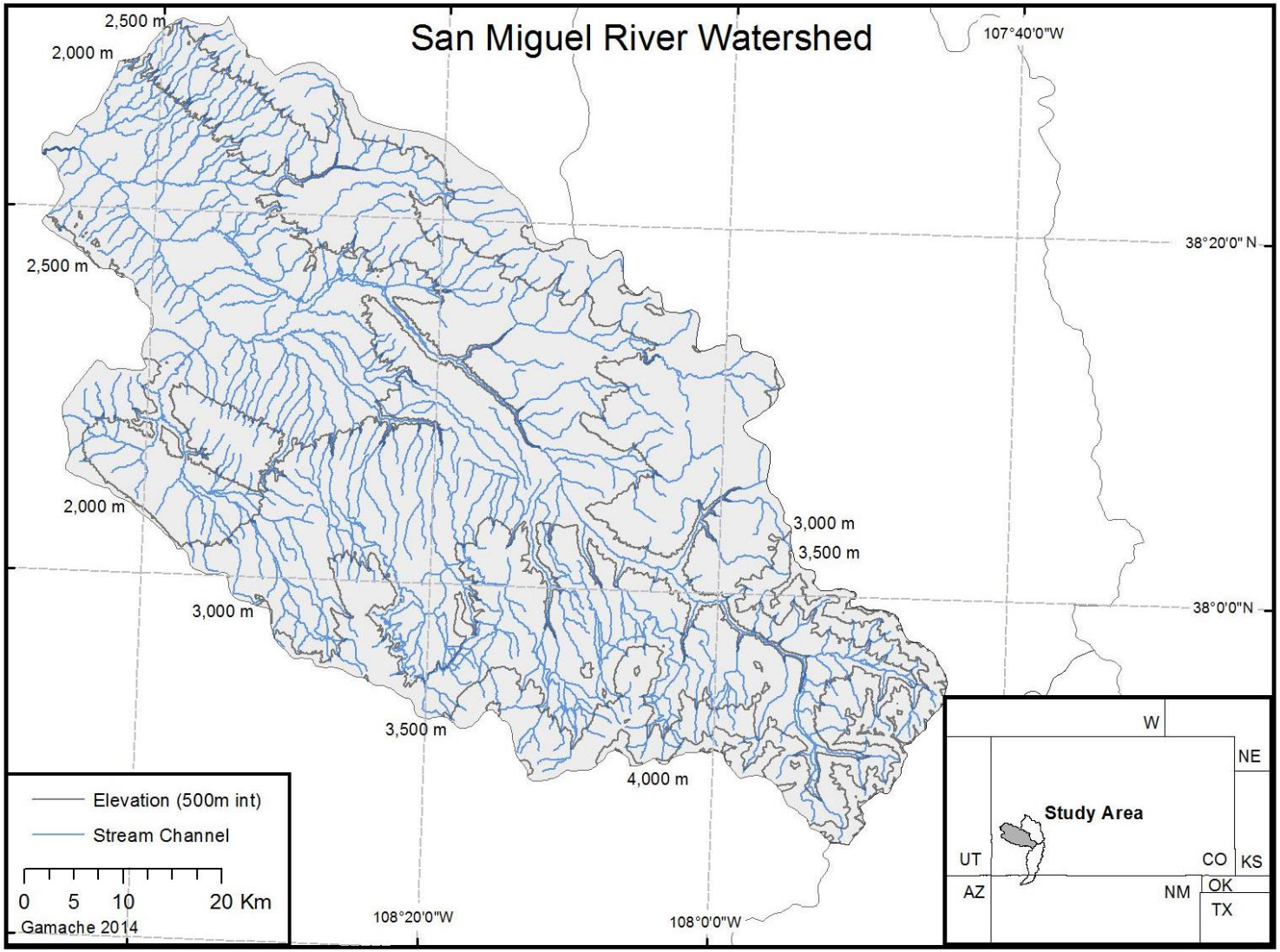

Figure 20: SMRW topography and stream network for Objective 2.

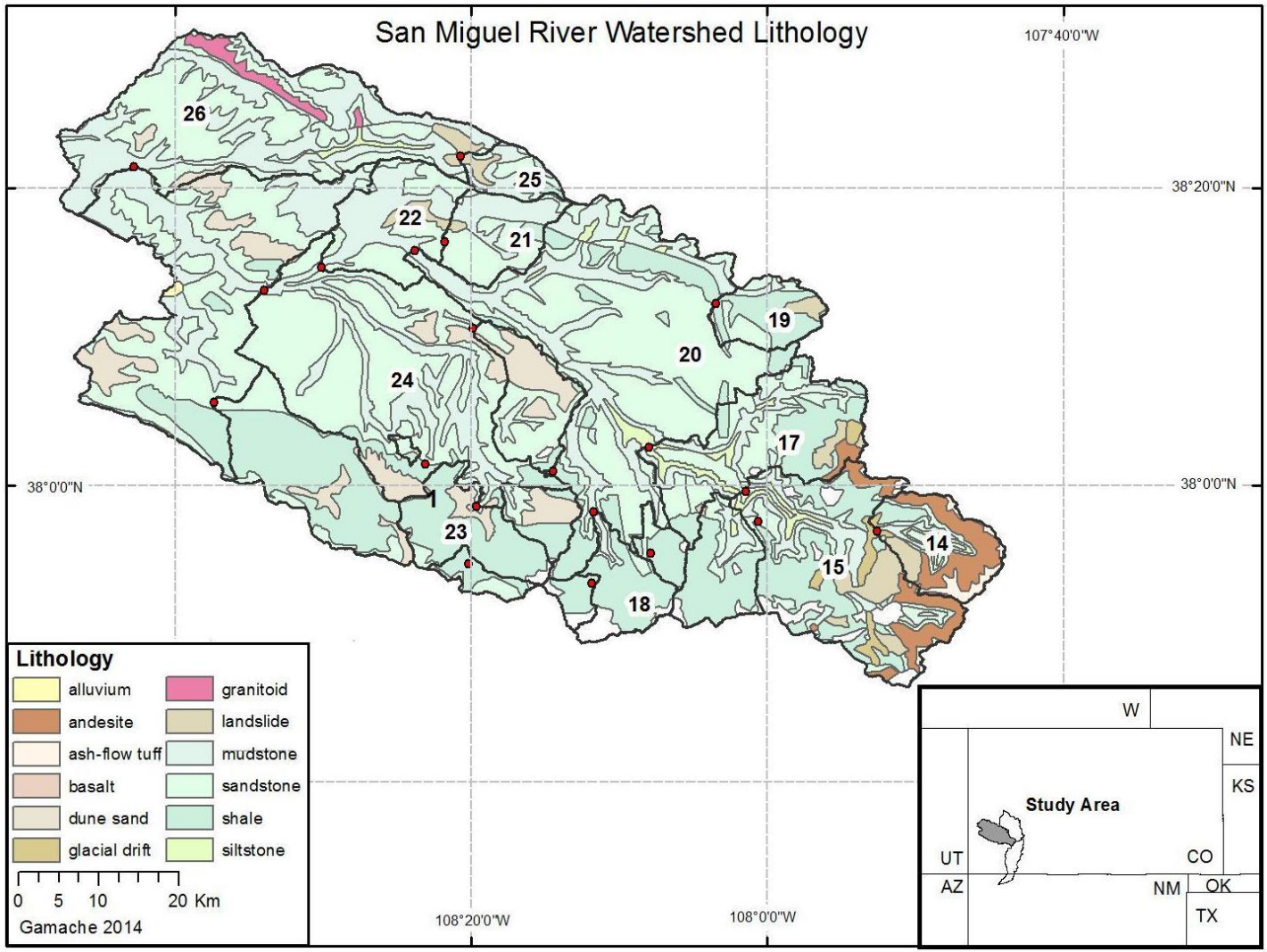

Figure 21: SMRW surface lithology and subbasin delineations for Objective 2. Numbered subbasins correspond to data in Table 12. Lithologic data provided by USGS.

Methods

Weighted least squares (WLS) regression was used to identify significant relationships between geologic and geomorphic variables and the timing of montane streamflow regimes. Forty five subbasins, within three watersheds were analyzed with varying periods of record. The Uncompahgre River watershed (URW), San Miguel River watershed (SMRW) and Animas River watershed (ARW) were each divided into multiple gauged subbasins, which were delineated using USGS stream gauges as pour points. Each subbasin was characterized by eight predictor variables: drainage area, average basin slope, average basin elevation, percentage of subbasin area above 2,250 m (A_{2250}), dominant basin aspect, lithologic rippability, landcover and average annual precipitation. For each subbasin, the onset of the spring pulse, peak and end of annual streamflow were used as response variables. Collectively, 1,126 years of streamflow data were used to determine the average date of when streamflow began, peaked and ended for each subbasin.

Daily streamflow data for each subbasin were obtained through the USGS, Hydro-Climate Data Network (HCDN) (Slack & Landwehr, 1994). The HCDN includes stream-flow measurements with few anthropogenic influences (diversions, dams, reservoirs) and are considered to be representative of natural flows. Kircher and others (1985) defined natural streamflow as streamflow having less than approximately 10 percent of the mean-annual streamflow volume affected by anthropogenic activity. Daily-mean streamflow data for each of the three locations were used to model the annual flow regime for each watershed. Flow regimes were modeled using calendar

years rather than water years because water years split the streamflow record at a time that did not accurately capture summer precipitation.

The timing of flow regimes was characterized by the beginning, peak and end of annual stream-flows. Beginning of annual streamflow represents the onset of the spring pulse, which is defined as the date at which the variance of the daily streamflow increases significantly (Stewart, 2004). A moving five-day streamflow variance method was used to determine the date at which the variance within any five-day-period exceeds a threshold of five percent of the maximum variance. The moving variance method was used to avoid bias created by using the standard percentile method (McCabe and Wolock 2002; McCabe and Clark 2005) which did not capture the desired information. The same method was used to determine the end of annual streamflow, with the end of streamflow being defined as the date at which the variance of the daily streamflow decreases significantly. Similar to other studies, (McCabe et al., 2005; Regonda et al., 2005; Stewart et al., 2004) the peak is characterized by the calendar date at which fifty percent of the annual flow volume was achieved. For simplification, data for February 29th in leap years is averaged with data for February 28th, placed in the record for February 28th, and then the leap day was excluded from the analysis. For each stream gauge, the annual dates for the three streamflow events were averaged over the corresponding period of record. All data processing was completed using R©, an open source statistical computing environment capable of processing large data sets (Team, 2005).

As previously mentioned, the three observed watersheds were separated into multiple subbasins, which were delineated using USGS stream gauges as pour points.

Delineation was completed using three meter digital elevation models (DEM) in conjunction with ArcHydro©. Stream networks were created using a channel threshold area method. To achieve the desired level of stream network accuracy and detail, 0.5 ha was chosen as the channel threshold. To provide consistency when comparing subbasins, the 0.5 ha threshold was used for all subbasins. This threshold area is comparable to other studies in similar topographic systems (McGlynn and Seibert, 2003; McGuire et al., 2005) Accuracy of the stream network was determined by comparing results of the threshold area method with stream networks provided by the National Hydrography Dataset (NHD).

The delineated subbasins were characterized by eight physical characteristics that were chosen to represent the dominant geologic and geomorphic characteristics; one weather variable was used to facilitate comparisons of relative significance (Tables 11 - 13). The physical characteristics included: drainage area, average basin slope, average basin elevation, percentage of basin area above 2,250 m, dominant basin aspect, lithologic rippability, landcover and average annual precipitation. These eight physical parameters were based on the results of previous regional streamflow studies conducted in Colorado and neighboring states (Hortness and Berenbrock, 2001; Hortness, 2006; Waltemeyer, 2006; and Kenney and others, 2007) and on the availability of readily accessible data.

Table 11: URW subbasins for Objective 2. Numbers in far left column refer to subbasin locations in Figure 16.

	Station Number	Latitude (deg)	Longitude (deg)	Years of record	Drainage Area	Average Slope (%)	Average Elevation (m)	A_{2250} (%)	Dominant Aspect	Lithology	Rippability Index	Landcover	Average Annual Precipitation (mm)
1	9144500	37.96	-107.66	8	47	48.4	3475	100	E	Andesite	Non-Rippable	Alpine	1025.40
2	9145000	38.02	-107.68	7	109	53.3	3475	100	N	Andesite	Non-Rippable	Forested	986.03
3	9146000	38.03	-107.68	15	195	58.4	3434	100	NW	Andesite	Non-Rippable	Forested	967.74
4	9146200	38.18	-107.75	54	386	51.4	3170	94.2	NW	Andesite/ Shale	Non-Rippable	Forested	842.26
5	9146400	38.07	-107.85	14	37	38.5	3114	100	NE	Glacial Drift	Rippable	Alpine/ Forested	784.86
6	9146500	38.09	-107.81	14	44	50.3	3334	100	N	Andesite /landslide	Marginally Rippable	Forested	894.08
7	9146550	38.12	-107.82	7	32	34.2	2859	100	N	Shale/ Landslide/ Andesite	Marginally Rippable	Forested	694.18
8	9146600	38.15	-107.92	11	21	11.8	2759	100	E	Shale	Marginally Rippable	Forested	655.32
9	9147000	38.18	-107.76	52	252	28.1	2793	91.4	N	Andesite/ Shale	Non-Rippable	Forested	668.02
10	9147025	38.24	-107.76	25	673	45.9	3036	87.8	N	Andesite/ Shale	Non-Rippable	Forested	784.35
11	9147100	38.15	-107.64	17	118	55.6	3268	100	NW	Andesite	Non-Rippable	Alpine /Forested	855.98
12	9147500	38.33	-107.78	98	1160	42.1	2665	72.6	N	Sandstone/ shale/ Andesite	Rippable	Scrub	669.29
13	9149500	38.74	-108.08	75	2888	21.3	2393	52.1	N	Sandstone/ shale/ Andesite	Rippable	Forested	482.85

Table 12: SMRW subbasins for Objective 2. Numbers in far left column refer to subbasin locations in Figure 21.

	Station Number	Latitude (deg)	Longitude (deg)	Years of record	Drainage Area	Average Slope (%)	Average Elevation (m)	A_{2250} (%)	Dominant Aspect	Lithology	Rippability Index	Landcover	Average Annual Precipitation (mm)
14	9171200	37.94	-107.87	5	111	53.3	3414	100	W	Andesite/ Sandstone	Marginally Rippable	Alpine/ Forested	933.95
15	9172000	37.96	-108.01	17	87	31.2	3060	100	W	Shale	Marginally Rippable	Forested	815.34
16	9172100	38.1	-107.92	7	23	23.1	2917	100	W	Shale	Marginally Rippable	Forested	686.05
17	9172500	38.04	-108.13	72	803	37.6	3031	99	NW	Shale/ Sandstone	Marginally Rippable	Forested	769.62
18	9173000	37.97	-108.20	28	105	23.6	3078	100	N	Shale	Marginally Rippable	Forested	872.99
19	9173500	38.20	-108.05	8	75	11.5	2707	100	W	Shale	Marginally Rippable	Forested	632.97
20	9174000	38.26	-108.40	8	1681	27.9	2807	92.4	NW	Sandstone	Rippable	Forested	684.27
21	9174500	38.27	-108.36	8	101	16.1	2330	54.7	W	Sandstone	Rippable	Scrub	500.38
22	9174600	38.24	-108.50	17	1906	26.5	2731	85.3	NW	Sandstone	Rippable	Forested	655.57
23	9175000	37.98	-108.33	16	137	16.9	2648	100	N	Shale	Marginally Rippable	Forested	665.48
24	9175500	38.22	-108.57	51	2769	22.6	2586	73.3	NW	Sandstone	Rippable	Scrub	601.98
25	9176500	38.37	-108.35	6	44	16.8	2731	100	W	Sandstone	Rippable	Scrub	798.57
26	9177000	38.35	-108.71	42	3882	21.2	2445	59.1	NW	Sandstone	Rippable	Forested	558.04

Table 13: ARW subbasins for Objective 2. Numbers in far left column refer to subbasin locations in Figure 19.

	Station Number	Latitude (deg)	Longitude (deg)	Years of record	Drainage Area	Average Slope (%)	Average Elevation (m)	A_{2250} (%)	Dominant Aspect	Lithology	Rippability Index	Landcover	Average Annual Precipitation (mm)
27	9357500	37.83	-107.60	46	145	54.4	3638	100	S	Andesite/ Tuff	Marginally Rippable	Alpine/ Forested	1135.38
28	9358000	37.81	-107.66	19	183	55.1	3597	100	S	Andesite	Non-rippable	Alpine/ Forested	1117.35
29	9358550	37.82	-107.66	19	52	54.5	3488	100	S	Andesite	Non-rippable	Forested	1028.70
30	9358900	37.85	-107.73	6	29	45.8	3566	100	S	Andesite	Non-rippable	Alpine/ Forested	1081.53
31	9359000	37.80	-107.70	12	114	51.9	3527	100	N	Andesite	Non-rippable	Alpine/ Forested	1046.48
32	9359010	37.80	-107.67	19	136	52	3505	100	E	Andesite/ Sandstone	Marginally Rippable	Forested	1038.86
33	9359020	37.79	-107.67	20	378	53.4	3536	100	S	Andesite	Non-rippable	Forested	1066.29
34	9359500	37.57	-107.78	10	901	52.1	3414	99.9	SW	Gneiss/ Sandstone/ Andesite	Marginally Rippable	Forested	1033.78
35	9361000	37.42	-107.85	46	445	46.7	2924	98.7	SE	Sandstone	Rippable	Forested	855.98
36	9361200	37.367	-107.87	5	19	49.1	2694	89.2	SE	Sandstone	Rippable	Forested	728.22
37	9361400	37.33	-107.91	5	68	53.9	2868	97.5	S	Sandstone	Rippable	Forested	870.97
38	9361500	37.28	-107.88	96	1792	46.6	3093	93.5	S	Sandstone	Rippable	Forested	911.86
39	9362000	37.60	-107.89	21	171	33	2491	68.7	W	Sandstone	Rippable	Forested	629.92
40	9362550	37.24	-107.84	6	17	15.7	2137	6.65	SW	Sandstone	Rippable	Forested	547.62
41	9362900	37.38	-107.66	7	178	33.4	3231	100	S	Sandstone/ Granite	Marginally Rippable	Forested	926.85
42	9363000	37.33	-107.75	39	252	34.1	3048	99.4	SW	Sandstone	Rippable	Forested	873.76
43	9363050	37.30	-107.79	14	277	33	2972	95	SW	Sandstone	Rippable	Forested	848.36
44	9363100	37.14	-107.75	21	46	6.8	2061	0	SW	Siltstone	Rippable	Forested	429.26
45	9363200	37.06	-107.87	21	572	22	2530	50.9	S	Gravel/ Shale/ Siltstone	Rippable	Forested	655.07

Drainage area, slope, elevation and aspect are topographic factors that are significant in influencing the amount and distribution of precipitation, runoff and infiltration that will occur; all of which affect stream-flow hydrographs. These factors are largely responsible for influencing microclimatic conditions that can significantly affect the amount and type of available precipitation within a watershed. These topographic data were derived using three-meter DEMs in conjunction with the Spatial Analyst extension in ArcMap©. Drainage area is measured in Km^2 and represents the amount of area contributing runoff to an individual stream gauge. Average subbasin slope is measured in percent. Average subbasin elevation is measured in meters-above-NGVD 29. To determine if a threshold occurs at which elevation becomes a significant factor, an additional elevation factor was included: percentage of subbasin area above 2,250 m (A_{2250}). Dominant basin Aspect was described by cardinal and intercardinal directions: N, S, E, W, NW, NE, SE, and SW.

Surface lithology and landcover have a significant influence on runoff and are critical in determining stream pattern, stream spacing and rates of erosion, all of which are known to affect a streams hydrograph. Lithologic data was collected using digital 1:24,000 scale USGS geologic maps (http://www.usgs.gov/pubprod/data.html#data). To accommodate the needs of the statistical methods, lithology was collapsed into three categories using a rippability index, which describes lithology as non-rippable, marginally rippable, or rippable. Rippability is a measure commonly used by engineering geologists to describe the ability of a rock to be excavated using conventional excavation equipment (Caterpillar©, 2013). In the context of this study,

rippability serves as a surrogate for erosion potential and surface roughness. The rippability of specific rocks can be found in several engineering geology or civil engineering texts. For this study, rippability was determined using a classification based on seismic wave velocities provided by Caterpillar© (Figure 22).

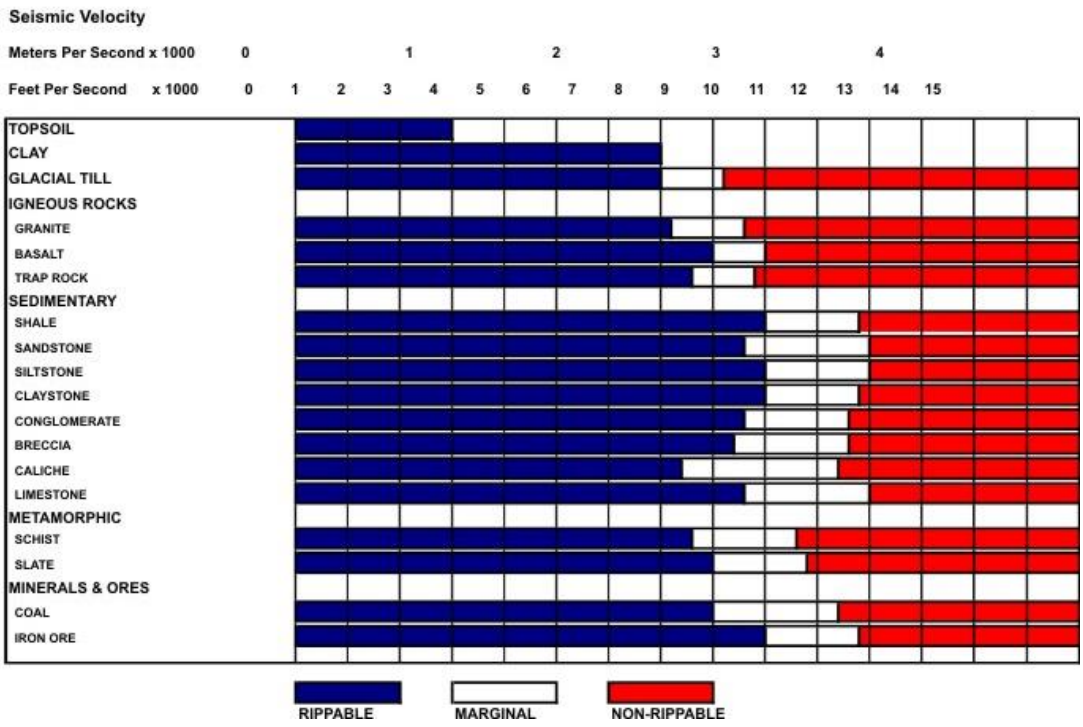

Figure 22: Caterpillar© Lithologic Rippability Index. Rippability is based on seismic wave velocities.

Similar to lithology, it was also necessary to collapse landcover into fewer categorical variables. Land cover data were obtained through the National Land Cover Database 2006 (NLCD) (http://www.mrlc.gov/). Land cover is described as alpine, alpine/forested, forested, or scrub. These categories describe the predominant landcover

of a subbasin based on the greatest percent of area covered by a specific type of landcover.

Average annual precipitation values were collected for each subbasin through the USGS StreamStats© program. Precipitation values were validated through the precipitation frequency atlas for the western United States (Daly, Neilson et al. 1994; Carroll, Cline et al. 2006).

The previously mentioned data were compiled into excel spreadsheets that could be imported into JMP©, a statistical analysis software developed by SAS©. Using JMP©, a weighted least squares regression analyses was conducted using the onset of the spring pulse, peak and end of annual streamflow as response variables, and the subbasin characteristics as predictor variables. The analysis was weighted by the data duration for each subbasin. Individual effects tests were conducted for each subbasin characteristic. To compare the impacts of each of these variables, the adjusted coefficient of determination (Adj. R^2) and percent standard error of prediction (SE%) were used as performance metrics.

Results

Weighted least squares (WLS) regression identified significant relationships between geologic and geomorphic watershed characteristics and the timing of montane streamflow regimes. Forty five subbasins, within three watersheds were analyzed. The Uncompahgre River watershed (URW), San Miguel River watershed (SMRW) and Animas River watershed (ARW) were each divided into multiple gauged subbasins,

which were delineated using USGS stream gauges as pour points. Each subbasin was characterized by eight explanatory variables: drainage area, average basin slope, average basin elevation, percentage of basin area above 2,250 m, dominant basin aspect, lithologic rippability, landcover and average annual precipitation. For each subbasin, the spring pulse onset, peak and end of annual streamflow were used as response variables.

Weighted least squares regression identified multiple significant ($\alpha < 0.01$) relationships between the explanatory variables and response variables. The analyzed explanatory variables were able to explain variance amongst the response variables, suggesting that geologic and geomorphic variables are significant in determining montane streamflow regimes. For all 45 subbasins, the model suggests with a level of significance greater than 0.99, that 83 percent of the variance of the average onset date of the spring pulse can be explained by the eight explanatory variables, 76 percent of the variance of the average date of peak flow, and 72 percent of the variance of the date at which streamflow ends, or substantially declines (Figure 23, Table 14).

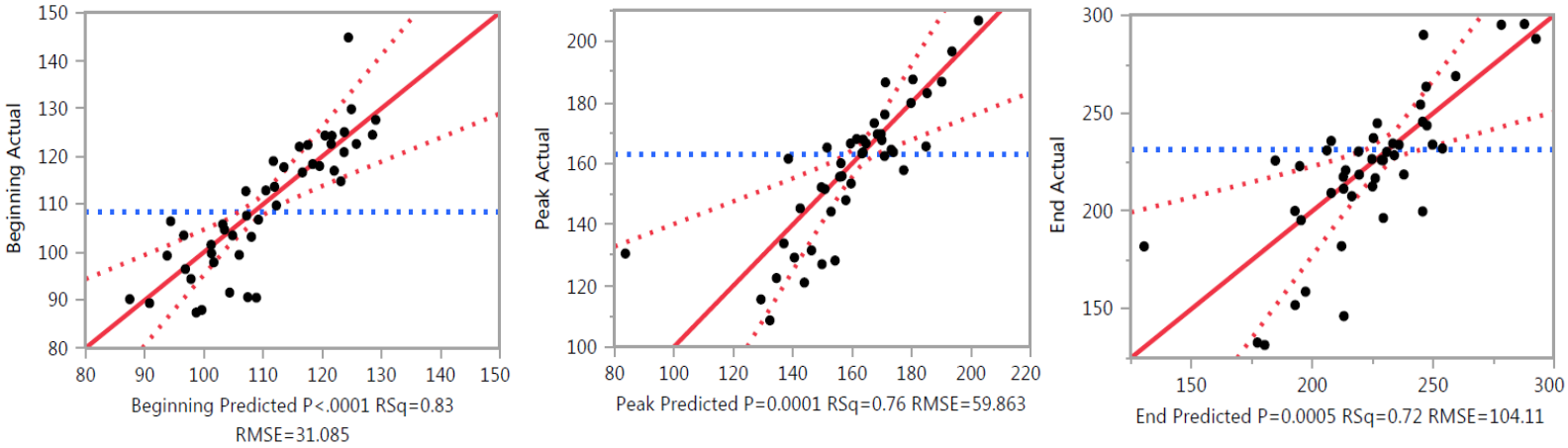

Figure 23: Actual by predicted plots for beginning, peak and end of annual streamflow using all eight explanatory variables. The mean of the response is demonstrated by the blue-dotted-line, and the limits of the 0.90 confidence intervals are represented by the red-dotted-lines.

Table 14: Coefficients of determination for individual model outputs for models including all 45 subbasins and all eight explanatory variables**.**

Model	R^2	Adjusted R^2	Mean	RMSE	P-value
Beginning	0.83	0.73	108	31	P < 0.0001
Peak	0.76	0.61	163	60	P = 0.0001
End	0.72	0.55	232	104	P = 0.0005

In analyzing individual effects tests of each explanatory variable, the most influential explanatory variables for the beginning of annual streamflow are drainage area and the percent of the subbasin above 2,250 m, with p-values of 0.048 and 0.015 respectively (Figure 24). Although less statistically significant ($\alpha > 0.05$), average elevation was also relatively influential, with a p-value of 0.09.

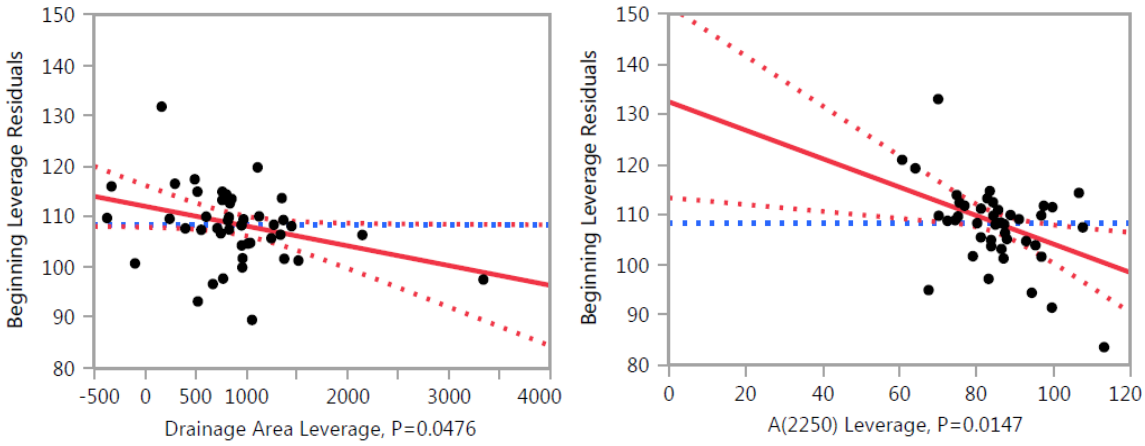

Figure 24: Individual leverage plots for the effects of drainage area and the percentage of area above 2,250 m elevation on the timing of spring pulse onset. The mean of the response is demonstrated by the blue-dotted-line, and the limits of the 0.90 confidence intervals are represented by the red-dotted-lines.

In addition to elevation, multiple less significant variables were seen to have influential effects on the timing of the onset of the spring pulse. For example in analyzing the least squares means results (Table 15) for the rippability index leverage plot, it can be seen that subbasins characterized as being marginally rippable on average have an onset of the spring pulse approximately ten days later than subbasins characterized as having a rippable lithology. Similarly, in analyzing the least squares

means results (Table 16) for the landcover leverage plot, on average, streamflow begins approximately twenty days later for subbasins characterized as alpine/forested when compared to subbasins characterized by dominantly scrub landcover.

Table 15: Average number of days at which spring pulse onset begins for subbasins of varying lithologic rippability

Rippability	Standard Error	Mean Spring Pulse Onset (No. of days after 1 Jan)
Marginally Rippable	5.86	114
Non-rippable	5.87	113
Rippable	3.59	103

Table 16: Average number of days at which spring pulse onset begins for subbasins of varying landcover.

Landcover	Standard Error	Mean Spring Pulse Onset (No. of days after 1 Jan)
Alpine/ Forested	4.65	122
Alpine	12.76	118
Forested	2.79	107
Scrub	4.98	103

Individual effects tests suggest that the most influential explanatory variables for the date at which streamflow peaks are average subbasin elevation, the percent of the subbasin above 2,250 m, and average annual precipitation, with p-values of 0.006, 0.001, and 0.002 respectively (Figure 25). Dominant aspect was less significant ($\alpha < 0.05$), with a p-value of 0.01.

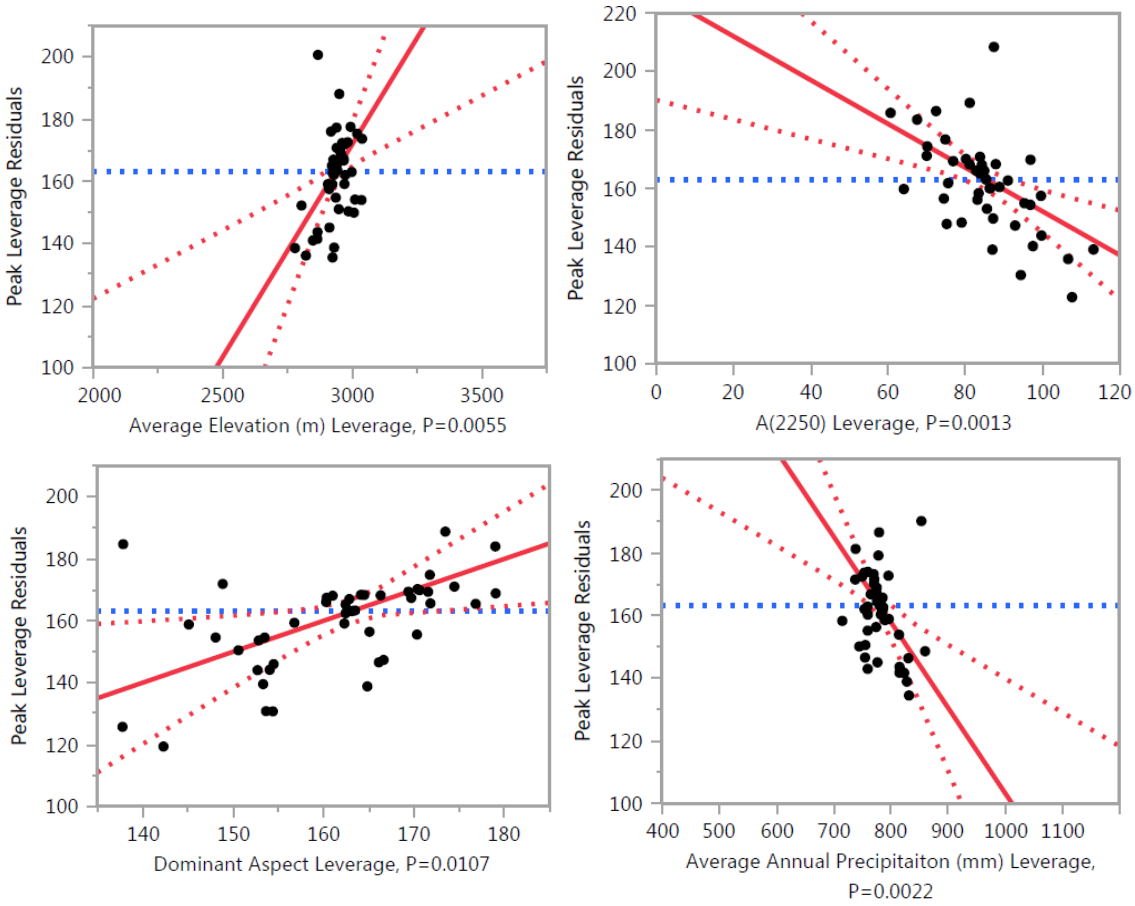

Figure 25: Individual leverage plots for statistically significant watershed characteristics. The average effects of average subbasin elevation, the percentage of area above 2,250 m elevation, average annual subbasin precipitation, and dominant subbasin aspect on the timing of peak streamflow are demonstrated by the solid red line. The mean of the response is demonstrated by the blue-dotted-line, and the limits of the 0.90 confidence intervals are represented by the red-dotted-lines.

In comparison to the first two models, fewer variables were found to be significant when predicting the timing of the decline of streamflow. Individual effects tests suggest that the most influential explanatory variable for the date at which streamflow declines is the dominant aspect, with a corresponding p-value of 0.03 (Figure 26).

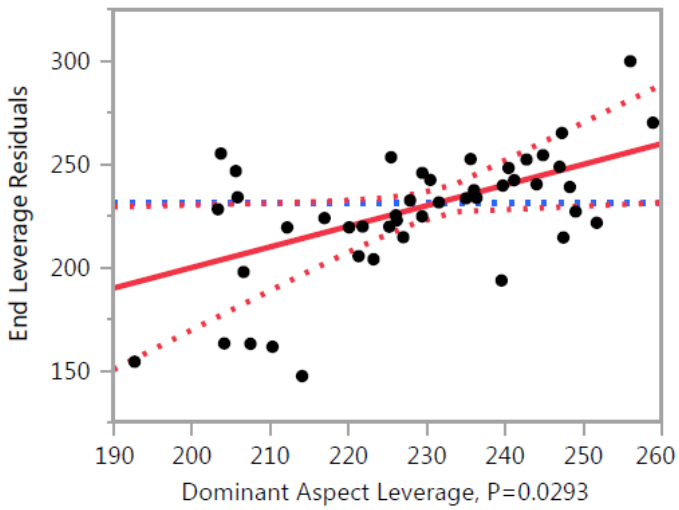

Figure 26: Individual leverage plot for the effects of dominant aspect on the average timing of the date at which streamflow ends or substantially subsides. The mean of the response is demonstrated by the blue-dotted-line, and the limits of the 0.90 confidence intervals are represented by the red-dotted-lines.

In analyzing the results of the least squares means of the individual cardinal and intercardinal aspect directions, some aspects have more of an effect than others (Table 17). Subbasins with predominantly northern facing slopes maintain streamflow for an average of approximately forty days longer than subbasins with predominantly southern facing slopes, and approximately sixty days longer than subbasins with predominantly eastern facing slopes (Table 17).

Table 17: Average number of days at which streamflow ends for subbasins of varying aspect.

Aspect	Standard Error	Average number of days at which streamflow ends (No. of days after 1 Jan)
N	12.81	252
NE	40.85	246
NW	13.54	231
S	18.09	224
SW	23.51	214
SE	24.04	195
W	18.13	192
E	20.12	191

The individual effects test for all eight parameters for each the three models can be best understood in analyzing Table 18. In general, the percentage of subbasin area above 2,250 m elevation and aspect have the most influence on the overall timing of montane streamflow regimes. When considering the timing of individual streamflow, however, specific variables may be more significant for one event than another.

Table 18: Statistical significance of individual parameter effects for each streamflow. (Levels of significance: * $\alpha = 0.05$; ** $\alpha = 0.01$)

Variable	Beginning	Peak	End
	Probability > F		
Drainage Area	0.0476 *	0.9222	0.9026
Average Slope	0.7577	0.1405	0.0910
Average Elevation	0.0944	0.0055 **	0.4121
$A_{2,250}$	0.0147 *	0.0013 **	0.0583
Dominant Aspect	0.7091	0.0107 *	0.0293 *
Rippability Index	0.2098	0.9805	0.9245
Landcover	0.5319	0.6913	0.1961
Average Annual Precipitation	0.9912	0.0022 **	0.1560

Discussion and Conclusions

Changes in the timing and volume of montane streamflow regimes are typically attributed to earlier snowmelt and the reduction of snow pack (Tague, 2009; Viviroli et al., 2011). Although snow accumulation and melt are the primary hydrologic inputs from a montane streamflow perspective, several other first-order controls affect the spatial variability of the hydrologic response to weather phenomena (Jasper, 2004; Tague, 2008, 2009; Uhlenbrook, 2005, Viviroli et al., 2011). Considerable research (Jasper, 2004; Tague, 2008, 2009; Uhlenbrook, 2005, Viviroli et al., 2011) has shown that hydrographs for montane streams are significantly affected by geologic controls. Such geologic factors, however, are rarely considered first-order controls on spatial variation in the hydrologic response to weather phenomena (Tague, 2008). Spatial differences in geologic and geomorphic controls may have an equally significant influence on the response of streamflow as does the spatial relationship associated with the accumulation and melt of snow.

To provide a better overall picture of how stream-flow in a specific region will be affected by weather phenomena, it is crucial to understand all processes involved. To date, the majority of research concerned with determining future stream-flow has focused primarily on climate-mediated changes in snowpack and regimes of melt (Tague, Grant, 2009). A better understanding of the impact of relevant geologic controls would help to improve assessments of the impacts of weather phenomena on stream-flow.

The research presented in this paper focused on determining if geology and geomorphology have a significant effect on the timing of montane streamflow regimes; more specifically, if drainage area, slope, elevation, aspect, lithology, and landcover have a significant effect on the timing of spring pulse onset, the peak and the end of annual streamflow. Weighted least squares (WLS) regression was used to identify significant relationships between geologic and geomorphic variables and timing of streamflow. Multiple highly significant correlations were observed, suggesting that the inclusion of geologic and geomorphic watershed characteristics in hydrologic analyses would be beneficial. The results from this research should be used to improve understanding of changing streamflow regimes in an effort to make critical decisions by water resource managers more efficient and effective. By determining which watershed characteristics are most influential for changing flow regimes, it is possible to identify specific subbasins that are more vulnerable to changes in streamflow and plan according to the average changes observed for the corresponding characteristics.

As previously mentioned, many hydrological applications require an accurate and effective means to predict the timing of streamflow regimes. By determining which factors affect streamflow timing, it may be possible to improve estimates. When considering hydrology at a watershed scale, many of the systems and feedbacks are not fully understood (McGlynn, 2004). For example, the effects of drainage area on runoff generation have yet to be explicitly defined (Band, 2000; McDonnel, 2007; McGlynn, 2003). Results from this study indicate, however, that drainage area is one of the most significant of the eight analyzed variables in terms of influencing the onset of the spring

pulse. This finding is significant in the sense that the timing of streamflow is largely related to runoff generation. Thus, knowing that drainage area is critical in determining the timing of montane streamflow regimes could help to identify previously unrecognized linkages between geomorphology and subbasin hydrology. In general, it was observed that as the drainage area of a subbasin increases, the date at which the onset of the spring pulse occurs shifts to earlier in the year. Although statistical analyses did not reveal any significant levels of autocorrelation, this may be an auto-correlative artifact. For example, drainage area may also be highly correlated to another parameter which is known to affect the average date of the onset of the spring pulse. For instance, in the specific regions that were observed, larger subbasins may contain a higher percentage of lower elevation surface area. Such a relationship would certainly affect the date of the onset of the spring pulse as elevation is known to affect the timing of snow melt, which would subsequently affect flow regimes.

As previously mentioned, the relationship between elevation and snowmelt runoff is well understood. This relationship was evident in the highly significant correlation between the percentage of subbasin area above 2,250 m (A_{2250}) elevation and the timing of spring pulse onset. With a greater percentage of a subbasin at higher elevation, snow pack is likely to last longer, resulting in a later onset of the spring pulse. Conversely, with a greater percentage of a subbasin area at lower elevations, snowpack is likely to melt sooner, resulting in an earlier onset of the spring pulse. The effect of A_{2250} had a more significant influence than the average basin elevation on the onset of the spring pulse. The significance of A_{2250} suggests that it may be possible to develop

thresholds at which elevation becomes a critical factor in determining the onset of the spring pulse. The significance of correlation between A_{2250} and the onset of the spring pulse proves that not only meteorological measurements are required to assess changes in flow regimes, but topographic catchment parameters as well.

Subbasin elevation proved to be highly influential in regard to the timing of peak streamflow as well. Peak streamflow, or the time at which fifty percent of annual streamflow has passed, however, was influenced by average subbasin elevation and A_{2250}, with A_{2250} being slightly more significant. The dominant subbasin aspect was also determined to be influential in determining the timing of peak flow. In the northern hemisphere, northern slopes receive less solar exposure than slopes with other aspects (Dettinger, Cayan et al. 1998; Lehning 2006; Resler 2006; Kunkel, Palecki et al. 2007; Elliott and Kipfmueller 2010; Rittger, Kahl et al. 2011). As a result, northern facing slopes are able to maintain snowpack for longer, leading to a later peak streamflow in subbasins dominated by northern facing slopes. The opposite effect is true for subbasins with predominantly south facing slopes. With constantly improving spatially explicit digital elevation models, it is becoming increasingly easier to make detailed measurements of parameters, such as elevation and aspect, for study areas ranging from subbasin scale to watershed scale. In knowing that such topographic information is significant in determining the timing of peak streamflow, and being able to readily access detailed and accurate aspect information, including such variables in hydrological assessments would likely improve effectiveness.

Being able to predict the average time that montane streamflow will end, or significantly decline is imperative for many water resource applications. Because montane watersheds are often very complex and spatially diverse, it is often difficult to determine how processes and characteristics upstream may affect flow regimes downstream. The research in this study found that fewer of the analyzed predictor variables had an effect on the timing of the end of streamflow than on the beginning or peak. This result is not necessarily surprising considering that by the time average annual streamflow typically subsides (mid-to-late summer), a majority of snowmelt has already occurred. Because snowmelt is the primary source for montane streamflow, it is logical that the parameters that are known to affect the rate and timing of snowmelt (i.e. elevation and aspect) would have less of an effect. Linear regression determined, however, that the most influential predictor variable for the date at which streamflow ends is the dominant subbasin aspect. More specifically, north facing subbasins were seen to be most significant. This could possibly be because aspect is related to rates of evaporation. In the mid-to-late summer, south-facing slopes may lose more water to evaporation, and contribute less water to streamflow. The significance of aspect could also be related to a rain shadow effect. In the region of interest, most summer precipitation comes from the east. If windward slopes receive the majority of this precipitation, then aspect would likely cause spatial variations in summer streamflow patterns.

Of the eight selected parameters, several did not prove to be significant ($\alpha = 0.01$), but can still be determined as relatively influential. For example, when

considering the timing of the onset of the spring pulse, subbasins characterized as having non-rippable lithology were seen to have a noticeable effect. This is likely because non-rippable lithology does not promote infiltration, so a higher percentage of precipitation is contributed to streamflow. In comparing the significance of slope between the three streamflows, slope is increasingly more significant later in the year; (i.e. slope has less of an effect on the onset of the spring pulse, and more of an effect on streamflow subsidence) this is likely because of the relationship between rates of runoff and type of precipitation. Slope is not nearly as influential in determining the rates of runoff when the dominant type of precipitation is snow, as compared to when the dominant type of precipitation is rain (Hay and McCabe 2002; Dahlke, 2009). This could possibly explain why slope is less influential earlier in the year when the main streamflow contribution is snowmelt as compared to rain which occurs later in the year.

Earlier snowmelt and streamflow are likely to be an increasingly challenging problem for many water resource management systems. With changing weather phenomena, snowmelt dominated streams are becoming less predictable and less reliable. Although the complex nature of montane hydrologic systems is not fully understood, the ability to characterize which watershed characteristics significantly impact streamflow regimes is a crucial step towards understanding future changes and the vulnerability of water resources. The research presented in this study was able to develop the following general conclusions: 1) Geology and geomorphology have a significant effect on the timing of montane streamflow regimes. 2) Drainage area and the percentage of a subbasin over 2,250 m elevation are highly significant in determining the

timing of the beginning of montane streamflow. 3) Average subbasin elevation, the percent of the subbasin above 2,250 m, dominant aspect, and average annual precipitation are highly significant in determining the date at which 50 percent of annual streamflow is achieved. 4) Dominant aspect is highly significant in determining the date at which annual streamflow significantly subsides. Although regionally specific, these conclusions suggest that geological and geomorphic characteristic should be considered when assessing streamflow in montane regions. It is likely that similar characteristics would be significant for other montane regions.

CHAPTER IV

THE INFLUENCE OF SPATIAL VARIATIONS ON THE FREQUENCY AND MAGNITUDE OF LOW STREAMFLOW

Synopsis

In the western United States, limited availability of fresh water coupled with growing agricultural and urban demands are causing large urban locations to be heavily dependant on montane water resources as supplemental sources of water supply. Unfortunately, montane water resources are delicate and highly dependent upon persistent weather and climatic conditions. With current research indicating dramatic changes from climate warming, water resources in montane areas are approaching excessive liability. The problem of reduced water resources is being accelerated by the decreasing volume of readily available fresh water and population increasing. Thus, predicting the impact of weather trends and variability on water resources is necessary to ensure that demands for water for irrigation and municipal water supply can be met.

Changes in the timing and volume of montane streamflow regimes are typically attributed to earlier snowmelt and the reduction of snow pack. Although snow accumulation and melt are the primary hydrologic inputs from a montane streamflow perspective, several other first-order controls affect the spatial variability of the hydrologic response to weather phenomena. Considerable research has shown that hydrographs for montane streams are significantly affected by geologic controls. Such geologic factors, however, are rarely considered first-order controls on spatial variation

in the hydrologic response to weather phenomena. Spatial differences in geologic and geomorphic controls may have an equally significant influence on the response of streamflow as does the spatial relationship associated with the accumulation and melt of snow. To understand the hydrologic response related to weather phenomena in montane regions, it is necessary to ask: Do weather phenomena and spatial variations in geology, and geomorphology reduce or shift the timing and volume of montane streamflow regimes?

Weighted least squares (WLS) regression was used to identify significant relationships between geologic and geomorphic variables and low streamflow characteristics. The Uncompahgre River watershed (URW), San Miguel River watershed (SMRW) and Animas River watershed (ARW) were each divided into multiple gauged subbasins, which were delineated using USGS stream gages as pour points. A total of forty-five subbasins, within the three watersheds were analyzed. Each subbasin was characterized by eight explanatory variables: drainage area, average basin slope, average basin elevation, percentage of basin area above 2,250 m, dominant basin aspect, lithologic rippability, landcover and average annual precipitation. For each subbasin, the average monthly frequency and discharge of low streamflows were used as response variables.

For all forty-five subbasins, the model suggests with a level of significance greater than 0.99, that on average, 69 percent of the variance associated with average number of monthly low streamflows can be explained by the eight explanatory variables. At a level of significance greater than 0.95, the chosen explanatory variables were able

to explain approximately 67 percent of the variance associated with average monthly low streamflow discharge. The results from this research suggest that the inclusion of geologic and geomorphic watershed characteristics in hydrologic analyses would be beneficial. Such knowledge should be used to improve understanding of changing streamflow regimes in an effort to make critical decisions for water resource management more efficient and effective.

Introduction

When considering the impact of weather on streamflow, changes in the patterns of streamflows have typically been attributed to earlier snowmelt and the reduction of snowpack (Tague, 2009; Viviroli et al., 2011). Although snow accumulation and melt are the primary hydrologic inputs from a montane streamflow perspective, several other first-order controls affect the spatial variability of the hydrologic response to weather phenomena (Jasper, 2004; Tague, 2008, 2009; Uhlenbrook, 2005, Viviroli et al., 2011). Spatial differences in geologic and geomorphic controls may have an equally significant influence on the response of streamflow as does the spatial relationship associated with the accumulation and melt of snow.

Spatial differences in lithology and land cover have the potential to affect the drainage system in a region, thus, affecting the temporal response of the streamflow (Tague, 2008, 2009). Similarly, topographic and geomorphic controls, such as slope, aspect, elevation, and landcover also have the potential to affect the input pathway of runoff to streamflow. By understanding the affects of such spatial differences on the

relationship between drainage systems and streamflow, it may be possible to better understand the hydrologic response to weather phenomena that can occur in montane regions.

Research (Nolin, 2012; Nydick, 2012; Rangwala, 2011) has been conducted on topics relating to the effects of climate change on streamflow; however, little attention has been focused on how spatial variations in geology and geomorphology may potentially control the impact of weather phenomena on streamflow in montane drainage basins. The next level of research must focus on this aspect. One can ask: Do weather phenomena and spatial variations in geology, and geomorphology reduce or shift the timing and volume of montane streamflow regimes?

In the western United States, limited fresh water availability coupled with growing agricultural and urban demands are causing large urban locations to be heavily dependant on montane water resources as supplemental sources of water supply. Unfortunately, montane water resources are delicate and highly dependent upon persistent weather and climatic conditions. With current research indicating dramatic changes resulting from climate warming, water resources in montane areas are approaching excessive liability. The problem of reduced water resources is being accelerated by the volume of readily available fresh water decreasing and population increasing (Vörösmarty and Vorosmarty 2000). Thus, predicting the impact of weather trends and variability on water resources is necessary to determine if demands for water for irrigation and municipal water supply can be met.

Understanding the frequency and duration of extreme hydrologic events is critical to effective water resource management. Considerable attention has focused on understanding and predicting flood frequency and magnitude (Jarrett and Costa 1988). Relatively little attention, however, has focused on the understanding of low streamflow characteristics. Understanding the nature of low streamflows is becoming increasingly important as the demand for freshwater continues to increase. The research presented in this paper is focused on determining the extent to which spatial variations in geology and geomorphology may affect the frequency and magnitude of low streamflows in montane drainage basins. The results of this paper should help in providing water resource planners a better understanding of which watershed characteristics can be used to describe and predict low streamflows.

As noted by Kroll (2004), knowledge of low streamflows is important for water quantity management, and water quality management as well. Low streamflows greatly influence policy on water use in regions where streamflow provides critical dilution of nonpoint source and point source pollution (Kroll, 2004). For example, the Clean Water Act of 1977 requires all states to provide estimates of low streamflow statistics to renew National Pollution Discharge Elimination System permits. Low streamflow statistics are also used to plan water supply, hydropower, irrigation, and to make decisions regarding allowable basin withdrawals (Kroll, 2004). Furthermore, low streamflow is critical to sensitive ecological systems and aquatic habitats.

Typically, low streamflow statistics are obtained through frequency analysis when sufficient historic record is available (Riggs 1965, 1980). For ungaged streams, or

locations lacking sufficient record, however, regional regression models may be developed (Garen 1992; Griffis and Stedinger 2007). Regional regression techniques require a relationship between low streamflow and watershed characteristics to be developed. In most cases, the standard errors associated with low flow regression models have been relatively high (Vogel and Kroll, 1992; Smakhtin, 2001). Luce (2009) suggests that high standard errors are likely the result of hydrologic relationships being too complex to model with linear regression. Errors in regional regression, however, may also be the result of inadequate characterization of watershed characteristics. The research presented in this paper aims to determine which watershed characteristics are crucial for modeling low flow in montane regions of southwestern Colorado in an effort to improve montane regional regression models.

This research differs from most regional regression modeling studies in that the spatial scale is much smaller and the watershed characteristics are determined using higher resolution data. Most regional regression analyses are focused on determining low flow characteristics for entire states or even the coterminous US as a whole, and, thus, often use spatial data at a resolution up to 1Km (Reilly and Kroll 2003; Capesius, Stephens et al. 2009). The research presented in this paper will model low flows at a subbasin scale, using 3m spatial resolution to derive watershed characteristics. Furthermore, most regional regression studies are limited to the eastern US, in which watershed and weather characteristics are substantially different than those of montane watersheds. It is crucial to have an understanding of the specific systems operating in montane watersheds, as mountain river basins, associated reservoirs, and underlying

aquifers supply water demands for over sixty million people in the western United States (Barnett, 2005; Viviroli et al., 2011).

Description of the Study Area

This study focuses on three adjacent watersheds located in the San Juan Mountains of south-western Colorado: the Uncompahgre, San Miguel, and Animas River Watersheds (Figure 27). These watersheds are most suitable for this study because they represent varying hydrologic, geologic and geomorphic conditions, and have sufficient periods of record. The geographic orientations of the three watersheds are ideal for making comparisons in terms of how slope, aspect and elevation may control changes in stream-flow. Although all three watersheds are adjacent, the main river reaches of each watershed flow in contrasting directions and have significantly different slopes and surface lithology.

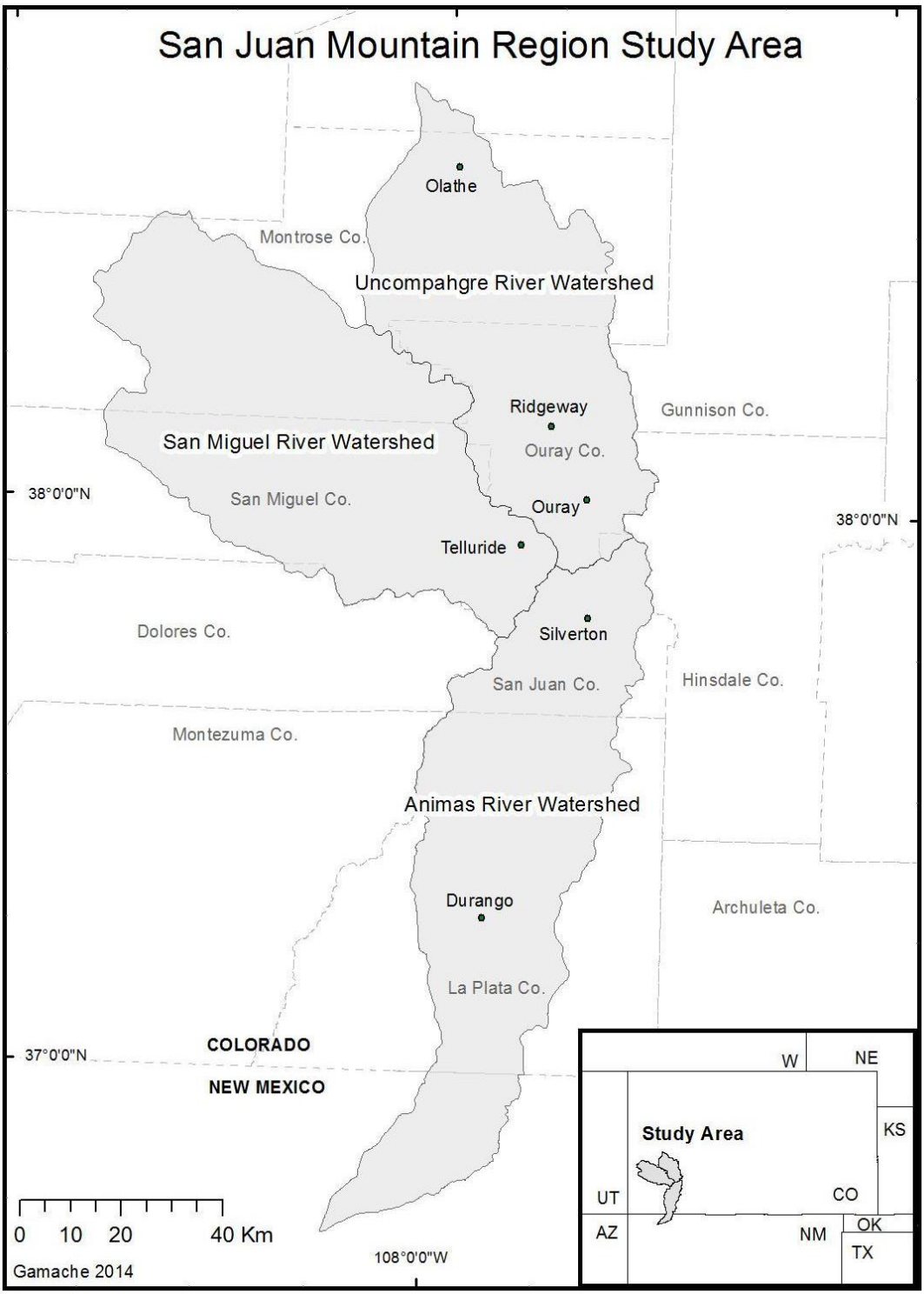

Figure 27: Location of study area for Objective 3. The Uncompahgre (HUC: 14020006), Animas (HUC: 14080104), and San Miguel (HUC: 14030003) River watersheds, located in the San Juan Mountains of southwestern Colorado, USA.

The Uncompahgre River flows to the north with an average slope of one degree, and in general is much steeper than the Animas River which flows to the south with an average slope of 0.5 degrees. The San Miguel River, which flows to the west, is characterized by a much more variable profile, with high relief stream channels in the headwaters, and more a more shallow relief at lower elevations, in comparison to the Uncompahgre and Animas Rivers (Figure 28).

These watersheds are ideal for stream-flow analyses because they are considered by the Hydro-Climate Data Network (HCDN) as having minimum anthropogenic influences (diversions, dams, reservoirs) (Slack & Landwehr, 1994). Thus, stream-flow records can be interpreted as natural flows. The San Miguel River is well known as one of the last free-flowing rivers in the U.S., making it ideal for hydrologic analysis.

To date, the majority of hydrological research focused on the Uncompahgre River, San Miguel River, and Animas River watersheds is concerned with impaired water quality as a result of historic mining activity. In recent years, however, research of the San Juan Mountains (Rangwala, 2010, 2011) has focused on how changing weather phenomena will affect the volume of stream-flow, with the primary concern being the affects on ecological systems. No available research has focused on the reduction of, and shift in peak timing of stream flow with respect to weather phenomena, geologic and geomorphic spatial variations, for this study area.

Figure 28: Variable topographic relief of the SMRW. The San Miguel River is characterized by high relief headwaters, as seen in the photograph on the left, and a much lower relief further down stream, as seen in the photograph on the right.

Uncompahgre River Watershed

The Uncompahgre River Watershed (Hydrologic Unit Code (HUC): 14020006) (38° N, 107° W) is located in the San Juan Mountains of south-western Colorado, USA (Figure 29). From north to south, the Uncompahgre River Watershed spans Delta, Montrose and Ouray counties, draining 2,888 km^2 (Nydick, 2012). The Uncompahgre River flows to the north, with the headwaters beginning near Ouray and flowing through Olathe where it joins the Gunnison River. In total, the Uncompahgre River flows approximately 120 km with a total elevation loss of approximately 2,100 m, resulting in a relatively steep gradient. The Uncompahgre River Watershed contains one storage

dam and approximately 30 known diversion dams to supply irrigation water to over 26,000 hectares in Delta, Gunnison, and Montrose counties (Uncompahgre Watershed Partnership, 2012). As previously mentioned, according to the Hydro-Climate Data Network (HCDN), the stream-flow for the Uncompahgre River is considered to be representative of natural flows. Natural streamflow is considered as streamflow having less than ten percent of the mean-annual streamflow volume affected by anthropogenic activity (Kircher, 1985).

The topography of the Uncompahgre watershed is highly varied, ranging from alpine and sub-alpine landscape, to grassland, agricultural land, and barren desert (Figure 29). This variable topography results in unique and extremely variable patterns of temperature and precipitation. The weather varies substantially between the southern and northern parts of the watershed because of the significant differences in elevation and landscape features (Nydick, 2012).

Landscape features are defined as orographic or landcover characteristics that have the potential to influence weather patterns (Nydick, 2012). The climate in the northern, lower elevation region of the watershed is semi-arid with a low relative humidity. Precipitation is less than 25 cm/yr (Uncompahgre Watershed Partnership, 2013). The maximum monthly rainfall usually occurs in August (28 mm) and reflects the influence of summer, convection thunderstorms (Uncompahgre Watershed Partnership, 2013). Winters at lower elevations are relatively mild when compared to winters at higher elevations, with occasional snowfall, and summers are hot and dry. Average temperatures range from -2°C in the winter to 32°C in the summer (Uncompahgre Watershed Partnership, 2013).

Above 2,250 m, the mountainous conditions result in an increase in precipitation and cooler temperatures. Annual precipitation averages over 76 cm in the high mountains, with 350 cm of snow in Ouray each year (Uncompahgre Watershed Partnership, 2013). Average monthly snowpack is greatest in March and April. Temperatures range from -12°C in the winter to 27°C in the summer (Uncompahgre Watershed Partnership, 2013).

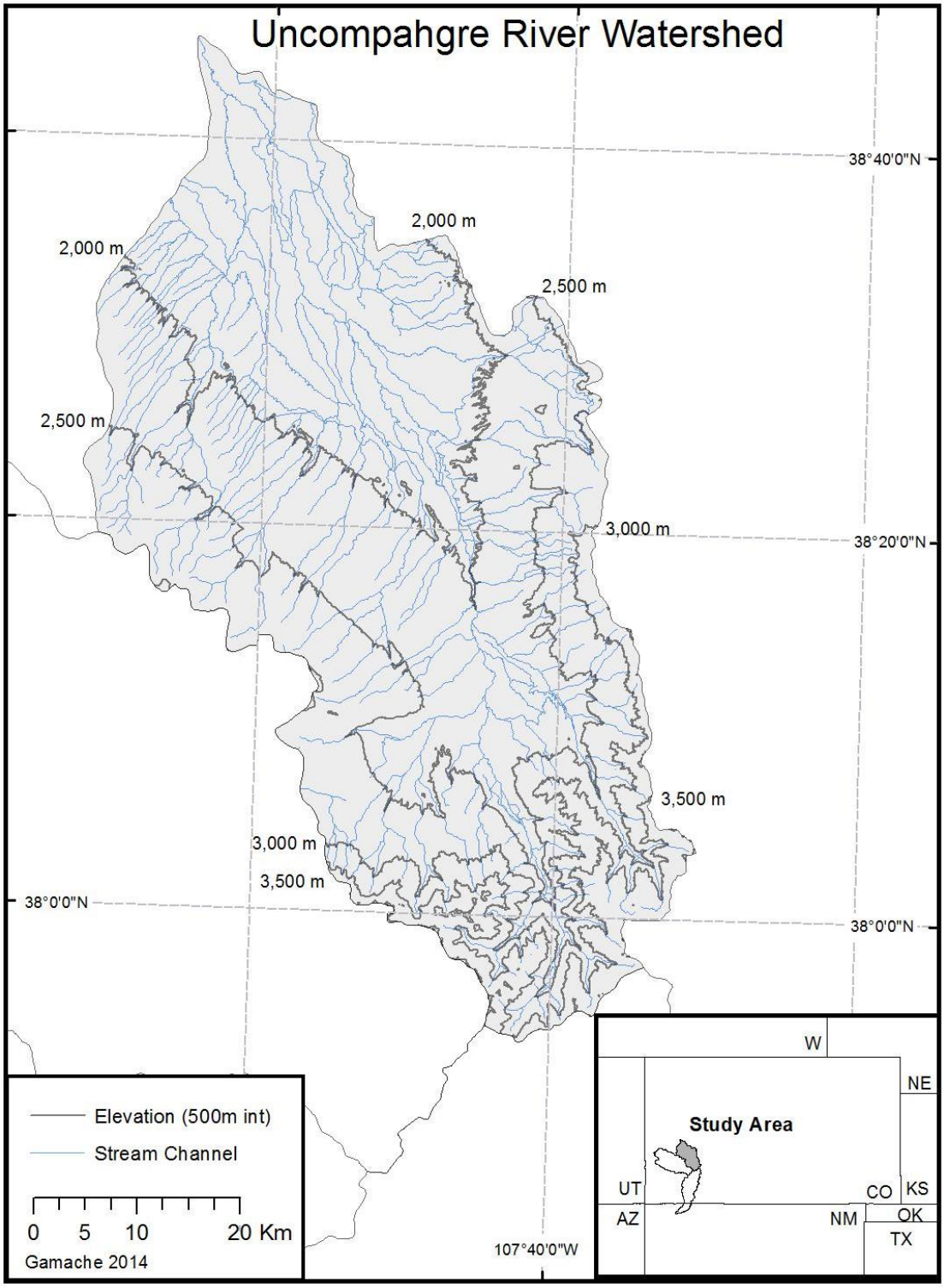

Figure 29: URW topography and stream network for Objective 3.

The Uncompahgre Watershed covers portions of two distinct physiographic regions: the Southern Rocky Mountains south of Ridgway and the Colorado Plateau to the north (Blair, 1996). Differences in geology, landscape and climate between the regions create varying hydrologic conditions. The San Juan Mountains are a mixture of pre-Cambrian metamorphics with mid-Tertiary Andesitic volcanic intrusions (Figure 30) (Uncompahgre Watershed Partnership, 2013). Soils of the valley range in age from recent alluvial deposits in the flood plains to the well-weathered soils of higher terraces and benches. The alluvial deposits contain relatively coarse, unconsolidated and stratified soils of poorly graded, well-sorted sand and gravel derived from igneous and sedimentary rock formations (Uncompahgre Watershed Partnership, 2013).

Evidence of the glacial activity that sculpted the Uncompahgre River valley is still visible in the wide valley floor at Ridgeway. When the glaciers melted at the end of the Pleistocene, approximately 10,000 years B.P., valley train deposits filled the U-shaped valley bottom between Ouray and Ridgway, flattening the valley floor (Blair, 1996).

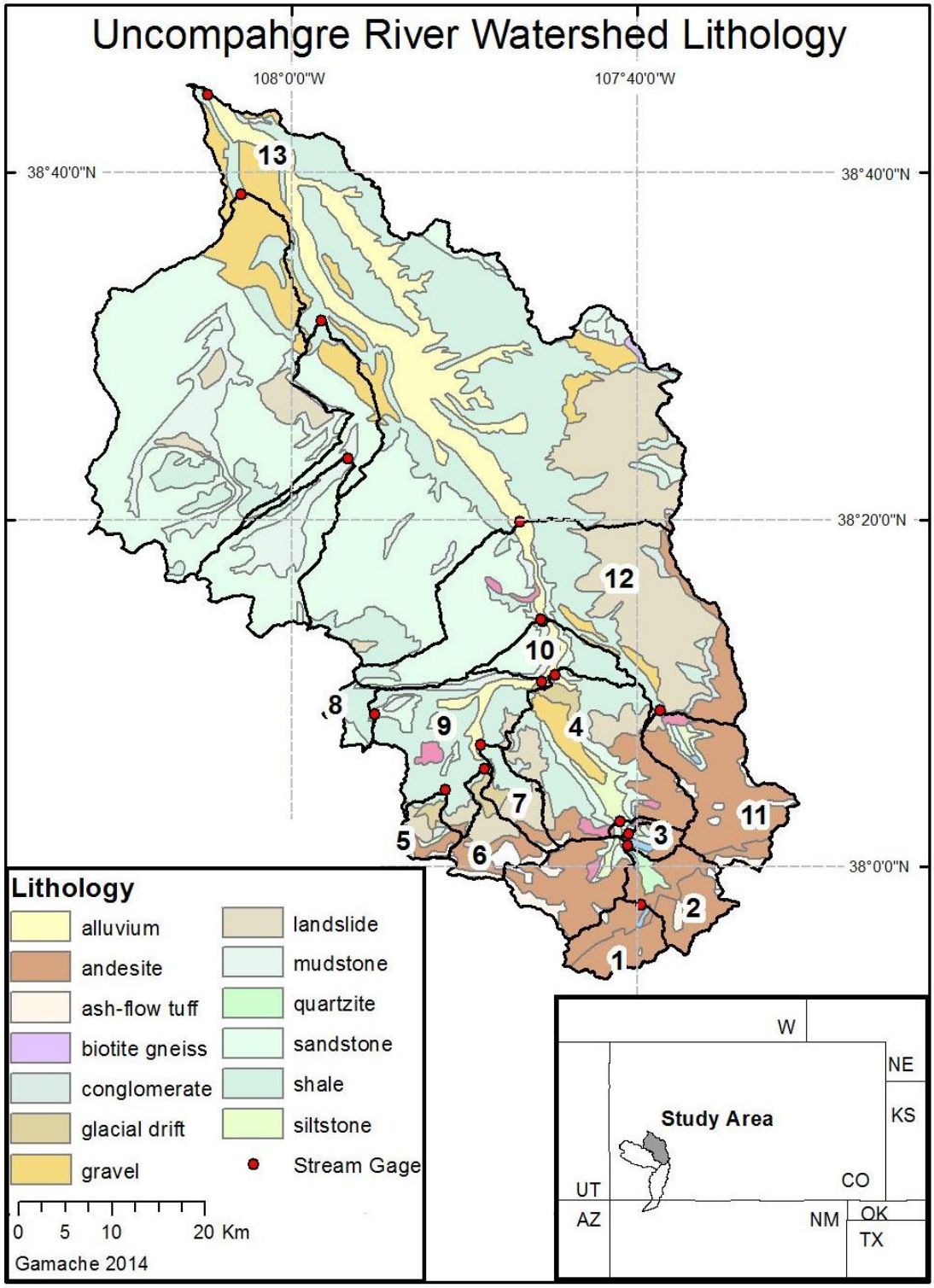

Figure 30: URW surface lithology and subbasin delineations for Objective 3. Numbered subbasins correspond to data in Table 19. Lithologic data provided by USGS.

Groundwater in the Uncompahgre River Watershed is directly related to the local geology. Sedimentary rock aquifers are shallow and have highly variable yields. Hydraulic properties of igneous aquifers vary considerably as the result of differences in type of rock, density and orientation of joints and fractures (Uncompahgre Watershed Partnership, 2013).

The ecological setting of the Uncompahgre River Watershed is a reflection of its diverse geology, topography, climate and landuse (Watershed Partnership, 2013). Landcover in the Uncompahgre River Watershed consists of a mix of range/grassland (44%), forested land (36%), and cropland (13%); approximately 5% of the land is classified as "rock or barren" (NRCS, 2009). Less than one percent of the watershed is residential/commercial (NRCS, 2009). Landcover is critical in determining the amount of and rate at which surface runoff enters a stream system. Variable landcover results in significantly different streamflow response throughout the watershed.

Animas River Watershed

The Animas River Watershed (HUC: 14080104) (37°N, 107°W) is located to the south of the Uncompahgre River Watershed (Figure 31). The Animas River flows from north to south, draining 3,515 km^2. The watershed includes San Juan and La Plata Counties, with the headwaters beginning north of the town of Silverton and passing through the city of Durango, Colorado, flowing as far south as Farmington, New Mexico where it meets the Rio Grande. Elevations range from more than 4,300 m at the headwaters to less than 1,830 m at the confluence with the San Juan River near Aztec, New Mexico.

The climate is highly variable throughout the watershed, with average annual precipitation ranging from 112 cm at the highest elevations to 33 cm at the lowest elevations (Colorado State University, 2008). The primary sources of precipitation in the watershed are winter snowfall and late summer monsoonal thunderstorms. Approximately 40% of the watershed is above 2,250 m, allowing snowpack to accumulate from late fall to early spring (Colorado State University, 2008).

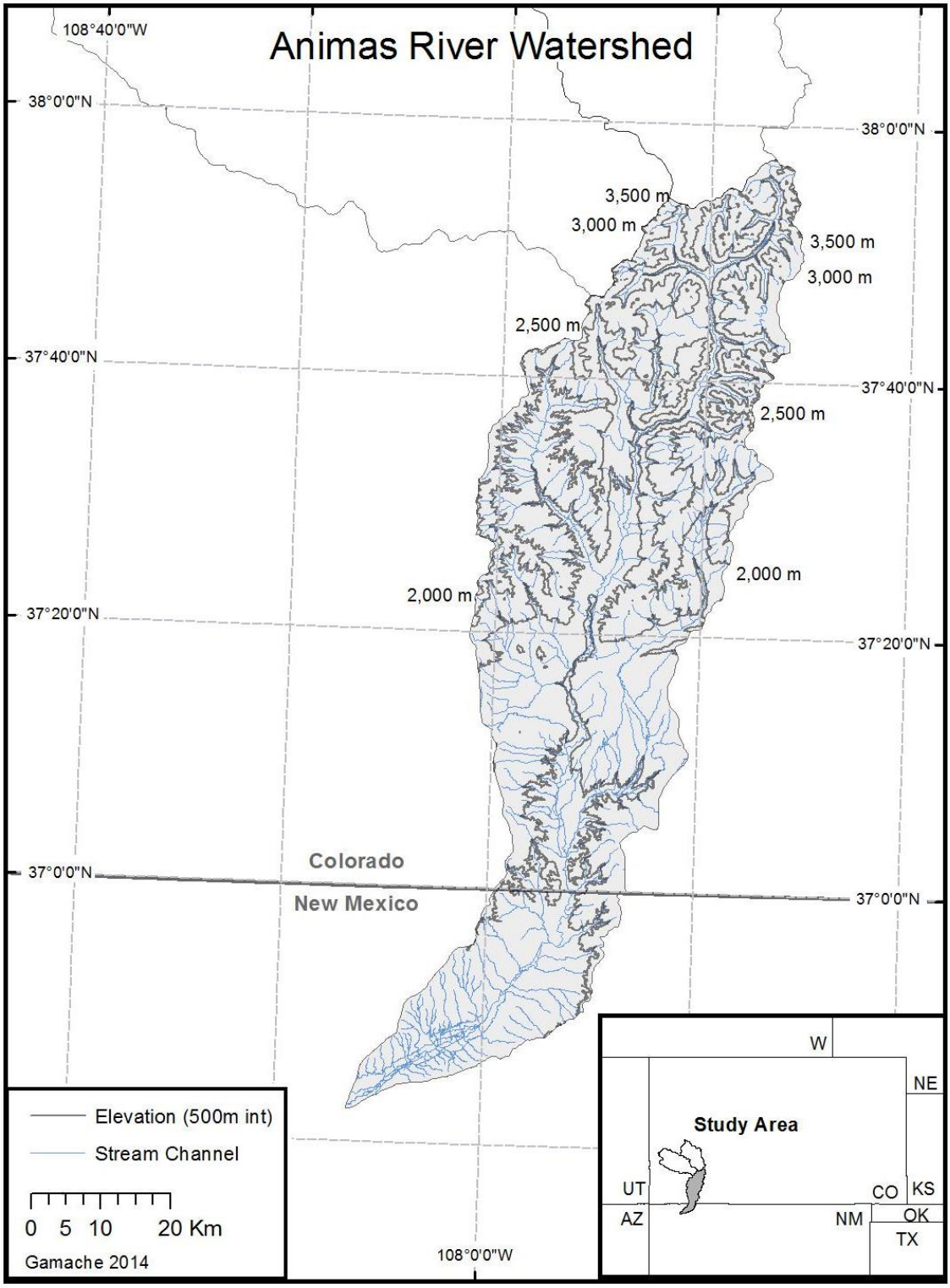

Figure 31: ARW topography and stream network for Objective 3.

The surface lithology is primarily of Precambrian age in the eastern part of the drainage basin, in the Animas Canyon area south of Silverton, with Paleozoic and Mesozoic sedimentary outcrops in the southern part of the drainage basin. The headwaters of the Animas River watershed are underlain by the Tertiary igneous intrusive and volcanic rocks (Figure 32) that formed as a result of late Tertiary episodes of andesitic to dacitic volcanism followed by a later episode of ash-flows, lava flows and intrusions of dacitic to rhyolitic composition (Bush, 1959). This area of the Animas River watershed above Silverton has been extensively fractured, hydrothermally altered, and mineralized by Miocene hydrothermal activity (Casadevall and Ohmoto, 1977).

Similar to landcover, lithology acts as a control to precipitation and runoff. The surface roughness of exposed bedrock determines the rate at which precipitation will be delivered to stream channels, and the degree of fracture of dissection determines the amount of, and rate at which precipitation will enter the groundwater system. All of theses factors affect the timing of streamflow regimes.

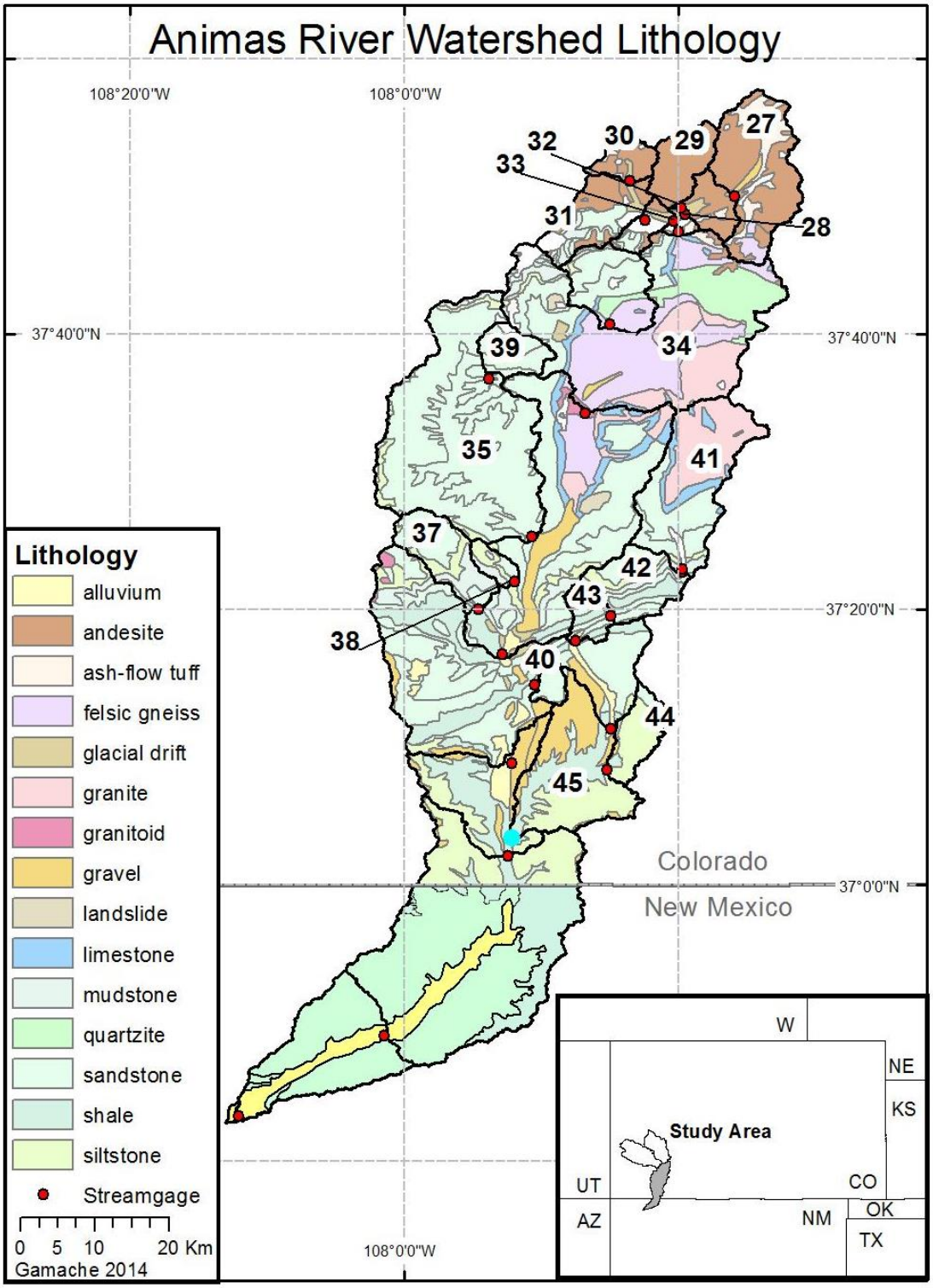

Figure 32: ARW surface lithology and subbasin delineations for Objective 3. Numbered subbasins correspond to data in Table 21. Lithologic data provided by USGS.

Land use for the Animas River Watershed includes 56% forest, 29 % rangeland, 8% agriculture, 5% developed land, 1% water, and less than 1% wetlands and barren land (NRCS, 2009). As previously mentioned, variable landuse and landcover contribute to varying rates of surface runoff. The rate at which surface runoff enters a stream system has a significant influence on the timing of a stream flow regime.

San Miguel River Watershed

The San Miguel River Watershed (HUC: 14030003) (37°N, 107°W), located to the west of the Animas and Uncompahgre watersheds, drains 4,050 km^2 (Figure 33). The watershed includes portions of San Miguel County and western Montrose County. The headwaters begin above Telluride, at elevations above 4,000 m, with the main river channel flows 145 km northwest, to the confluence with the Dolores River. The San Miguel River System is considered one of the few remaining intact river systems in the U.S. (Inyan, 2001). With the exception of the affects of acid mine drainage, very little research has focused on the San Miguel Watershed (Inyan, 2001).

San Miguel River watershed is characterized by predominantly sedimentary rocks of late Paleozoic and Mesozoic age (Atwood, 1932; Bush, 1959). In the southern portion of the watershed the Paleozoic and Mesozoic age sedimentary rocks are covered by younger sedimentary and volcanic rocks, and are intruded by sills and dikes in the Wilson and Dolores Peaks mountain groups, which together form the San Miguel Mountains (Figure 34) (Atwood, 1932; Bush, 1959).

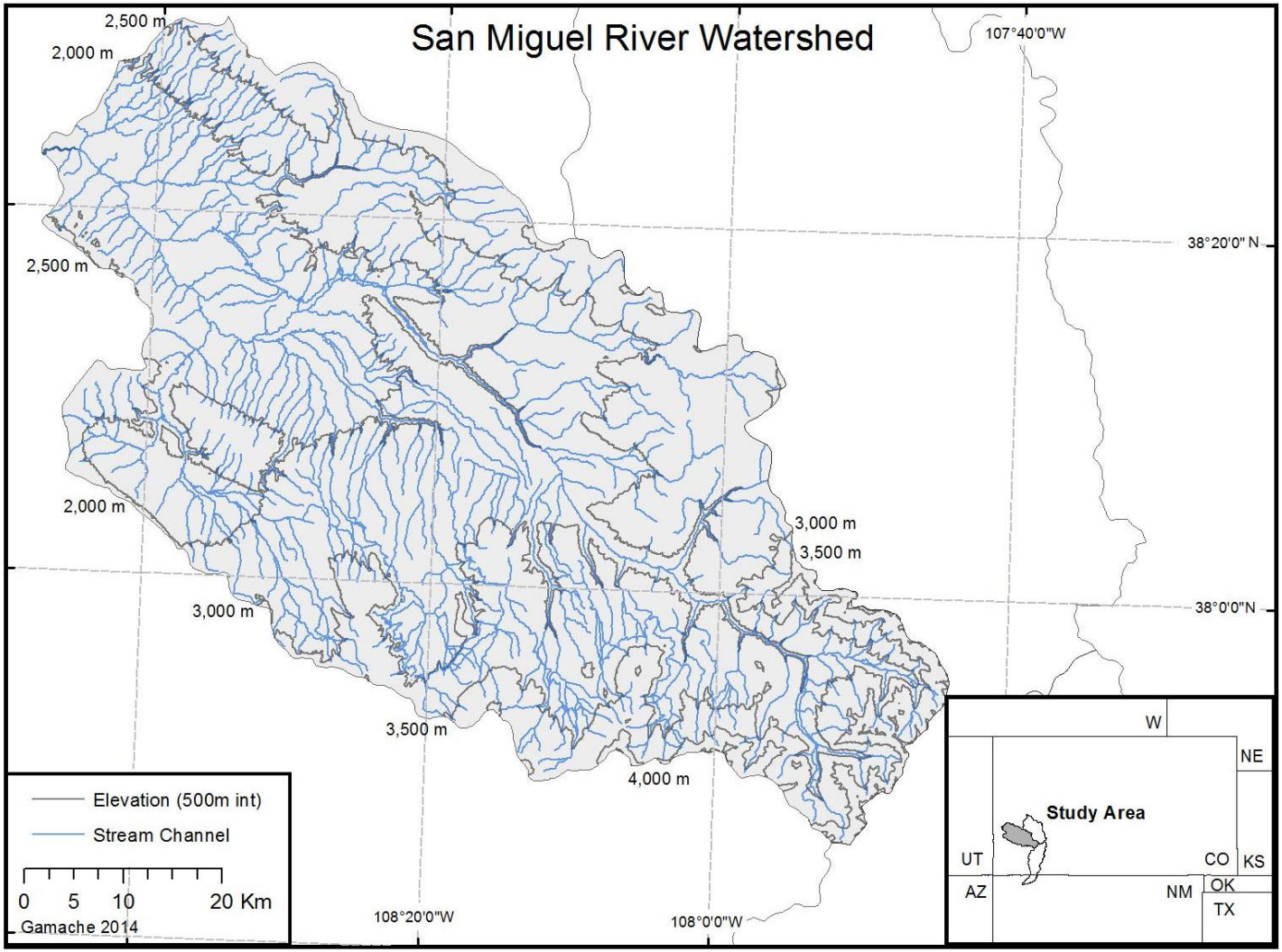

Figure 33: SMRW topography and stream network for Objective 3.

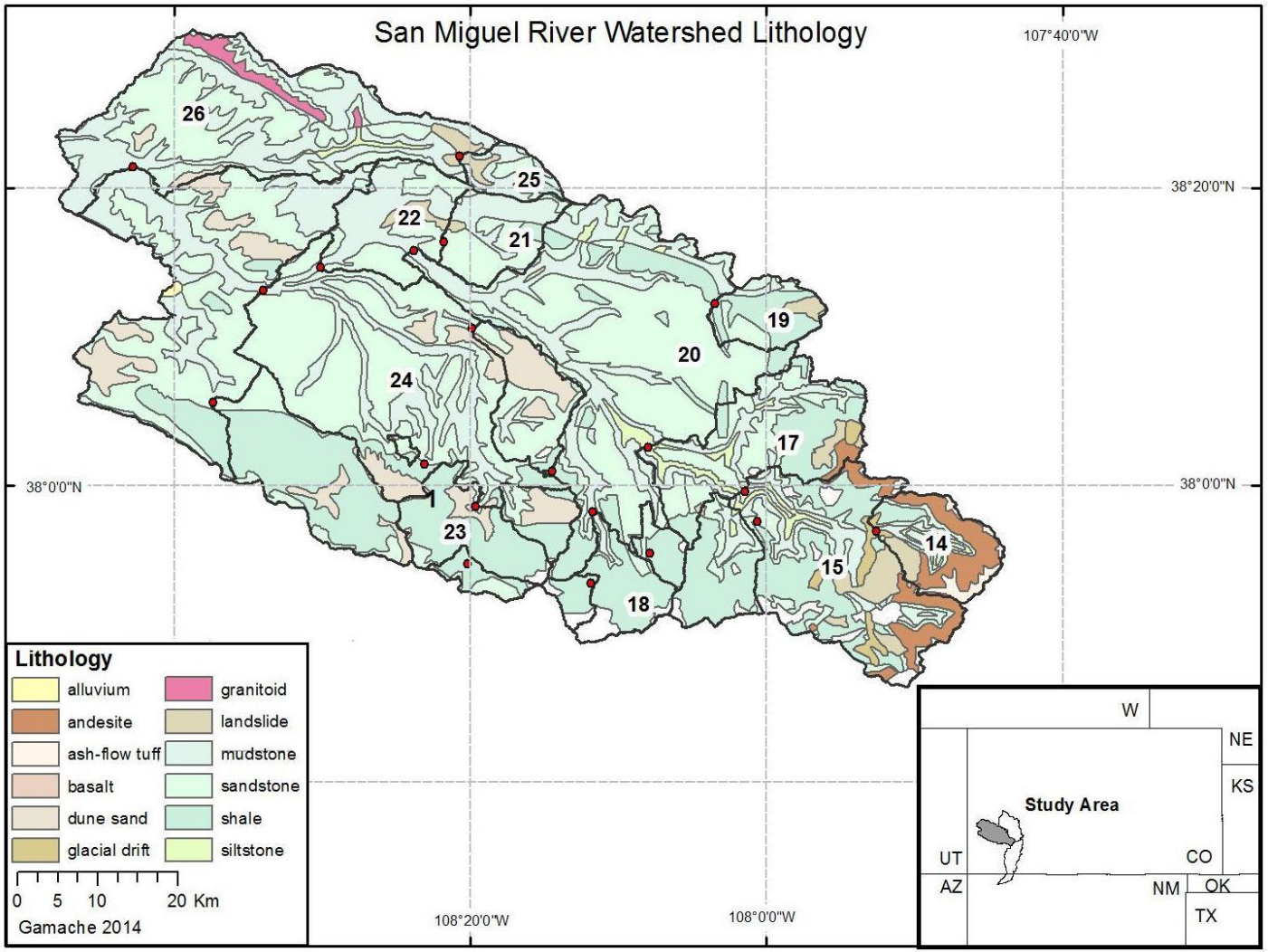

Figure 34: SMRW surface lithology and subbasin delineations for Objective 3. Numbered subbasins correspond to data in Table 20. Lithologic data provided by USGS.

Methods

Weighted least squares (WLS) regression was used to identify significant relationships between geologic and geomorphic variables and the frequency and magnitude of low streamflows. A total of forty-five subbasins, within three watersheds were analyzed with varying periods of record. The Uncompahgre River watershed (URW), San Miguel River watershed (SMRW) and Animas River watershed (ARW) were each divided into multiple gauged subbasins, which were delineated using USGS stream gages as pour points. Each subbasin was characterized by eight explanatory variables: drainage area, average basin slope, average basin elevation, percentage of subbasin area above 2,250 m (A_{2250}), dominant basin aspect, lithologic rippability, landcover and average annual precipitation. For each subbasin, the monthly average low streamflow frequency and monthly average low streamflow discharge were used as response variables. To avoid the influence of frozen streams, only data for April through September were analyzed. Collectively, 1,126 years of streamflow data were used to find the averages of each low streamflow characteristic.

Daily streamflow data for each watershed was obtained through the USGS, Hydro-Climate Data Network (HCDN) (Slack & Landwehr, 1994). The HCDN includes stream-flow measurements with little or no anthropogenic influences (diversions, dams, reservoirs) and are considered to be representative of natural flows. Kircher and others (1985) defined natural streamflow as streamflow having less than approximately ten percent of the mean-annual streamflow volume affected by anthropogenic activity.

Daily-mean streamflow data for each of the three locations were used to calculate the average monthly low flow characteristics. For the purposes of calculating average monthly low streamflow frequency, low streamflow was defined as any daily streamflow value that is less than seventy percent of the corresponding monthly average streamflow. Because high variability exists amongst flow magnitudes, it was necessary to use a percentage of monthly streamflow as a threshold rather than a specific threshold value. The seventy percent value is commonly used as a low streamflow threshold in many ecological studies (Tetzlaff, 2007; Spence, 2010).

Monthly average low flow discharge is defined as the average of the ten lowest monthly streamflows, represented as a percentage of the corresponding average monthly streamflow. This value was calculated as follows: 1) calculate the daily average streamflow, by month, for every year of record 2) divide individual daily flows by the corresponding monthly average flow (This represents the flow on each day as a percentage of the average daily flow for that month) 3) calculate the average percentage for the ten lowest values by month. The decision to calculate the average monthly low streamflow discharge using the ten lowest streamflow percentages is based on the results of the average low flow frequency. For simplification, streamflow data for February 29th in leap years is averaged with data for February 28th, placed in the record for February 28th, and then the leap day was excluded from the analysis. All data processing was completed using R©, an open source statistical computing environment capable of processing large data sets (Team 2005).

As previously mentioned, the three observed watersheds were separated into multiple subbasins which were delineated using USGS stream gages as pour points. Delineation was completed using three meter digital elevation models (DEM) in conjunction with ArcHydro©. Stream networks were created using a channel threshold area method. To achieve the desired level of stream network accuracy and detail, 0.5 ha was chosen as the channel threshold. To provide consistency when comparing subbasins, the 0.5 ha threshold was used for all subbasins. This threshold area is comparable to other studies in similar topographic systems (McGlynn and Seibert, 2003; McGuire et al., 2005). Accuracy of the stream network was determined by comparing results of the threshold area method with stream networks provided by the National Hydrography Dataset (NHD).

The delineated subbasins were characterized by eight physical characteristics that were selected to represent the dominant geologic and geomorphic characteristics; one weather variable was used to make comparisons of relative significance (Tables 19 - 21). The watershed characteristics included: drainage area, average basin slope, average basin elevation, percentage of basin area above 2,250 m, dominant basin aspect, lithologic rippability, landcover and average annual precipitation. These eight parameters were based on the results of previous regional streamflow studies conducted in Colorado and neighboring states (Hortness and Berenbrock, 2001; Hortness, 2006; Waltemeyer, 2006; and Kenney and others, 2007) and on the availability of readily accessible data.

Table 19: URW subbasins for Objective 3. Numbers in far left column refer to subbasin locations in Figure 30.

	Station Number	Latitude (deg)	Longitude (deg)	Years of record	Drainage Area	Average Slope (%)	Average Elevation (m)	A_{2250} (%)	Dominant Aspect	Lithology	Rippability Index	Landcover	Average Annual Precipitation (mm)
1	9144500	37.96	-107.66	8	47	48.4	3475	100	E	Andesite	Non-Rippable	Alpine	1025.40
2	9145000	38.02	-107.68	7	109	53.3	3475	100	N	Andesite	Non-Rippable	Forested	986.03
3	9146000	38.03	-107.68	15	195	58.4	3434	100	NW	Andesite	Non-Rippable	Forested	967.74
4	9146200	38.18	-107.75	54	386	51.4	3170	94.2	NW	Andesite/ Shale	Non-Rippable	Forested	842.26
5	9146400	38.07	-107.85	14	37	38.5	3114	100	NE	Glacial Drift	Rippable	Alpine/ Forested	784.86
6	9146500	38.09	-107.81	14	44	50.3	3334	100	N	Andesite /landslide	Marginally Rippable	Forested	894.08
7	9146550	38.12	-107.82	7	32	34.2	2859	100	N	Shale/ Landslide/ Andesite	Marginally Rippable	Forested	694.18
8	9146600	38.15	-107.92	11	21	11.8	2759	100	E	Shale	Marginally Rippable	Forested	655.32
9	9147000	38.18	-107.76	52	252	28.1	2793	91.4	N	Andesite/ Shale	Non-Rippable	Forested	668.02
10	9147025	38.24	-107.76	25	673	45.9	3036	87.8	N	Andesite/ Shale	Non-Rippable	Forested	784.35
11	9147100	38.15	-107.64	17	118	55.6	3268	100	NW	Andesite	Non-Rippable	Alpine /Forested	855.98
12	9147500	38.33	-107.78	98	1160	42.1	2665	72.6	N	Sandstone/ shale/ Andesite	Rippable	Scrub	669.29
13	9149500	38.74	-108.08	75	2888	21.3	2393	52.1	N	Sandstone/ shale/ Andesite	Rippable	Forested	482.85

Table 20: SMRW subbasins for Objective 3. Numbers in far left column refer to subbasin locations in Figure 34.

	Station Number	Latitude (deg)	Longitude (deg)	Years of record	Drainage Area	Average Slope (%)	Average Elevation (m)	A_{2250} (%)	Dominant Aspect	Lithology	Rippability Index	Landcover	Average Annual Precipitation (mm)
14	9171200	37.94	-107.87	5	111	53.3	3414	100	W	Andesite/ Sandstone	Marginally Rippable	Alpine/ Forested	933.95
15	9172000	37.96	-108.01	17	87	31.2	3060	100	W	Shale	Marginally Rippable	Forested	815.34
16	9172100	38.1	-107.92	7	23	23.1	2917	100	W	Shale	Marginally Rippable	Forested	686.05
17	9172500	38.04	-108.13	72	803	37.6	3031	99	NW	Shale/ Sandstone	Marginally Rippable	Forested	769.62
18	9173000	37.97	-108.20	28	105	23.6	3078	100	N	Shale	Marginally Rippable	Forested	872.99
19	9173500	38.20	-108.05	8	75	11.5	2707	100	W	Shale	Marginally Rippable	Forested	632.97
20	9174000	38.26	-108.40	8	1681	27.9	2807	92.4	NW	Sandstone	Rippable	Forested	684.27
21	9174500	38.27	-108.36	8	101	16.1	2330	54.7	W	Sandstone	Rippable	Scrub	500.38
22	9174600	38.24	-108.50	17	1906	26.5	2731	85.3	NW	Sandstone	Rippable	Forested	655.57
23	9175000	37.98	-108.33	16	137	16.9	2648	100	N	Shale	Marginally Rippable	Forested	665.48
24	9175500	38.22	-108.57	51	2769	22.6	2586	73.3	NW	Sandstone	Rippable	Scrub	601.98
25	9176500	38.37	-108.35	6	44	16.8	2731	100	W	Sandstone	Rippable	Scrub	798.57
26	9177000	38.35	-108.71	42	3882	21.2	2445	59.1	NW	Sandstone	Rippable	Forested	558.04

Table 21: ARW subbasins for Objective 3. Numbers in far left column refer to subbasin locations in Figure 32.

	Station Number	Latitude (deg)	Longitude (deg)	Years of record	Drainage Area	Average Slope (%)	Average Elevation (m)	A_{2250} (%)	Dominant Aspect	Lithology	Rippability Index	Landcover	Average Annual Precipitation (mm)
27	9357500	37.83	-107.60	46	145	54.4	3638	100	S	Andesite/ Tuff	Marginally Rippable	Alpine/ Forested	1135.38
28	9358000	37.81	-107.66	19	183	55.1	3597	100	S	Andesite	Non-rippable	Alpine/ Forested	1117.35
29	9358550	37.82	-107.66	19	52	54.5	3488	100	S	Andesite	Non-rippable	Forested	1028.70
30	9358900	37.85	-107.73	6	29	45.8	3566	100	S	Andesite	Non-rippable	Alpine/ Forested	1081.53
31	9359000	37.80	-107.70	12	114	51.9	3527	100	N	Andesite	Non-rippable	Alpine/ Forested	1046.48
32	9359010	37.80	-107.67	19	136	52	3505	100	E	Andesite/ Sandstone	Marginally Rippable	Forested	1038.86
33	9359020	37.79	-107.67	20	378	53.4	3536	100	S	Andesite	Non-rippable	Forested	1066.29
34	9359500	37.57	-107.78	10	901	52.1	3414	99.9	SW	Gneiss/ Sandstone/ Andesite	Marginally Rippable	Forested	1033.78
35	9361000	37.42	-107.85	46	445	46.7	2924	98.7	SE	Sandstone	Rippable	Forested	855.98
36	9361200	37.367	-107.87	5	19	49.1	2694	89.2	SE	Sandstone	Rippable	Forested	728.22
37	9361400	37.33	-107.91	5	68	53.9	2868	97.5	S	Sandstone	Rippable	Forested	870.97
38	9361500	37.28	-107.88	96	1792	46.6	3093	93.5	S	Sandstone	Rippable	Forested	911.86
39	9362000	37.60	-107.89	21	171	33	2491	68.7	W	Sandstone	Rippable	Forested	629.92
40	9362550	37.24	-107.84	6	17	15.7	2137	6.65	SW	Sandstone	Rippable	Forested	547.62
41	9362900	37.38	-107.66	7	178	33.4	3231	100	S	Sandstone/ Granite	Marginally Rippable	Forested	926.85
42	9363000	37.33	-107.75	39	252	34.1	3048	99.4	SW	Sandstone	Rippable	Forested	873.76
43	9363050	37.30	-107.79	14	277	33	2972	95	SW	Sandstone	Rippable	Forested	848.36
44	9363100	37.14	-107.75	21	46	6.8	2061	0	SW	Siltstone	Rippable	Forested	429.26
45	9363200	37.06	-107.87	21	572	22	2530	50.9	S	Gravel/ Shale/ Siltstone	Rippable	Forested	655.07

Drainage area, slope, elevation and aspect are topographic factors that are significant in influencing the amount of precipitation, runoff and infiltration that will occur; all of which affect stream-flow hydrographs. These factors are largely responsible for creating microclimatic conditions that can significantly affect the amount and type of available precipitation within a watershed. These topographic data were derived using three-meter DEMs in conjunction with the Spatial Analyst extension in ArcMap©. Drainage area is measured in square kilometers and represents the amount of area contributing runoff to an individual stream gage. Average subbasin slope is measured in percent. Average subbasin elevation is measured in meters-above-NGVD 29. To determine if a threshold occurs at which elevation becomes a significant factor, an additional elevation factor was included: percentage of subbasin area above 2,250 m (A_{2250}). Dominant basin Aspect was described by cardinal and intercardinal directions: N, S, E, W, NW, NE, SE, SW.

Surface lithology and landcover have a significant influence on runoff and are critical in determining stream pattern, stream spacing and rates of erosion, all of which are known to affect a streams hydrograph (Woods 2003; Troch 2009; Spence 2010; Spence, Guan et al. 2010; Richardson, Ketcheson et al. 2012). Lithologic data was collected using digital 1:24,000 scale USGS geologic maps (http://www.usgs.gov/pubprod/data.html#data). To accommodate the needs of the statistical methods, lithology was collapsed into three categories using a rippability index which describes lithology as non-rippable, marginally rippable, or rippable. Rippability is a measure commonly used by engineering geologists to describe the

ability of rock to be excavated using conventional excavation equipment. In the context of this study, rippability serves as a surrogate for erosion potential and surface roughness. The rippability of specific rocks can be found in several engineering geology or civil engineering texts. For this study, rippability was determined using a classification based on seismic wave velocities provided by Caterpillar© (Figure 35).

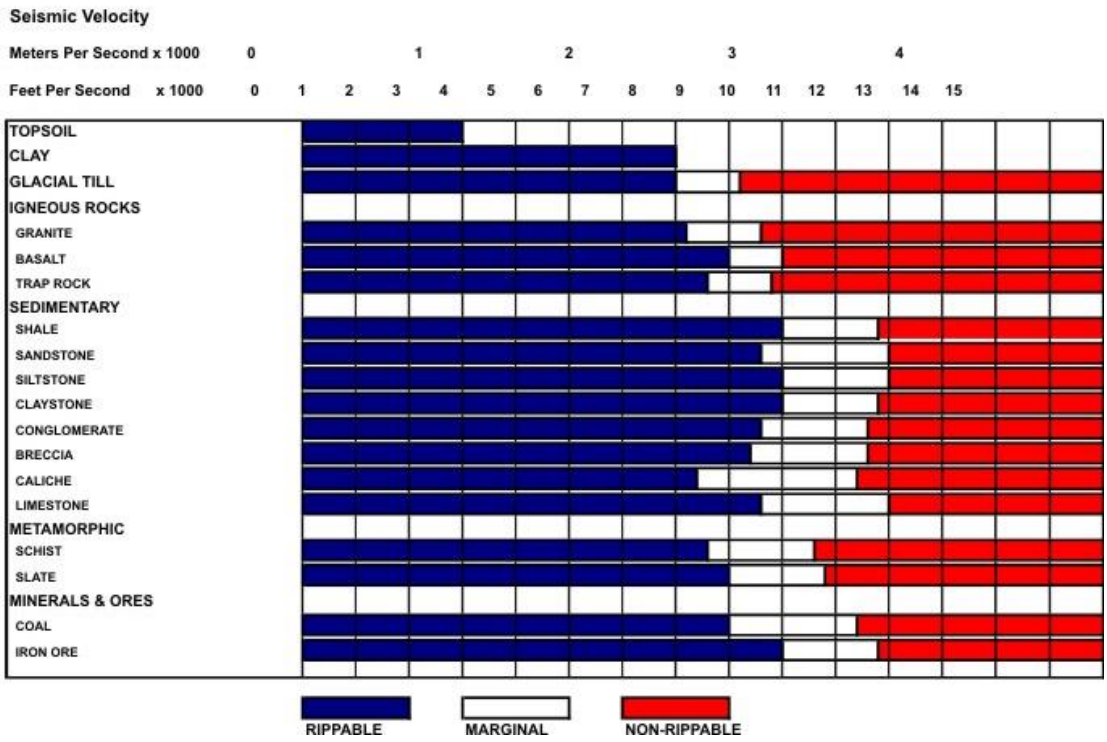

Figure 35: Lithologic Rippability Index. Rippability is based on seismic wave velocities provided by Caterpillar©.

Similar to lithology, it was also necessary to collapse landcover into fewer categorical variables. Land cover data were obtained through the National Land Cover Database 2006 (NLCD). Land cover was described as alpine, alpine/forested, forested, or scrub. These categories describe the predominant landcover of a subbasin based on the greatest percentage of area covered by a specific type of landcover.

Average annual precipitation values were collected for each subbasin through the USGS StreamStats© program. Precipitation values were validated through the precipitation frequency atlas for the western United States (Daly, Neilson et al. 1994; Carroll, Cline et al. 2006).

The previously mentioned data were compiled into Microsoft Excel© spreadsheets that were imported into JMP©, a statistical analysis software developed by SAS©. Using JMP©, a weighted least squares regression analyses was conducted using the frequency of monthly average low streamflow and discharge as response variables, and the subbasin characteristics as explanatory variables. The analysis was weighted by the data duration for each subbasin. Individual effects tests were conducted for each subbasin characteristic. To compare the impacts of each of these variables, the adjusted coefficient of determination (Adj. R^2) and percent standard error of prediction (SE%) were used as performance metrics.

Results

Weighted least squares (WLS) regression was used to identify significant relationships between geologic and geomorphic watershed characteristics and the

magnitude and frequency of low streamflows. A total of forty-five subbasins, within three watersheds were analyzed (Tables 19 – 21). The Uncompahgre River watershed (URW), San Miguel River watershed (SMRW) and Animas River watershed (ARW) were each divided into multiple gauged subbasins, which were delineated using USGS stream gauges as pour points. Each subbasin was characterized by eight explanatory variables: drainage area, average basin slope, average basin elevation, percentage of basin area above 2,250 m, dominant basin aspect, lithologic rippability, landcover and average annual precipitation. For each subbasin, the average monthly frequency and magnitude of low streamflows were used as response variables.

Weighted least squares regression identified multiple highly significant ($\alpha < 0.05$) relationships between explanatory variables and response variables. The analyzed explanatory variables were able to explain much of the variance associated with the response variables, suggesting that geologic and geomorphic characteristics are significant in influencing low streamflow characteristics in montane drainage basins.

In analyzing the results of the WLS regression model of low streamflow frequency, the numbers of low streamflows in summer months are better described by the chosen explanatory variables than the number of low streamflows in spring months. Study of Table 22 shows an average coefficient of determination (R^2) of 0.69 for the summer months (June, July, August, September) with an average P-value (Prob >F) of 0.01, compared to an average coefficient of determination of 0.57 and an average P-value of 0.045 for the observed spring months (April and May).

Table 22: WLS model fit coefficients for low flow frequency and watershed characteristics.

Month	R2	Adjusted R2	RMSE	Mean Frequency (days)	Prob > F
April	0.56	0.28	12.8	14.1	0.049*
May	0.57	0.30	11.7	12.7	0.041*
June	0.76	0.61	11.1	11.7	<0.001**
July	0.57	0.29	14.6	15.5	0.045*
August	0.72	0.54	13.0	13.3	0.0007**
September	0.71	0.53	16.2	13.0	0.0007**

As previously mentioned, results indicate that WLS regression using the chosen variables is more successful for modeling low flow frequency in summer than spring; this can be seen in the individual effects tests as well. In general, results form effects tests show that more explanatory variables become significant later in the summer than in spring (Figure 36). Individual effects tests suggest that the most influential watershed characteristic for determining the number of low streamflows is the average basin slope. For all months observed, average basin slope was the most influential, with a level of significance greater than 0.99 (Table 23).

Table 23: P-values for individual watershed characteristic effects tests for modeling low flow frequency.

Watershed Characteristic	Prob >F					
	April	**May**	**June**	**July**	**August**	**September**
Drainage Area	0.291	0.330	0.401	0.539	0.655	0.943
Average Slope	0.006**	0.005**	0.002**	0.004**	0.004**	0.008**
Average Elevation	0.926	0.816	0.124	0.752	0.212	0.031*
A(2250)	0.711	0.438	0.001**	0.029*	0.002**	0.057
Dominant Aspect	0.880	0.446	0.127	0.601	0.129	0.039*
Rippability Index	0.922	0.389	0.493	0.209	0.383	0.371
Landcover	0.393	0.618	0.700	0.380	0.094	0.448
Average Annual Precipitation	0.626	0.936	0.125	0.927	0.244	0.002**

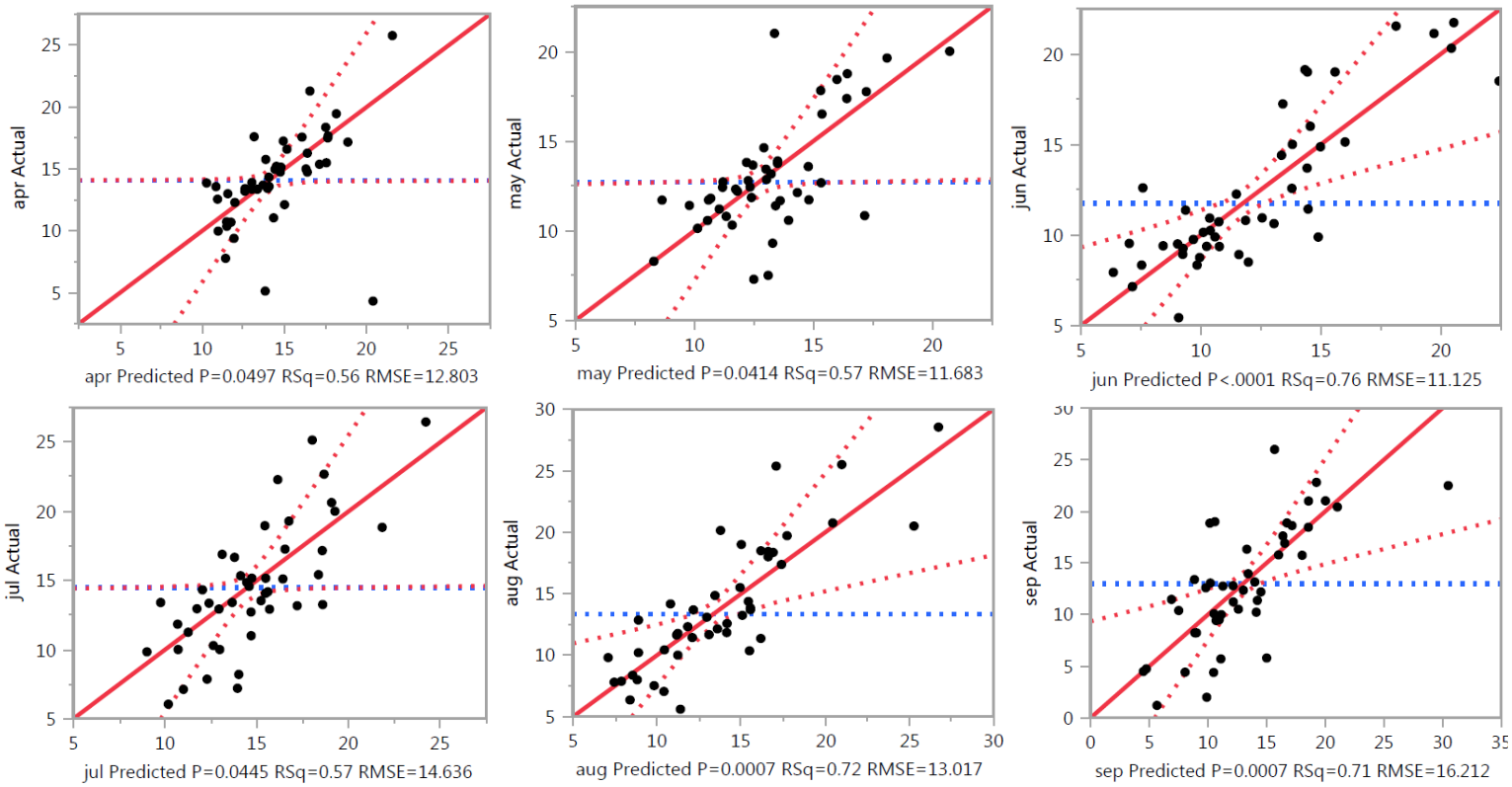

Figure 36: WLS regression model fits for average monthly low streamflow frequency in number of days. The mean of the response is demonstrated by the blue-dotted-line, and the limits of the 0.90 confidence intervals are represented by the red-dotted-lines.

Estimates of individual parameters for the average basin slope shows that for all months observed, a negative trend exists with a consistent slope of approximately - 0.25 (Table 24). On average, for approximately four percent increase in average basin slope, approximately one less day of low streamflow occurs each month (Figure 37). Such a consistent trend would likely be helpful in predicting low streamflows in montane regions. Analysis also showed the percentage of basin area above 2,250 m elevation ($A_{2,250}$) is influential, however, more so in the summer months than the spring or fall.

Table 24: Monthly parameter estimates for the effects of average basin slope on low streamflow frequency.

Month	Estimate
April	- 0.23
May	- 0.22
June	- 0.23
July	- 0.28
August	- 0.25
September	- 0.28

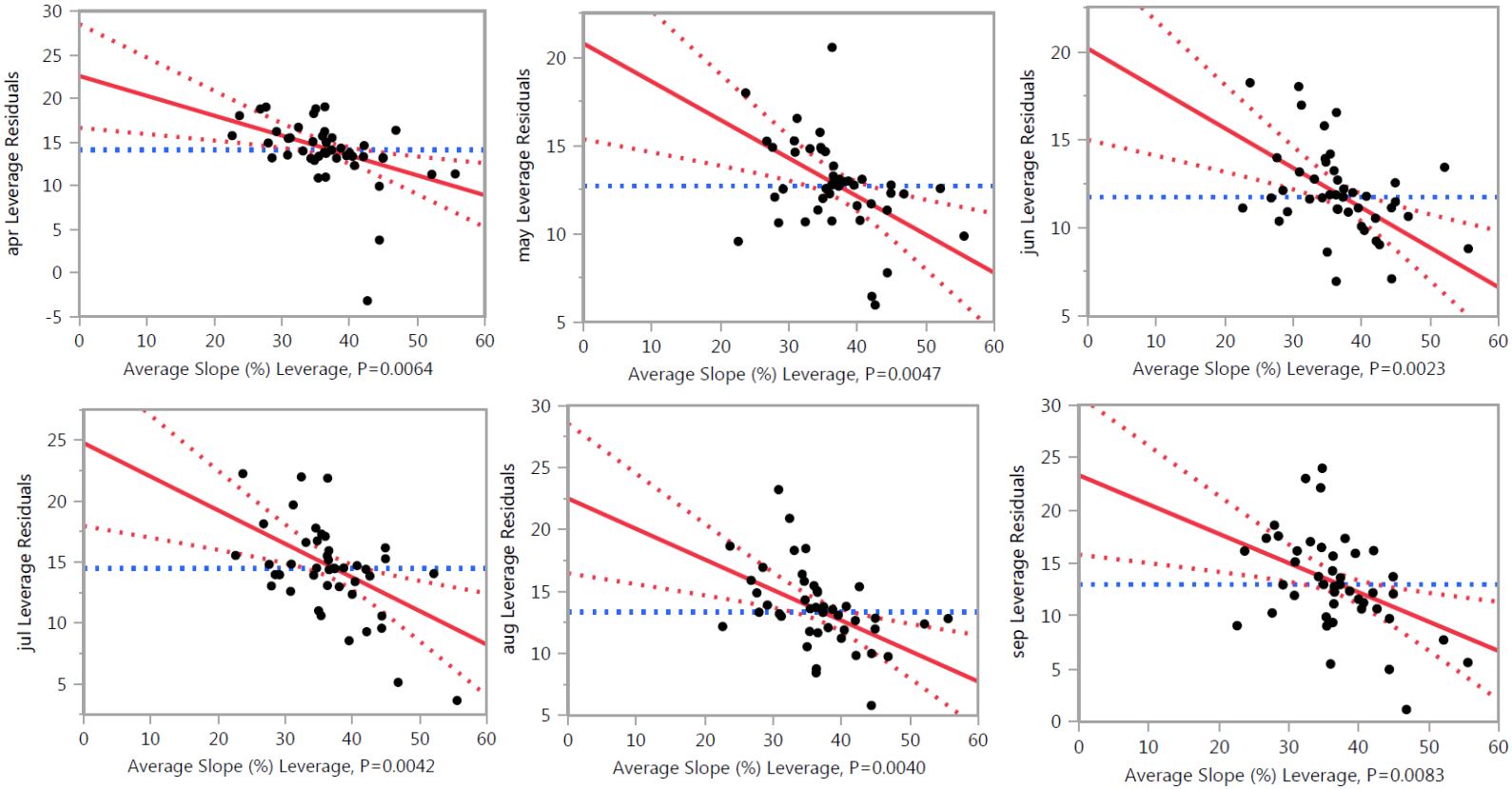

Figure 37: Monthly leverage plots for average subbasin slope and low streamflow frequency (in number of days). The mean of the response is demonstrated by the blue-dotted-line, and the limits of the 0.90 confidence intervals are represented by the red-dotted-lines.

WLS regression was also successful at modeling significant relationships between watershed characteristics and the magnitude of monthly average low streamflow discharge. At a level of significance greater than 0.95, the chosen explanatory variables were able to explain approximately 67 percent of the variance associated with average monthly low streamflow discharge. For all months observed, an average coefficient of determination (R^2) of 0.67 was observed. Similar to the low streamflow frequency model, the low streamflow discharge model is also most successful at modeling low streamflow discharges for the late summer months (figure 38). Although all months resulted in significant ($\alpha < 0.05$) relationships, the model was able to predict the magnitude of low flows in August and September with a confidence level greater than 0.99 (Table 25).

Table 25: WLS model fit coefficients for low flow magnitude and watershed characteristics.

Month	R2	Adjusted R2	RMSE	Mean Discharge (cfs)	Prob > F
April	0.63	0.40	0.45	0.51	0.009**
May	0.58	0.31	0.40	0.58	0.034*
June	0.69	0.49	0.37	0.64	0.002**
July	0.63	0.39	0.43	0.63	0.011*
August	0.76	0.60	0.39	0.65	0.0001**
September	0.74	0.57	0.40	0.67	0.0003**

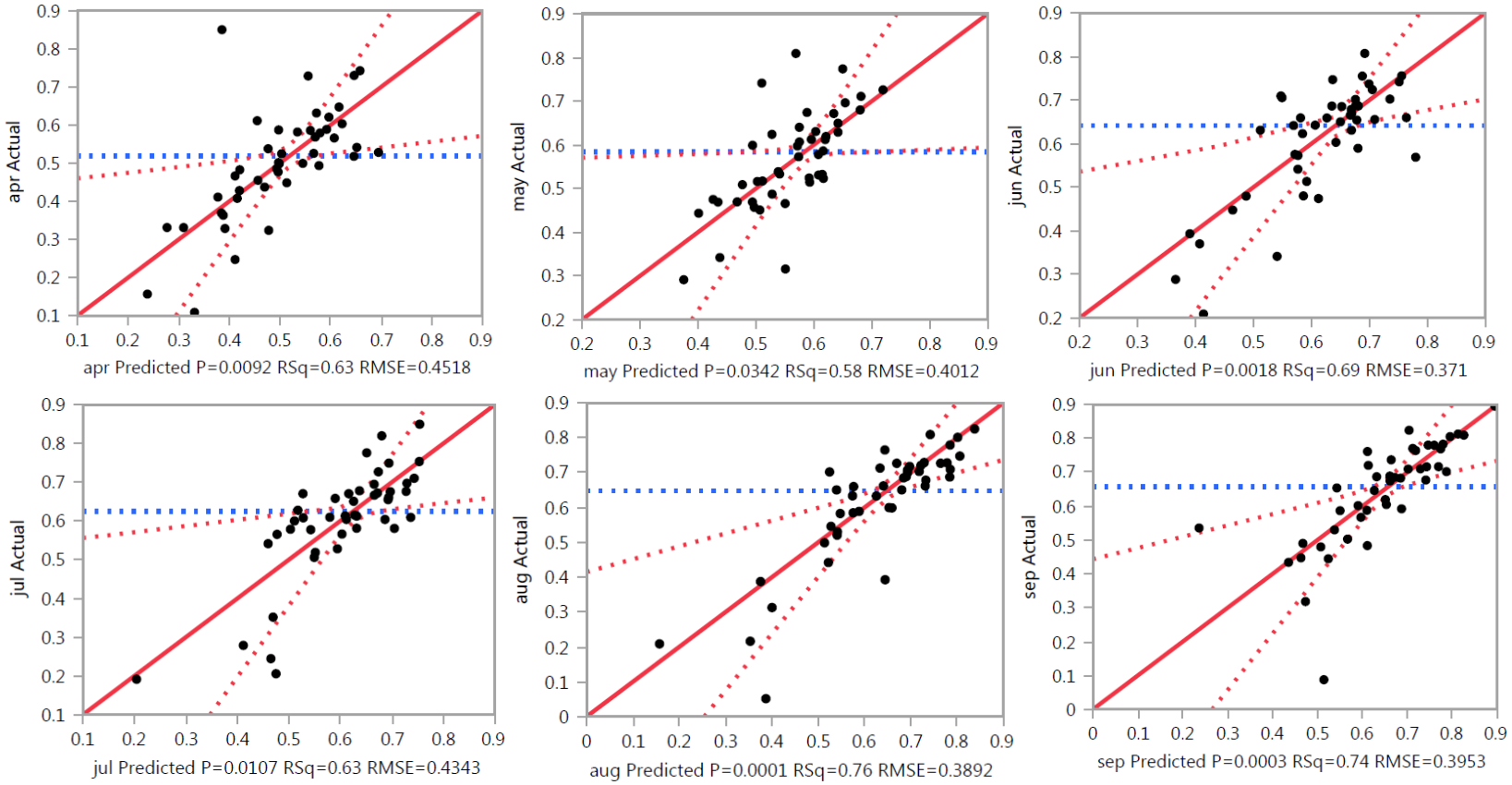

Figure 38: WLS regression model fits for monthly average low flow discharge (in percentage of average monthly discharge). The mean of the response is demonstrated by the blue-dotted-line, and the limits of the 0.90 confidence intervals are represented by the red-dotted-lines.

Individual effects tests showed that the most significant of the observed watershed characteristics was average subbasin slope (Table 26). With the exception of May, all months showed, with a level of significance greater than 0.99, that average subbasin slope is influential at determining average monthly low streamflow magnitude. Other significant watershed characteristics were the percentage of subbasin area above 2,250 m elevation and average annual precipitation.

Table 26: P-values for individual watershed characteristic effects tests for modeling low flow magnitude.

Watershed Characteristic	Prob >F					
	April	**May**	**June**	**July**	**August**	**September**
Drainage Area	0.971	0.139	0.120	0.215	0.579	0.482
Average Slope	0.0007**	0.485	0.008**	0.0003**	0.0004**	0.0002**
Average Elevation	0.960	0.250	0.433	0.854	0.046*	0.143
A(2250)	0.745	0.295	0.016*	0.314	0.007**	0.048*
Dominant Aspect	0.363	0.243	0.142	0.297	0.130	0.146
Rippability Index	0.852	0.643	0.349	0.094	0.524	0.084
Landcover	0.258	0.499	0.810	0.702	0.202	0.125
Average Annual Precipitation	0.647	0.251	0.444	0.117	0.009**	0.011*

Discussion and Conclusions

Changes in the timing and volume of montane streamflow regimes are typically attributed to earlier snowmelt and the reduction of snow pack (Tague, 2009; Viviroli et al., 2011). Although snow accumulation and melt are the primary hydrologic inputs from a montane streamflow perspective, several other first-order controls affect the spatial variability of the hydrologic response to weather phenomena (Jasper, 2004; Tague, 2008, 2009; Uhlenbrook, 2005, Viviroli et al., 2011). Considerable research (Jasper, 2004;

Tague, 2008, 2009; Uhlenbrook, 2005, Viviroli et al., 2011) has shown that hydrographs for montane streams are significantly affected by geologic controls. Such geologic factors, however, are rarely considered first-order controls on spatial variation in the hydrologic response to weather phenomena (Tague, 2008). Spatial differences in geologic and geomorphic controls may have an equally significant influence on the response of streamflow as does the spatial relationship associated with the accumulation and melt of snow.

To provide a better overall picture of how stream-flow in a specific region will be affected by weather phenomena, it is crucial to understand all involved processes. To date, the majority of research concerned with determining future stream-flow has focused primarily on climate-mediated changes in snowpack and regimes of melt (Tague, Grant, 2009). A better understanding of the influence of relevant geologic controls would help to improve assessments of the impacts of weather phenomena on stream-flow.

It is crucial to have an understanding of the specific systems operating in montane watersheds, as mountain river basins, associated reservoirs, and underlying aquifers supply water demands for over sixty million people in the western United States (Milly, Dunne et al. 2005; Pagano and Garen 2005; Ray, Barsugli et al. 2008; Rangwala, Barsugli et al. 2012; Rangwala and Miller 2012). Changes in montane hydrology could have a significant impact on water resource management. Thus, understanding the frequency and duration of extreme hydrologic events is critical to effective management

of montane water resources. As the demand for freshwater continues to increase, it is becoming increasingly necessary to understand the nature of low streamflows.

The research presented in this paper is focused on determining the extent to which spatial variations in geology and geomorphology may affect the frequency and magnitude of low streamflows in montane drainage basins. More specifically, this paper aims to determine which watershed characteristics are crucial for modeling low flow in montane regions of southwestern Colorado. Weighted least squares (WLS) regression was used to identify significant relationships between watershed characteristics and the magnitude and frequency of low streamflows. Multiple highly significant correlations were observed, suggesting that the inclusion of geologic and geomorphic watershed characteristics in low streamflow analyses would be beneficial. The results of this paper should help in providing water resource planners a better understanding of which watershed characteristics can be used to describe and predict low streamflows.

In general, it was found that the eight selected watershed characteristics can sufficiently describe the average frequency and average discharge of low streamflows. The selected explanatory variables were more successful, however, at describing low streamflows in the summer rather than the spring. For all months observed, the most significant explanatory variable for predicting frequency and magnitude of low streamflow was average subbasin slope. A consistent negative trend was associated with average subbasin slope, warranting further analysis as to whether a specific threshold value could be developed and utilized for future low flow predictions.

As previously mentioned, many hydrological applications require an accurate and effective means to predict the frequency and volume of low streamflows. In knowing that specific watershed characteristics are significant at determining low streamflow characteristics, it may be possible to improve regional regression analyses. Because all of the watershed characteristics data used in this study are readily available through public sources and can be relatively easily calculated through geographic information software, it is possible to include these variables in regional regression analyses for almost anywhere in the US weather the basin is gauged or ungaged. Furthermore, this research showed that regional regression models are not limited to kilometer scale resolution. With the appropriate data resolution and appropriate watershed characteristics, significant linear relationships are evident at the subbasin scale, suggesting that regional regression could be effective at the subbasin scale.

Future research would involve a comparison of traditional regional regression techniques to a regional regression model that incorporates the watershed characteristics that were proven to be statistically for the selected study area. Future research should also consider the relative influence of baseflow.

CHAPTER V

CONCLUSIONS

Conclusions

In the previous chapters, the research was motivated by the need to better understand and predict the trends and variability in montane water resources. The study focused on three topics of montane streamflow for the Uncompahgre River, San Miguel River and Animas River watersheds. The first study was focused on establishing a link between weather phenomena and timing and volume of streamflow regimes. The second established a link between watershed characteristics and the timing of the onset of the spring pulse, peak streamflow and summer streamflow subsidence. The third study determined the extent to which watershed characteristics influence the frequency and magnitude of low streamflows.

The study of streamflow timing and weather phenomena suggests that: 1) The timing of montane streamflow regimes can be sufficiently explained by average monthly maximum and minimum temperatures and average monthly precipitation 2) Increases in average maximum temperatures for winter months have the most substantial effect in terms of shifting the onset of the spring pulse later 3) Increases in average minimum temperatures for spring months have the most substantial effect in terms of shifting the onset of the spring pulse earlier.

The study of streamflow timing and watershed characteristics suggests that: 1) Geology and geomorphology have a significant effect on the timing of montane

streamflow regimes. 2) Drainage area and the percentage of a subbasin over 2,250 m elevation are highly significant in determining the timing of the beginning of montane streamflow. 3) Average subbasin elevation, the percent of the subbasin above 2,250 m, dominant aspect, and average annual precipitation are highly significant in determining the date at which 50 percent of annual streamflow is achieved. 4) Dominant aspect is highly significant in determining the date at which annual streamflow significantly subsides.

The study of low streamflow frequency and magnitude suggests that: 1) The eight selected watershed characteristics can sufficiently describe the average frequency and average discharge of low streamflows. 2) The selected explanatory variables were more successful, however, at describing low streamflows in the summer rather than the spring. 3) For all months observed, the most significant explanatory variable for predicting frequency and magnitude of low streamflow was average subbasin slope. 4) A consistent negative trend was associated with average subbasin slope, warranting further analysis as to whether a specific threshold value could be developed and utilized for future low flow predictions.

REFERENCES

Anderton, S. P. (2002). "Micro-scale spatial variability and the timing of snow melt runoff in a high mountain catchment." Journal of Hydrology **268**(1-4): 158-176.

Arnell, N. W. (1996). Global warming, river flows and water resources, John Wiley & Sons Ltd. Hoboken, New Jersey.

Atwood, W. W. and K. F. Mather (1932). Physiography and quaternary geology of the San Juan Mountains, Colorado, US Government Printing Office.

Bales, R. C. (2006). "Mountain hydrology of the western United States." Water Resources Research **42**(8): 8432.

Band, L. E., C. L. Tague, et al. (2000). "Modelling watersheds as spatial object hierarchies: structure and dynamics." Transactions in GIS **4**(3): 181-196.

Barnett, T. (2004). "The effects of climate change on water resources in the west: introduction and overview." Climatic Change **62**(1-3): 1.

Barnett, T. P. (2005). "Potential impacts of a warming climate on water availability in snow-dominated regions." Nature **438**(7066): 303.

Bernstein, L., P. Bosch, et al. (2007). Climate change 2007: synthesis report. Summary for policymakers. IPCC. Washington D.C.

Blair, R., T. A. Casey, et al. (1996). The Western San Juan Mountains: their geology, ecology, and human history, University Press of Colorado Boulder.

Bush, A.L., Bromfield, C.S., Pierson, C.T. (1959) "Areal Geology of the Placerville Quadrangle, San Miguel County, Colorado". USGS Bulletin 1072-E, 229-384

Capesius, J. P., V. C. Stephens, et al. (2009). Regional regression equations for estimation of natural streamflow statistics in Colorado, US Department of the Interior, US Geological Survey. Washington D.C.

Carroll, T., D. Cline, et al. (2006). NOAA's national snow analyses. 74th Annual Meeting of the Western Snow Conference 2006. Pasadena, California.

Casadevall, T. and H. Ohmoto (1977). "Sunnyside Mine, Eureka mining district, San Juan County, Colorado; geochemistry of gold and base metal ore deposition in a volcanic environment." Economic Geology **72**(7): 1285-1320.

Cayan, D. R. (1996). "Interannual climate variability and snowpack in the western United States." Journal of Climate **9**(5): 928-948.

Christensen, N. S. (2004). "The effects of climate change on the hydrology and water resources of the Colorado River basin." Climatic Change **62**(1-3): 337.

Christensen, N. S. and D. P. Lettenmaier (2007). "A multimodel ensemble approach to assessment of climate change impacts on the hydrology and water resources of the Colorado River Basin." Hydrology & Earth System Sciences **11**(4): 228.

Clow, D. W. (2010). "Changes in the timing of snowmelt and streamflow in Colorado: A response to recent warming." Journal of Climate **23**(9): 144.

Cole, J. P. and C. A. King (1968). Quantitative geography: techniques and theories in geography, Wiley. London.

Dahlke, H. E. (2009). "Modelling variable source area dynamics in a CEAP watershed." Ecohydrology **2**(3): 337-349.

Daly, C., R. P. Neilson, et al. (1994). "A statistical-topographic model for mapping climatological precipitation over mountainous terrain." Journal of Applied Meteorology **33**(2): 140-158.

Dettinger, M. D. and D. R. Cayan (1995). "Large-scale atmospheric forcing of recent trends toward early snowmelt runoff in California." Journal of Climate **8**(3): 606-623.

Dettinger, M. D., D. R. Cayan, et al. (1998). "North--South precipitation patterns in western North America on interannual-to-decadal timescales." Journal of Climate **11**(12): 221-256.

Dettinger, M. D. and H. F. Diaz (2000). "Global characteristics of stream flow seasonality and variability." Journal of Hydrometeorology **1**(4): 289-310.

Diaz, H. F. and R. S. Bradley (1997). “Temperature variations during the last century at high elevation sites.” Climatic Change at High Elevation Sites, Springer Netherlands**:** 21-47.

Eischeid, J. K., C. Bruce Baker, et al. (1995). "The quality control of long-term climatological data using objective data analysis." Journal of Applied Meteorology **34**(12): 2787-2795.

Elliott, G. P. and K. F. Kipfmueller (2010). "Multi-scale influences of slope aspect and spatial pattern on ecotonal dynamics at upper treeline in the Southern Rocky Mountains, USA." Arctic, Antarctic, and Alpine Research **42**(1): 45-56.

Ficklin, D. L., I. T. Stewart, et al. (2013). "Climate change impacts on streamflow and subbasin-scale hydrology in the upper Colorado River basin." PloS One **8**(8): e71297.

Garen, D. C. (1992). "Improved techniques in regression-based streamflow volume forecasting." Journal of Water Resources Planning and Management **118**(6): 654-670.

Geladi, P. and B. R. Kowalski (1986). "Partial least-squares regression: a tutorial." Analytica Chimica Acta **185**: 1-17.

Griffis, V. and J. Stedinger (2007). "The use of GLS regression in regional hydrologic analyses." Journal of Hydrology **344**(1): 82-95.

Harding, B., A. Wood, et al. (2012). "The implications of climate change scenario selection for future streamflow projection in the Upper Colorado River Basin." Hydrology & Earth System Sciences Discussions **9**(1):12-47.

Hay, L. E. and G. J. McCabe (2002). "Spatial variability in water-balance model performance in the coterminous United States." JAWRA Journal of the American Water Resources Association **38**(3): 847-860.

Helsel, D. and R. Hirsch (2002). Statistical methods in water resources: US Geological Survey techniques of water resources investigations. United States Geological Survey. Washington D.C.

Hidalgo, H., T. Das, et al. (2009). "Detection and attribution of streamflow timing changes to Climate Change in the Western United States." Journal of Climate **22**(13): 21-44.

Hodgkins, G. A. and R. W. Dudley (2006). "Changes in the timing of winter–spring streamflows in eastern North America, 1913–2002." Geophysical Research Letters **33**(6): 56-75.

Hortness, J. E. (2006). Estimating low-flow frequency statistics for unregulated streams in Idaho, US Department of the Interior, US Geological Survey. Washington D.C.

Hortness, J. E. and C. Berenbrock (2001). Estimating monthly and annual streamflow statistics at ungaged sites in Idaho, US Department of the Interior, US Geological Survey. Washington D.C.

Inyan, B. J. and M. W. Williams (2001). "Protection of headwater catchments from future degradation: San Miguel River Basin, Colorado." Mountain Research and Development **21**(1): 54-60.

Jarrett, R. D. and J. E. Costa (1988). Evaluation of the flood hydrology in the Colorado Front Range using precipitation, streamflow, and paleoflood data for the Big Thompson River Basin, Department of the Interior, US Geological Survey. Washington D.C.

Jasper, K. (2004). "Differential impacts of climate change on the hydrology of two alpine river basins." Climate Research **26**(2): 113.

Kenney, T. A., C. D. Wilkowske, et al. (2007). "Methods for estimating magnitude and frequency of peak flows for natural streams in Utah." US Geological Survey. Washington D.C.

Kircher, J. E., A. F. Choquette, et al. (1985). Estimation of natural streamflow characteristics in western Colorado, US Geological Survey. Washington D.C.

Knowles, N. and D. R. Cayan (2002). "Potential effects of global warming on the Sacramento/San Joaquin watershed and the San Francisco estuary." Geophysical Research Letters **29**(18): 38-31-38-34.

Knowles, N., M. D. Dettinger, et al. (2006). "Trends in snowfall versus rainfall in the western United States." Journal of Climate **19**(18): 14-52.

Kroll, C., J. Luz, et al. (2004). "Developing a watershed characteristics database to improve low streamflow prediction." Journal of Hydrologic Engineering **9**(2): 116-125.

Kundzewicz, Z. W. (2008). "The implications of projected climate change for freshwater resources and their management." Hydrological Sciences Bulletin **53**(1): 3.

Kunkel, K. E., M. A. Palecki, et al. (2007). "Trend identification in twentieth-century US snowfall: The challenges." Journal of Atmospheric & Oceanic Technology **24**(1): 3.

Lehning, M. (2006). "ALPINE3D: A detailed model of mountain surface processes and its application to snow hydrology." Hydrological Processes **20**(10): 2111-2128.

Leung, L. R. (2005). "Effects of climate variability and change on mountain water resources in the western U.S." Global Change and Mountain Regions: 355-364.

Lins, H. F. and J. R. Slack (2005). "Seasonal and regional characteristics of US streamflow trends in the United States from 1940 to 1999." Physical Geography **26**(6): 489-501.

Luce, C. H. and Z. A. Holden (2009). "Declining annual streamflow distributions in the Pacific Northwest United States, 1948–2006." Geophysical Research Letters **36**(16): 12.

McCabe, G. J. and M. P. Clark (2005). "Trends and variability in snowmelt runoff in the western United States." Journal of Hydrometeorology **6**(4): 476-482.

McCabe, G. J. and D. M. Wolock (2002). "A step increase in streamflow in the conterminous United States." Geophysical Research Letters **29**(24): 38-31-38-34.

McCabe, G. J. and D. M. Wolock (2007). "Warming may create substantial water supply shortages in the Colorado River basin." Geophysical Research Letters **34**(22): 12.

McDonnell, J. J. (2007). "Moving beyond heterogeneity and process complexity: A new vision for watershed hydrology." Water Resources Research **43**(7): 17-34.

McGlynn, B., J. McDonnell, et al. (2003). "On the relationships between catchment scale and streamwater mean residence time." Hydrological Processes **17**(1): 175-181.

McGlynn, B. L., J. J. McDonnell, et al. (2004). "Scale effects on headwater catchment runoff timing, flow sources, and groundwater‐streamflow relations." Water Resources Research **40**(7): 14-27.

McGuire, K., J. McDonnell, et al. (2005). "The role of topography on catchment‐scale water residence time." Water Resources Research **41**(5): 288-317.

Milly, P. C., K. A. Dunne, et al. (2005). "Global pattern of trends in streamflow and water availability in a changing climate." Nature **438**(7066): 347-350.

Montgomery, D. C., E. A. Peck, et al. (2012). Introduction to linear regression analysis, John Wiley & Sons. Hoboken, New Jersey.

Mote, P. W., A. F. Hamlet, et al. (2005). "Declining mountain snowpack in western North America." Bulletin of American Meteorolgical Society **86**(39): 221

Nolin, A. W. (2012). "Perspectives on climate change, mountain hydrology, and water resources in the Oregon Cascades, USA." Mountain Research and Development **32**(S1): S35-S46.

Nydick, K., Crawford, J., Bidwell, M., Livensperger, C., Rangwala, I. and Cozetto, K. (2012). "Climate Change Assessment for the San Juan Mountain Regions, Southwestern Colorado, USA: A Reveiew of Scientific Research". Prepared by Mountain Studies Institute in cooperation with USDA San Juan National Forest Service and USDOI Bureau of Land Management Tres Rios Field Office. Durango, CO. Available for download from www.mountainstudies.org

Pagano, T. and D. Garen (2005). "A recent increase in western US streamflow variability and persistence." Journal of Hydrometeorology **6**(2): 445-498.

Rangwala, I., J. Barsugli, et al. (2012). "Mid-21st century projections in temperature extremes in the southern Colorado Rocky Mountains from regional climate models." Climate Dynamics **39**(7-8): 1823-1840.

Rangwala, I. and J. Miller (2011). "Long-term temperature trends in the San Juan Mountains." Eastern San Juan Mountains: Their Geology, Ecology and Human History. University Press of Colorado, Boulder.

Rangwala, I. and J. R. Miller (2010). "Twentieth century temperature trends in Colorado's San Juan Mountains." Arctic, Antarctic, and Alpine Research **42**(1): 89-97.

Rangwala, I. and J. R. Miller (2012). "Climate change in mountains: a review of elevation-dependent warming and its possible causes." Climatic Change **114**(3-4): 527-547.

Ray, A., J. Barsugli, et al. (2008). "Climate change in Colorado: a synthesis to support water resources management and adaptation." Report for the Colorado Water Conservation Board. University of Colorado, Boulder.

Regonda, S. K., B. Rajagopalan, et al. (2005). "Seasonal cycle shifts in hydroclimatology over the western United States." Journal of Climate **18**(2): 372-384.

Reilly, C. F. and C. N. Kroll (2003). "Estimation of 7 - day, 10 - year low - streamflow statistics using baseflow correlation." Water Resources Research **39**(9): 227.

Resler, L. M. (2006). "Geomorphic controls of spatial pattern and process at alpine treeline." The Professional Geographer **58**(2): 124-138.

Richardson, M., S. Ketcheson, et al. (2012). "The influences of catchment geomorphology and scale on runoff generation in a northern peatland complex." Hydrological Processes **26**(12): 1805-1817.

Riggs, H. (1965). "Estimating probability distributions of drought flows." Water and Sewage Works **112**(5): 153-157.

Riggs, H. C. (1980). "Characteristics of low flows." Journal of the Hydraulics Division **106**(5): 717-731.

Rittger, K., A. Kahl, et al. (2011). Topographic distribution of snow water equivalent in the Sierra Nevada. 79th Western Snow Conference 2011. Stateline, Nevada.

Service, R. F. (2004). "As the west goes dry." Science **303**(5661): 1124.

Slack, J. R. and J. M. Landwehr (1994). Hydro-climatic data network (HCDN): A US Geological Survey streamflow data set for the United States for the study of climate variations, 1874-1988, US Geological Survey. Washington D.C.

Smakhtin, V. (2001). "Low flow hydrology: a review." Journal of Hydrology **240**(3): 147-186.

Spence, C. (2010). "A paradigm shift in hydrology: Storage thresholds across scales influence catchment runoff generation." Geography Compass **4**(7): 819-833.

Spence, C., X. Guan, et al. (2010). "Storage dynamics and streamflow in a catchment with a variable contributing area." Hydrological Processes **24**(16): 2209-2221.

Stewart, I. T., D. R. Cayan, et al. (2004). "Changes in snowmelt runoff timing in western North America under abusiness as usual'climate change scenario." Climatic Change **62**(1-3): 217-232.

Stewart, I. T., D. R. Cayan, et al. (2005). "Changes toward earlier streamflow timing across western North America." Journal of Climate **18**(8): 1136-1155.

Tague, C., G. Grant, et al. (2008). "Deep groundwater mediates streamflow response to climate warming in the Oregon Cascades." Climatic Change **86**(1): 189-210.

Tague, C. and G. E. Grant (2009). "Groundwater dynamics mediate low-flow response to global warming in snow-dominated alpine regions." Water Resources Research **45**(7): 225-276.

Tague, C. L. (2009). "Assessing climate change impacts on alpine stream-flow and vegetation water use: mining the linkages with subsurface hydrologic processes." Hydrological Processes **23**: 1815-1819.

Team, R. C. (2005). "R: A language and environment for statistical computing." R Foundation for Statistical Computing. San Angelo, Texas.

Tetzlaff, D. (2007). "Connectivity between landscapes and riverscapes—a unifying theme in integrating hydrology and ecology in catchment science?" Hydrological Processes **21**(10): 1385.

Timilsena, J., T. Piechota, et al. (2009). "Associations of interdecadal/interannual climate variability and long-term colorado river basin streamflow." Journal of Hydrology **365**(3): 289-301.

Troch, P. A. (2009). "Dealing with landscape heterogeneity in watershed hydrology: a review of recent progress toward new hydrological theory." Geography Compass **3**(1): 375.

Uncompahgre Watershed Partnership. Uncompahgre Watershed Plan. (2013). Available for download from www.uncompahgrewatershed.org.

Uhlenbrook, S., U. M. Huber, et al. (2005). “Runoff generation processes on hillslopes and their susceptibility to global change.” Global Change and Mountain Regions. Springer Netherlands.

Viviroli, D., D. Archer, et al. (2011). "Climate change and mountain water resources: overview and recommendations for research, management and policy." Hydrology and Earth System Sciences **15**(2): 471-504.

Vogel, R. M. and C. N. Kroll (1992). "Regional geohydrologic‐geomorphic relationships for the estimation of low‐flow statistics." Water Resources Research **28**(9): 2451-2458.

Vörösmarty, C. J. and Vorosmarty (2000). "Global water resources: vulnerability from climate change and population growth." Science **289**(5477): 284.

Waltemeyer, S. (2006). "Analysis of the magnitude and frequency of peak discharges for the Navajo Nation in Arizona." Utah, Colorado, and New Mexico: US Geological Survey Scientific Investigations Report **5306**: 42.

Woods, R. (2003). "The relative roles of climate, soil, vegetation and topography in determining seasonal and long-term catchment dynamics." Advances in Water Resources **26**(3): 295-309.

APPENDIX A

Response Moving.var

Actual by Predicted Plot

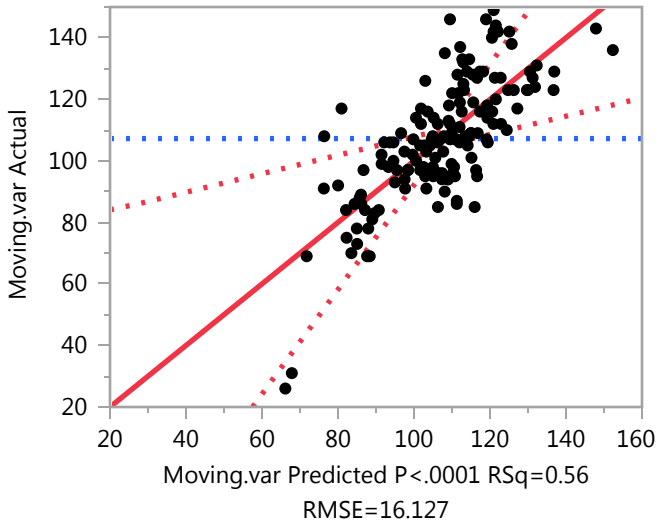

Summary of Fit

RSquare	0.556945
RSquare Adj	0.354774
Root Mean Square Error	16.12651
Mean of Response	107.2318
Observations (or Sum Wgts)	151

Analysis of Variance

Source	DF	Sum of Squares	Mean Square	F Ratio
Model	47	33672.262	716.431	2.7548
Error	103	26786.625	260.064	**Prob > F**
C. Total	150	60458.887		<.0001 *

Parameter Estimates

Term	Estimate	Std Error	t Ratio	Prob>|t|
Intercept	111.90531	30.33906	3.69	0.0004 *
tmax.jan	1.6707854	1.665617	1.00	0.3182
tmax.feb	2.8150368	1.383619	2.03	0.0445 *
tmax.mar	-1.635784	1.488112	-1.10	0.2742
tmax.apr	0.3203564	1.704055	0.19	0.8512
tmax.may	-0.290722	1.616701	-0.18	0.8576
tmin.jan	1.320968	1.373139	0.96	0.3383
tmin.feb	-1.373243	1.293866	-1.06	0.2910
tmin.mar	1.9238655	1.413987	1.36	0.1766

Response Moving.var

Parameter Estimates

Term	Estimate	Std Error	t Ratio	Prob>|t|
tmin.apr	-2.315664	2.016222	-1.15	0.2534
tmin.may	-3.330547	2.243597	-1.48	0.1407
prcp.jan	-0.149598	0.285584	-0.52	0.6015
prcp.feb	-0.131322	0.222628	-0.59	0.5566
prcp.mar	-0.222436	0.180528	-1.23	0.2207
prcp.apr	0.7313114	0.221808	3.30	0.0013 *
prcp.may	0.2166679	0.280681	0.77	0.4419
(tmax.jan-2.34132)*site[Colona]	-4.781086	2.574446	-1.86	0.0661
(tmax.jan-2.34132)*site[Durango]	0.4759602	2.084579	0.23	0.8198
(tmax.feb-3.69126)*site[Colona]	1.7395812	2.321909	0.75	0.4554
(tmax.feb-3.69126)*site[Durango]	-2.050493	1.678081	-1.22	0.2245
(tmax.mar-6.17911)*site[Colona]	1.977831	2.200347	0.90	0.3708
(tmax.mar-6.17911)*site[Durango]	0.2872416	2.122339	0.14	0.8926
(tmax.apr-10.6453)*site[Colona]	0.4095203	2.718166	0.15	0.8805
(tmax.apr-10.6453)*site[Durango]	-2.04698	2.244289	-0.91	0.3639
(tmax.may-16.2904)*site[Colona]	0.772146	2.59326	0.30	0.7665
(tmax.may-16.2904)*site[Durango]	0.7531898	2.057926	0.37	0.7151
(tmin.jan+14.4807)*site[Colona]	1.3197691	2.391484	0.55	0.5822
(tmin.jan+14.4807)*site[Durango]	-1.129527	1.607707	-0.70	0.4839
(tmin.feb+12.8394)*site[Colona]	0.8443984	2.115407	0.40	0.6906
(tmin.feb+12.8394)*site[Durango]	1.6904966	1.51454	1.12	0.2669
(tmin.mar+9.44288)*site[Colona]	-1.954539	2.199077	-0.89	0.3762
(tmin.mar+9.44288)*site[Durango]	-1.193492	1.793451	-0.67	0.5072
(tmin.apr+4.62791)*site[Colona]	0.3417193	3.306645	0.10	0.9179
(tmin.apr+4.62791)*site[Durango]	1.22368	2.416336	0.51	0.6136
(tmin.may+0.18882)*site[Colona]	-6.229034	3.683516	-1.69	0.0938
(tmin.may+0.18882)*site[Durango]	2.6040311	2.65495	0.98	0.3290
(prcp.jan-13.0782)*site[Colona]	-1.174031	0.396752	-2.96	0.0038 *
(prcp.jan-13.0782)*site[Durango]	0.4667682	0.38211	1.22	0.2247
(prcp.feb-15.1946)*site[Colona]	-0.488277	0.311176	-1.57	0.1197
(prcp.feb-15.1946)*site[Durango]	-0.20982	0.286349	-0.73	0.4654
(prcp.mar-18.5581)*site[Colona]	0.3192594	0.269453	1.18	0.2388
(prcp.mar-18.5581)*site[Durango]	-0.165757	0.242169	-0.68	0.4952
(prcp.apr-17.0011)*site[Colona]	0.3933669	0.320704	1.23	0.2228
(prcp.apr-17.0011)*site[Durango]	-0.610694	0.31877	-1.92	0.0582
(prcp.may-13.4067)*site[Colona]	0.2380858	0.37152	0.64	0.5230
(prcp.may-13.4067)*site[Durango]	0.0820368	0.41739	0.20	0.8446
site[Colona]	16.83293	10.25746	1.64	0.1038

Response Moving.var

Parameter Estimates

Term	Estimate	Std Error	t Ratio	Prob>|t|
site[Durango]	-1.56	7.687672	-0.20	0.8396

Effect Tests

Source	Nparm	DF	Sum of Squares	F Ratio	Prob > F
tmax.jan	1	1	261.6808	1.0062	0.3182
tmax.feb	1	1	1076.5051	4.1394	0.0445 *
tmax.mar	1	1	314.2401	1.2083	0.2742
tmax.apr	1	1	9.1914	0.0353	0.8512
tmax.may	1	1	8.4096	0.0323	0.8576
tmin.jan	1	1	240.6780	0.9255	0.3383
tmin.feb	1	1	292.9525	1.1265	0.2910
tmin.mar	1	1	481.4367	1.8512	0.1766
tmin.apr	1	1	343.0480	1.3191	0.2534
tmin.may	1	1	573.0889	2.2036	0.1407
prcp.jan	1	1	71.3620	0.2744	0.6015
prcp.feb	1	1	90.4887	0.3479	0.5566
prcp.mar	1	1	394.8221	1.5182	0.2207
prcp.apr	1	1	2827.0362	10.8705	0.0013 *
prcp.may	1	1	154.9688	0.5959	0.4419
tmax.jan*site	2	2	1060.1589	2.0383	0.1355
tmax.feb*site	2	2	388.5436	0.7470	0.4763
tmax.mar*site	2	2	378.1375	0.7270	0.4858
tmax.apr*site	2	2	283.9932	0.5460	0.5809
tmax.may*site	2	2	138.2296	0.2658	0.7671
tmin.jan*site	2	2	130.6622	0.2512	0.7783
tmin.feb*site	2	2	699.6864	1.3452	0.2650
tmin.mar*site	2	2	659.8999	1.2687	0.2855
tmin.apr*site	2	2	126.6201	0.2434	0.7844
tmin.may*site	2	2	743.9775	1.4304	0.2439
prcp.jan*site	2	2	2278.9137	4.3814	0.0149 *
prcp.feb*site	2	2	1109.0833	2.1323	0.1238
prcp.mar*site	2	2	367.1614	0.7059	0.4960
prcp.apr*site	2	2	964.2421	1.8539	0.1618
prcp.may*site	2	2	195.8225	0.3765	0.6872
site	2	2	1441.9111	2.7722	0.0672

Scaled Estimates

Nominal factors expanded to all levels

APPENDIX B

Response X50th

Actual by Predicted Plot

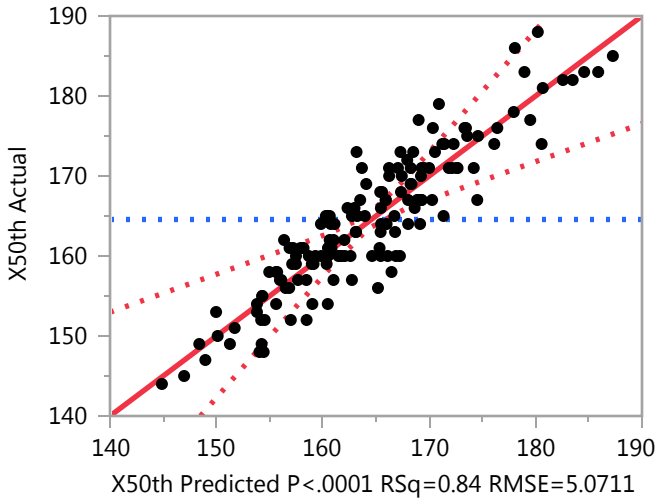

Summary of Fit

RSquare	0.836985
RSquare Adj	0.678259
Root Mean Square Error	5.071092
Mean of Response	164.5629
Observations (or Sum Wgts)	151

Analysis of Variance

Source	DF	Sum of Squares	Mean Square	F Ratio
Model	74	10034.738	135.605	5.2732
Error	76	1954.414	25.716	**Prob > F**
C. Total	150	11989.152		<.0001 *

Parameter Estimates

Term	Estimate	Std Error	t Ratio	Prob>|t|
Intercept	197.33214	20.90056	9.44	<.0001 *
tmax.jan	0.3133667	0.627808	0.50	0.6191
tmax.feb	1.2490442	0.562783	2.22	0.0294 *
tmax.mar	-0.510504	0.521218	-0.98	0.3305
tmax.apr	-0.030113	0.635262	-0.05	0.9623
tmax.may	-1.550924	0.655926	-2.36	0.0206 *
tmax.jun	-1.412993	0.718126	-1.97	0.0528
tmax.jul	0.0253211	0.665297	0.04	0.9697
tmax.aug	0.6078142	0.649819	0.94	0.3526
tmin.jan	0.6668363	0.495831	1.34	0.1827

Response X50th

Parameter Estimates

Term	Estimate	Std Error	t Ratio	Prob>|t|
tmin.feb	-0.596708	0.515088	-1.16	0.2503
tmin.mar	0.0047488	0.506526	0.01	0.9925
tmin.apr	0.7986832	0.738148	1.08	0.2827
tmin.may	-2.064006	0.899988	-2.29	0.0246 *
tmin.jun	-0.273532	0.887645	-0.31	0.7588
tmin.jul	0.8330537	0.793821	1.05	0.2973
tmin.aug	0.3713569	0.803742	0.46	0.6454
prcp.jan	-0.00931	0.10619	-0.09	0.9304
prcp.feb	-0.022891	0.081986	-0.28	0.7808
prcp.mar	-0.093114	0.066714	-1.40	0.1669
prcp.apr	0.1543429	0.082401	1.87	0.0649
prcp.may	0.0706614	0.106506	0.66	0.5090
prcp.jun	0.0309562	0.089007	0.35	0.7290
prcp.jul	0.1124453	0.092958	1.21	0.2302
prcp.aug	0.1576224	0.0838	1.88	0.0638
(tmax.jan-2.34132)*site[Colona]	-0.035367	0.967357	-0.04	0.9709
(tmax.jan-2.34132)*site[Durango]	0.9369389	0.806954	1.16	0.2492
(tmax.feb-3.69126)*site[Colona]	0.9252243	0.96672	0.96	0.3416
(tmax.feb-3.69126)*site[Durango]	-0.758952	0.675399	-1.12	0.2647
(tmax.mar-6.17911)*site[Colona]	-0.177965	0.770448	-0.23	0.8179
(tmax.mar-6.17911)*site[Durango]	0.2709333	0.749401	0.36	0.7187
(tmax.apr-10.6453)*site[Colona]	0.6750241	1.021518	0.66	0.5107
(tmax.apr-10.6453)*site[Durango]	-0.062158	0.848653	-0.07	0.9418
(tmax.may-16.2904)*site[Colona]	0.7389186	1.065288	0.69	0.4900
(tmax.may-16.2904)*site[Durango]	-0.924235	0.864199	-1.07	0.2882
(tmax.jun-22.038)*site[Colona]	-0.623701	1.201426	-0.52	0.6052
(tmax.jun-22.038)*site[Durango]	0.2494664	0.817012	0.31	0.7609
(tmax.jul-24.6205)*site[Colona]	-0.699904	1.059946	-0.66	0.5110
(tmax.jul-24.6205)*site[Durango]	0.7762964	0.896904	0.87	0.3895
(tmax.aug-23.3124)*site[Colona]	-2.040768	0.985852	-2.07	0.0418 *
(tmax.aug-23.3124)*site[Durango]	2.116972	0.877634	2.41	0.0183 *
(tmin.jan+14.4807)*site[Colona]	-0.129601	0.851096	-0.15	0.8794
(tmin.jan+14.4807)*site[Durango]	-0.370469	0.575026	-0.64	0.5213
(tmin.feb+12.8394)*site[Colona]	-0.530622	0.851165	-0.62	0.5349
(tmin.feb+12.8394)*site[Durango]	0.5883277	0.586965	1.00	0.3194
(tmin.mar+9.44288)*site[Colona]	-0.4067	0.795277	-0.51	0.6106
(tmin.mar+9.44288)*site[Durango]	0.008381	0.631735	0.01	0.9894
(tmin.apr+4.62791)*site[Colona]	1.0944407	1.24048	0.88	0.3804

Response X50th

Parameter Estimates

Term	Estimate	Std Error	t Ratio	Prob>|t|
(tmin.apr+4.62791)*site[Durango]	-1.308504	0.885442	-1.48	0.1436
(tmin.may+0.18882)*site[Colona]	-2.657288	1.531224	-1.74	0.0867
(tmin.may+0.18882)*site[Durango]	2.1535723	1.062526	2.03	0.0462 *
(tmin.jun-3.14379)*site[Colona]	-0.07806	1.384989	-0.06	0.9552
(tmin.jun-3.14379)*site[Durango]	-0.284161	1.100298	-0.26	0.7969
(tmin.jul-6.41007)*site[Colona]	0.6176639	1.306463	0.47	0.6377
(tmin.jul-6.41007)*site[Durango]	-1.86637	0.98025	-1.90	0.0607
(tmin.aug-6.07391)*site[Colona]	1.4908229	1.287702	1.16	0.2506
(tmin.aug-6.07391)*site[Durango]	-0.501068	1.037551	-0.48	0.6305
(prcp.jan-13.0782)*site[Colona]	0.0770073	0.152521	0.50	0.6151
(prcp.jan-13.0782)*site[Durango]	-0.033715	0.140419	-0.24	0.8109
(prcp.feb-15.1946)*site[Colona]	0.0955975	0.113244	0.84	0.4012
(prcp.feb-15.1946)*site[Durango]	-0.126502	0.110313	-1.15	0.2551
(prcp.mar-18.5581)*site[Colona]	0.1464482	0.099657	1.47	0.1458
(prcp.mar-18.5581)*site[Durango]	-0.059068	0.087547	-0.67	0.5019
(prcp.apr-17.0011)*site[Colona]	0.0498796	0.120691	0.41	0.6806
(prcp.apr-17.0011)*site[Durango]	0.0098279	0.117836	0.08	0.9338
(prcp.may-13.4067)*site[Colona]	-0.190435	0.148348	-1.28	0.2031
(prcp.may-13.4067)*site[Durango]	0.0141585	0.157102	0.09	0.9284
(prcp.jun-10.5593)*site[Colona]	-0.099551	0.123287	-0.81	0.4219
(prcp.jun-10.5593)*site[Durango]	0.0462209	0.115346	0.40	0.6898
(prcp.jul-19.6642)*site[Colona]	-0.068005	0.13696	-0.50	0.6210
(prcp.jul-19.6642)*site[Durango]	0.1283032	0.127344	1.01	0.3169
(prcp.aug-21.9434)*site[Colona]	-0.003795	0.127355	-0.03	0.9763
(prcp.aug-21.9434)*site[Durango]	-0.047409	0.117204	-0.40	0.6870
site[Colona]	10.056593	4.602592	2.18	0.0320 *
site[Durango]	-11.77129	3.608814	-3.26	0.0017 *

Effect Tests

Source	Nparm	DF	Sum of Squares	F Ratio	Prob > F
tmax.jan	1	1	6.40700	0.2491	0.6191
tmax.feb	1	1	126.67067	4.9258	0.0294 *
tmax.mar	1	1	24.66962	0.9593	0.3305
tmax.apr	1	1	0.05778	0.0022	0.9623
tmax.may	1	1	143.77216	5.5908	0.0206 *
tmax.jun	1	1	99.55944	3.8715	0.0528
tmax.jul	1	1	0.03725	0.0014	0.9697
tmax.aug	1	1	22.49880	0.8749	0.3526

Response X50th

Effect Tests

Source	Nparm	DF	Sum of Squares	F Ratio	Prob > F
tmin.jan	1	1	46.51289	1.8087	0.1827
tmin.feb	1	1	34.51155	1.3420	0.2503
tmin.mar	1	1	0.00226	0.0001	0.9925
tmin.apr	1	1	30.10683	1.1707	0.2827
tmin.may	1	1	135.25443	5.2595	0.0246 *
tmin.jun	1	1	2.44197	0.0950	0.7588
tmin.jul	1	1	28.32072	1.1013	0.2973
tmin.aug	1	1	5.48976	0.2135	0.6454
prcp.jan	1	1	0.19766	0.0077	0.9304
prcp.feb	1	1	2.00467	0.0780	0.7808
prcp.mar	1	1	50.09507	1.9480	0.1669
prcp.apr	1	1	90.22207	3.5084	0.0649
prcp.may	1	1	11.31934	0.4402	0.5090
prcp.jun	1	1	3.11063	0.1210	0.7290
prcp.jul	1	1	37.62814	1.4632	0.2302
prcp.aug	1	1	90.98106	3.5379	0.0638
tmax.jan*site	2	2	45.89616	0.8924	0.4139
tmax.feb*site	2	2	34.33954	0.6677	0.5159
tmax.mar*site	2	2	3.37396	0.0656	0.9366
tmax.apr*site	2	2	16.48995	0.3206	0.7267
tmax.may*site	2	2	29.41529	0.5719	0.5668
tmax.jun*site	2	2	6.93242	0.1348	0.8741
tmax.jul*site	2	2	19.82041	0.3854	0.6815
tmax.aug*site	2	2	170.06037	3.3065	0.0420 *
tmin.jan*site	2	2	25.10996	0.4882	0.6156
tmin.feb*site	2	2	26.04499	0.5064	0.6047
tmin.mar*site	2	2	8.99005	0.1748	0.8400
tmin.apr*site	2	2	56.24147	1.0935	0.3403
tmin.may*site	2	2	113.92028	2.2150	0.1162
tmin.jun*site	2	2	2.90504	0.0565	0.9451
tmin.jul*site	2	2	112.20584	2.1816	0.1199
tmin.aug*site	2	2	36.18554	0.7036	0.4980
prcp.jan*site	2	2	6.57422	0.1278	0.8802
prcp.feb*site	2	2	38.67859	0.7520	0.4749
prcp.mar*site	2	2	55.58789	1.0808	0.3445
prcp.apr*site	2	2	8.23971	0.1602	0.8523
prcp.may*site	2	2	55.82016	1.0853	0.3430

Response X50th

Effect Tests

Source	Nparm	DF	Sum of Squares	F Ratio	Prob > F
prcp.jun*site	2	2	17.26890	0.3358	0.7158
prcp.jul*site	2	2	26.12938	0.5080	0.6037
prcp.aug*site	2	2	7.12723	0.1386	0.8708
site	2	2	278.06214	5.4064	0.0064 *

Scaled Estimates

Nominal factors expanded to all levels

Continuous factors centered by mean, scaled by range/2

Term	Scaled Estimate	Std Error	t Ratio	Prob
Intercept	166.34954	2.688717	61.87	<.00
tmax.jan	1.9529821	3.912663	0.50	0.61
tmax.feb	6.9299647	3.122443	2.22	0.02
tmax.mar	-2.891756	2.952445	-0.98	0.33
tmax.apr	-0.187653	3.958743	-0.05	0.96
tmax.may	-8.017275	3.390712	-2.36	0.02
tmax.jun	-7.719652	3.923359	-1.97	0.05
tmax.jul	0.1114947	2.929454	0.04	0.96
tmax.aug	2.6136011	2.794224	0.94	0.35
tmin.jan	7.062012	5.251015	1.34	0.18
tmin.feb	-5.744383	4.958641	-1.16	0.25
tmin.mar	0.0419882	4.478672	0.01	0.99
tmin.apr	5.2175586	4.822102	1.08	0.28
tmin.may	-12.72027	5.54654	-2.29	0.02
tmin.jun	-1.810782	5.876209	-0.31	0.75
tmin.jul	5.0480367	4.810297	1.05	0.29
tmin.aug	2.2655765	4.903473	0.46	0.64
prcp.jan	-0.172383	1.966224	-0.09	0.93
prcp.feb	-0.530125	1.898709	-0.28	0.78
prcp.mar	-2.335349	1.673231	-1.40	0.16
prcp.apr	3.7755212	2.015682	1.87	0.06
prcp.may	1.2696257	1.913668	0.66	0.50
prcp.jun	0.6660747	1.91514	0.35	0.72
prcp.jul	2.8292688	2.338941	1.21	0.23
prcp.aug	3.9583561	2.104461	1.88	0.06
(tmax.jan-2.34132)*site[Colona]	-0.220416	6.02882	-0.04	0.97
(tmax.jan-2.34132)*site[Durango]	5.8392451	5.029148	1.16	0.24
(tmax.jan-2.34132)*site[Placerville]	-5.618829	5.496781	-1.02	0.30

APPENDIX C

Response Moving.var.end

Actual by Predicted Plot

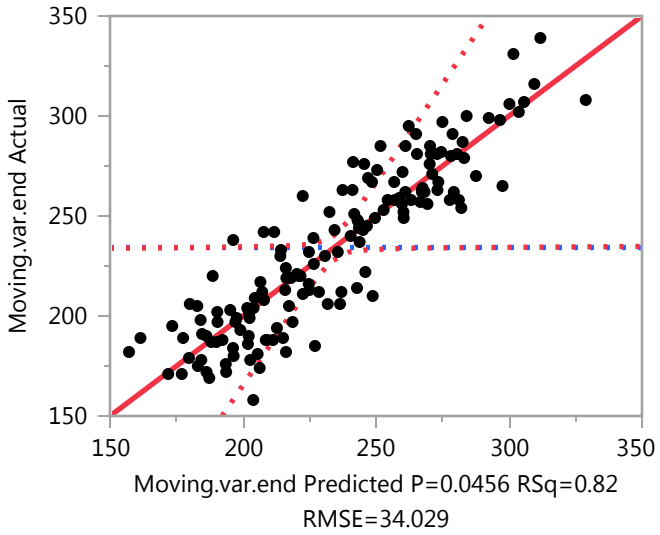

Summary of Fit

RSquare	0.81504
RSquare Adj	0.306401
Root Mean Square Error	34.0289
Mean of Response	234.2384
Observations (or Sum Wgts)	151

Analysis of Variance

Source	DF	Sum of Squares	Mean Square	F Ratio
Model	110	204106.79	1855.52	1.6024
Error	40	46318.63	1157.97	**Prob > F**
C. Total	150	250425.42		0.0456 *

Parameter Estimates

Term	Estimate	Std Error	t Ratio	Prob>|t|
Intercept	339.16279	223.1356	1.52	0.1364
tmax.jan	3.646697	5.236455	0.70	0.4902
tmax.feb	-5.909508	5.46148	-1.08	0.2857
tmax.mar	-6.060984	5.211559	-1.16	0.2517
tmax.apr	5.8990729	6.681523	0.88	0.3826
tmax.may	-7.030969	6.437041	-1.09	0.2813
tmax.jun	-1.175905	5.937652	-0.20	0.8440
tmax.jul	1.5736576	6.527425	0.24	0.8107
tmax.aug	2.7347588	6.884228	0.40	0.6933

Response Moving.var.end

Parameter Estimates

Term	Estimate	Std Error	t Ratio	Prob>|t|
tmax.sep	-8.731546	4.971707	-1.76	0.0867
tmax.oct	-1.750598	3.350934	-0.52	0.6043
tmax.nov	10.563749	5.19146	2.03	0.0485 *
tmax.dec	-9.521954	4.730385	-2.01	0.0509
tmin.jan	-3.225269	4.171457	-0.77	0.4440
tmin.feb	6.5491514	4.512202	1.45	0.1545
tmin.mar	0.3019772	5.24649	0.06	0.9544
tmin.apr	-5.290654	7.500747	-0.71	0.4847
tmin.may	0.7934468	8.888574	0.09	0.9293
tmin.jun	1.4178194	7.963165	0.18	0.8596
tmin.jul	10.600372	8.257889	1.28	0.2066
tmin.aug	-12.22809	8.405407	-1.45	0.1535
tmin.sep	7.7518036	7.369086	1.05	0.2991
tmin.oct	6.758536	5.452262	1.24	0.2224
tmin.nov	-10.63342	5.966287	-1.78	0.0823
tmin.dec	4.1554484	5.632971	0.74	0.4650
prcp.jan	1.1798891	1.042069	1.13	0.2643
prcp.feb	-0.004316	0.803129	-0.01	0.9957
prcp.mar	-1.259527	0.659136	-1.91	0.0632
prcp.apr	-0.166729	0.834617	-0.20	0.8427
prcp.may	0.0858308	0.958197	0.09	0.9291
prcp.jun	-0.227804	1.010841	-0.23	0.8228
prcp.jul	-0.193606	0.845631	-0.23	0.8201
prcp.aug	1.2473291	0.892479	1.40	0.1699
prcp.sep	1.0652018	0.624151	1.71	0.0956
prcp.oct	-0.199299	0.548712	-0.36	0.7184
prcp.nov	0.8449281	0.905602	0.93	0.3564
prcp.dec	-0.7738	0.829712	-0.93	0.3566
(tmax.jan-2.34132)*site[Colona]	-5.661636	7.982687	-0.71	0.4823
(tmax.jan-2.34132)*site[Durango]	-4.186914	6.564342	-0.64	0.5272
(tmax.feb-3.69126)*site[Colona]	-7.096468	8.800835	-0.81	0.4248
(tmax.feb-3.69126)*site[Durango]	12.47398	6.814341	1.83	0.0746
(tmax.mar-6.17911)*site[Colona]	-0.998783	7.314014	-0.14	0.8921
(tmax.mar-6.17911)*site[Durango]	-4.371271	8.219498	-0.53	0.5978
(tmax.apr-10.6453)*site[Colona]	-3.406522	9.089519	-0.37	0.7098
(tmax.apr-10.6453)*site[Durango]	14.074692	10.11534	1.39	0.1718
(tmax.may-16.2904)*site[Colona]	-0.891892	10.31815	-0.09	0.9315
(tmax.may-16.2904)*site[Durango]	-9.735314	7.897386	-1.23	0.2249

Response Moving.var.end

Parameter Estimates

Term	Estimate	Std Error	t Ratio	Prob>|t|
(tmax.jun-22.038)*site[Colona]	12.199914	9.625752	1.27	0.2123
(tmax.jun-22.038)*site[Durango]	-7.212912	6.877112	-1.05	0.3006
(tmax.jul-24.6205)*site[Colona]	-12.03311	10.64282	-1.13	0.2649
(tmax.jul-24.6205)*site[Durango]	18.660426	8.685659	2.15	0.0378 *
(tmax.aug-23.3124)*site[Colona]	-0.815825	11.49084	-0.07	0.9438
(tmax.aug-23.3124)*site[Durango]	6.6097727	8.667501	0.76	0.4502
(tmax.sep-19.9138)*site[Colona]	0.5080432	7.646149	0.07	0.9474
(tmax.sep-19.9138)*site[Durango]	-7.414811	6.568614	-1.13	0.2657
(tmax.oct-14.2443)*site[Colona]	3.9574805	5.22546	0.76	0.4533
(tmax.oct-14.2443)*site[Durango]	-5.393212	4.601172	-1.17	0.2481
(tmax.nov-7.03187)*site[Colona]	13.481256	8.257177	1.63	0.1104
(tmax.nov-7.03187)*site[Durango]	-7.910754	7.495222	-1.06	0.2976
(tmax.dec-2.64597)*site[Colona]	-3.069954	7.453339	-0.41	0.6826
(tmax.dec-2.64597)*site[Durango]	7.8197151	5.634225	1.39	0.1729
(tmin.jan+14.4807)*site[Colona]	5.5422189	7.008058	0.79	0.4337
(tmin.jan+14.4807)*site[Durango]	5.5713498	4.813875	1.16	0.2540
(tmin.feb+12.8394)*site[Colona]	4.808277	7.262003	0.66	0.5117
(tmin.feb+12.8394)*site[Durango]	-11.00688	5.072801	-2.17	0.0360 *
(tmin.mar+9.44288)*site[Colona]	6.4770624	7.790036	0.83	0.4107
(tmin.mar+9.44288)*site[Durango]	3.9767117	6.38199	0.62	0.5367
(tmin.apr+4.62791)*site[Colona]	-2.821789	11.12093	-0.25	0.8010
(tmin.apr+4.62791)*site[Durango]	-10.02028	9.757899	-1.03	0.3106
(tmin.may+0.18882)*site[Colona]	24.320752	14.80953	1.64	0.1084
(tmin.may+0.18882)*site[Durango]	-0.305915	10.13031	-0.03	0.9761
(tmin.jun-3.14379)*site[Colona]	-16.75564	11.62816	-1.44	0.1574
(tmin.jun-3.14379)*site[Durango]	-3.659743	9.552892	-0.38	0.7037
(tmin.jul-6.41007)*site[Colona]	5.343371	12.69534	0.42	0.6761
(tmin.jul-6.41007)*site[Durango]	-8.995928	10.00288	-0.90	0.3739
(tmin.aug-6.07391)*site[Colona]	0.9956633	12.57396	0.08	0.9373
(tmin.aug-6.07391)*site[Durango]	7.8808906	11.27618	0.70	0.4887
(tmin.sep-2.319)*site[Colona]	1.8050942	10.02795	0.18	0.8581
(tmin.sep-2.319)*site[Durango]	8.1393729	10.22581	0.80	0.4308
(tmin.oct+2.68914)*site[Colona]	-3.370944	8.331917	-0.40	0.6879
(tmin.oct+2.68914)*site[Durango]	5.1370609	7.470733	0.69	0.4957
(tmin.nov+8.98778)*site[Colona]	-15.27814	10.24624	-1.49	0.1438
(tmin.nov+8.98778)*site[Durango]	9.8441944	7.723404	1.27	0.2098
(tmin.dec+13.6122)*site[Colona]	4.8650224	8.455522	0.58	0.5683
(tmin.dec+13.6122)*site[Durango]	-12.71955	6.972139	-1.82	0.0756

Response Moving.var.end

Parameter Estimates

Term	Estimate	Std Error	t Ratio	Prob>|t|
(prcp.jan-13.0782)*site[Colona]	-1.499473	1.410639	-1.06	0.2942
(prcp.jan-13.0782)*site[Durango]	-1.457466	1.297355	-1.12	0.2680
(prcp.feb-15.1946)*site[Colona]	0.962803	0.996516	0.97	0.3398
(prcp.feb-15.1946)*site[Durango]	1.4614497	1.016727	1.44	0.1584
(prcp.mar-18.5581)*site[Colona]	0.1021801	0.915324	0.11	0.9117
(prcp.mar-18.5581)*site[Durango]	-0.771728	1.032604	-0.75	0.4592
(prcp.apr-17.0011)*site[Colona]	-1.25401	1.193915	-1.05	0.2999
(prcp.apr-17.0011)*site[Durango]	2.4555054	1.287439	1.91	0.0637
(prcp.may-13.4067)*site[Colona]	-0.963994	1.321433	-0.73	0.4699
(prcp.may-13.4067)*site[Durango]	-0.563973	1.314996	-0.43	0.6703
(prcp.jun-10.5593)*site[Colona]	0.3836751	1.308533	0.29	0.7709
(prcp.jun-10.5593)*site[Durango]	0.9945504	1.24103	0.80	0.4276
(prcp.jul-19.6642)*site[Colona]	1.2613941	1.211416	1.04	0.3040
(prcp.jul-19.6642)*site[Durango]	-0.549605	1.169491	-0.47	0.6409
(prcp.aug-21.9434)*site[Colona]	-0.103734	1.275544	-0.08	0.9356
(prcp.aug-21.9434)*site[Durango]	-0.055277	1.295994	-0.04	0.9662
(prcp.sep-19.8212)*site[Colona]	-0.189095	0.894981	-0.21	0.8337
(prcp.sep-19.8212)*site[Durango]	-0.370596	0.788889	-0.47	0.6411
(prcp.oct-18.6979)*site[Colona]	0.7712231	0.798735	0.97	0.3401
(prcp.oct-18.6979)*site[Durango]	-0.217915	0.696986	-0.31	0.7562
(prcp.nov-14.6841)*site[Colona]	1.8169473	1.127046	1.61	0.1148
(prcp.nov-14.6841)*site[Durango]	-0.828116	1.246418	-0.66	0.5102
(prcp.dec-13.3255)*site[Colona]	-1.091375	1.147634	-0.95	0.3473
(prcp.dec-13.3255)*site[Durango]	0.0746403	1.005518	0.07	0.9412
site[Colona]	-46.83476	49.71081	-0.94	0.3518
site[Durango]	2.8536071	45.0754	0.06	0.9498

Effect Tests

Source	Nparm	DF	Sum of Squares	F Ratio	Prob > F
tmax.jan	1	1	561.5913	0.4850	0.4902
tmax.feb	1	1	1355.7440	1.1708	0.2857
tmax.mar	1	1	1566.1984	1.3525	0.2517
tmax.apr	1	1	902.6352	0.7795	0.3826
tmax.may	1	1	1381.5085	1.1930	0.2813
tmax.jun	1	1	45.4162	0.0392	0.8440
tmax.jul	1	1	67.3027	0.0581	0.8107
tmax.aug	1	1	182.7356	0.1578	0.6933
tmax.sep	1	1	3571.6343	3.0844	0.0867

Response Moving.var.end

Effect Tests

Source	Nparm	DF	Sum of Squares	F Ratio	Prob > F
tmax.oct	1	1	316.0361	0.2729	0.6043
tmax.nov	1	1	4794.6057	4.1405	0.0485 *
tmax.dec	1	1	4691.9673	4.0519	0.0509
tmin.jan	1	1	692.2326	0.5978	0.4440
tmin.feb	1	1	2439.4314	2.1067	0.1545
tmin.mar	1	1	3.8362	0.0033	0.9544
tmin.apr	1	1	576.1100	0.4975	0.4847
tmin.may	1	1	9.2271	0.0080	0.9293
tmin.jun	1	1	36.7085	0.0317	0.8596
tmin.jul	1	1	1908.0940	1.6478	0.2066
tmin.aug	1	1	2450.7303	2.1164	0.1535
tmin.sep	1	1	1281.3681	1.1066	0.2991
tmin.oct	1	1	1779.2930	1.5366	0.2224
tmin.nov	1	1	3678.1863	3.1764	0.0823
tmin.dec	1	1	630.1681	0.5442	0.4650
prcp.jan	1	1	1484.5178	1.2820	0.2643
prcp.feb	1	1	0.0334	0.0000	0.9957
prcp.mar	1	1	4228.2478	3.6514	0.0632
prcp.apr	1	1	46.2108	0.0399	0.8427
prcp.may	1	1	9.2912	0.0080	0.9291
prcp.jun	1	1	58.8103	0.0508	0.8228
prcp.jul	1	1	60.6977	0.0524	0.8201
prcp.aug	1	1	2261.8408	1.9533	0.1699
prcp.sep	1	1	3372.7217	2.9126	0.0956
prcp.oct	1	1	152.7630	0.1319	0.7184
prcp.nov	1	1	1007.9992	0.8705	0.3564
prcp.dec	1	1	1007.1593	0.8698	0.3566
tmax.jan*site	2	2	1978.8928	0.8545	0.4331
tmax.feb*site	2	2	3982.8899	1.7198	0.1921
tmax.mar*site	2	2	811.4330	0.3504	0.7066
tmax.apr*site	2	2	2505.8116	1.0820	0.3486
tmax.may*site	2	2	2713.3029	1.1716	0.3203
tmax.jun*site	2	2	2105.6838	0.9092	0.4110
tmax.jul*site	2	2	5510.3683	2.3793	0.1056
tmax.aug*site	2	2	1040.3839	0.4492	0.6413
tmax.sep*site	2	2	1976.3203	0.8534	0.4336
tmax.oct*site	2	2	1593.3972	0.6880	0.5084

Response Moving.var.end

Effect Tests

Source	Nparm	DF	Sum of Squares	F Ratio	Prob > F
tmax.nov*site	2	2	3106.1755	1.3412	0.2730
tmax.dec*site	2	2	2328.1236	1.0053	0.3750
tmin.jan*site	2	2	5478.7283	2.3657	0.1069
tmin.feb*site	2	2	5647.0821	2.4384	0.1002
tmin.mar*site	2	2	1990.5338	0.8595	0.4310
tmin.apr*site	2	2	2000.8891	0.8640	0.4292
tmin.may*site	2	2	4501.4390	1.9437	0.1565
tmin.jun*site	2	2	3347.5545	1.4454	0.2477
tmin.jul*site	2	2	937.1257	0.4046	0.6699
tmin.aug*site	2	2	872.3010	0.3767	0.6886
tmin.sep*site	2	2	1093.0274	0.4720	0.6272
tmin.oct*site	2	2	547.5881	0.2364	0.7905
tmin.nov*site	2	2	2659.3545	1.1483	0.3274
tmin.dec*site	2	2	3907.9316	1.6874	0.1979
prcp.jan*site	2	2	3581.8907	1.5466	0.2254
prcp.feb*site	2	2	3795.7541	1.6390	0.2070
prcp.mar*site	2	2	903.2698	0.3900	0.6796
prcp.apr*site	2	2	4278.2205	1.8473	0.1709
prcp.may*site	2	2	1364.8252	0.5893	0.5594
prcp.jun*site	2	2	918.0756	0.3964	0.6753
prcp.jul*site	2	2	1257.5780	0.5430	0.5852
prcp.aug*site	2	2	20.5441	0.0089	0.9912
prcp.sep*site	2	2	448.4794	0.1936	0.8247
prcp.oct*site	2	2	1086.2613	0.4690	0.6290
prcp.nov*site	2	2	3085.4221	1.3323	0.2753
prcp.dec*site	2	2	1071.9814	0.4629	0.6328
site	2	2	2149.1314	0.9280	0.4037

Scaled Estimates

Nominal factors expanded to all levels

Continuous factors centered by mean, scaled by range/2

Term	Scaled Estimate	Std Error	t Ratio	Prob
Intercept	215.54221	30.62778	7.04	<.00
tmax.jan	22.727157	32.63494	0.70	0.49
tmax.feb	-32.78722	30.30146	-1.08	0.28
tmax.mar	-34.33254	29.52096	-1.16	0.25
tmax.apr	36.761056	41.63702	0.88	0.38

APPENDIX D

Least Squares Fit

Weight: Number of Years

Response Beginning

Whole Model

Actual by Predicted Plot

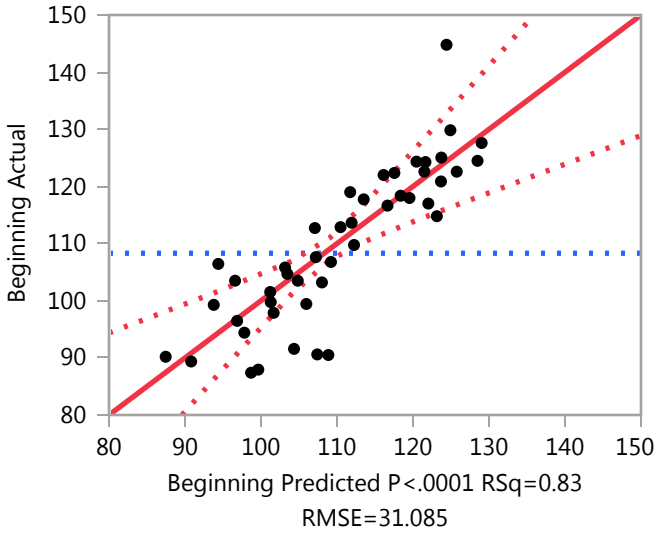

Summary of Fit

RSquare	0.833933
RSquare Adj	0.729372
Root Mean Square Error	31.08464
Mean of Response	108.3086
Observations (or Sum Wgts)	1114

Analysis of Variance

Source	DF	Sum of Squares	Mean Square	F Ratio
Model	17	131009.72	7706.45	7.9756
Error	27	26088.88	966.25	**Prob > F**
C. Total	44	157098.59		<.0001 *

Parameter Estimates

Term	Estimate	Std Error	t Ratio	Prob>|t|
Intercept	13.103391	36.35097	0.36	0.7213
Drainage Area	-0.003918	0.001888	-2.07	0.0476 *
Average Slope (%)	0.0582592	0.186948	0.31	0.7577
Average Elevation (m)	0.0405672	0.02355	1.72	0.0964
A(2250)	-0.283368	0.10872	-2.61	0.0147 *

Least Squares Fit

Response Beginning

Whole Model

Parameter Estimates

Term	Estimate	Std Error	t Ratio	Prob>|t|
Dominant Aspect[E]	-4.527993	5.728389	-0.79	0.4362
Dominant Aspect[N]	0.7344133	3.319721	0.22	0.8266
Dominant Aspect[NE]	4.263393	9.860006	0.43	0.6689
Dominant Aspect[NW]	1.19212	3.81041	0.31	0.7568
Dominant Aspect[S]	-1.844365	3.597141	-0.51	0.6123
Dominant Aspect[SE]	-5.823256	5.448996	-1.07	0.2947
Dominant Aspect[SW]	5.4001374	4.487761	1.20	0.2393
Rippability Index[Marginally Rippable]	0.4833107	2.413786	0.20	0.8428
Rippability Index[Non-Rippable]	-4.606918	2.671438	-1.72	0.0960
Landcover[Alpine]	-0.3845	9.676983	-0.04	0.9686
Landcover[Alpine/Forrested]	-4.568528	4.575333	-1.00	0.3269
Landcover[Forrested]	0.8361671	3.547173	0.24	0.8154
Average Annual Precipitaiton (mm)	-0.000467	0.041999	-0.01	0.9912

Effect Tests

Source	Nparm	DF	Sum of Squares	F Ratio	Prob > F
Drainage Area	1	1	4160.1203	4.3054	0.0476 *
Average Slope (%)	1	1	93.8379	0.0971	0.7577
Average Elevation (m)	1	1	2867.2792	2.9674	0.0964
A(2250)	1	1	6564.0422	6.7933	0.0147 *
Dominant Aspect	7	7	4414.3539	0.6526	0.7091
Rippability Index	2	2	3199.3992	1.6556	0.2098
Landcover	3	3	2174.0622	0.7500	0.5319
Average Annual Precipitaiton (mm)	1	1	0.1195	0.0001	0.9912

Least Squares Fit

Response Beginning

Whole Model

Residual by Predicted Plot

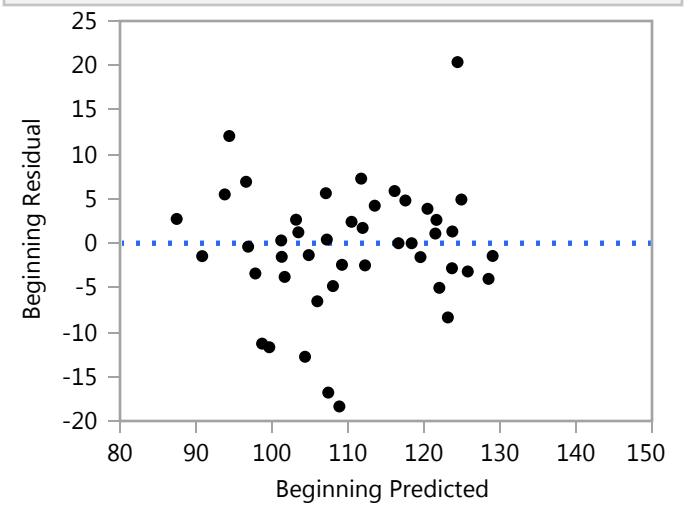

Drainage Area

Leverage Plot

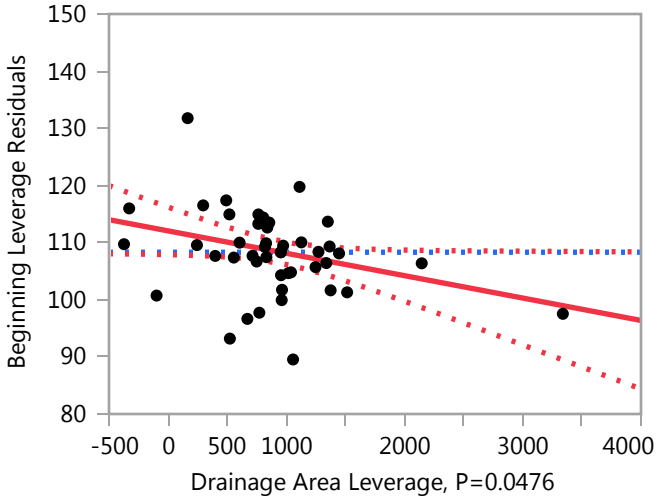

Least Squares Fit

Response Beginning

Average Slope (%)

Leverage Plot

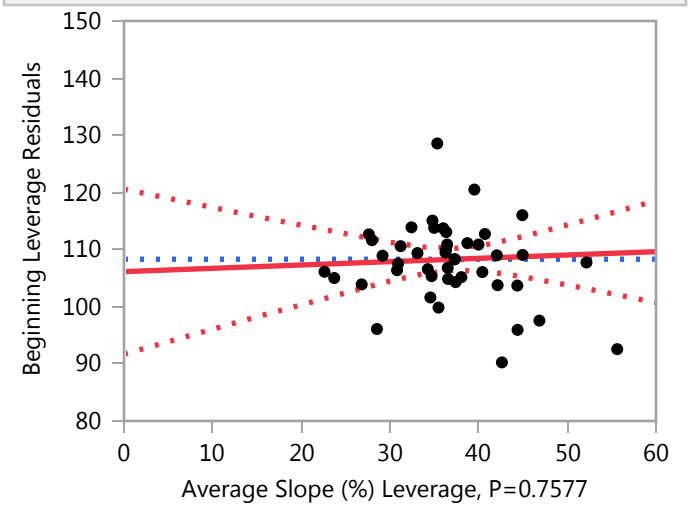

Average Elevation (m)

Leverage Plot

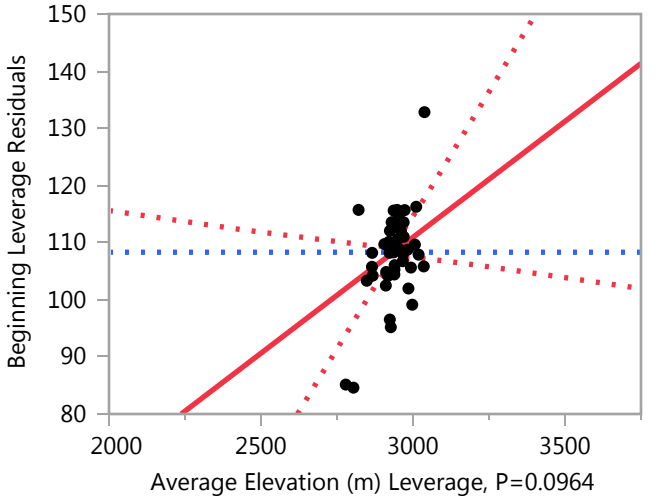

Least Squares Fit

Response Beginning

A(2250)

Leverage Plot

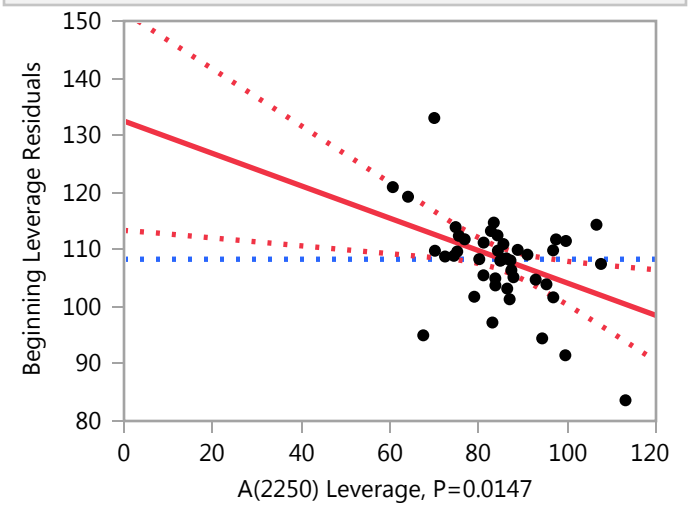

Dominant Aspect

Leverage Plot

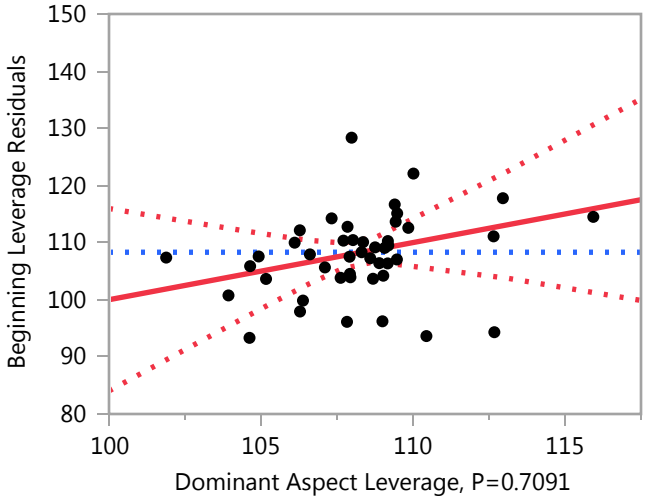

Least Squares Fit

Response Beginning

Dominant Aspect

Least Squares Means Table

Level	Least Sq Mean	Std Error	Mean
E	101.56228	6.007799	114.947
N	106.82468	3.823616	103.479
NE	110.35366	12.198010	116.643
NW	107.28239	4.043411	104.594
S	104.24591	5.402511	116.653
SE	100.26702	7.178948	103.000
SW	111.49041	7.020144	116.667
W	106.69582	5.412290	105.444

Rippability Index

Leverage Plot

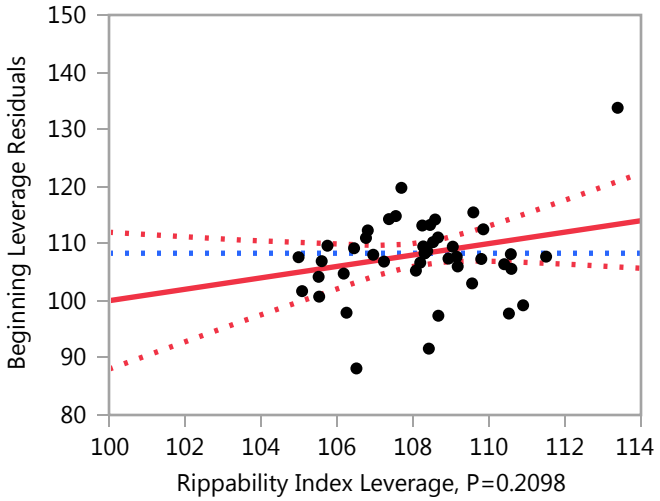

Least Squares Means Table

Level	Least Sq Mean	Std Error	Mean
Marginally Rippable	106.57358	5.8606699	114.045
Non-Rippable	101.48335	5.8736365	113.381
Rippable	110.21388	3.5873615	103.553

Least Squares Fit

Response Beginning

Landcover

Leverage Plot

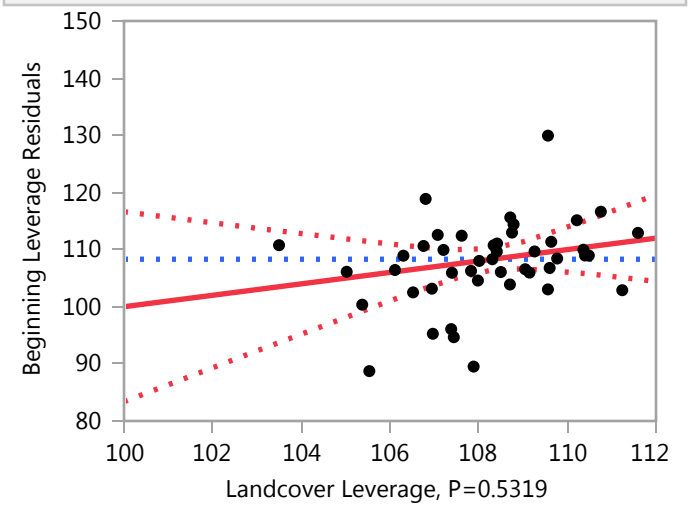

Least Squares Means Table

Level	Least Sq Mean	Std Error	Mean
Alpine	105.70577	12.767962	118.375
Alpine/Forrested	101.52174	4.658852	122.227
Forrested	106.92644	2.790387	107.133
Scrub	110.20713	4.984632	103.595

Least Squares Fit

Response Beginning

Average Annual Precipitaiton (mm)

Leverage Plot

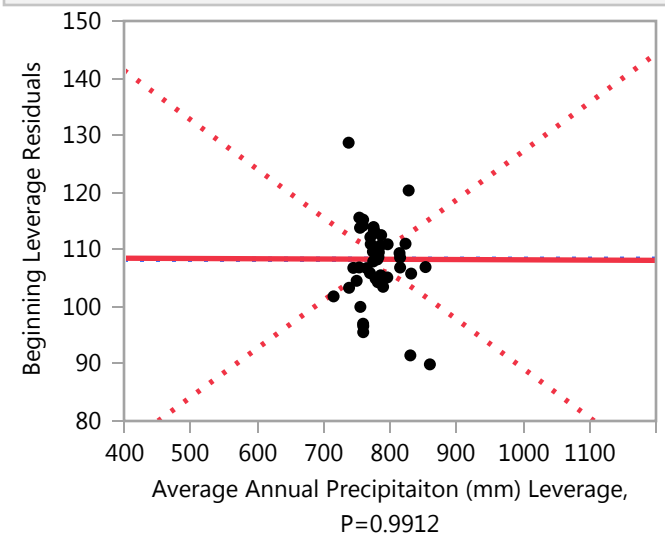

Response Peak

Whole Model

Actual by Predicted Plot

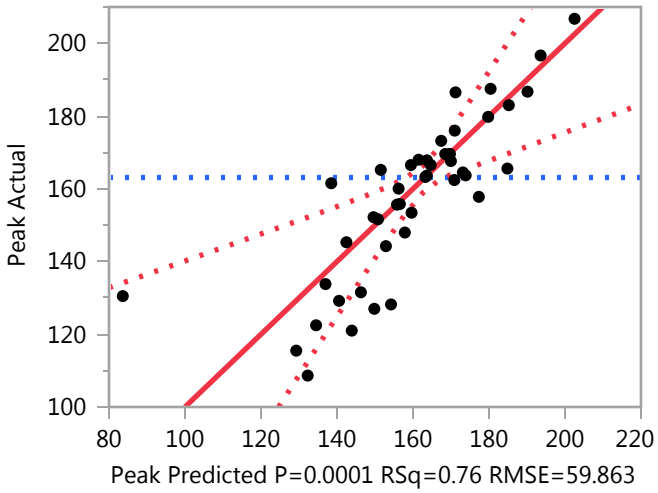

Least Squares Fit

Response Peak

Whole Model

Summary of Fit

RSquare	0.759816
RSquare Adj	0.60859
Root Mean Square Error	59.86273
Mean of Response	163.1104
Observations (or Sum Wgts)	1114

Analysis of Variance

Source	DF	Sum of Squares	Mean Square	F Ratio
Model	17	306085.24	18005.0	5.0244
Error	27	96755.77	3583.5	**Prob > F**
C. Total	44	402841.00		0.0001 *

Parameter Estimates

Term	Estimate	Std Error	t Ratio	Prob>|t|
Intercept	19.85201	70.00463	0.28	0.7789
Drainage Area	0.0003586	0.003636	0.10	0.9222
Average Slope (%)	0.5467666	0.360024	1.52	0.1405
Average Elevation (m)	0.1368482	0.045352	3.02	0.0055 *
A(2250)	-0.749478	0.209374	-3.58	0.0013 *
Dominant Aspect[E]	-16.9279	11.03172	-1.53	0.1365
Dominant Aspect[N]	6.4630462	6.393112	1.01	0.3210
Dominant Aspect[NE]	9.2184123	18.98838	0.49	0.6313
Dominant Aspect[NW]	-10.87642	7.33808	-1.48	0.1499
Dominant Aspect[S]	8.198467	6.927366	1.18	0.2469
Dominant Aspect[SE]	6.6384342	10.49367	0.63	0.5323
Dominant Aspect[SW]	16.07677	8.642522	1.86	0.0738
Rippability Index[Marginally Rippable]	0.8015072	4.648463	0.17	0.8644
Rippability Index[Non-Rippable]	-0.308385	5.144649	-0.06	0.9526
Landcover[Alpine]	14.317867	18.63591	0.77	0.4490
Landcover[Alpine/Forrested]	-6.437836	8.811167	-0.73	0.4713
Landcover[Forrested]	-1.322734	6.831139	-0.19	0.8479
Average Annual Precipitaiton (mm)	-0.273444	0.080882	-3.38	0.0022 *

Least Squares Fit

Response Peak

Whole Model

Effect Tests

Source	Nparm	DF	Sum of Squares	F Ratio	Prob > F
Drainage Area	1	1	34.853	0.0097	0.9222
Average Slope (%)	1	1	8265.203	2.3064	0.1405
Average Elevation (m)	1	1	32628.575	9.1051	0.0055 *
A(2250)	1	1	45918.454	12.8137	0.0013 *
Dominant Aspect	7	7	83889.971	3.3443	0.0107 *
Rippability Index	2	2	141.605	0.0198	0.9805
Landcover	3	3	5281.241	0.4912	0.6913
Average Annual Precipitaiton (mm)	1	1	40958.900	11.4297	0.0022 *

Residual by Predicted Plot

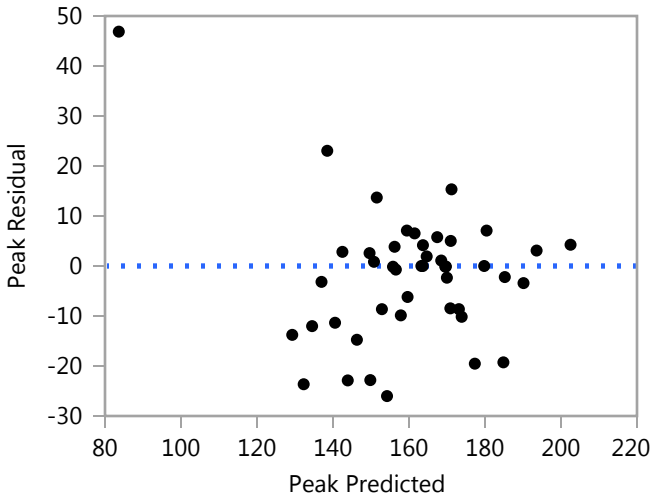

Least Squares Fit

Response Peak

Whole Model

Residual by Predicted Plot

Drainage Area

Leverage Plot

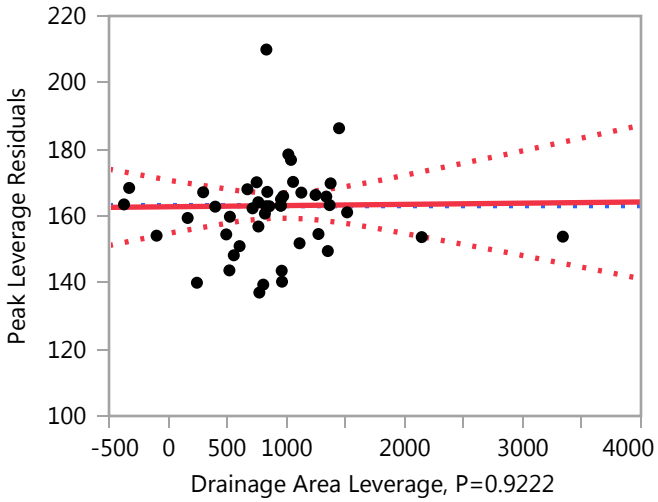

Average Slope (%)

Leverage Plot

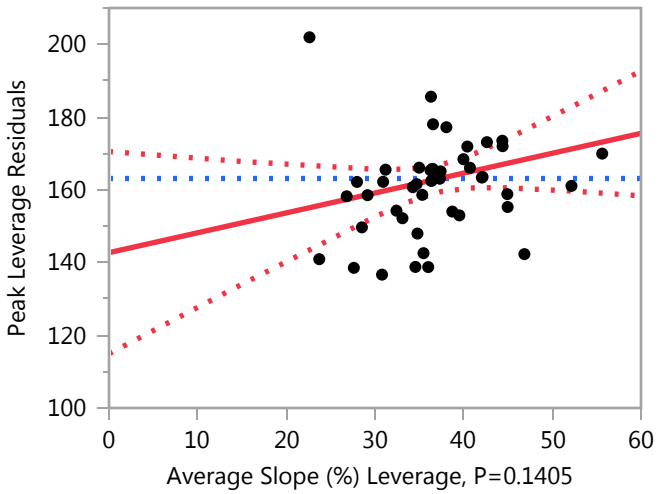

Least Squares Fit

Response Peak

Average Elevation (m)

Leverage Plot

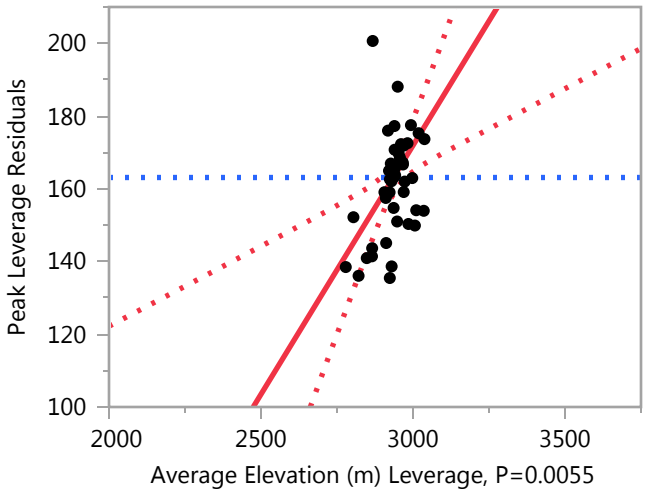

A(2250)

Leverage Plot

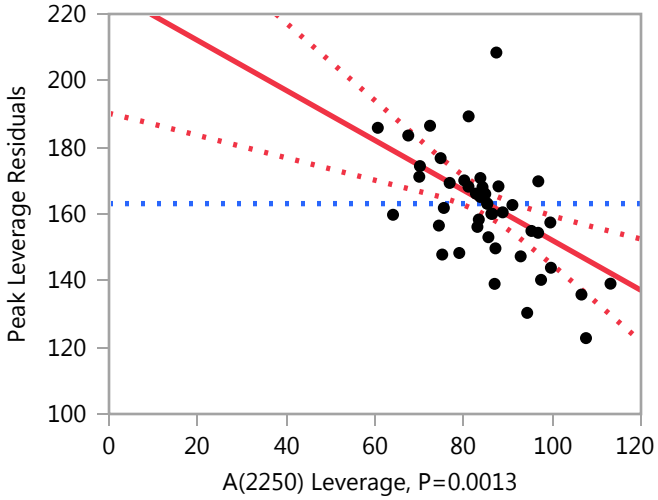

Least Squares Fit

Response Peak

Dominant Aspect

Leverage Plot

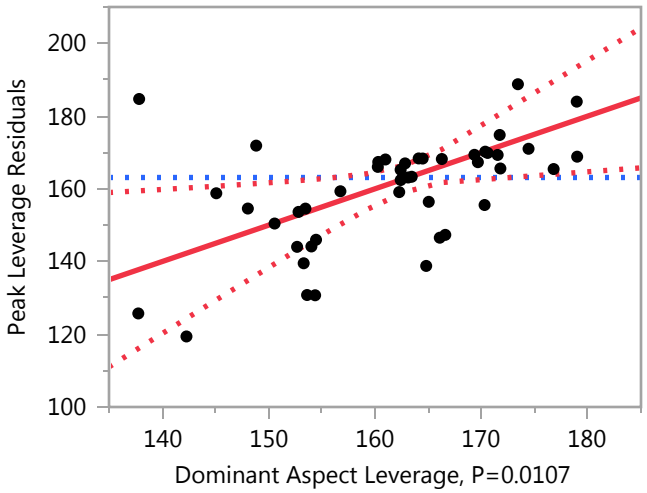

Least Squares Means Table

Level	Least Sq Mean	Std Error	Mean
E	147.91730	11.569808	148.500
N	171.30825	7.363513	174.371
NE	174.06361	23.490903	179.786
NW	153.96878	7.786793	159.761
S	173.04367	10.404145	162.360
SE	171.48363	13.825203	143.627
SW	180.92197	13.519380	170.667
W	146.05439	10.422977	135.028

Least Squares Fit

Response Peak

Rippability Index

Leverage Plot

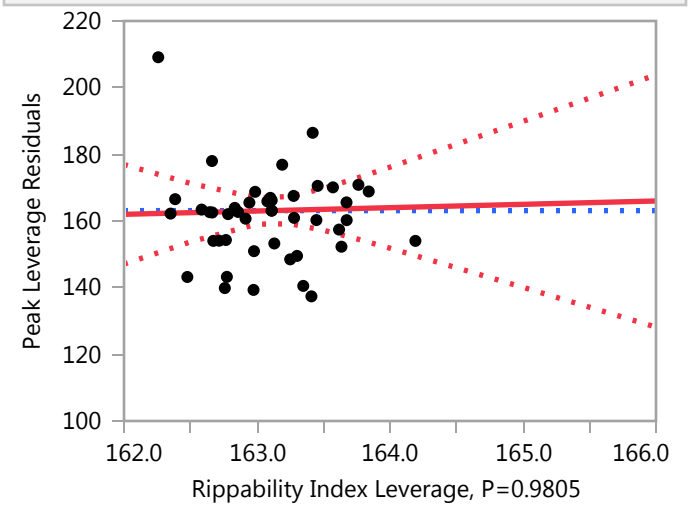

Least Squares Means Table

Level	Least Sq Mean	Std Error	Mean
Marginally Rippable	165.64671	11.286467	156.150
Non-Rippable	164.53681	11.311438	171.787
Rippable	164.35208	6.908534	162.528

Landcover

Leverage Plot

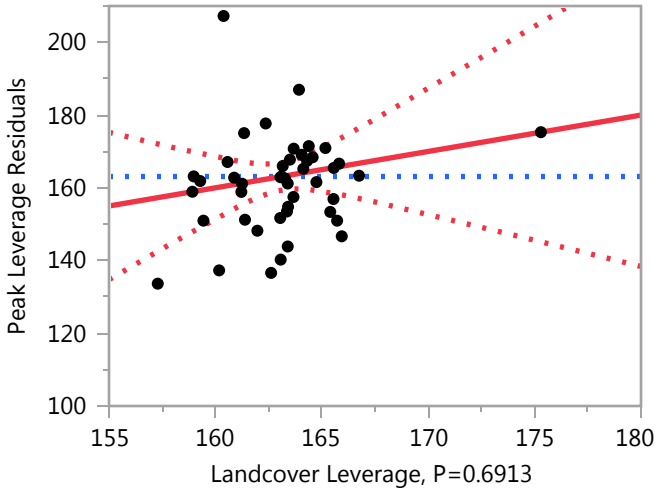

Least Squares Fit

Response Peak

Landcover

Leverage Plot

Landcover Leverage, P=0.6913

Least Squares Means Table

Level	Least Sq Mean	Std Error	Mean
Alpine	179.16307	24.588516	163.625
Alpine/Forrested	158.40736	8.972009	167.412
Forrested	163.52247	5.373721	163.268
Scrub	158.28790	9.599395	159.147

Average Annual Precipitaiton (mm)

Leverage Plot

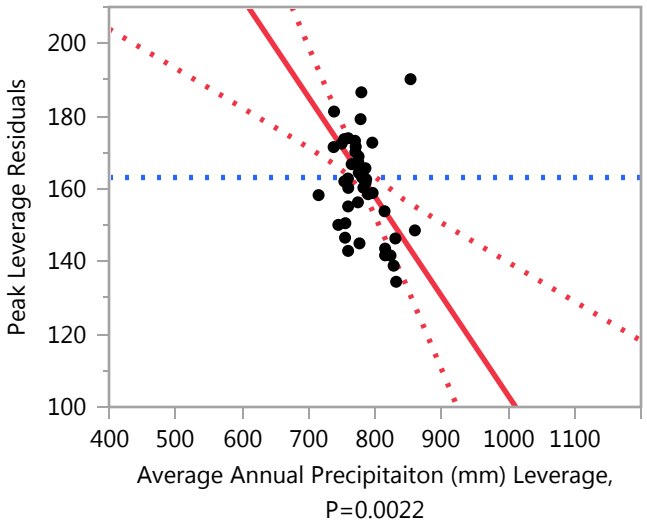

Least Squares Fit

Response Peak

Average Annual Precipitaiton (mm)

Response End

Whole Model

Actual by Predicted Plot

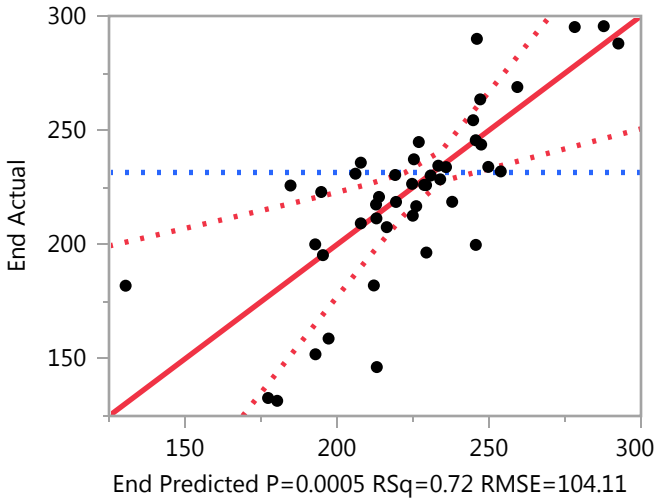

Summary of Fit

RSquare	0.724343
RSquare Adj	0.550781
Root Mean Square Error	104.1076
Mean of Response	231.5458
Observations (or Sum Wgts)	1114

Analysis of Variance

Source	DF	Sum of Squares	Mean Square	F Ratio
Model	17	768960.3	45233.0	4.1734
Error	27	292636.5	10838.4	**Prob > F**
C. Total	44	1061596.8		0.0005 *

Least Squares Fit

Response End

Whole Model

Parameter Estimates

Term	Estimate	Std Error	t Ratio	Prob>|t|
Intercept	208.18337	121.7454	1.71	0.0987
Drainage Area	0.000781	0.006323	0.12	0.9026
Average Slope (%)	1.0972356	0.62612	1.75	0.0910
Average Elevation (m)	0.0657143	0.078872	0.83	0.4121
A(2250)	-0.720006	0.364123	-1.98	0.0583
Dominant Aspect[E]	-19.78377	19.18532	-1.03	0.3116
Dominant Aspect[N]	22.723277	11.11829	2.04	0.0508
Dominant Aspect[NE]	14.895855	33.02279	0.45	0.6555
Dominant Aspect[NW]	1.1352697	12.76169	0.09	0.9298
Dominant Aspect[S]	8.6205931	12.04742	0.72	0.4804
Dominant Aspect[SE]	-22.88807	18.24959	-1.25	0.2205
Dominant Aspect[SW]	18.961676	15.03025	1.26	0.2179
Rippability Index[Marginally Rippable]	-1.491345	8.084166	-0.18	0.8550
Rippability Index[Non-Rippable]	-3.422871	8.947086	-0.38	0.7050
Landcover[Alpine]	11.404074	32.40981	0.35	0.7277
Landcover[Alpine/Forrested]	3.8681399	15.32355	0.25	0.8026
Landcover[Forrested]	5.6810307	11.88007	0.48	0.6364
Average Annual Precipitaiton (mm)	-0.205291	0.140662	-1.46	0.1560

Effect Tests

Source	Nparm	DF	Sum of Squares	F Ratio	Prob > F
Drainage Area	1	1	165.34	0.0153	0.9026
Average Slope (%)	1	1	33285.07	3.0710	0.0910
Average Elevation (m)	1	1	7523.85	0.6942	0.4121
A(2250)	1	1	42378.09	3.9100	0.0583
Dominant Aspect	7	7	205049.67	2.7027	0.0293 *
Rippability Index	2	2	1706.80	0.0787	0.9245
Landcover	3	3	54428.39	1.6739	0.1961
Average Annual Precipitaiton (mm)	1	1	23086.27	2.1300	0.1560

Least Squares Fit

Response End

Whole Model

Residual by Predicted Plot

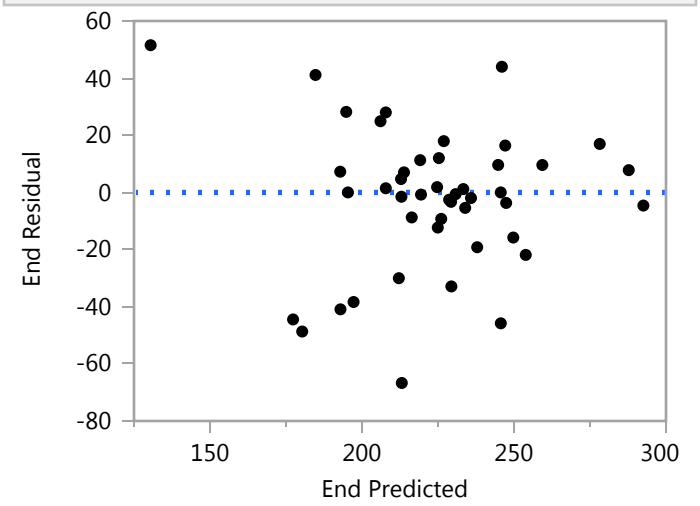

Drainage Area

Leverage Plot

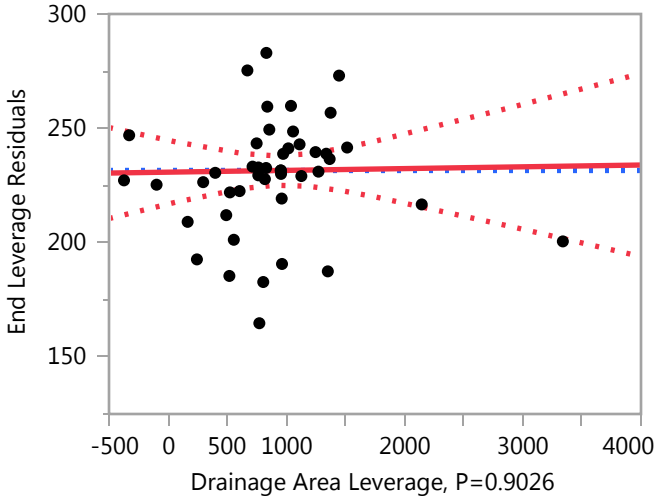

Least Squares Fit

Response End

Average Slope (%)

Leverage Plot

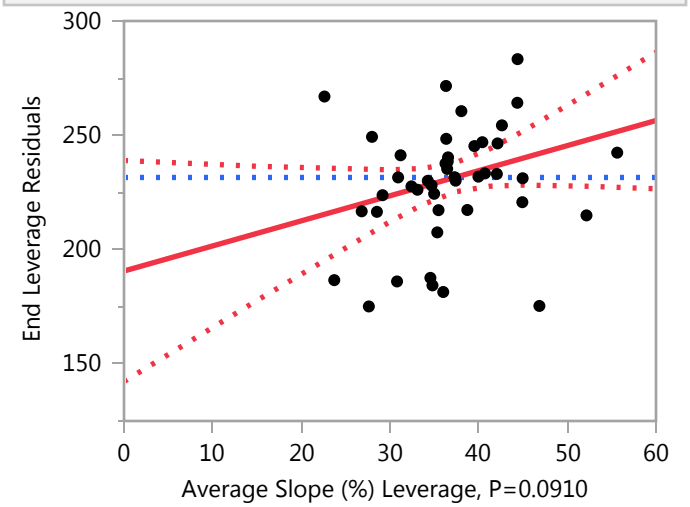

Average Elevation (m)

Leverage Plot

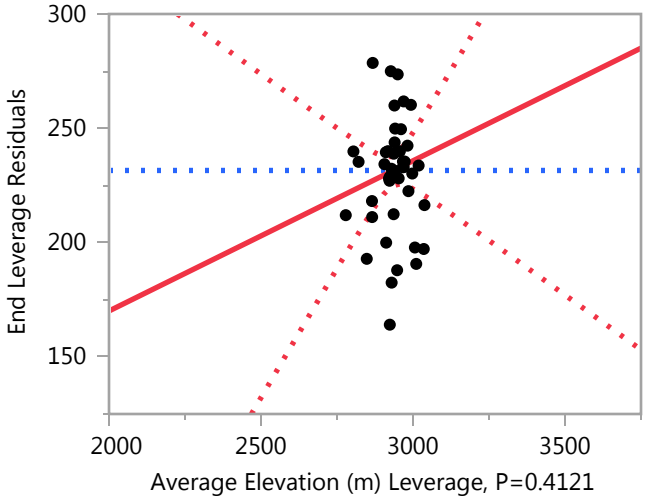

Least Squares Fit

Response End

A(2250)

Leverage Plot

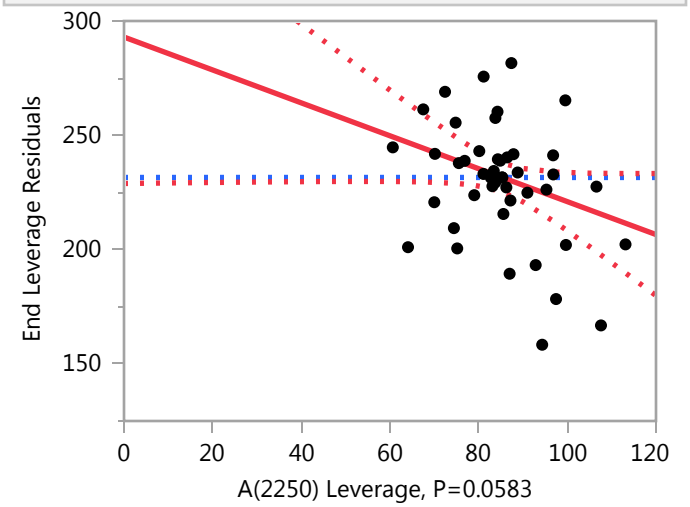

Dominant Aspect

Leverage Plot

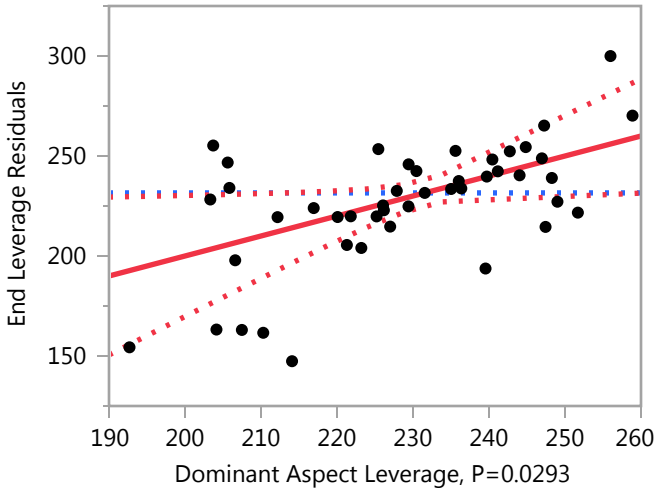

Least Squares Fit

Response End

Dominant Aspect

Least Squares Means Table

Level	Least Sq Mean	Std Error	Mean
E	201.24204	20.121111	190.737
N	243.74909	12.805922	252.341
NE	235.92167	40.853147	245.643
NW	222.16108	13.542051	230.688
S	229.64641	18.093901	223.749
SE	198.13774	24.043481	194.824
SW	239.98749	23.511621	244.967
W	197.36099	18.126651	192.278

Rippability Index

Leverage Plot

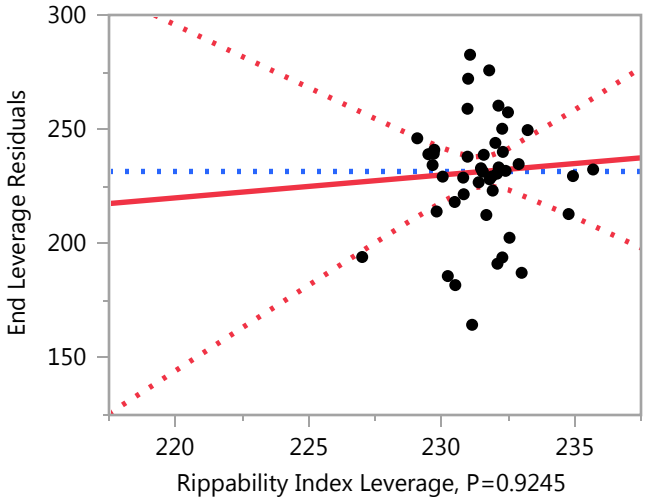

Least Squares Means Table

Level	Least Sq Mean	Std Error	Mean
Marginally Rippable	219.53447	19.628351	213.906
Non-Rippable	217.60294	19.671778	234.213
Rippable	225.94003	12.014666	238.346

Least Squares Fit

Response End

Landcover

Leverage Plot

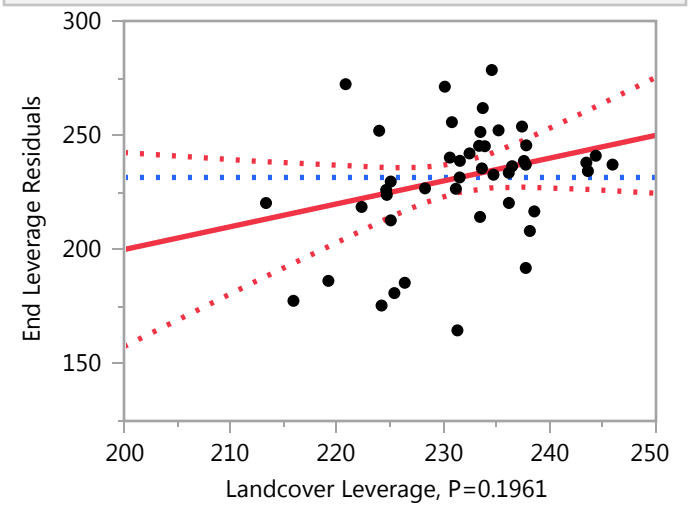

Least Squares Means Table

Level	Least Sq Mean	Std Error	Mean
Alpine	232.42989	42.762011	195.375
Alpine/Forrested	224.89395	15.603266	221.857
Forrested	226.70684	9.345466	233.574
Scrub	200.07257	16.694355	230.141

Least Squares Fit

Response End

Average Annual Precipitaiton (mm)

Leverage Plot

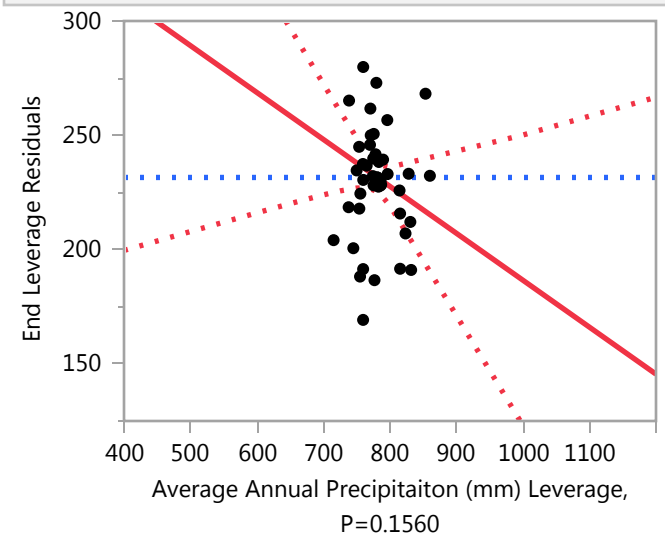

APPENDIX E

Least Squares Fit

Weight: Number of Years

Response apr

Whole Model

Actual by Predicted Plot

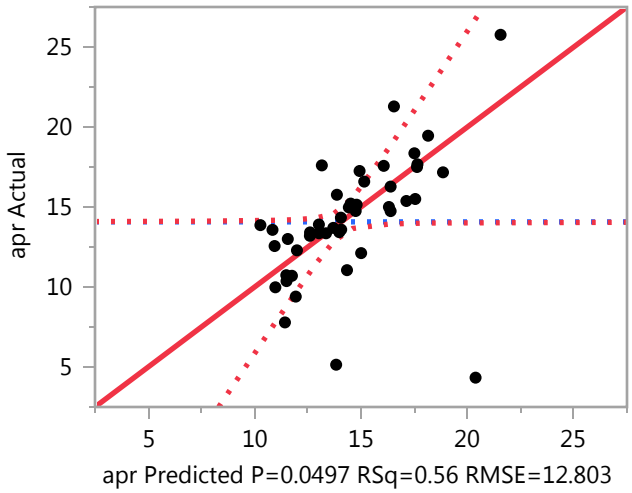

Summary of Fit

RSquare	0.559922
RSquare Adj	0.282836
Root Mean Square Error	12.80259
Mean of Response	14.07092
Observations (or Sum Wgts)	1114

Analysis of Variance

Source	DF	Sum of Squares	Mean Square	F Ratio
Model	17	5630.633	331.214	2.0207
Error	27	4425.471	163.906	Prob > F
C. Total	44	10056.104		0.0497 *

Parameter Estimates

Term	Estimate	Std Error	t Ratio	Prob>|t|
Intercept	21.556925	14.9578	1.44	0.1610
Drainage Area	-0.000837	0.000777	-1.08	0.2907
Average Slope (%)	-0.227754	0.076996	-2.96	0.0064 *
Average Elevation (m)	-0.00091	0.009689	-0.09	0.9259
A(2250)	-0.016747	0.044737	-0.37	0.7111
Dominant Aspect[E]	-0.521416	2.359497	-0.22	0.8268

Least Squares Fit

Response apr

Whole Model

Parameter Estimates

Term	Estimate	Std Error	t Ratio	Prob>|t|
Dominant Aspect[N]	0.0278931	1.366788	0.02	0.9839
Dominant Aspect[NE]	-2.609326	4.058969	-0.64	0.5257
Dominant Aspect[NW]	0.8114477	1.569179	0.52	0.6093
Dominant Aspect[S]	0.5610375	1.481788	0.38	0.7079
Dominant Aspect[SE]	1.9449148	2.24517	0.87	0.3940
Dominant Aspect[SW]	1.2091468	1.848238	0.65	0.5185
Rippability Index[Marginally Rippable]	0.1101038	0.994335	0.11	0.9126
Rippability Index[Non-Rippable]	-0.392158	1.098986	-0.36	0.7240
Landcover[Alpine]	1.2728931	3.985608	0.32	0.7519
Landcover[Alpine/Forrested]	0.7498836	1.884157	0.40	0.6938
Landcover[Forrested]	-1.68227	1.460933	-1.15	0.2596
Average Annual Precipitaiton (mm)	0.0085167	0.017291	0.49	0.6263

Effect Tests

Source	Nparm	DF	Sum of Squares	F Ratio	Prob > F
Drainage Area	1	1	190.3924	1.1616	0.2907
Average Slope (%)	1	1	1434.1473	8.7498	0.0064 *
Average Elevation (m)	1	1	1.4454	0.0088	0.9259
A(2250)	1	1	22.9684	0.1401	0.7111
Dominant Aspect	7	7	483.3291	0.4213	0.8804
Rippability Index	2	2	26.8415	0.0819	0.9216
Landcover	3	3	508.2386	1.0336	0.3934
Average Annual Precipitaiton (mm)	1	1	39.7664	0.2426	0.6263

Least Squares Fit

Response apr

Whole Model

Residual by Predicted Plot

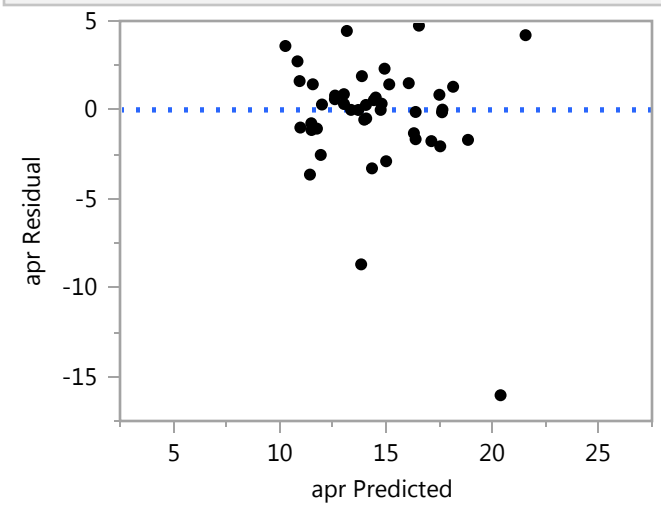

Expanded Estimates

Nominal factors expanded to all levels

Term	Estimate	Std Error	t Ratio	Prob>|t|
Intercept	21.556925	14.9578	1.44	0.1610
Drainage Area	-0.000837	0.000777	-1.08	0.2907
Average Slope (%)	-0.227754	0.076996	-2.96	0.0064 *
Average Elevation (m)	-0.00091	0.009689	-0.09	0.9259
A(2250)	-0.016747	0.044737	-0.37	0.7111
Dominant Aspect[E]	-0.521416	2.359497	-0.22	0.8268
Dominant Aspect[N]	0.0278931	1.366788	0.02	0.9839
Dominant Aspect[NE]	-2.609326	4.058969	-0.64	0.5257
Dominant Aspect[NW]	0.8114477	1.569179	0.52	0.6093
Dominant Aspect[S]	0.5610375	1.481788	0.38	0.7079
Dominant Aspect[SE]	1.9449148	2.24517	0.87	0.3940
Dominant Aspect[SW]	1.2091468	1.848238	0.65	0.5185
Dominant Aspect[W]	-1.423698	1.613732	-0.88	0.3854
Rippability Index[Marginally Rippable]	0.1101038	0.994335	0.11	0.9126
Rippability Index[Non-Rippable]	-0.392158	1.098986	-0.36	0.7240
Rippability Index[Rippable]	0.2820545	1.631132	0.17	0.8640
Landcover[Alpine]	1.2728931	3.985608	0.32	0.7519
Landcover[Alpine/Forrested]	0.7498836	1.884157	0.40	0.6938
Landcover[Forrested]	-1.68227	1.460933	-1.15	0.2596

Least Squares Fit

Response apr

Whole Model

Expanded Estimates

Term	Estimate	Std Error	t Ratio	Prob>|t|
Landcover[Scrub]	-0.340507	1.81726	-0.19	0.8528
Average Annual Precipitaiton (mm)	0.0085167	0.017291	0.49	0.6263

Drainage Area

Leverage Plot

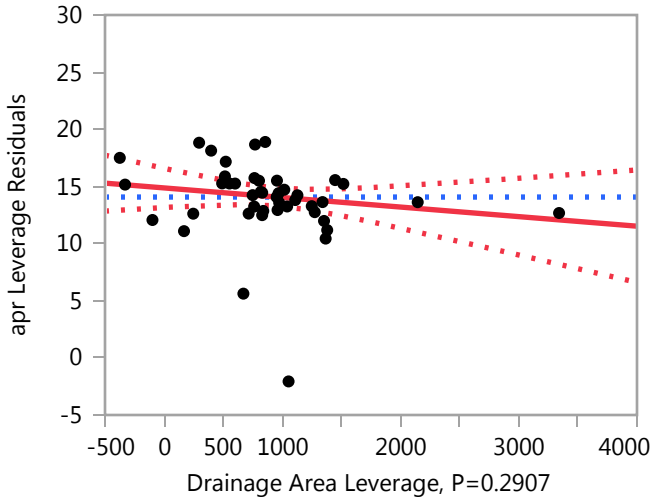

Average Slope (%)

Leverage Plot

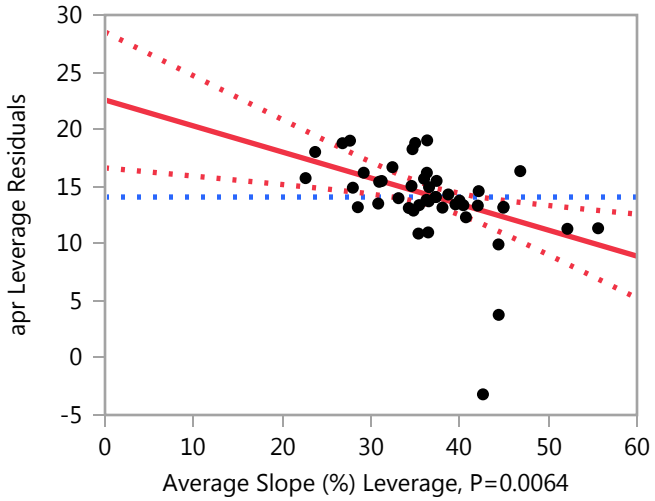

Least Squares Fit

Response apr

Average Elevation (m)

Leverage Plot

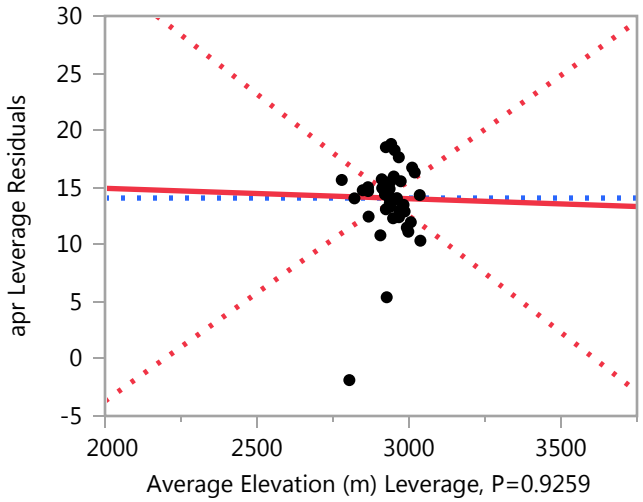

A(2250)

Leverage Plot

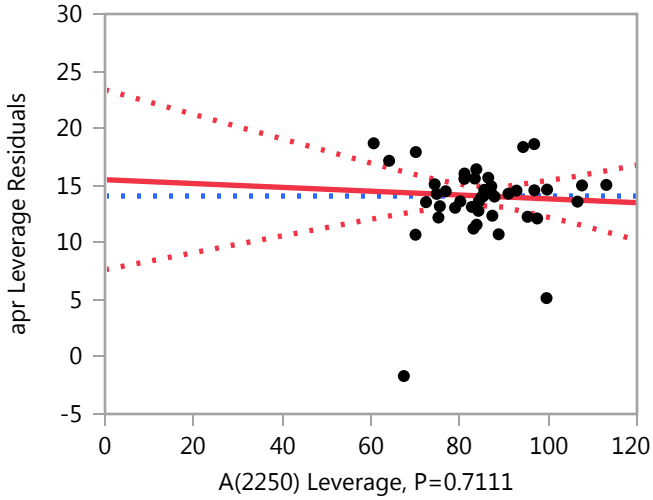

Least Squares Fit

Response apr

Dominant Aspect

Leverage Plot

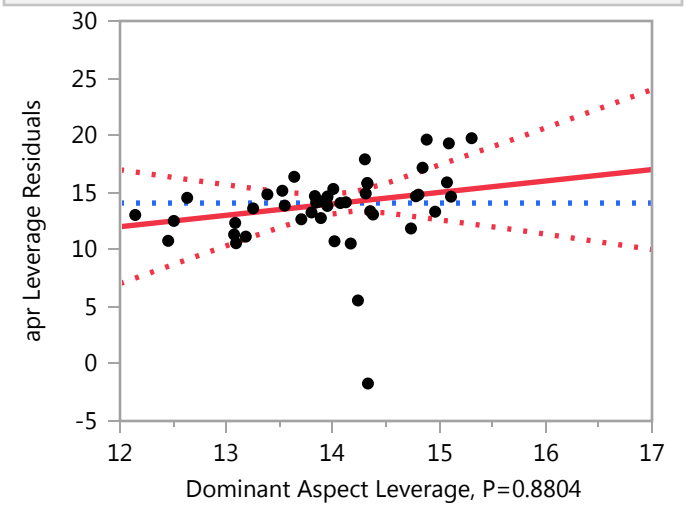

Least Squares Means Table

Level	Least Sq Mean	Std Error	Mean
E	14.293395	2.4743486	14.1053
N	14.842703	1.5751421	13.8533
NE	12.205484	5.0207926	13.3571
NW	15.626258	1.6651911	13.6377
S	15.375848	2.2249617	13.4435
SE	16.759725	2.9574806	13.9804
SW	16.023957	2.8902445	17.4667
W	13.391112	2.2292721	14.7639

Least Squares Fit

Response apr

Rippability Index

Leverage Plot

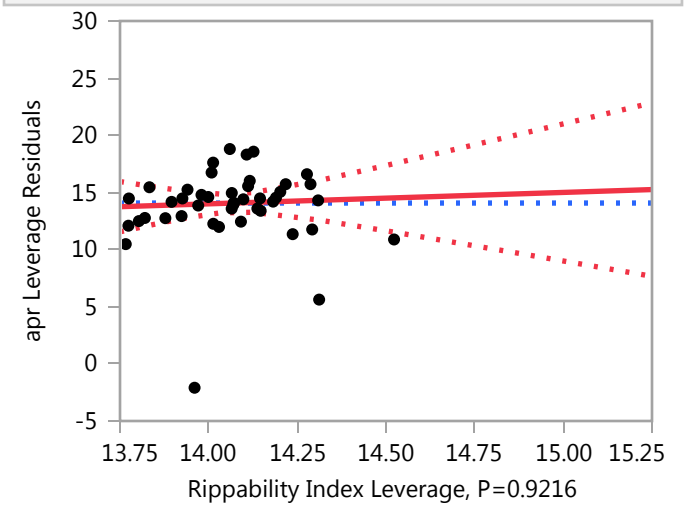

Least Squares Means Table

Level	Least Sq Mean	Std Error	Mean
Marginally Rippable	14.924914	2.4130652	14.6255
Non-Rippable	14.422652	2.4169811	12.5039
Rippable	15.096865	1.4775669	14.4924

Landcover

Leverage Plot

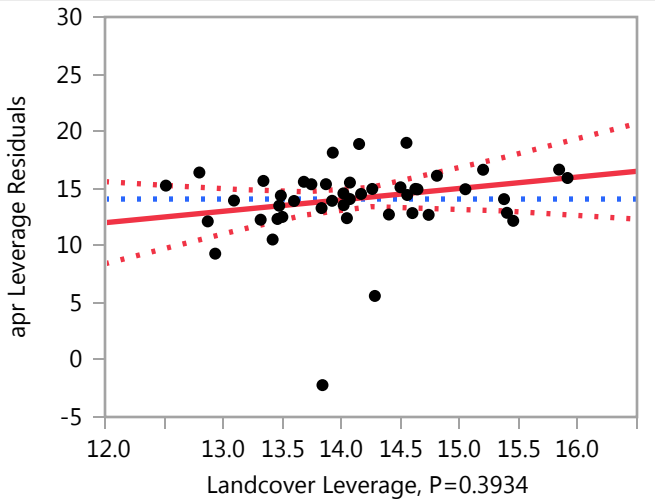

Least Squares Fit

Response apr

Landcover

Least Squares Means Table

Level	Least Sq Mean	Std Error	Mean
Alpine	16.087703	5.2583997	14.7500
Alpine/Forrested	15.564694	1.9172079	14.2605
Forrested	13.132541	1.1484632	13.9490
Scrub	14.474303	2.0528563	14.5153

Average Annual Precipitaiton (mm)

Leverage Plot

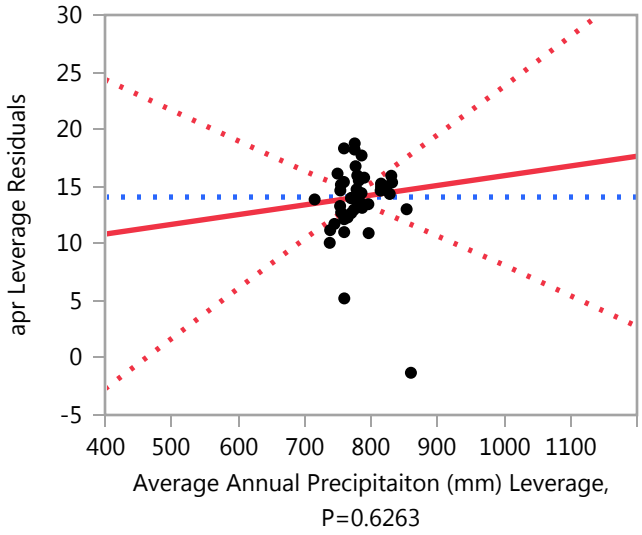

Least Squares Fit

Response apr

Average Annual Precipitaiton (mm)

Response may

Whole Model

Actual by Predicted Plot

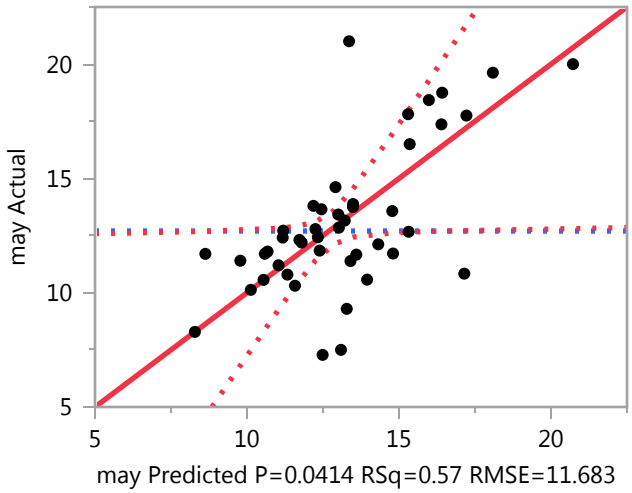

Summary of Fit

RSquare	0.56912
RSquare Adj	0.297826
Root Mean Square Error	11.68271
Mean of Response	12.69928
Observations (or Sum Wgts)	1114

Analysis of Variance

Source	DF	Sum of Squares	Mean Square	F Ratio
Model	17	4867.4200	286.319	2.0978
Error	27	3685.1121	136.486	**Prob > F**
C. Total	44	8552.5320		0.0414 *

Least Squares Fit

Response may

Whole Model

Parameter Estimates

Term	Estimate	Std Error	t Ratio	Prob>|t|
Intercept	11.866337	13.64939	0.87	0.3923
Drainage Area	-0.000703	0.000709	-0.99	0.3300
Average Slope (%)	-0.21637	0.070261	-3.08	0.0047 *
Average Elevation (m)	0.0020794	0.008842	0.24	0.8158
A(2250)	0.0321646	0.040824	0.79	0.4376
Dominant Aspect[E]	2.9356103	2.153104	1.36	0.1840
Dominant Aspect[N]	0.8608827	1.24723	0.69	0.4959
Dominant Aspect[NE]	-6.214114	3.703917	-1.68	0.1049
Dominant Aspect[NW]	-0.462758	1.431918	-0.32	0.7491
Dominant Aspect[S]	1.1679844	1.352171	0.86	0.3953
Dominant Aspect[SE]	2.0490256	2.048778	1.00	0.3261
Dominant Aspect[SW]	-0.689665	1.686567	-0.41	0.6858
Rippability Index[Marginally Rippable]	-0.884705	0.907357	-0.98	0.3382
Rippability Index[Non-Rippable]	0.7748486	1.002854	0.77	0.4464
Landcover[Alpine]	-4.07216	3.636974	-1.12	0.2727
Landcover[Alpine/Forrested]	2.1966328	1.719344	1.28	0.2123
Landcover[Forrested]	1.2609082	1.33314	0.95	0.3526
Average Annual Precipitaiton (mm)	-0.001284	0.015778	-0.08	0.9357

Effect Tests

Source	Nparm	DF	Sum of Squares	F Ratio	Prob > F
Drainage Area	1	1	134.3185	0.9841	0.3300
Average Slope (%)	1	1	1294.3705	9.4836	0.0047 *
Average Elevation (m)	1	1	7.5485	0.0553	0.8158
A(2250)	1	1	84.7261	0.6208	0.4376
Dominant Aspect	7	7	966.1096	1.0112	0.4455
Rippability Index	2	2	266.9445	0.9779	0.3890
Landcover	3	3	247.2407	0.6038	0.6182
Average Annual Precipitaiton (mm)	1	1	0.9037	0.0066	0.9357

Least Squares Fit

Response may

Whole Model

Residual by Predicted Plot

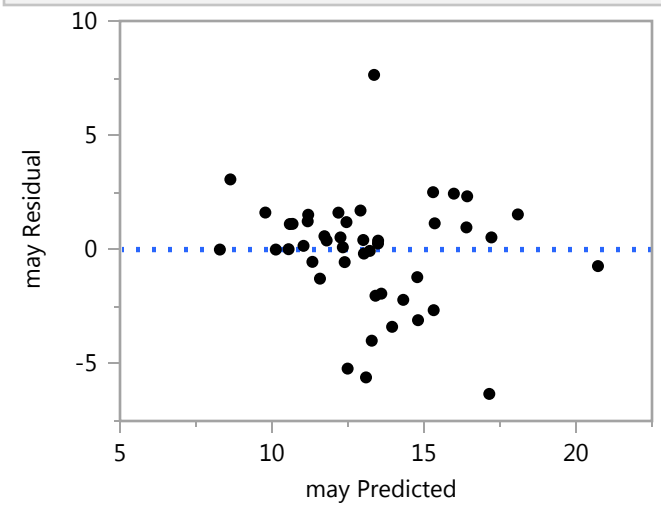

Expanded Estimates

Nominal factors expanded to all levels

Term	Estimate	Std Error	t Ratio	Prob>|t|
Intercept	11.866337	13.64939	0.87	0.3923
Drainage Area	-0.000703	0.000709	-0.99	0.3300
Average Slope (%)	-0.21637	0.070261	-3.08	0.0047 *
Average Elevation (m)	0.0020794	0.008842	0.24	0.8158
A(2250)	0.0321646	0.040824	0.79	0.4376
Dominant Aspect[E]	2.9356103	2.153104	1.36	0.1840
Dominant Aspect[N]	0.8608827	1.24723	0.69	0.4959
Dominant Aspect[NE]	-6.214114	3.703917	-1.68	0.1049
Dominant Aspect[NW]	-0.462758	1.431918	-0.32	0.7491
Dominant Aspect[S]	1.1679844	1.352171	0.86	0.3953
Dominant Aspect[SE]	2.0490256	2.048778	1.00	0.3261
Dominant Aspect[SW]	-0.689665	1.686567	-0.41	0.6858
Dominant Aspect[W]	0.3530345	1.472573	0.24	0.8123
Rippability Index[Marginally Rippable]	-0.884705	0.907357	-0.98	0.3382
Rippability Index[Non-Rippable]	0.7748486	1.002854	0.77	0.4464
Rippability Index[Rippable]	0.1098566	1.488452	0.07	0.9417
Landcover[Alpine]	-4.07216	3.636974	-1.12	0.2727
Landcover[Alpine/Forrested]	2.1966328	1.719344	1.28	0.2123
Landcover[Forrested]	1.2609082	1.33314	0.95	0.3526

Least Squares Fit

Response may

Whole Model

Expanded Estimates

Term	Estimate	Std Error	t Ratio	Prob>|t|
Landcover[Scrub]	0.6146192	1.658298	0.37	0.7138
Average Annual Precipitaiton (mm)	-0.001284	0.015778	-0.08	0.9357

Drainage Area

Leverage Plot

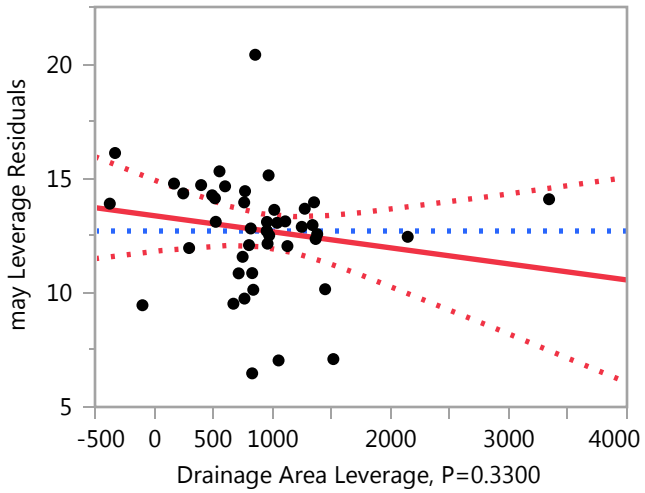

Average Slope (%)

Leverage Plot

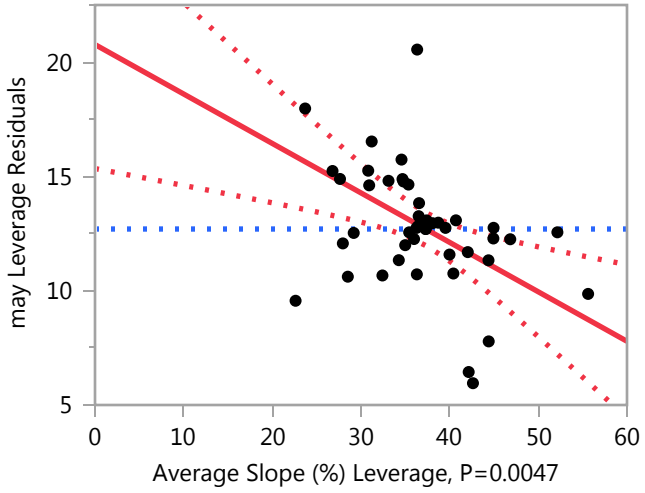

Least Squares Fit

Response may

Average Slope (%)

Leverage Plot

Average Elevation (m)

Leverage Plot

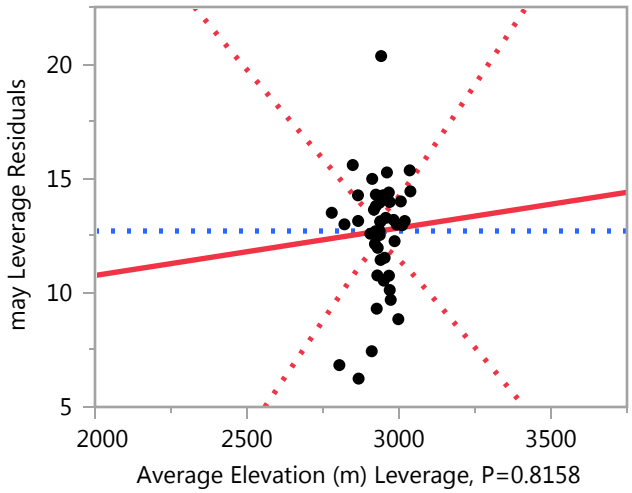

A(2250)

Leverage Plot

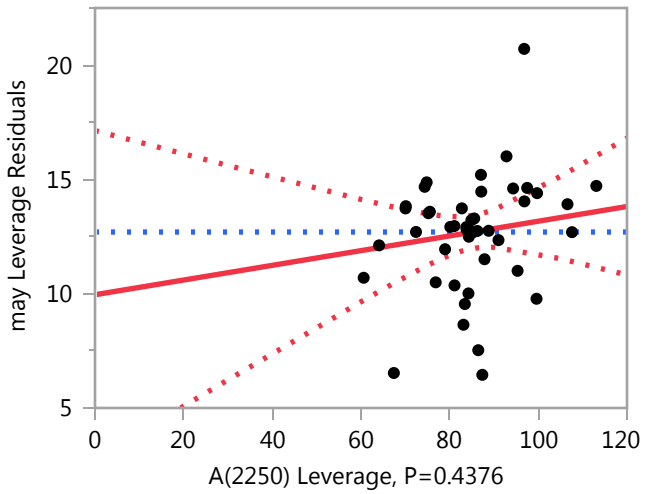

Least Squares Fit

Response may

Dominant Aspect

Leverage Plot

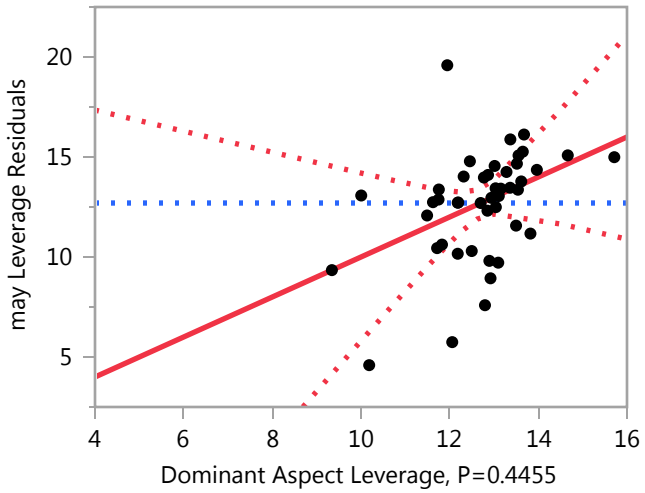

Least Squares Means Table

Level	Least Sq Mean	Std Error	Mean
E	13.906795	2.2579093	14.6316
N	11.832068	1.4373593	13.3204
NE	4.757071	4.5816075	8.2857
NW	10.508427	1.5195314	11.5688
S	12.139170	2.0303371	12.2845
SE	13.020211	2.6987802	12.9412
SW	10.281520	2.6374254	13.1667
W	11.324220	2.0342704	14.6111

Least Squares Fit

Response may

Rippability Index

Leverage Plot

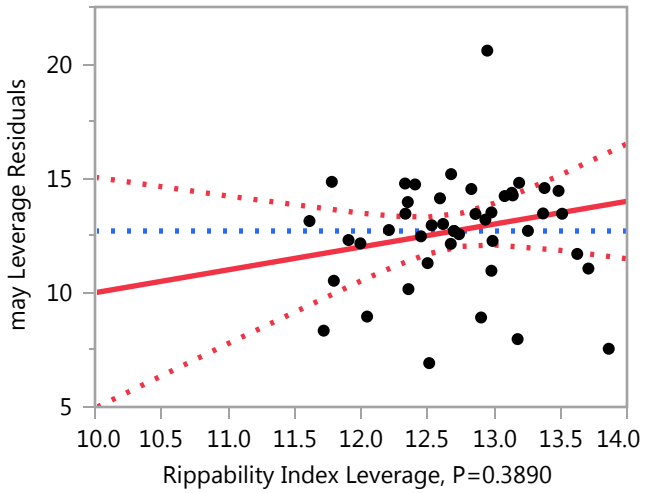

Least Squares Means Table

Level	Least Sq Mean	Std Error	Mean
Marginally Rippable	10.086480	2.2019865	13.4307
Non-Rippable	11.746034	2.2055599	12.7205
Rippable	11.081042	1.3483193	12.3609

Landcover

Leverage Plot

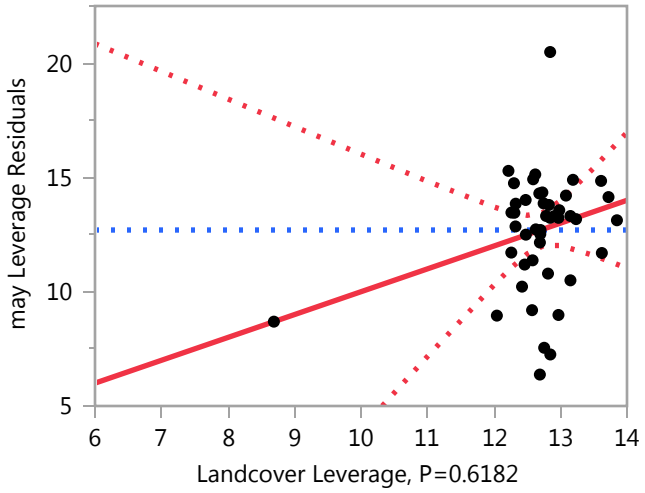

Least Squares Fit

Response may

Landcover

Leverage Plot

Landcover Leverage, P=0.6182

Least Squares Means Table

Level	Least Sq Mean	Std Error	Mean
Alpine	6.899025	4.7984303	10.1250
Alpine/Forrested	13.167818	1.7495035	11.8487
Forrested	12.232093	1.0480034	13.0728
Scrub	11.585804	1.8732863	11.5583

Average Annual Precipitaiton (mm)

Leverage Plot

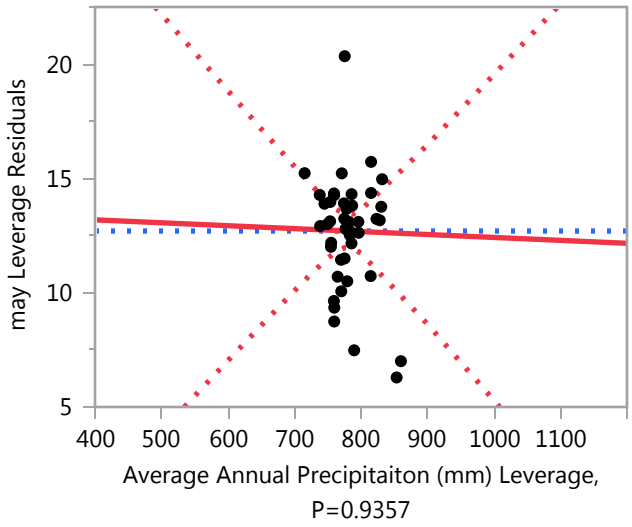

Least Squares Fit

Response may

Average Annual Precipitaiton (mm)

Response jun

Whole Model

Actual by Predicted Plot

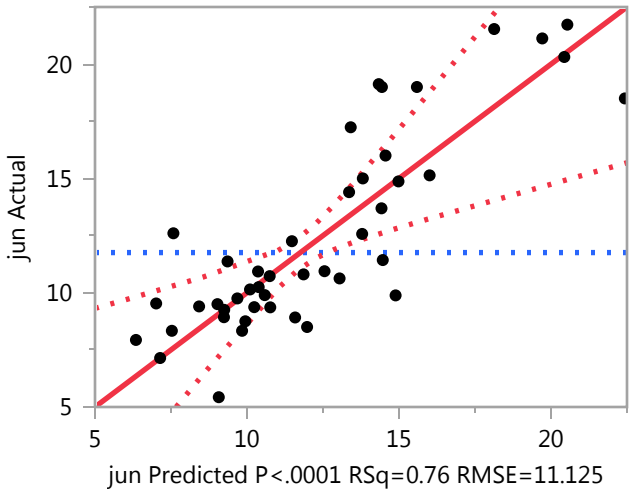

Summary of Fit

RSquare	0.762046
RSquare Adj	0.612223
Root Mean Square Error	11.1248
Mean of Response	11.75583
Observations (or Sum Wgts)	1114

Analysis of Variance

Source	DF	Sum of Squares	Mean Square	F Ratio
Model	17	10701.306	629.489	5.0863
Error	27	3341.551	123.761	Prob > F
C. Total	44	14042.857		<.0001 *

Least Squares Fit

Response jun

Whole Model

Parameter Estimates

Term	Estimate	Std Error	t Ratio	Prob>|t|
Intercept	27.58771	12.99756	2.12	0.0431 *
Drainage Area	-0.000576	0.000675	-0.85	0.4010
Average Slope (%)	-0.225016	0.066905	-3.36	0.0023 *
Average Elevation (m)	-0.013362	0.00842	-1.59	0.1242
A(2250)	0.1430964	0.038874	3.68	0.0010 *
Dominant Aspect[E]	2.4166174	2.050283	1.18	0.2488
Dominant Aspect[N]	1.7988393	1.187669	1.51	0.1415
Dominant Aspect[NE]	-5.143792	3.527037	-1.46	0.1563
Dominant Aspect[NW]	-0.8674	1.363537	-0.64	0.5300
Dominant Aspect[S]	0.4607795	1.287598	0.36	0.7232
Dominant Aspect[SE]	1.1589973	1.950939	0.59	0.5574
Dominant Aspect[SW]	-1.211541	1.606025	-0.75	0.4572
Rippability Index[Marginally Rippable]	-0.890836	0.864027	-1.03	0.3117
Rippability Index[Non-Rippable]	0.3734708	0.954962	0.39	0.6988
Landcover[Alpine]	-2.479346	3.463291	-0.72	0.4802
Landcover[Alpine/Forrested]	1.4883791	1.637237	0.91	0.3714
Landcover[Forrested]	1.0630917	1.269476	0.84	0.4097
Average Annual Precipitaiton (mm)	0.0237881	0.015025	1.58	0.1250

Effect Tests

Source	Nparm	DF	Sum of Squares	F Ratio	Prob > F
Drainage Area	1	1	90.0956	0.7280	0.4010
Average Slope (%)	1	1	1399.8740	11.3111	0.0023 *
Average Elevation (m)	1	1	311.7001	2.5186	0.1242
A(2250)	1	1	1676.9464	13.5499	0.0010 *
Dominant Aspect	7	7	1566.4769	1.8082	0.1266
Rippability Index	2	2	179.7926	0.7264	0.4929
Landcover	3	3	177.7907	0.4789	0.6997
Average Annual Precipitaiton (mm)	1	1	310.2358	2.5067	0.1250

Least Squares Fit

Response jun

Whole Model

Residual by Predicted Plot

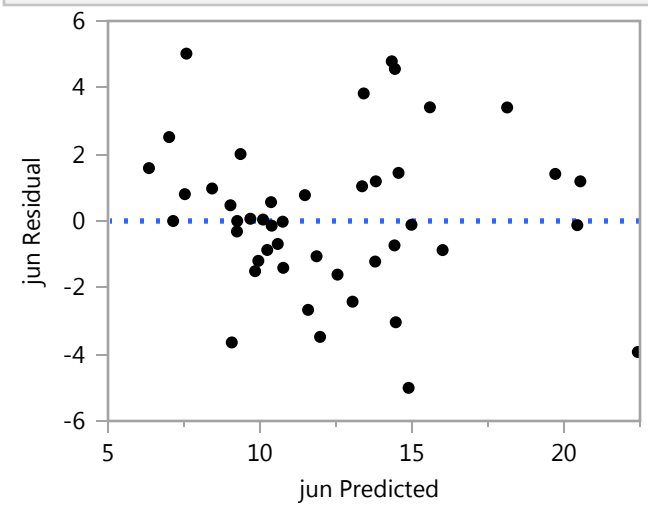

Expanded Estimates

Nominal factors expanded to all levels

Term	Estimate	Std Error	t Ratio	Prob>|t|
Intercept	27.58771	12.99756	2.12	0.0431 *
Drainage Area	-0.000576	0.000675	-0.85	0.4010
Average Slope (%)	-0.225016	0.066905	-3.36	0.0023 *
Average Elevation (m)	-0.013362	0.00842	-1.59	0.1242
A(2250)	0.1430964	0.038874	3.68	0.0010 *
Dominant Aspect[E]	2.4166174	2.050283	1.18	0.2488
Dominant Aspect[N]	1.7988393	1.187669	1.51	0.1415
Dominant Aspect[NE]	-5.143792	3.527037	-1.46	0.1563
Dominant Aspect[NW]	-0.8674	1.363537	-0.64	0.5300
Dominant Aspect[S]	0.4607795	1.287598	0.36	0.7232
Dominant Aspect[SE]	1.1589973	1.950939	0.59	0.5574
Dominant Aspect[SW]	-1.211541	1.606025	-0.75	0.4572
Dominant Aspect[W]	1.3874996	1.402251	0.99	0.3312
Rippability Index[Marginally Rippable]	-0.890836	0.864027	-1.03	0.3117
Rippability Index[Non-Rippable]	0.3734708	0.954962	0.39	0.6988
Rippability Index[Rippable]	0.5173652	1.417371	0.37	0.7179
Landcover[Alpine]	-2.479346	3.463291	-0.72	0.4802
Landcover[Alpine/Forrested]	1.4883791	1.637237	0.91	0.3714
Landcover[Forrested]	1.0630917	1.269476	0.84	0.4097

Least Squares Fit

Response jun

Whole Model

Expanded Estimates

Term	Estimate	Std Error	t Ratio	Prob>|t|
Landcover[Scrub]	-0.072125	1.579106	-0.05	0.9639
Average Annual Precipitaiton (mm)	0.0237881	0.015025	1.58	0.1250

Drainage Area

Leverage Plot

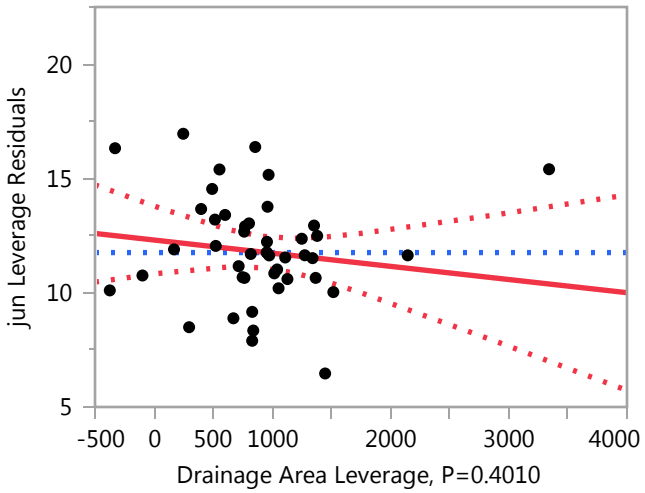

Average Slope (%)

Leverage Plot

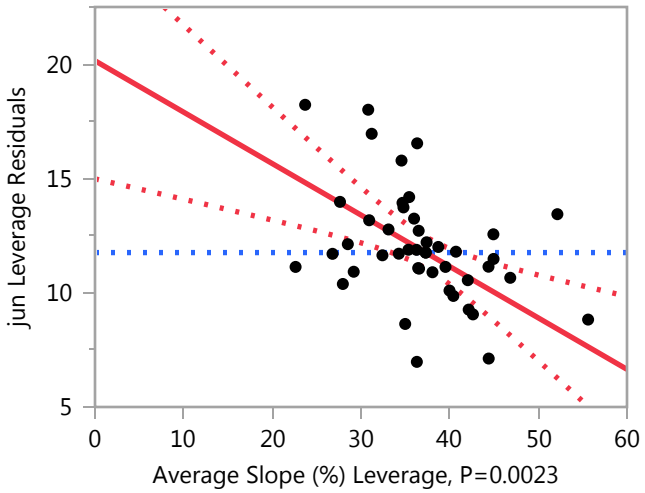

Least Squares Fit

Response jun

Average Slope (%)

Leverage Plot

Average Elevation (m)

Leverage Plot

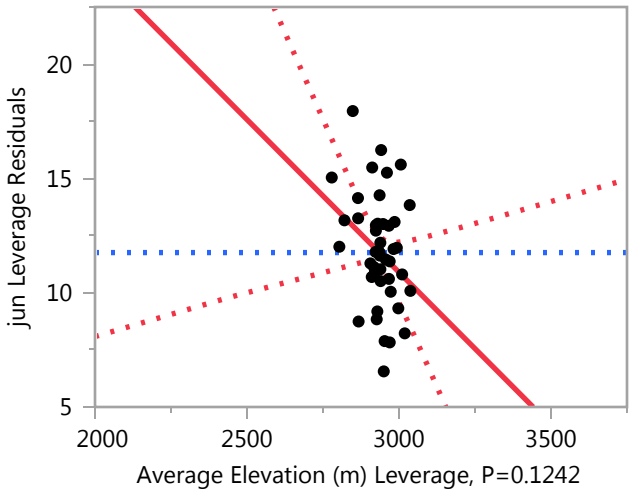

A(2250)

Leverage Plot

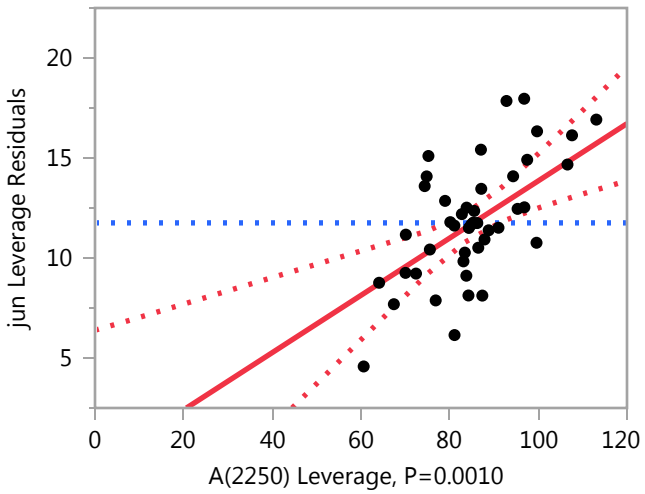

Least Squares Fit

Response jun

Dominant Aspect

Leverage Plot

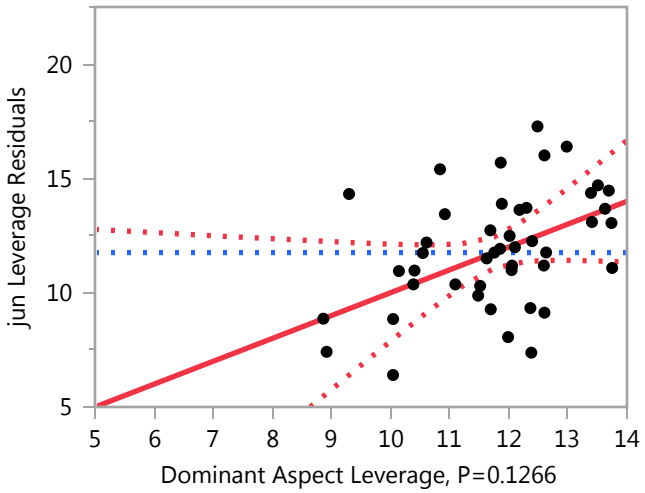

Least Squares Means Table

Level	Least Sq Mean	Std Error	Mean
E	12.622502	2.1500830	13.1842
N	12.004724	1.3687182	12.7395
NE	5.062093	4.3628131	7.1429
NW	9.338485	1.4469663	9.5580
S	10.666665	1.9333784	11.0418
SE	11.364882	2.5699001	14.8235
SW	8.994345	2.5114753	12.1111
W	11.593385	1.9371240	15.5139

Least Squares Fit

Response jun

Rippability Index

Leverage Plot

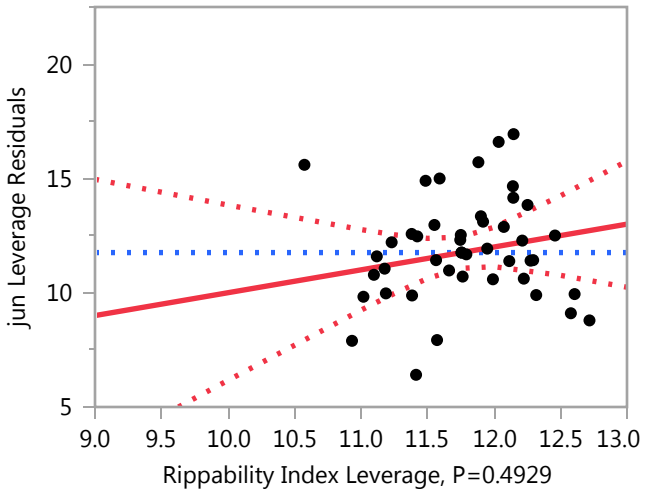

Least Squares Means Table

Level	Least Sq Mean	Std Error	Mean
Marginally Rippable	9.315049	2.0968307	12.5768
Non-Rippable	10.579356	2.1002335	10.4094
Rippable	10.723250	1.2839304	11.9629

Landcover

Leverage Plot

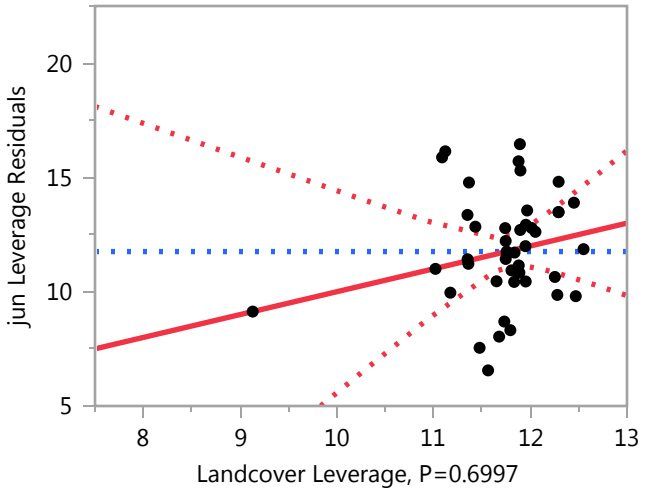

Least Squares Fit

Response jun

Landcover

Leverage Plot

Landcover Leverage, P=0.6997

Least Squares Means Table

Level	Least Sq Mean	Std Error	Mean
Alpine	7.726539	4.5692815	9.2500
Alpine/Forrested	11.694264	1.6659560	9.0924
Forrested	11.268977	0.9979560	12.2876
Scrub	10.133760	1.7838276	11.1350

Average Annual Precipitaiton (mm)

Leverage Plot

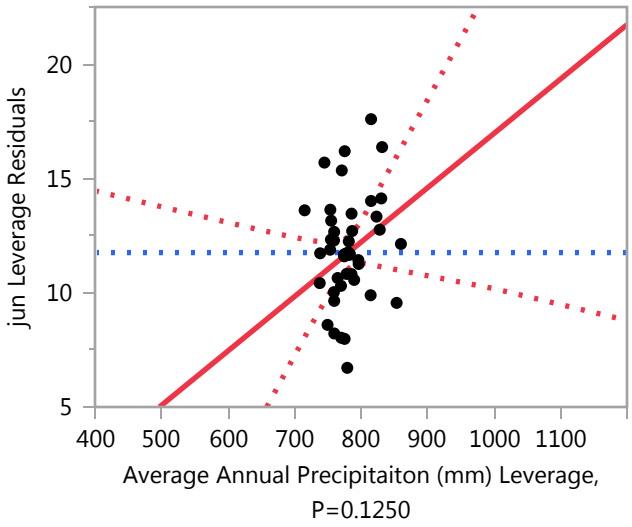

Least Squares Fit

Response jun

Average Annual Precipitaiton (mm)

Response jul

Whole Model

Actual by Predicted Plot

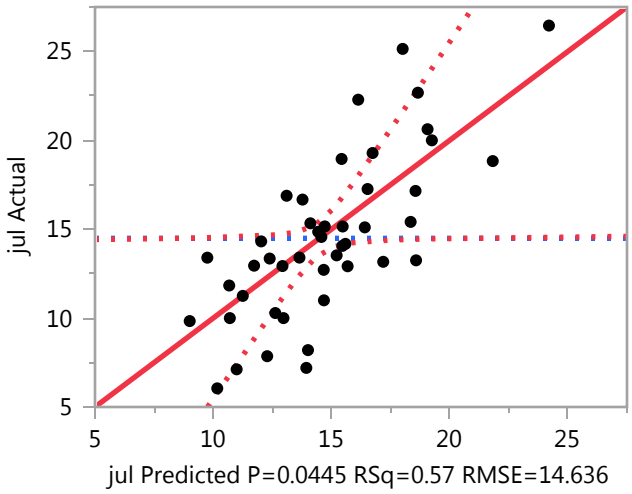

Summary of Fit

RSquare	0.565486
RSquare Adj	0.291903
Root Mean Square Error	14.63606
Mean of Response	14.48833
Observations (or Sum Wgts)	1114

Analysis of Variance

Source	DF	Sum of Squares	Mean Square	F Ratio
Model	17	7527.135	442.773	2.0670
Error	27	5783.784	214.214	**Prob > F**
C. Total	44	13310.920		0.0445 *

Least Squares Fit

Response jul

Whole Model

Parameter Estimates

Term	Estimate	Std Error	t Ratio	Prob>|t|
Intercept	0.2765213	17.09991	0.02	0.9872
Drainage Area	-0.000552	0.000888	-0.62	0.5394
Average Slope (%)	-0.275294	0.088022	-3.13	0.0042 *
Average Elevation (m)	0.0035364	0.011077	0.32	0.7520
A(2250)	0.1178088	0.051144	2.30	0.0292 *
Dominant Aspect[E]	4.9454217	2.697402	1.83	0.0778
Dominant Aspect[N]	1.168531	1.562527	0.75	0.4610
Dominant Aspect[NE]	-7.977976	4.640257	-1.72	0.0970
Dominant Aspect[NW]	0.8748532	1.793902	0.49	0.6297
Dominant Aspect[S]	0.744955	1.693995	0.44	0.6636
Dominant Aspect[SE]	1.1808392	2.566703	0.46	0.6492
Dominant Aspect[SW]	-0.920412	2.112926	-0.44	0.6666
Rippability Index[Marginally Rippable]	-1.892653	1.136735	-1.66	0.1075
Rippability Index[Non-Rippable]	-1.354157	1.256372	-1.08	0.2906
Landcover[Alpine]	-5.219085	4.55639	-1.15	0.2621
Landcover[Alpine/Forrested]	3.770384	2.153989	1.75	0.0914
Landcover[Forrested]	1.3888467	1.670154	0.83	0.4129
Average Annual Precipitaiton (mm)	0.0018348	0.019767	0.09	0.9267

Effect Tests

Source	Nparm	DF	Sum of Squares	F Ratio	Prob > F
Drainage Area	1	1	82.7676	0.3864	0.5394
Average Slope (%)	1	1	2095.3446	9.7815	0.0042 *
Average Elevation (m)	1	1	21.8341	0.1019	0.7520
A(2250)	1	1	1136.6244	5.3060	0.0292 *
Dominant Aspect	7	7	1186.4489	0.7912	0.6010
Rippability Index	2	2	711.5139	1.6608	0.2088
Landcover	3	3	684.9693	1.0659	0.3800
Average Annual Precipitaiton (mm)	1	1	1.8457	0.0086	0.9267

Least Squares Fit

Response jul

Whole Model

Residual by Predicted Plot

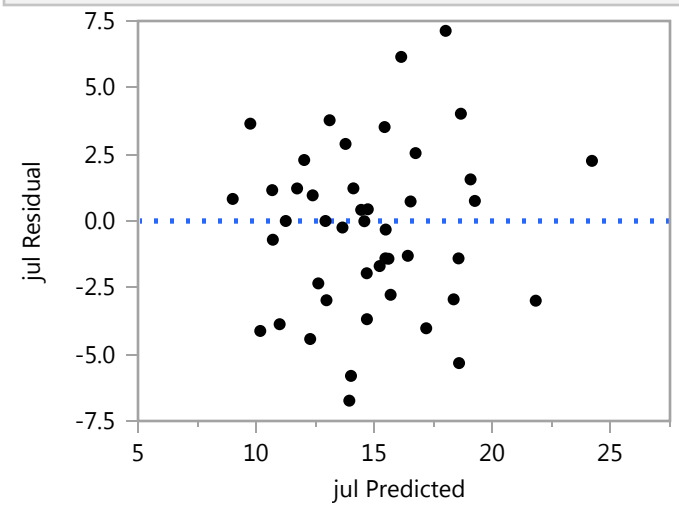

Expanded Estimates

Nominal factors expanded to all levels

Term	Estimate	Std Error	t Ratio	Prob>|t|
Intercept	0.2765213	17.09991	0.02	0.9872
Drainage Area	-0.000552	0.000888	-0.62	0.5394
Average Slope (%)	-0.275294	0.088022	-3.13	0.0042 *
Average Elevation (m)	0.0035364	0.011077	0.32	0.7520
A(2250)	0.1178088	0.051144	2.30	0.0292 *
Dominant Aspect[E]	4.9454217	2.697402	1.83	0.0778
Dominant Aspect[N]	1.168531	1.562527	0.75	0.4610
Dominant Aspect[NE]	-7.977976	4.640257	-1.72	0.0970
Dominant Aspect[NW]	0.8748532	1.793902	0.49	0.6297
Dominant Aspect[S]	0.744955	1.693995	0.44	0.6636
Dominant Aspect[SE]	1.1808392	2.566703	0.46	0.6492
Dominant Aspect[SW]	-0.920412	2.112926	-0.44	0.6666
Dominant Aspect[W]	-0.016212	1.844836	-0.01	0.9931
Rippability Index[Marginally Rippable]	-1.892653	1.136735	-1.66	0.1075
Rippability Index[Non-Rippable]	-1.354157	1.256372	-1.08	0.2906
Rippability Index[Rippable]	3.2468099	1.864728	1.74	0.0930
Landcover[Alpine]	-5.219085	4.55639	-1.15	0.2621
Landcover[Alpine/Forrested]	3.770384	2.153989	1.75	0.0914
Landcover[Forrested]	1.3888467	1.670154	0.83	0.4129

Least Squares Fit

Response jul

Whole Model

Expanded Estimates

Term	Estimate	Std Error	t Ratio	Prob>|t|
Landcover[Scrub]	0.0598542	2.077511	0.03	0.9772
Average Annual Precipitaiton (mm)	0.0018348	0.019767	0.09	0.9267

Drainage Area

Leverage Plot

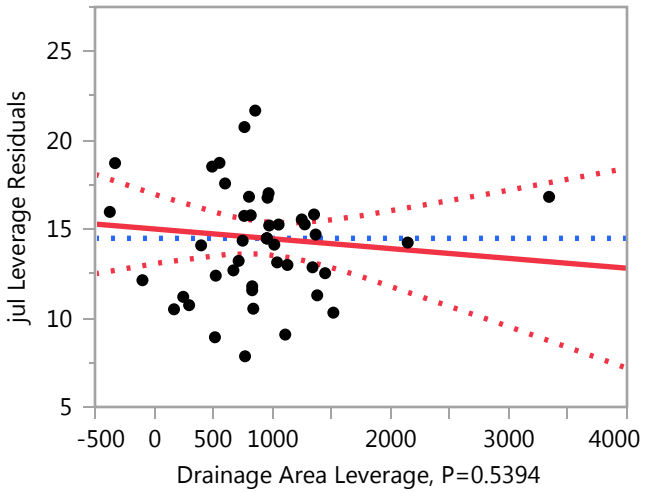

Average Slope (%)

Leverage Plot

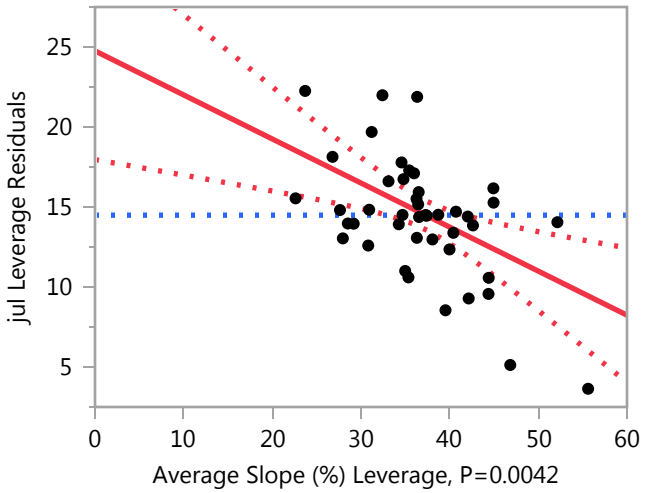

Least Squares Fit

Response jul

Average Slope (%)

Leverage Plot

Average Elevation (m)

Leverage Plot

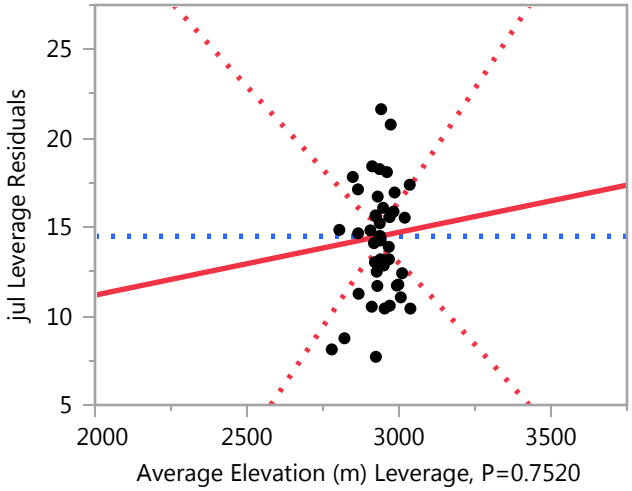

A(2250)

Leverage Plot

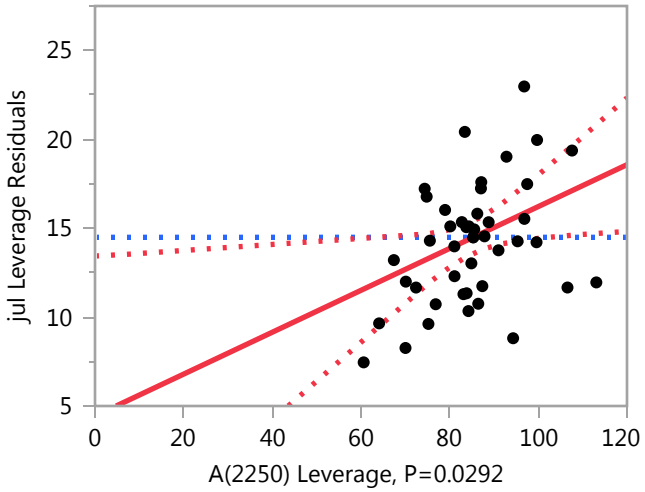

Least Squares Fit

Response jul

Dominant Aspect

Leverage Plot

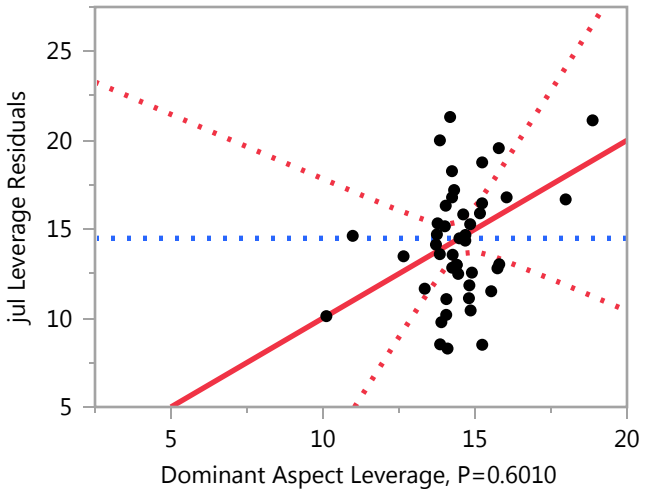

Least Squares Means Table

Level	Least Sq Mean	Std Error	Mean
E	16.292460	2.8287020	17.5789
N	12.515570	1.8007193	13.9461
NE	3.369063	5.7398241	12.9286
NW	12.221892	1.9036644	13.8043
S	12.091994	2.5436001	14.7322
SE	12.527878	3.3810237	16.2745
SW	10.426627	3.3041586	14.9000
W	11.330826	2.5485279	15.7083

Least Squares Fit

Response jul

Rippability Index

Leverage Plot

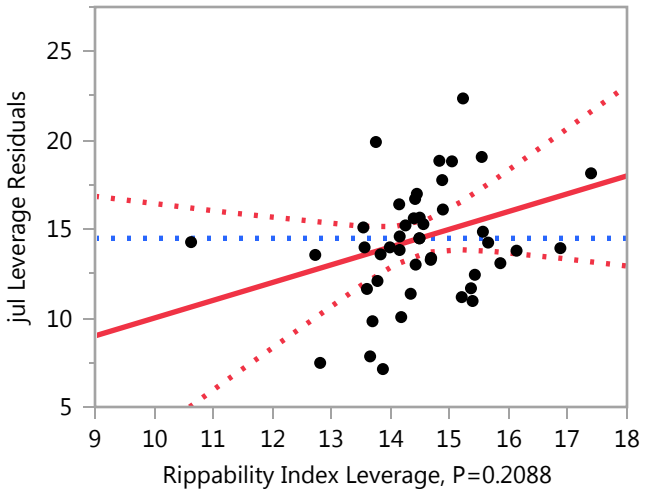

Least Squares Means Table

Level	Least Sq Mean	Std Error	Mean
Marginally Rippable	9.454386	2.7586421	15.4644
Non-Rippable	9.992881	2.7631188	12.8543
Rippable	14.593849	1.6891704	14.7487

Landcover

Leverage Plot

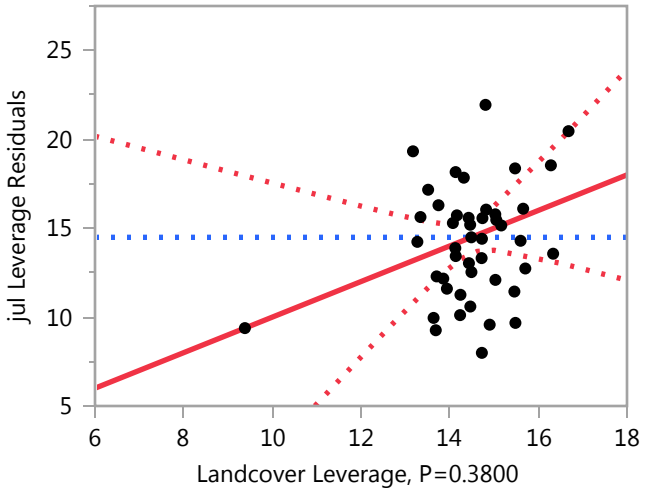

Least Squares Fit

Response jul

Landcover

Leverage Plot

Landcover Leverage, P=0.3800

Least Squares Means Table

Level	Least Sq Mean	Std Error	Mean
Alpine	6.127954	6.0114591	11.2500
Alpine/Forrested	15.117423	2.1917727	14.3697
Forrested	12.735885	1.3129355	14.7415
Scrub	11.406893	2.3468474	13.4540

Average Annual Precipitaiton (mm)

Leverage Plot

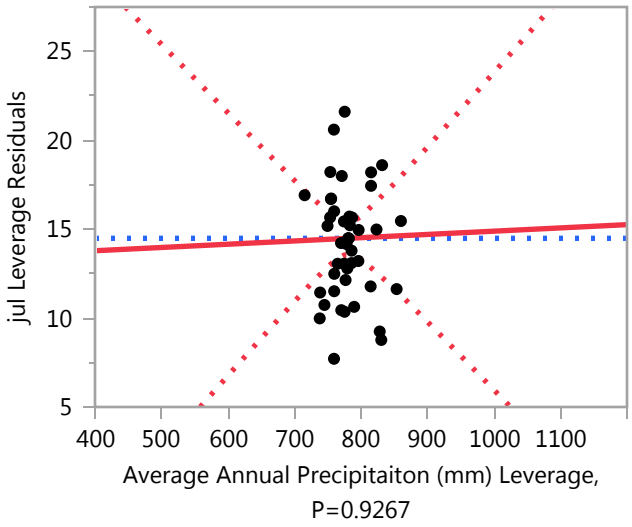

Least Squares Fit

Response jul

Average Annual Precipitaiton (mm)

Response aug

Whole Model

Actual by Predicted Plot

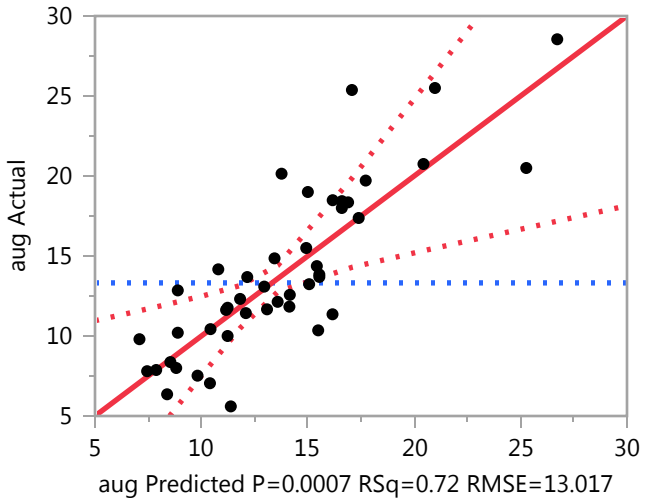

Summary of Fit

RSquare	0.716586
RSquare Adj	0.538139
Root Mean Square Error	13.0165
Mean of Response	13.31957
Observations (or Sum Wgts)	1114

Analysis of Variance

Source	DF	Sum of Squares	Mean Square	F Ratio
Model	17	11566.407	680.377	4.0157
Error	27	4574.593	169.429	**Prob > F**
C. Total	44	16141.001		0.0007 *

Least Squares Fit

Response aug

Whole Model

Parameter Estimates

Term	Estimate	Std Error	t Ratio	Prob>|t|
Intercept	26.967814	15.20772	1.77	0.0875
Drainage Area	-0.000357	0.00079	-0.45	0.6549
Average Slope (%)	-0.246253	0.078282	-3.15	0.0040 *
Average Elevation (m)	-0.012595	0.009851	-1.28	0.2119
A(2250)	0.1577105	0.045485	3.47	0.0018 *
Dominant Aspect[E]	7.5648855	2.398921	3.15	0.0039 *
Dominant Aspect[N]	0.9583841	1.389625	0.69	0.4963
Dominant Aspect[NE]	-6.950322	4.126788	-1.68	0.1037
Dominant Aspect[NW]	0.7477748	1.595398	0.47	0.6430
Dominant Aspect[S]	0.2356765	1.506546	0.16	0.8769
Dominant Aspect[SE]	-2.626638	2.282684	-1.15	0.2600
Dominant Aspect[SW]	-1.501942	1.87912	-0.80	0.4311
Rippability Index[Marginally Rippable]	-1.424591	1.010949	-1.41	0.1702
Rippability Index[Non-Rippable]	-0.388958	1.117348	-0.35	0.7305
Landcover[Alpine]	-7.823719	4.052202	-1.93	0.0641
Landcover[Alpine/Forrested]	5.0886873	1.915639	2.66	0.0131 *
Landcover[Forrested]	1.7778109	1.485343	1.20	0.2417
Average Annual Precipitaiton (mm)	0.0209552	0.01758	1.19	0.2436

Effect Tests

Source	Nparm	DF	Sum of Squares	F Ratio	Prob > F
Drainage Area	1	1	34.6181	0.2043	0.6549
Average Slope (%)	1	1	1676.5821	9.8955	0.0040 *
Average Elevation (m)	1	1	276.9537	1.6346	0.2119
A(2250)	1	1	2036.9628	12.0225	0.0018 *
Dominant Aspect	7	7	2131.4112	1.7971	0.1290
Rippability Index	2	2	336.8657	0.9941	0.3832
Landcover	3	3	1197.7902	2.3565	0.0940
Average Annual Precipitaiton (mm)	1	1	240.7441	1.4209	0.2436

Least Squares Fit

Response aug

Whole Model

Residual by Predicted Plot

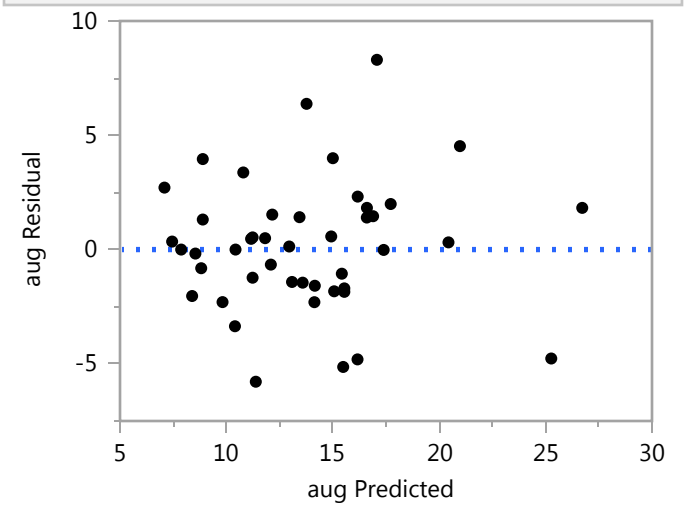

Expanded Estimates

Nominal factors expanded to all levels

Term	Estimate	Std Error	t Ratio	Prob>|t|
Intercept	26.967814	15.20772	1.77	0.0875
Drainage Area	-0.000357	0.00079	-0.45	0.6549
Average Slope (%)	-0.246253	0.078282	-3.15	0.0040 *
Average Elevation (m)	-0.012595	0.009851	-1.28	0.2119
A(2250)	0.1577105	0.045485	3.47	0.0018 *
Dominant Aspect[E]	7.5648855	2.398921	3.15	0.0039 *
Dominant Aspect[N]	0.9583841	1.389625	0.69	0.4963
Dominant Aspect[NE]	-6.950322	4.126788	-1.68	0.1037
Dominant Aspect[NW]	0.7477748	1.595398	0.47	0.6430
Dominant Aspect[S]	0.2356765	1.506546	0.16	0.8769
Dominant Aspect[SE]	-2.626638	2.282684	-1.15	0.2600
Dominant Aspect[SW]	-1.501942	1.87912	-0.80	0.4311
Dominant Aspect[W]	1.5721806	1.640695	0.96	0.3464
Rippability Index[Marginally Rippable]	-1.424591	1.010949	-1.41	0.1702
Rippability Index[Non-Rippable]	-0.388958	1.117348	-0.35	0.7305
Rippability Index[Rippable]	1.8135492	1.658386	1.09	0.2838
Landcover[Alpine]	-7.823719	4.052202	-1.93	0.0641
Landcover[Alpine/Forrested]	5.0886873	1.915639	2.66	0.0131 *
Landcover[Forrested]	1.7778109	1.485343	1.20	0.2417

Least Squares Fit

Response aug

Whole Model

Expanded Estimates

Term	Estimate	Std Error	t Ratio	Prob>|t|
Landcover[Scrub]	0.9572208	1.847624	0.52	0.6086
Average Annual Precipitaiton (mm)	0.0209552	0.01758	1.19	0.2436

Drainage Area

Leverage Plot

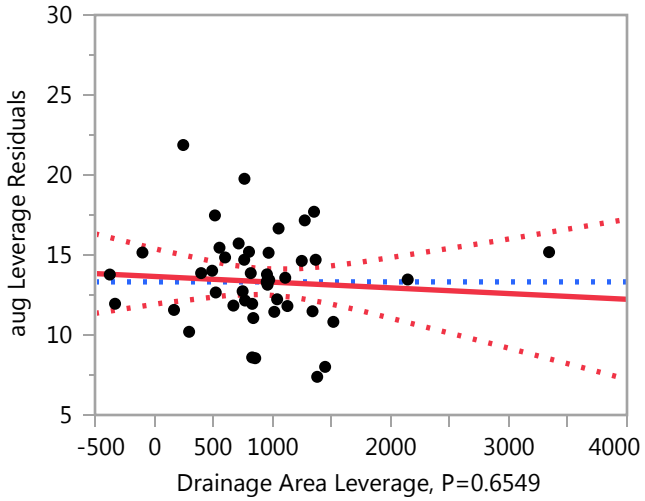

Average Slope (%)

Leverage Plot

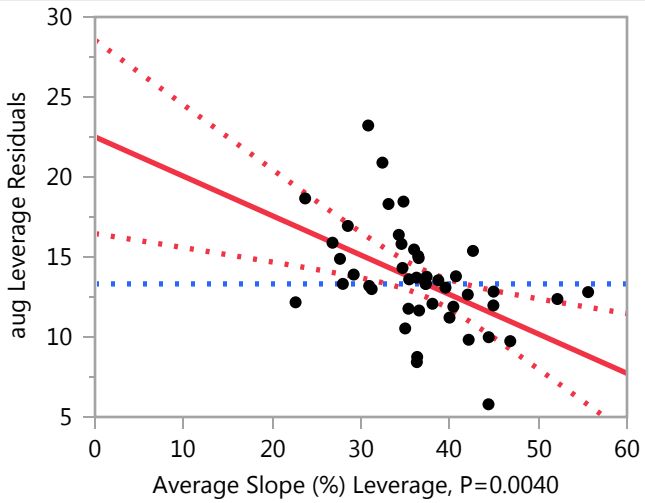

Least Squares Fit

Response aug

Average Slope (%)

Leverage Plot

Average Elevation (m)

Leverage Plot

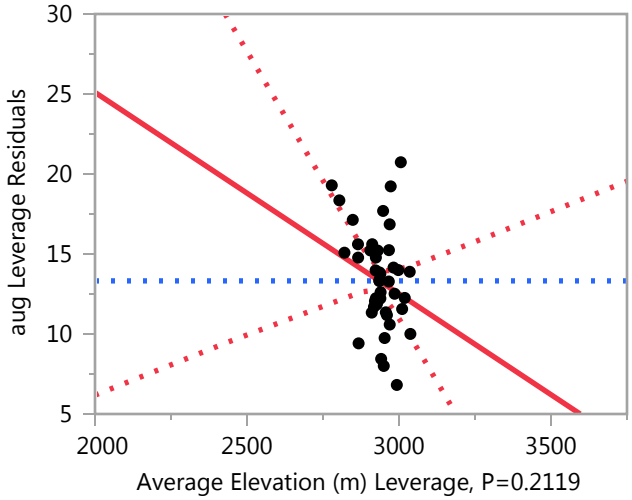

A(2250)

Leverage Plot

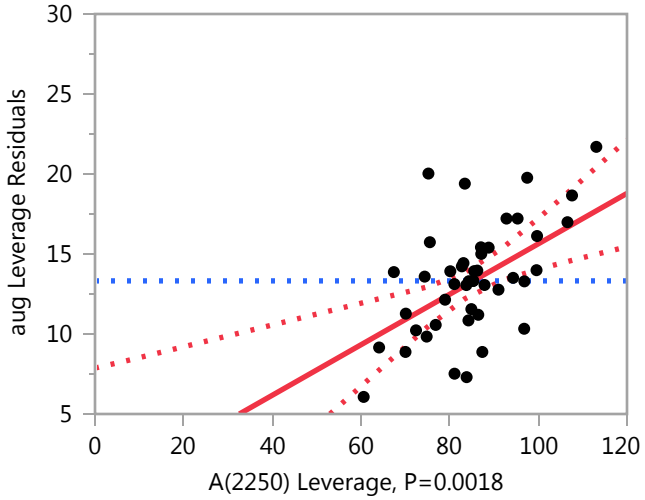

Least Squares Fit

Response aug

Dominant Aspect

Leverage Plot

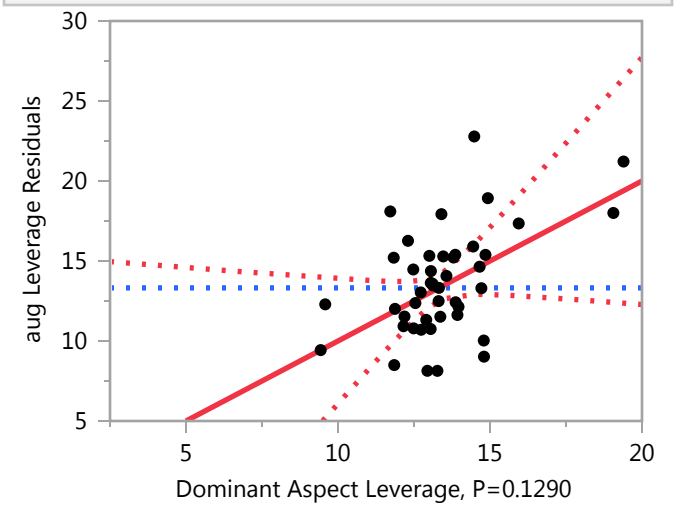

Least Squares Means Table

Level	Least Sq Mean	Std Error	Mean
E	17.852840	2.5156915	17.1053
N	11.246339	1.6014605	13.4072
NE	3.337633	5.1046829	10.4286
NW	11.035730	1.6930141	12.6775
S	10.523631	2.2621377	12.3891
SE	7.661317	3.0068959	12.7843
SW	8.786013	2.9385364	13.4556
W	11.860135	2.2665201	17.2361

Least Squares Fit

Response aug

Rippability Index

Leverage Plot

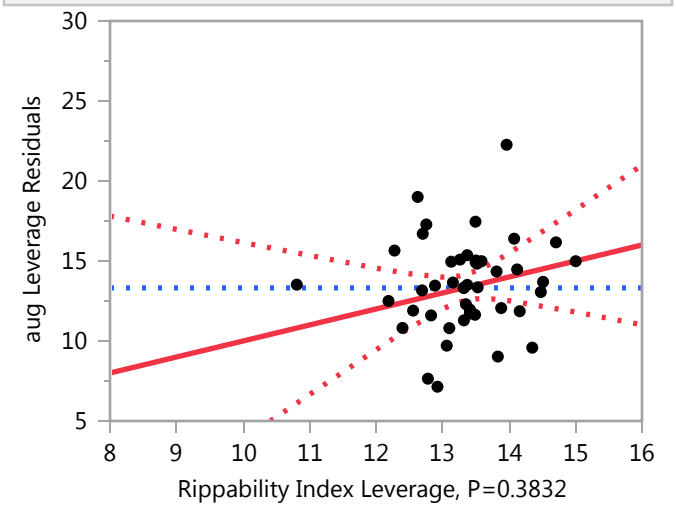

Least Squares Means Table

Level	Least Sq Mean	Std Error	Mean
Marginally Rippable	8.863364	2.4533841	14.1648
Non-Rippable	9.898996	2.4573654	10.9213
Rippable	12.101504	1.5022550	13.9663

Landcover

Leverage Plot

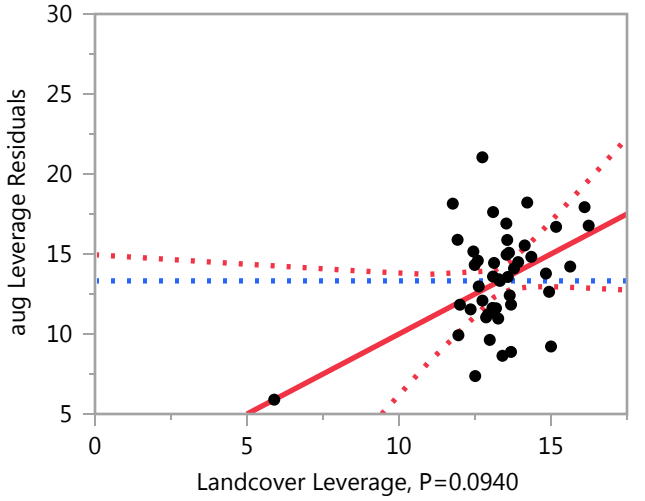

Least Squares Fit

Response aug

Landcover

Leverage Plot

Landcover Leverage, P=0.0940

Least Squares Means Table

Level	Least Sq Mean	Std Error	Mean
Alpine	2.464236	5.3462601	7.8750
Alpine/Forrested	15.376642	1.9492417	11.5966
Forrested	12.065766	1.1676524	13.5388
Scrub	11.245176	2.0871566	13.7362

Average Annual Precipitaiton (mm)

Leverage Plot

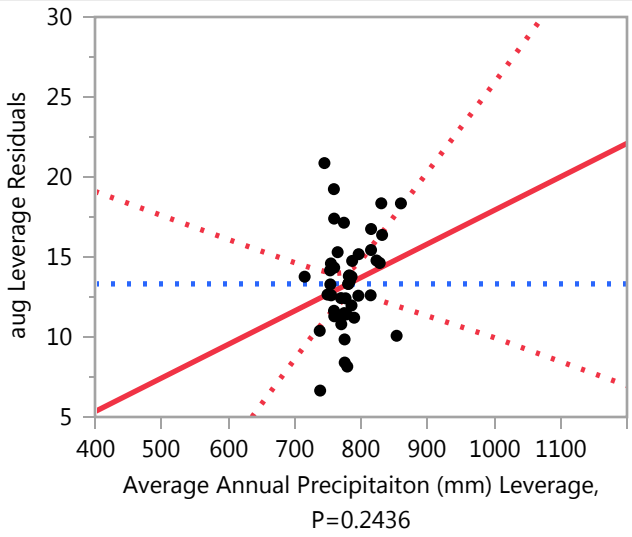

Least Squares Fit

Response aug

Average Annual Precipitaiton (mm)

Response sep

Whole Model

Actual by Predicted Plot

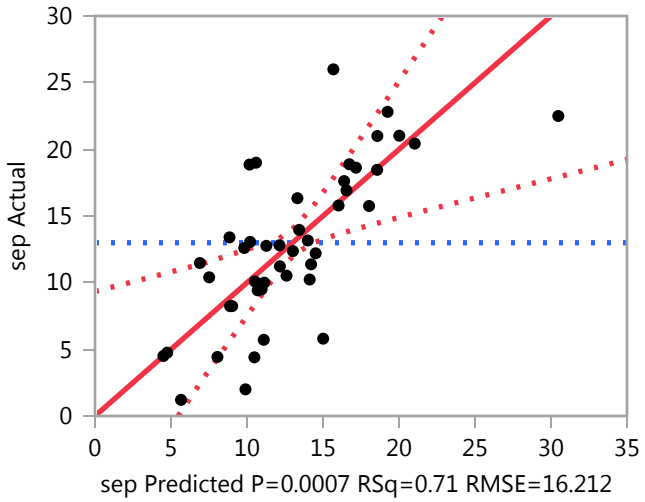

Summary of Fit

RSquare	0.713274
RSquare Adj	0.532742
Root Mean Square Error	16.21218
Mean of Response	12.99461
Observations (or Sum Wgts)	1114

Analysis of Variance

Source	DF	Sum of Squares	Mean Square	F Ratio
Model	17	17653.678	1038.45	3.9510
Error	27	7096.541	262.83	**Prob > F**
C. Total	44	24750.219		0.0007 *

Least Squares Fit

Response sep

Whole Model

Parameter Estimates

Term	Estimate	Std Error	t Ratio	Prob>|t|
Intercept	33.735282	18.94136	1.78	0.0862
Drainage Area	7.0436e-5	0.000984	0.07	0.9434
Average Slope (%)	-0.277522	0.097501	-2.85	0.0083 *
Average Elevation (m)	-0.028008	0.01227	-2.28	0.0305 *
A(2250)	0.1128598	0.056651	1.99	0.0566
Dominant Aspect[E]	-2.527218	2.987879	-0.85	0.4051
Dominant Aspect[N]	4.3355723	1.730791	2.50	0.0186 *
Dominant Aspect[NE]	-8.215095	5.139955	-1.60	0.1216
Dominant Aspect[NW]	4.7039988	1.987084	2.37	0.0253 *
Dominant Aspect[S]	-3.623786	1.876418	-1.93	0.0640
Dominant Aspect[SE]	2.4119096	2.843105	0.85	0.4037
Dominant Aspect[SW]	-0.480013	2.340462	-0.21	0.8390
Rippability Index[Marginally Rippable]	-1.749744	1.259147	-1.39	0.1760
Rippability Index[Non-Rippable]	-0.893539	1.391668	-0.64	0.5262
Landcover[Alpine]	-3.72591	5.047057	-0.74	0.4667
Landcover[Alpine/Forrested]	3.5152462	2.385947	1.47	0.1522
Landcover[Forrested]	0.0995432	1.850009	0.05	0.9575
Average Annual Precipitaiton (mm)	0.0757084	0.021895	3.46	0.0018 *

Effect Tests

Source	Nparm	DF	Sum of Squares	F Ratio	Prob > F
Drainage Area	1	1	1.3480	0.0051	0.9434
Average Slope (%)	1	1	2129.4034	8.1017	0.0083 *
Average Elevation (m)	1	1	1369.4958	5.2105	0.0305 *
A(2250)	1	1	1043.1350	3.9688	0.0566
Dominant Aspect	7	7	4644.7236	2.5245	0.0391 *
Rippability Index	2	2	540.6851	1.0286	0.3711
Landcover	3	3	718.9454	0.9118	0.4483
Average Annual Precipitaiton (mm)	1	1	3142.4079	11.9558	0.0018 *

Least Squares Fit

Response sep

Whole Model

Residual by Predicted Plot

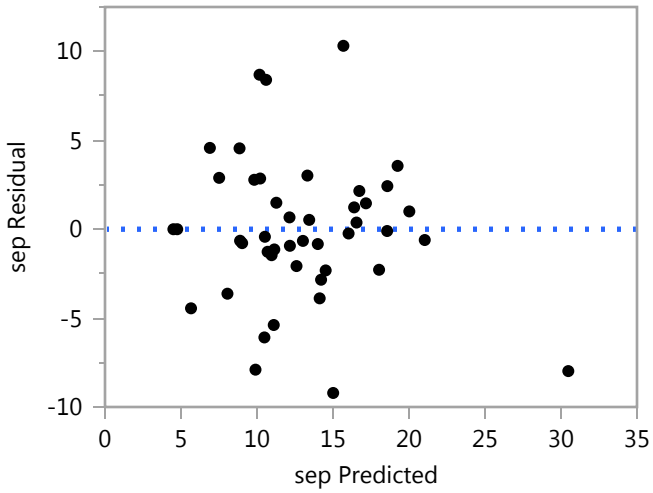

Expanded Estimates

Nominal factors expanded to all levels

Term	Estimate	Std Error	t Ratio	Prob>|t|
Intercept	33.735282	18.94136	1.78	0.0862
Drainage Area	7.0436e-5	0.000984	0.07	0.9434
Average Slope (%)	-0.277522	0.097501	-2.85	0.0083 *
Average Elevation (m)	-0.028008	0.01227	-2.28	0.0305 *
A(2250)	0.1128598	0.056651	1.99	0.0566
Dominant Aspect[E]	-2.527218	2.987879	-0.85	0.4051
Dominant Aspect[N]	4.3355723	1.730791	2.50	0.0186 *
Dominant Aspect[NE]	-8.215095	5.139955	-1.60	0.1216
Dominant Aspect[NW]	4.7039988	1.987084	2.37	0.0253 *
Dominant Aspect[S]	-3.623786	1.876418	-1.93	0.0640
Dominant Aspect[SE]	2.4119096	2.843105	0.85	0.4037
Dominant Aspect[SW]	-0.480013	2.340462	-0.21	0.8390
Dominant Aspect[W]	3.3946317	2.043501	1.66	0.1082
Rippability Index[Marginally Rippable]	-1.749744	1.259147	-1.39	0.1760
Rippability Index[Non-Rippable]	-0.893539	1.391668	-0.64	0.5262
Rippability Index[Rippable]	2.6432829	2.065536	1.28	0.2115
Landcover[Alpine]	-3.72591	5.047057	-0.74	0.4667
Landcover[Alpine/Forrested]	3.5152462	2.385947	1.47	0.1522
Landcover[Forrested]	0.0995432	1.850009	0.05	0.9575

Least Squares Fit

Response sep

Whole Model

Expanded Estimates

Term	Estimate	Std Error	t Ratio	Prob>|t|
Landcover[Scrub]	0.1111202	2.301233	0.05	0.9618
Average Annual Precipitaiton (mm)	0.0757084	0.021895	3.46	0.0018 *

Drainage Area

Leverage Plot

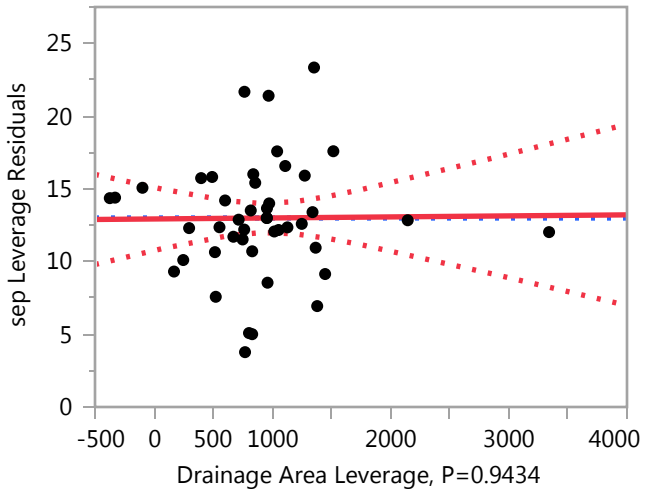

Average Slope (%)

Leverage Plot

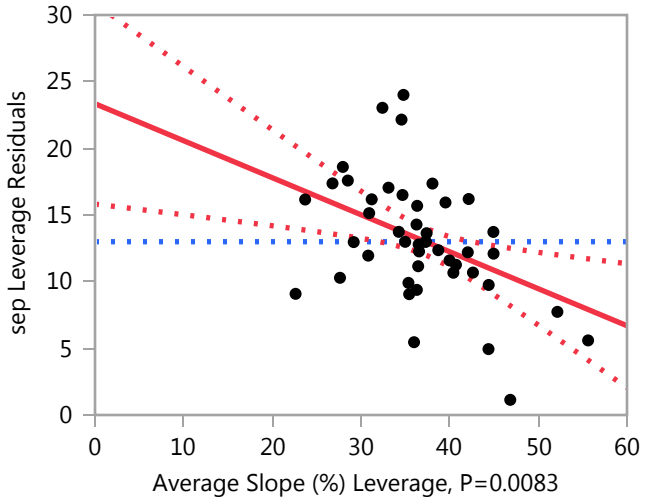

Least Squares Fit

Response sep

Average Slope (%)

Leverage Plot

Average Elevation (m)

Leverage Plot

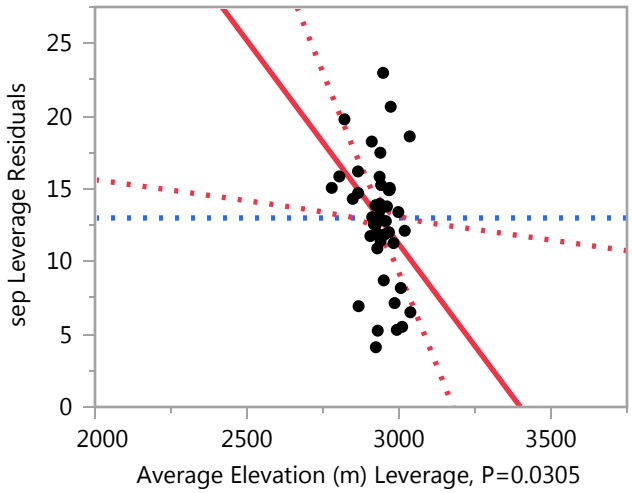

A(2250)

Leverage Plot

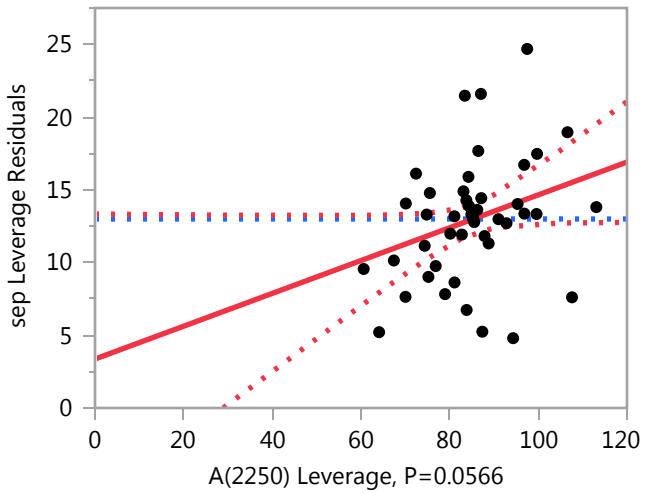

Least Squares Fit

Response sep

Dominant Aspect

Leverage Plot

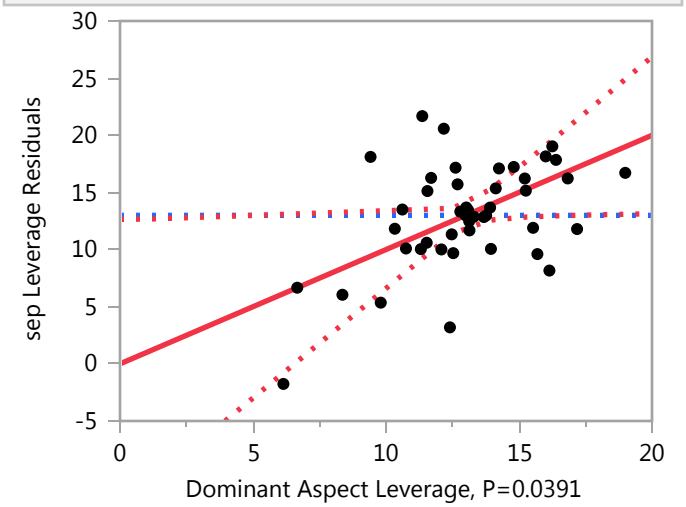

Least Squares Means Table

Level	Least Sq Mean	Std Error	Mean
E	7.455328	3.1333182	7.3158
N	14.318119	1.9946345	12.9880
NE	1.767452	6.3579320	4.5000
NW	14.686545	2.1086655	12.8116
S	6.358760	2.8175144	11.5732
SE	12.394456	3.7451180	19.5294
SW	9.502533	3.6599756	15.1778
W	13.377178	2.8229728	15.7361

Least Squares Fit

Response sep

Rippability Index

Leverage Plot

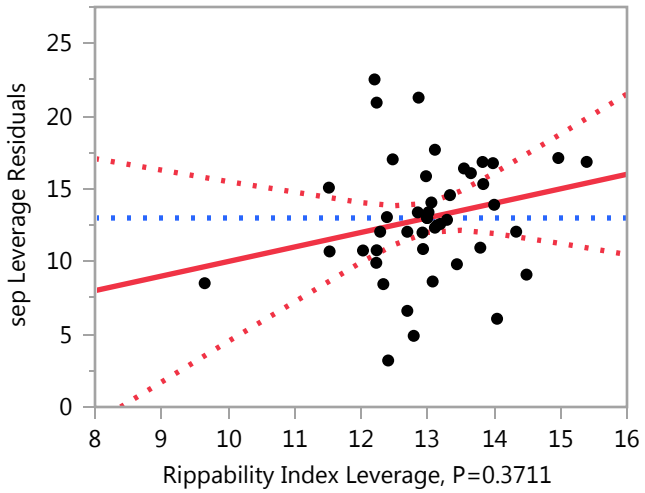

Least Squares Means Table

Level	Least Sq Mean	Std Error	Mean
Marginally Rippable	8.232802	3.0557136	12.5356
Non-Rippable	9.089007	3.0606725	10.1220
Rippable	12.625829	1.8710731	14.4317

Landcover

Leverage Plot

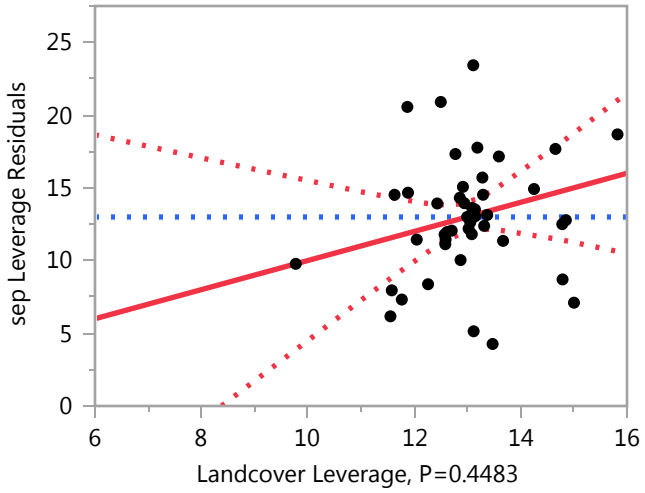

Least Squares Fit

Response sep

Landcover

Leverage Plot

Landcover Leverage, P=0.4483

Least Squares Means Table

Level	Least Sq Mean	Std Error	Mean
Alpine	6.256637	6.6588187	4.7500
Alpine/Forrested	13.497793	2.4277995	11.6218
Forrested	10.082089	1.4543224	12.8617
Scrub	10.093667	2.5995738	15.0736

Average Annual Precipitaiton (mm)

Leverage Plot

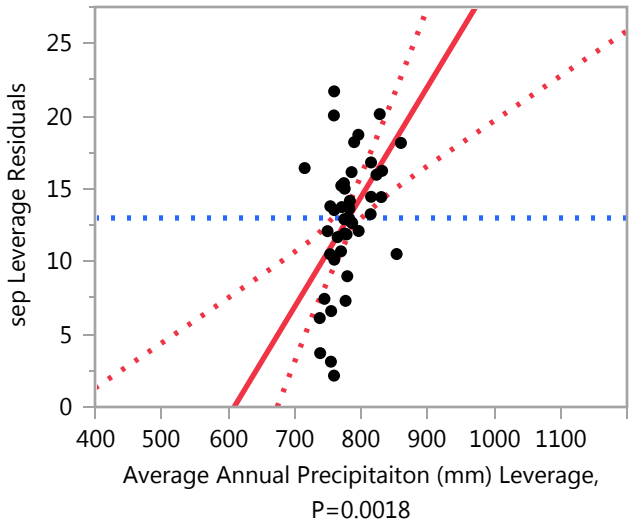

APPENDIX F

Least Squares Fit

Weight: Number of Years

Response apr

Whole Model

Actual by Predicted Plot

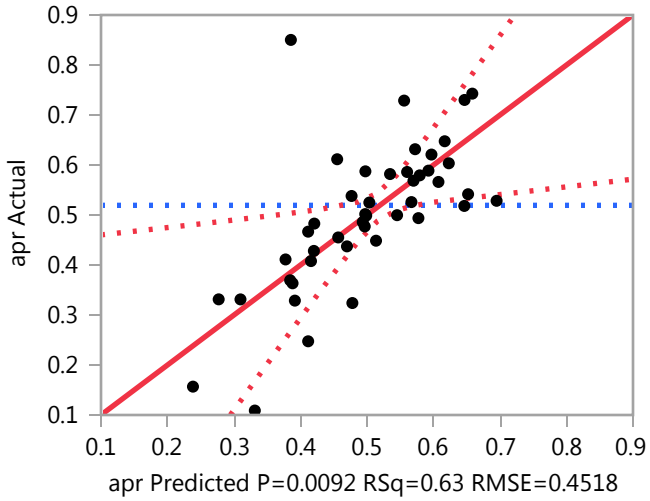

Summary of Fit

RSquare	0.634069
RSquare Adj	0.403668
Root Mean Square Error	0.451752
Mean of Response	0.519327
Observations (or Sum Wgts)	1114

Analysis of Variance

Source	DF	Sum of Squares	Mean Square	F Ratio
Model	17	9.547736	0.561632	2.7520
Error	27	5.510146	0.204079	**Prob > F**
C. Total	44	15.057882		0.0092 *

Parameter Estimates

Term	Estimate	Std Error	t Ratio	Prob>|t|
Intercept	0.406574	0.5278	0.77	0.4478
Drainage Area	1.0071e-6	2.741e-5	0.04	0.9710
Average Slope (%)	0.0103851	0.002717	3.82	0.0007 *
Average Elevation (m)	-1.741e-5	0.000342	-0.05	0.9598
A(2250)	-0.00052	0.001579	-0.33	0.7445
Dominant Aspect[E]	-0.032443	0.083257	-0.39	0.6998

Least Squares Fit

Response apr

Whole Model

Parameter Estimates

Term	Estimate	Std Error	t Ratio	Prob>|t|
Dominant Aspect[N]	0.0651499	0.048228	1.35	0.1880
Dominant Aspect[NE]	0.1053187	0.143225	0.74	0.4685
Dominant Aspect[NW]	0.0005133	0.05537	0.01	0.9927
Dominant Aspect[S]	0.0054147	0.052286	0.10	0.9183
Dominant Aspect[SE]	-0.120396	0.079223	-1.52	0.1402
Dominant Aspect[SW]	-0.058398	0.065217	-0.90	0.3785
Rippability Index[Marginally Rippable]	-0.011268	0.035086	-0.32	0.7506
Rippability Index[Non-Rippable]	-0.020393	0.038779	-0.53	0.6033
Landcover[Alpine]	0.0442812	0.140636	0.31	0.7553
Landcover[Alpine/Forrested]	-0.036436	0.066484	-0.55	0.5882
Landcover[Forrested]	0.0378568	0.05155	0.73	0.4691
Average Annual Precipitaiton (mm)	-0.000282	0.00061	-0.46	0.6473

Effect Tests

Source	Nparm	DF	Sum of Squares	F Ratio	Prob > F
Drainage Area	1	1	0.0002756	0.0014	0.9710
Average Slope (%)	1	1	2.9818251	14.6111	0.0007 *
Average Elevation (m)	1	1	0.0005291	0.0026	0.9598
A(2250)	1	1	0.0221165	0.1084	0.7445
Dominant Aspect	7	7	1.6434978	1.1505	0.3626
Rippability Index	2	2	0.0658182	0.1613	0.8519
Landcover	3	3	0.8701910	1.4213	0.2582
Average Annual Precipitaiton (mm)	1	1	0.0436812	0.2140	0.6473

Least Squares Fit

Response apr

Whole Model

Residual by Predicted Plot

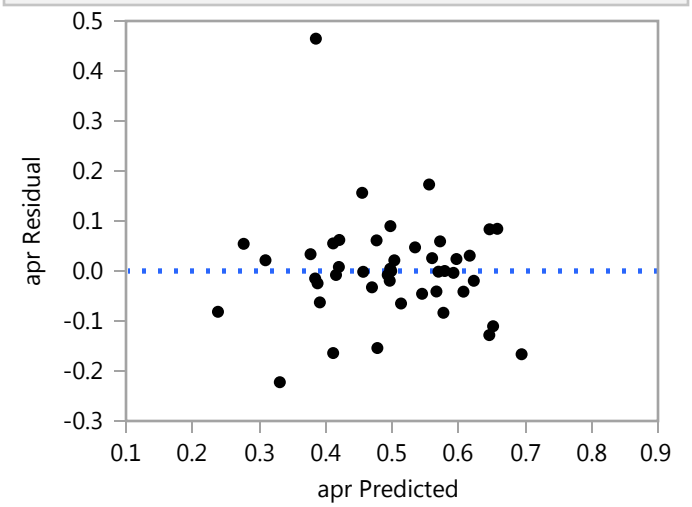

Expanded Estimates

Nominal factors expanded to all levels

Term	Estimate	Std Error	t Ratio	Prob>|t|
Intercept	0.406574	0.5278	0.77	0.4478
Drainage Area	1.0071e-6	2.741e-5	0.04	0.9710
Average Slope (%)	0.0103851	0.002717	3.82	0.0007 *
Average Elevation (m)	-1.741e-5	0.000342	-0.05	0.9598
A(2250)	-0.00052	0.001579	-0.33	0.7445
Dominant Aspect[E]	-0.032443	0.083257	-0.39	0.6998
Dominant Aspect[N]	0.0651499	0.048228	1.35	0.1880
Dominant Aspect[NE]	0.1053187	0.143225	0.74	0.4685
Dominant Aspect[NW]	0.0005133	0.05537	0.01	0.9927
Dominant Aspect[S]	0.0054147	0.052286	0.10	0.9183
Dominant Aspect[SE]	-0.120396	0.079223	-1.52	0.1402
Dominant Aspect[SW]	-0.058398	0.065217	-0.90	0.3785
Dominant Aspect[W]	0.0348401	0.056942	0.61	0.5458
Rippability Index[Marginally Rippable]	-0.011268	0.035086	-0.32	0.7506
Rippability Index[Non-Rippable]	-0.020393	0.038779	-0.53	0.6033
Rippability Index[Rippable]	0.0316616	0.057556	0.55	0.5868
Landcover[Alpine]	0.0442812	0.140636	0.31	0.7553
Landcover[Alpine/Forrested]	-0.036436	0.066484	-0.55	0.5882
Landcover[Forrested]	0.0378568	0.05155	0.73	0.4691

Least Squares Fit

Response apr

Whole Model

Expanded Estimates

Term	Estimate	Std Error	t Ratio	Prob>|t|
Landcover[Scrub]	-0.045702	0.064124	-0.71	0.4821
Average Annual Precipitaiton (mm)	-0.000282	0.00061	-0.46	0.6473

Drainage Area

Leverage Plot

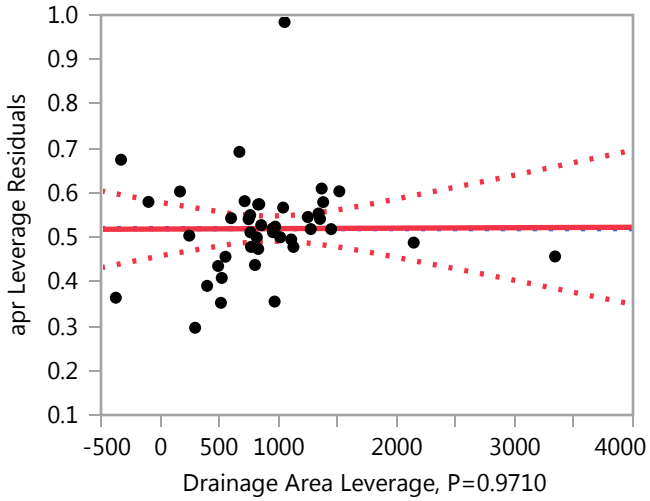

Average Slope (%)

Leverage Plot

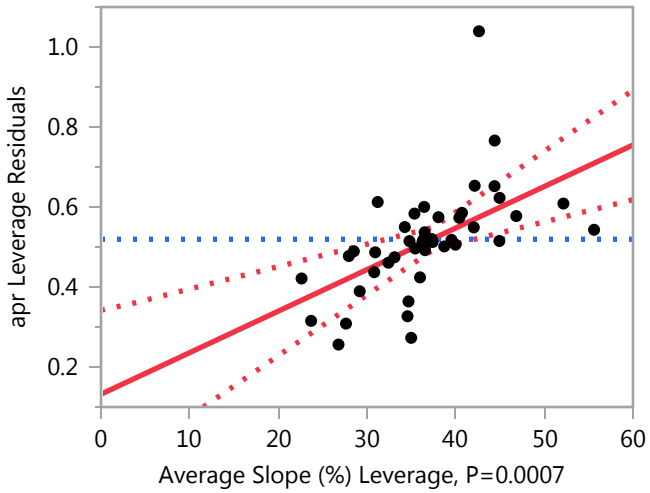

Least Squares Fit

Response apr

Average Elevation (m)

Leverage Plot

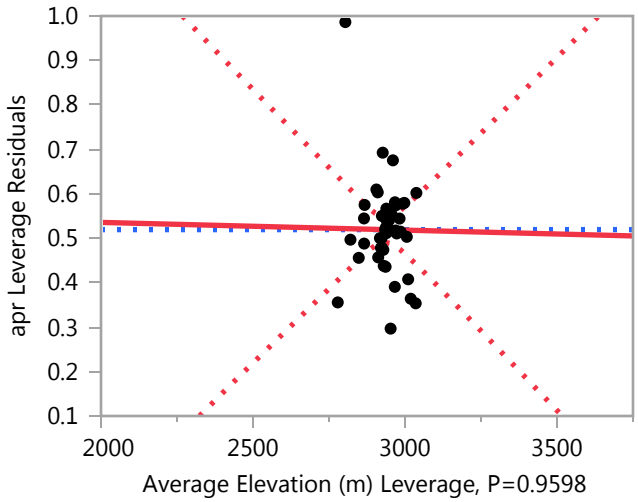

A(2250)

Leverage Plot

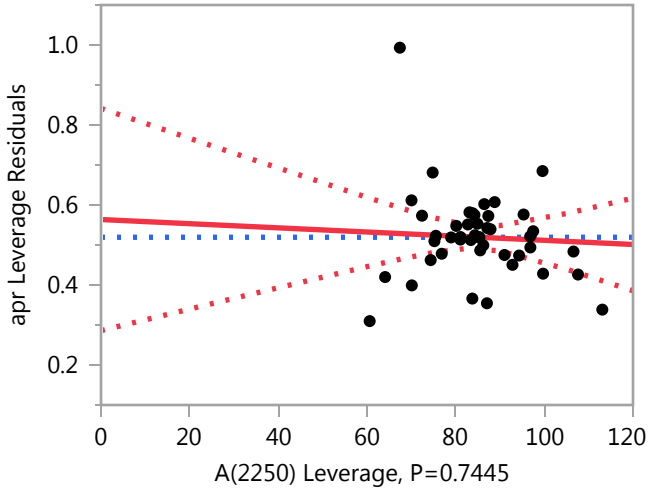

Least Squares Fit

Response apr

Dominant Aspect

Leverage Plot

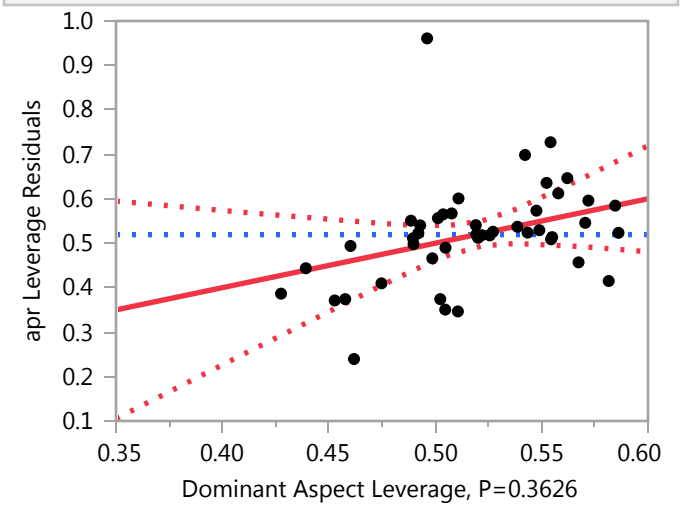

Least Squares Means Table

Level	Least Sq Mean	Std Error	Mean
E	0.44657967	0.08730974	0.441322
N	0.54417242	0.05558038	0.558249
NE	0.58434125	0.17716343	0.579270
NW	0.47953582	0.05875785	0.507212
S	0.48443726	0.07850989	0.550378
SE	0.35862655	0.10435751	0.504137
SW	0.42062461	0.10198502	0.407741
W	0.51386268	0.07866198	0.461906

Least Squares Fit

Response apr

Rippability Index

Leverage Plot

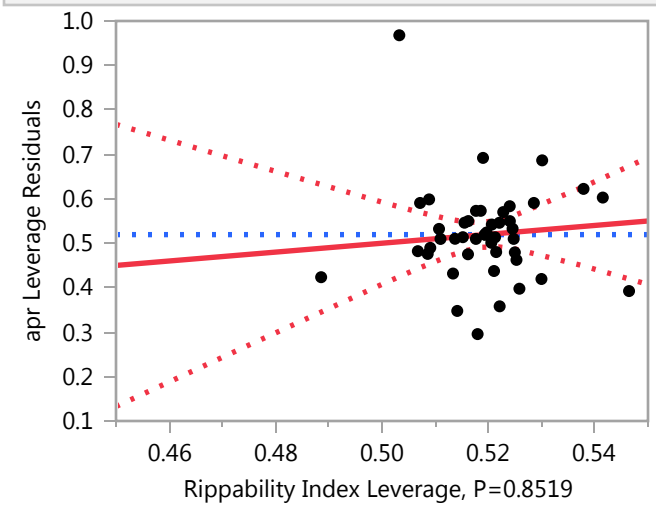

Least Squares Means Table

Level	Least Sq Mean	Std Error	Mean
Marginally Rippable	0.46775419	0.08514730	0.472090
Non-Rippable	0.45862932	0.08528547	0.568830
Rippable	0.51068409	0.05213735	0.519393

Landcover

Leverage Plot

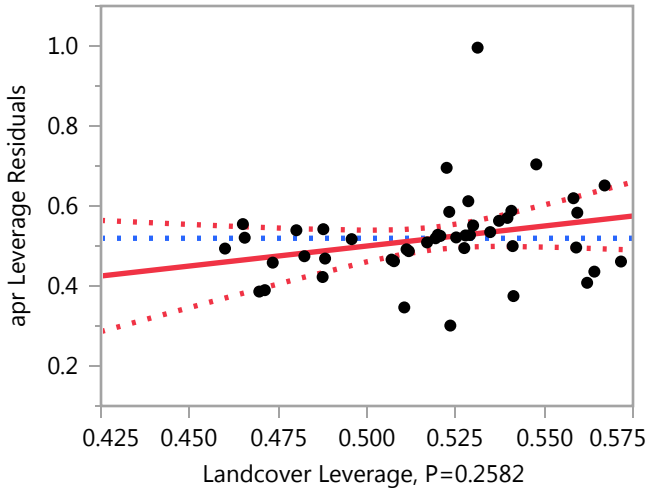

Least Squares Fit

Response apr

Landcover

Least Squares Means Table

Level	Least Sq Mean	Std Error	Mean
Alpine	0.52330375	0.18554762	0.498804
Alpine/Forrested	0.44258681	0.06765050	0.520649
Forrested	0.51687933	0.04052461	0.518856
Scrub	0.43332023	0.07243698	0.521753

Average Annual Precipitaiton (mm)

Leverage Plot

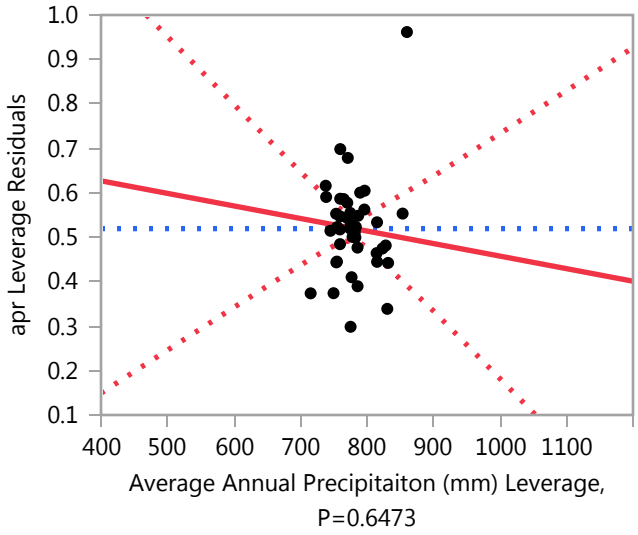

Least Squares Fit

Response apr

Average Annual Precipitaiton (mm)

Response may

Whole Model

Actual by Predicted Plot

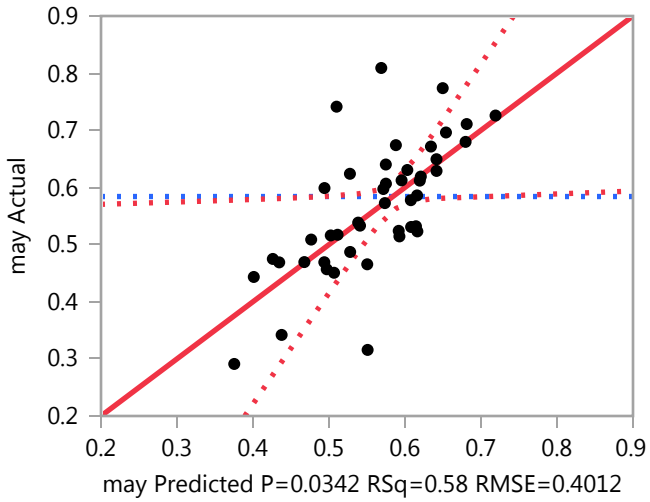

Summary of Fit

RSquare	0.578411
RSquare Adj	0.312967
Root Mean Square Error	0.401212
Mean of Response	0.584067
Observations (or Sum Wgts)	1114

Analysis of Variance

Source	DF	Sum of Squares	Mean Square	F Ratio
Model	17	5.962922	0.350760	2.1790
Error	27	4.346215	0.160971	Prob > F
C. Total	44	10.309138		0.0342 *

Least Squares Fit

Response may

Whole Model

Parameter Estimates

Term	Estimate	Std Error	t Ratio	Prob>|t|
Intercept	0.9389211	0.468752	2.00	0.0553
Drainage Area	3.7111e-5	2.434e-5	1.52	0.1390
Average Slope (%)	0.0017083	0.002413	0.71	0.4850
Average Elevation (m)	-0.000357	0.000304	-1.18	0.2501
A(2250)	0.0014975	0.001402	1.07	0.2949
Dominant Aspect[E]	-0.161062	0.073943	-2.18	0.0383 *
Dominant Aspect[N]	0.0237903	0.042833	0.56	0.5832
Dominant Aspect[NE]	0.2230539	0.127201	1.75	0.0909
Dominant Aspect[NW]	0.0503701	0.049175	1.02	0.3148
Dominant Aspect[S]	-0.072254	0.046437	-1.56	0.1314
Dominant Aspect[SE]	-0.041851	0.07036	-0.59	0.5569
Dominant Aspect[SW]	-0.030543	0.057921	-0.53	0.6023
Rippability Index[Marginally Rippable]	0.0183972	0.031161	0.59	0.5598
Rippability Index[Non-Rippable]	-0.020606	0.03444	-0.60	0.5546
Landcover[Alpine]	0.1348232	0.124902	1.08	0.2899
Landcover[Alpine/Forrested]	-0.089464	0.059046	-1.52	0.1414
Landcover[Forrested]	-0.023736	0.045783	-0.52	0.6084
Average Annual Precipitaiton (mm)	0.0006362	0.000542	1.17	0.2506

Effect Tests

Source	Nparm	DF	Sum of Squares	F Ratio	Prob > F
Drainage Area	1	1	0.3742105	2.3247	0.1390
Average Slope (%)	1	1	0.0806826	0.5012	0.4850
Average Elevation (m)	1	1	0.2223847	1.3815	0.2501
A(2250)	1	1	0.1836412	1.1408	0.2949
Dominant Aspect	7	7	1.5854011	1.4070	0.2432
Rippability Index	2	2	0.1443956	0.4485	0.6432
Landcover	3	3	0.3916299	0.8110	0.4989
Average Annual Precipitaiton (mm)	1	1	0.2219252	1.3787	0.2506

Least Squares Fit

Response may

Whole Model

Residual by Predicted Plot

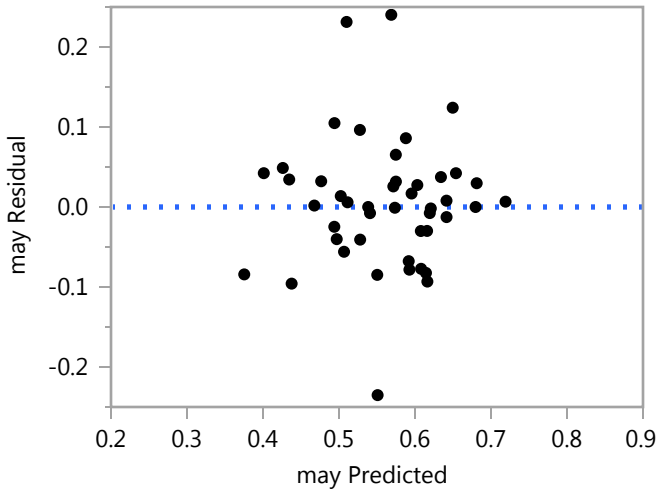

Expanded Estimates

Nominal factors expanded to all levels

Term	Estimate	Std Error	t Ratio	Prob>|t|
Intercept	0.9389211	0.468752	2.00	0.0553
Drainage Area	3.7111e-5	2.434e-5	1.52	0.1390
Average Slope (%)	0.0017083	0.002413	0.71	0.4850
Average Elevation (m)	-0.000357	0.000304	-1.18	0.2501
A(2250)	0.0014975	0.001402	1.07	0.2949
Dominant Aspect[E]	-0.161062	0.073943	-2.18	0.0383 *
Dominant Aspect[N]	0.0237903	0.042833	0.56	0.5832
Dominant Aspect[NE]	0.2230539	0.127201	1.75	0.0909
Dominant Aspect[NW]	0.0503701	0.049175	1.02	0.3148
Dominant Aspect[S]	-0.072254	0.046437	-1.56	0.1314
Dominant Aspect[SE]	-0.041851	0.07036	-0.59	0.5569
Dominant Aspect[SW]	-0.030543	0.057921	-0.53	0.6023
Dominant Aspect[W]	0.0084955	0.050572	0.17	0.8678
Rippability Index[Marginally Rippable]	0.0183972	0.031161	0.59	0.5598
Rippability Index[Non-Rippable]	-0.020606	0.03444	-0.60	0.5546
Rippability Index[Rippable]	0.0022088	0.051117	0.04	0.9659
Landcover[Alpine]	0.1348232	0.124902	1.08	0.2899
Landcover[Alpine/Forrested]	-0.089464	0.059046	-1.52	0.1414
Landcover[Forrested]	-0.023736	0.045783	-0.52	0.6084

Least Squares Fit

Response may

Whole Model

Expanded Estimates

Term	Estimate	Std Error	t Ratio	Prob>|t|
Landcover[Scrub]	-0.021623	0.05695	-0.38	0.7072
Average Annual Precipitaiton (mm)	0.0006362	0.000542	1.17	0.2506

Drainage Area

Leverage Plot

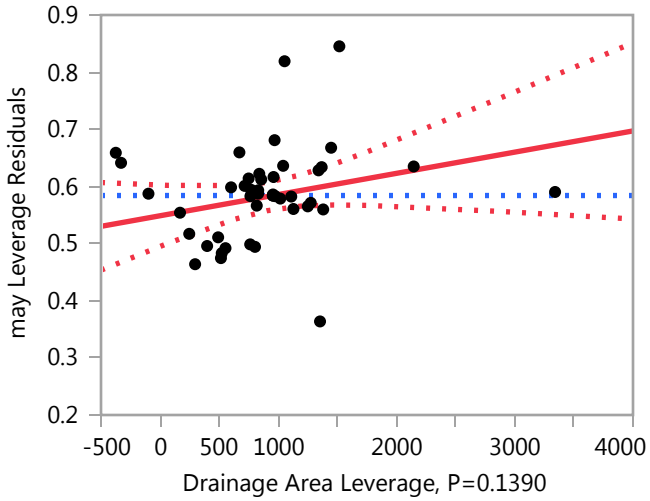

Average Slope (%)

Leverage Plot

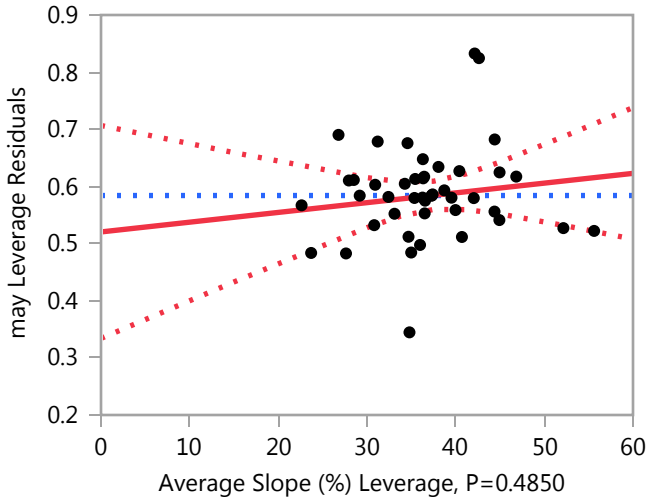

Least Squares Fit

Response may

Average Slope (%)

Leverage Plot

Average Elevation (m)

Leverage Plot

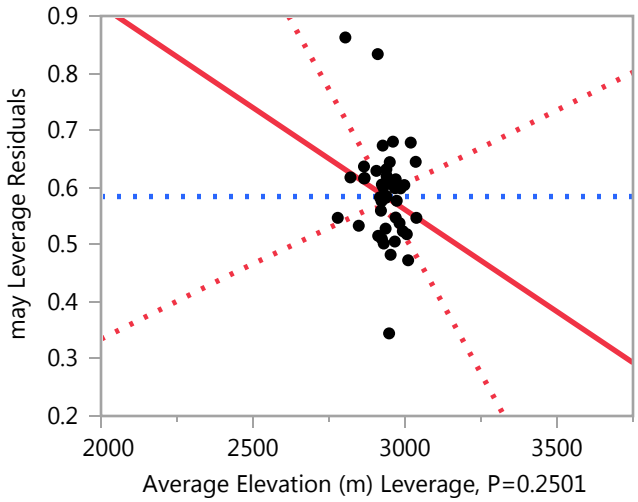

A(2250)

Leverage Plot

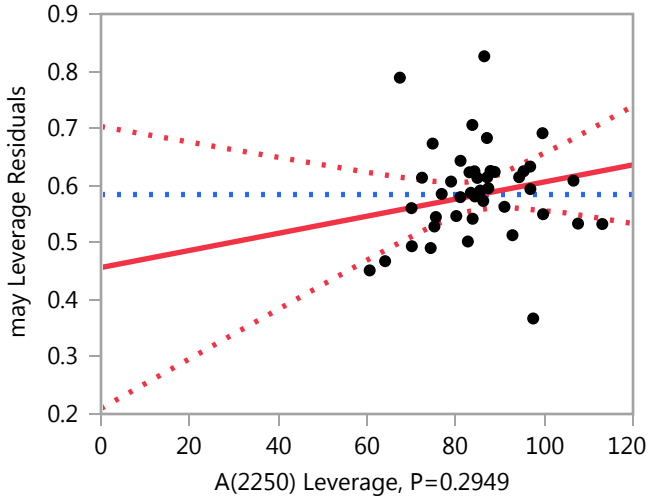

Least Squares Fit

Response may

Dominant Aspect

Leverage Plot

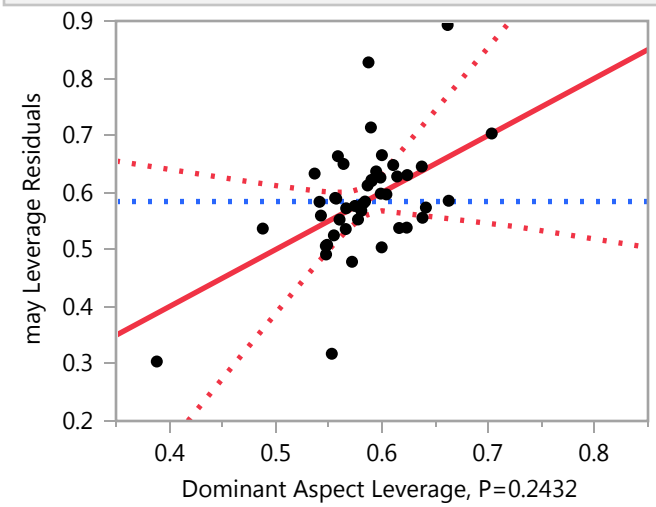

Least Squares Means Table

Level	Least Sq Mean	Std Error	Mean
E	0.45384239	0.07754196	0.435033
N	0.63869475	0.04936232	0.599890
NE	0.83795840	0.15734326	0.679712
NW	0.66527456	0.05218431	0.639159
S	0.54265080	0.06972659	0.529188
SE	0.57305326	0.09268251	0.618316
SW	0.58436179	0.09057544	0.541465
W	0.62339997	0.06986167	0.570710

Least Squares Fit

Response may

Rippability Index

Leverage Plot

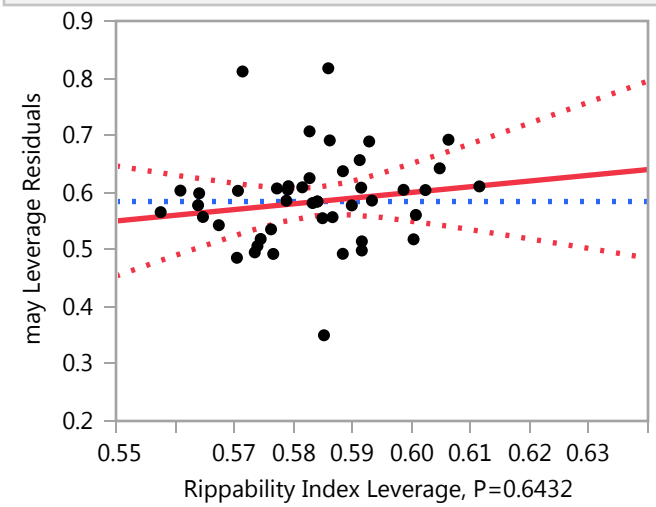

Least Squares Means Table

Level	Least Sq Mean	Std Error	Mean
Marginally Rippable	0.63330173	0.07562144	0.556369
Non-Rippable	0.59429842	0.07574415	0.533914
Rippable	0.61711331	0.04630448	0.618021

Landcover

Leverage Plot

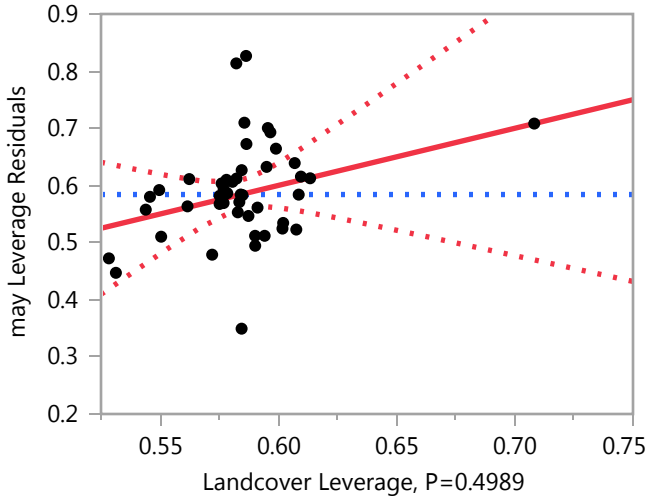

Least Squares Fit

Response may

Landcover

Leverage Plot

Landcover Leverage, P=0.4989

Least Squares Means Table

Level	Least Sq Mean	Std Error	Mean
Alpine	0.74972768	0.16478947	0.538398
Alpine/Forrested	0.52544020	0.06008210	0.494214
Forrested	0.59116853	0.03599092	0.584774
Scrub	0.59328156	0.06433309	0.648334

Average Annual Precipitaiton (mm)

Leverage Plot

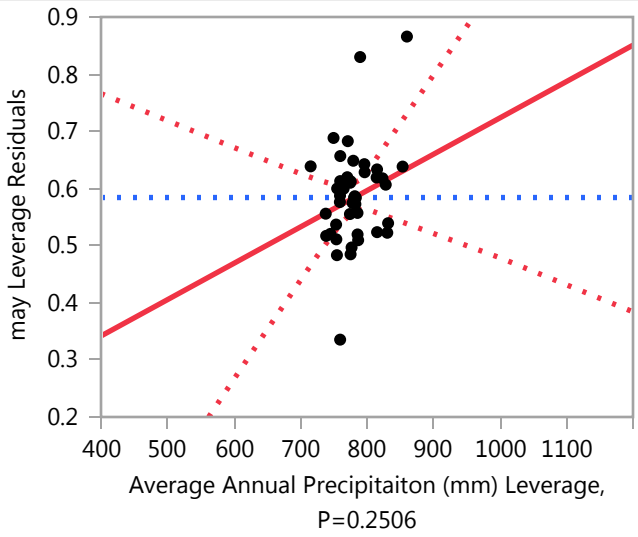

Least Squares Fit

Response may

Average Annual Precipitaiton (mm)

Response jun

Whole Model

Actual by Predicted Plot

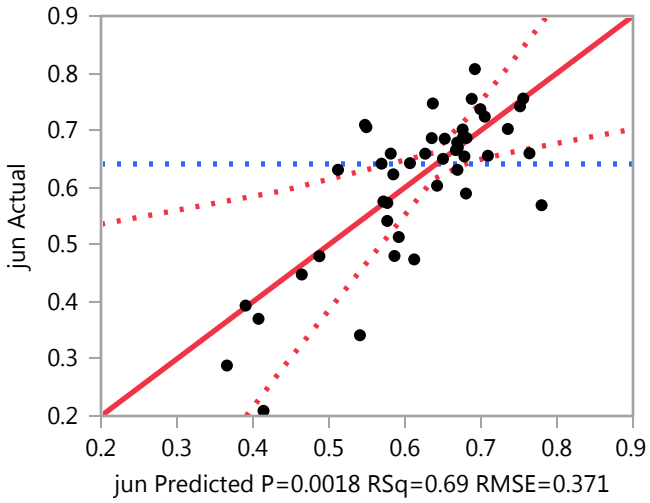

Summary of Fit

RSquare	0.687866
RSquare Adj	0.491336
Root Mean Square Error	0.371048
Mean of Response	0.641073
Observations (or Sum Wgts)	1114

Analysis of Variance

Source	DF	Sum of Squares	Mean Square	F Ratio
Model	17	8.191935	0.481879	3.5001
Error	27	3.717275	0.137677	**Prob > F**
C. Total	44	11.909211		0.0018 *

Least Squares Fit

Response jun

Whole Model

Parameter Estimates

Term	Estimate	Std Error	t Ratio	Prob>|t|
Intercept	0.3342798	0.433511	0.77	0.4473
Drainage Area	0.0000362	2.251e-5	1.61	0.1195
Average Slope (%)	0.0063422	0.002232	2.84	0.0084 *
Average Elevation (m)	0.0002236	0.000281	0.80	0.4328
A(2250)	-0.003335	0.001297	-2.57	0.0159 *
Dominant Aspect[E]	-0.069007	0.068384	-1.01	0.3219
Dominant Aspect[N]	-0.05972	0.039613	-1.51	0.1433
Dominant Aspect[NE]	0.1773439	0.117638	1.51	0.1433
Dominant Aspect[NW]	0.0283886	0.045478	0.62	0.5377
Dominant Aspect[S]	-0.025194	0.042946	-0.59	0.5623
Dominant Aspect[SE]	-0.042813	0.06507	-0.66	0.5161
Dominant Aspect[SW]	0.0334899	0.053566	0.63	0.5371
Rippability Index[Marginally Rippable]	0.0315476	0.028818	1.09	0.2833
Rippability Index[Non-Rippable]	-0.023622	0.031851	-0.74	0.4647
Landcover[Alpine]	0.0548871	0.115512	0.48	0.6385
Landcover[Alpine/Forrested]	-0.051164	0.054607	-0.94	0.3571
Landcover[Forrested]	-0.010797	0.042341	-0.26	0.8006
Average Annual Precipitaiton (mm)	-0.000389	0.000501	-0.78	0.4444

Effect Tests

Source	Nparm	DF	Sum of Squares	F Ratio	Prob > F
Drainage Area	1	1	0.3558742	2.5849	0.1195
Average Slope (%)	1	1	1.1120934	8.0776	0.0084 *
Average Elevation (m)	1	1	0.0873016	0.6341	0.4328
A(2250)	1	1	0.9108615	6.6159	0.0159 *
Dominant Aspect	7	7	1.6767974	1.7399	0.1417
Rippability Index	2	2	0.3018034	1.0961	0.3486
Landcover	3	3	0.1327425	0.3214	0.8098
Average Annual Precipitaiton (mm)	1	1	0.0829328	0.6024	0.4444

Least Squares Fit

Response jun

Whole Model

Residual by Predicted Plot

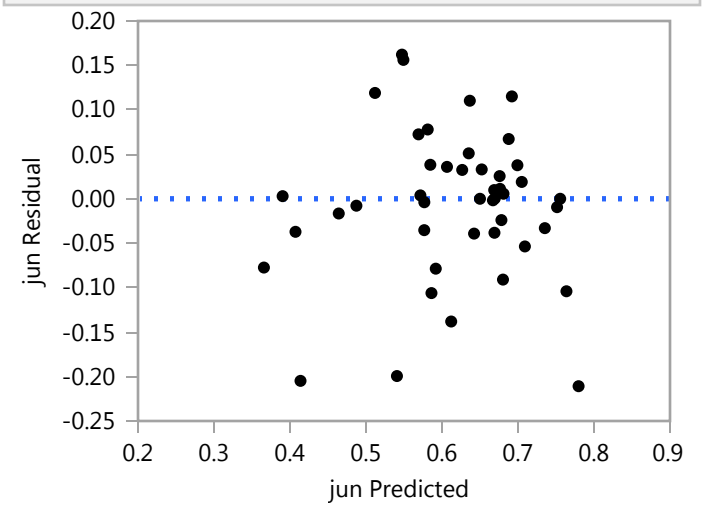

Expanded Estimates

Nominal factors expanded to all levels

Term	Estimate	Std Error	t Ratio	Prob>|t|
Intercept	0.3342798	0.433511	0.77	0.4473
Drainage Area	0.0000362	2.251e-5	1.61	0.1195
Average Slope (%)	0.0063422	0.002232	2.84	0.0084 *
Average Elevation (m)	0.0002236	0.000281	0.80	0.4328
A(2250)	-0.003335	0.001297	-2.57	0.0159 *
Dominant Aspect[E]	-0.069007	0.068384	-1.01	0.3219
Dominant Aspect[N]	-0.05972	0.039613	-1.51	0.1433
Dominant Aspect[NE]	0.1773439	0.117638	1.51	0.1433
Dominant Aspect[NW]	0.0283886	0.045478	0.62	0.5377
Dominant Aspect[S]	-0.025194	0.042946	-0.59	0.5623
Dominant Aspect[SE]	-0.042813	0.06507	-0.66	0.5161
Dominant Aspect[SW]	0.0334899	0.053566	0.63	0.5371
Dominant Aspect[W]	-0.042489	0.04677	-0.91	0.3717
Rippability Index[Marginally Rippable]	0.0315476	0.028818	1.09	0.2833
Rippability Index[Non-Rippable]	-0.023622	0.031851	-0.74	0.4647
Rippability Index[Rippable]	-0.007926	0.047274	-0.17	0.8681
Landcover[Alpine]	0.0548871	0.115512	0.48	0.6385
Landcover[Alpine/Forrested]	-0.051164	0.054607	-0.94	0.3571
Landcover[Forrested]	-0.010797	0.042341	-0.26	0.8006

Least Squares Fit

Response jun

Whole Model

Expanded Estimates

Term	Estimate	Std Error	t Ratio	Prob>|t|
Landcover[Scrub]	0.0070738	0.052668	0.13	0.8942
Average Annual Precipitaiton (mm)	-0.000389	0.000501	-0.78	0.4444

Drainage Area

Leverage Plot

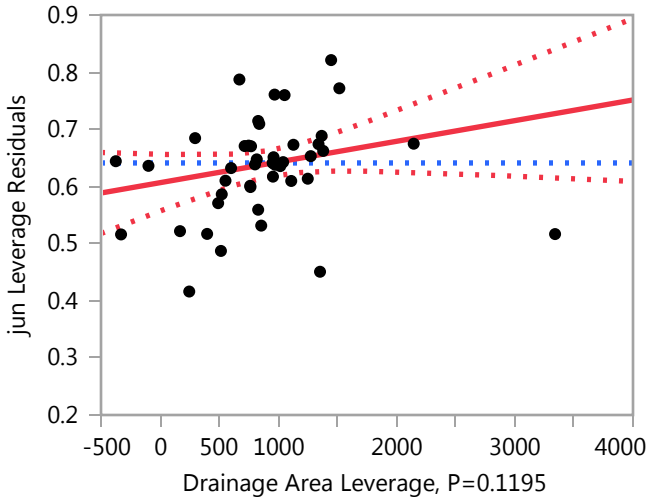

Average Slope (%)

Leverage Plot

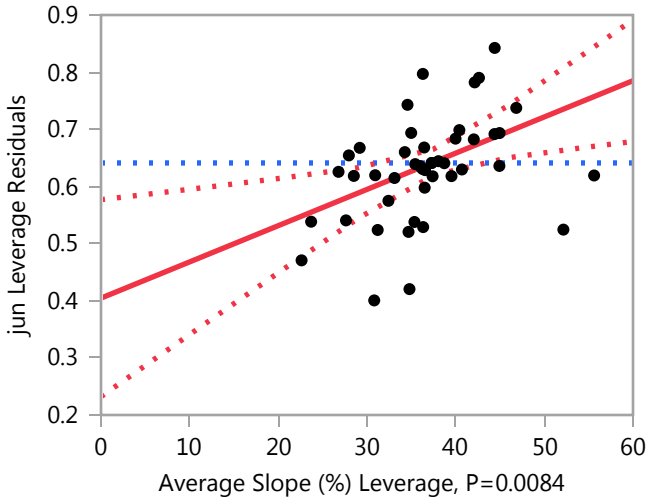

Least Squares Fit

Response jun

Average Slope (%)

Leverage Plot

Average Elevation (m)

Leverage Plot

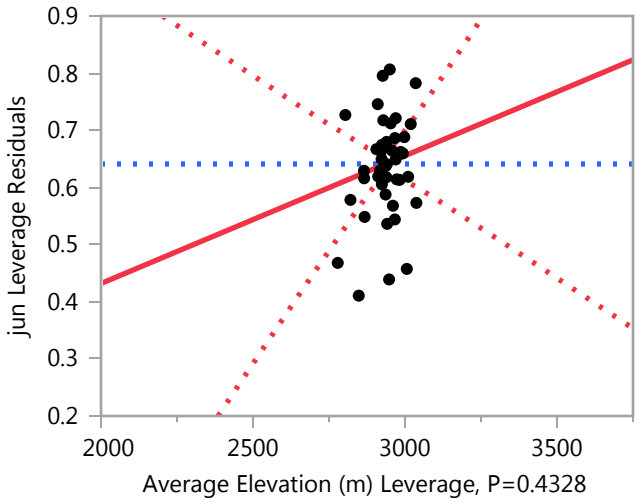

A(2250)

Leverage Plot

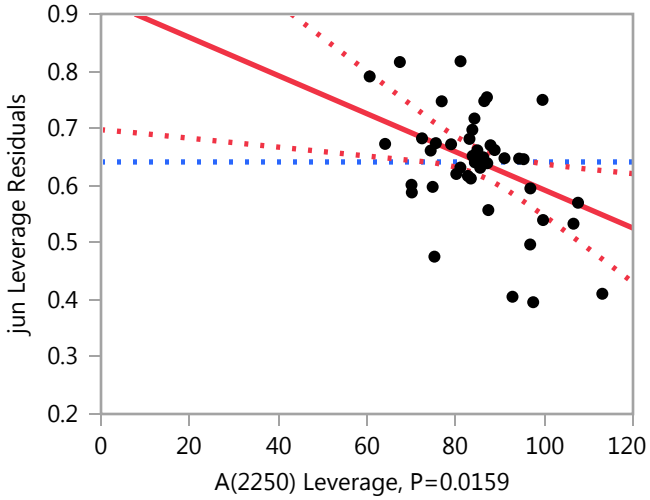

Least Squares Fit

Response jun

Dominant Aspect

Leverage Plot

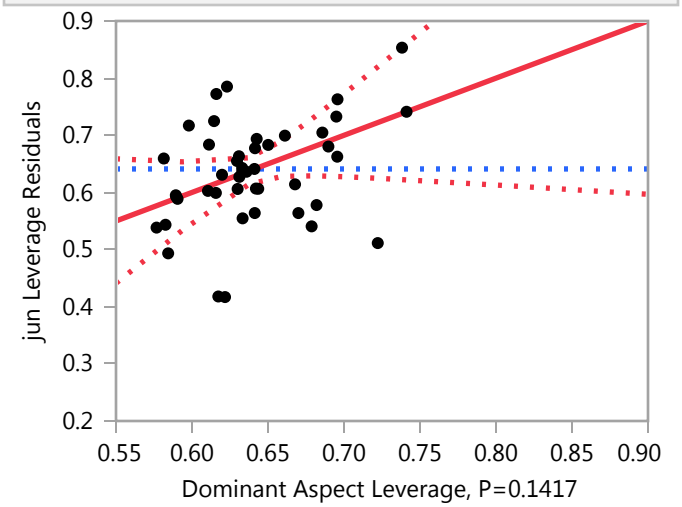

Least Squares Means Table

Level	Least Sq Mean	Std Error	Mean
E	0.60453489	0.07171228	0.583326
N	0.61382188	0.04565122	0.604986
NE	0.85088585	0.14551404	0.755518
NW	0.70193063	0.04826104	0.714650
S	0.64834819	0.06448447	0.656969
SE	0.63072920	0.08571455	0.579668
SW	0.70703194	0.08376589	0.637763
W	0.63105336	0.06460940	0.529520

Least Squares Fit

Response jun

Rippability Index

Leverage Plot

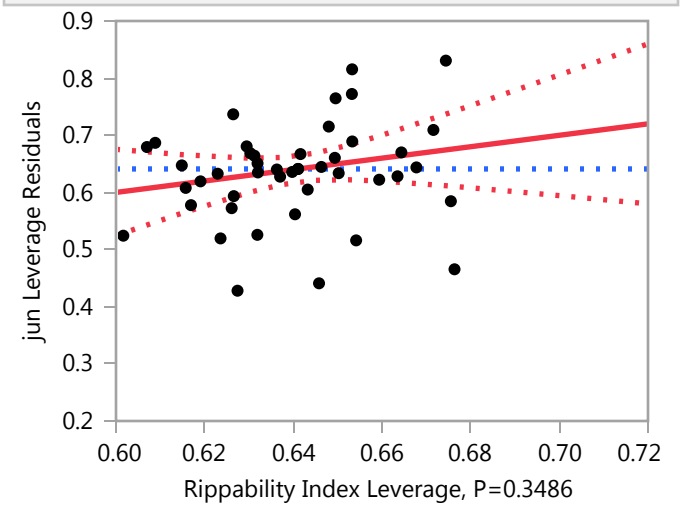

Least Squares Means Table

Level	Least Sq Mean	Std Error	Mean
Marginally Rippable	0.70508961	0.06993614	0.609826
Non-Rippable	0.64991999	0.07004963	0.639999
Rippable	0.66561638	0.04282327	0.655602

Landcover

Leverage Plot

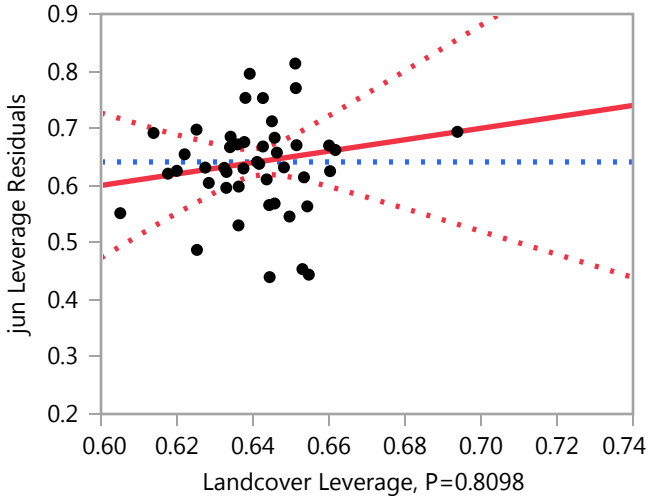

Least Squares Fit

Response jun

Landcover

Leverage Plot

Landcover Leverage, P=0.8098

Least Squares Means Table

Level	Least Sq Mean	Std Error	Mean
Alpine	0.72842909	0.15240044	0.649966
Alpine/Forrested	0.62237846	0.05556507	0.668293
Forrested	0.66274460	0.03328509	0.631888
Scrub	0.68061582	0.05949647	0.667197

Average Annual Precipitaiton (mm)

Leverage Plot

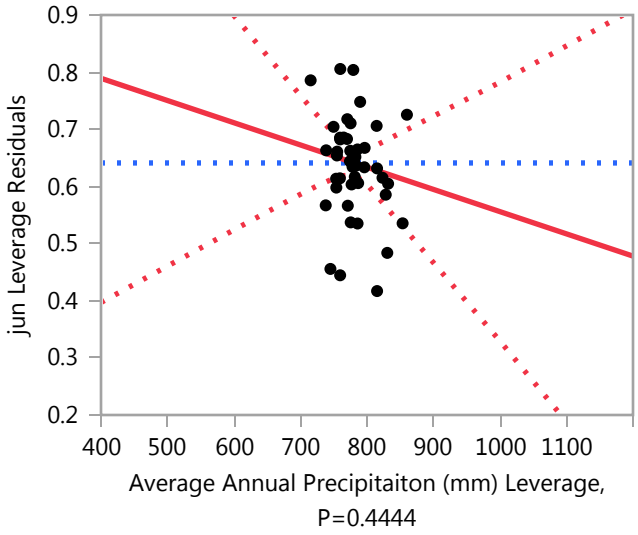

Least Squares Fit

Response jun

Average Annual Precipitaiton (mm)

Response jul

Whole Model

Actual by Predicted Plot

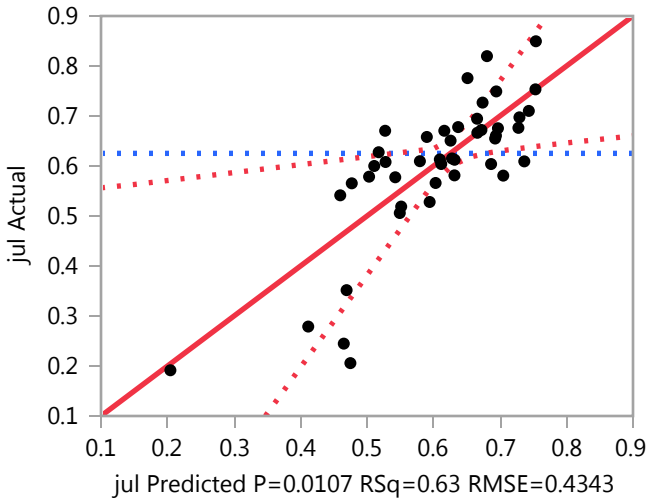

Summary of Fit

RSquare	0.6282
RSquare Adj	0.394104
Root Mean Square Error	0.434316
Mean of Response	0.625275
Observations (or Sum Wgts)	1114

Analysis of Variance

Source	DF	Sum of Squares	Mean Square	F Ratio
Model	17	8.605251	0.506191	2.6835
Error	27	5.093014	0.188630	**Prob > F**
C. Total	44	13.698265		0.0107 *

Least Squares Fit

Response jul

Whole Model

Parameter Estimates

Term	Estimate	Std Error	t Ratio	Prob>|t|
Intercept	0.9912191	0.507429	1.95	0.0612
Drainage Area	3.3485e-5	2.635e-5	1.27	0.2146
Average Slope (%)	0.010833	0.002612	4.15	0.0003 *
Average Elevation (m)	6.0915e-5	0.000329	0.19	0.8544
A(2250)	-0.001558	0.001518	-1.03	0.3139
Dominant Aspect[E]	-0.08135	0.080044	-1.02	0.3185
Dominant Aspect[N]	-0.082465	0.046367	-1.78	0.0866
Dominant Aspect[NE]	0.2494648	0.137697	1.81	0.0812
Dominant Aspect[NW]	-0.100382	0.053233	-1.89	0.0701
Dominant Aspect[S]	0.0422933	0.050268	0.84	0.4075
Dominant Aspect[SE]	0.0354838	0.076165	0.47	0.6450
Dominant Aspect[SW]	0.039093	0.0627	0.62	0.5382
Rippability Index[Marginally Rippable]	0.0697537	0.033732	2.07	0.0484 *
Rippability Index[Non-Rippable]	0.0509285	0.037282	1.37	0.1832
Landcover[Alpine]	0.1028755	0.135208	0.76	0.4533
Landcover[Alpine/Forrested]	-0.073812	0.063918	-1.15	0.2583
Landcover[Forrested]	-0.029066	0.049561	-0.59	0.5624
Average Annual Precipitaiton (mm)	-0.000949	0.000587	-1.62	0.1172

Effect Tests

Source	Nparm	DF	Sum of Squares	F Ratio	Prob > F
Drainage Area	1	1	0.3046486	1.6151	0.2146
Average Slope (%)	1	1	3.2446018	17.2009	0.0003 *
Average Elevation (m)	1	1	0.0064781	0.0343	0.8544
A(2250)	1	1	0.1986842	1.0533	0.3139
Dominant Aspect	7	7	1.6908788	1.2806	0.2969
Rippability Index	2	2	0.9763228	2.5879	0.0937
Landcover	3	3	0.2690772	0.4755	0.7019
Average Annual Precipitaiton (mm)	1	1	0.4940861	2.6193	0.1172

Least Squares Fit

Response jul

Whole Model

Residual by Predicted Plot

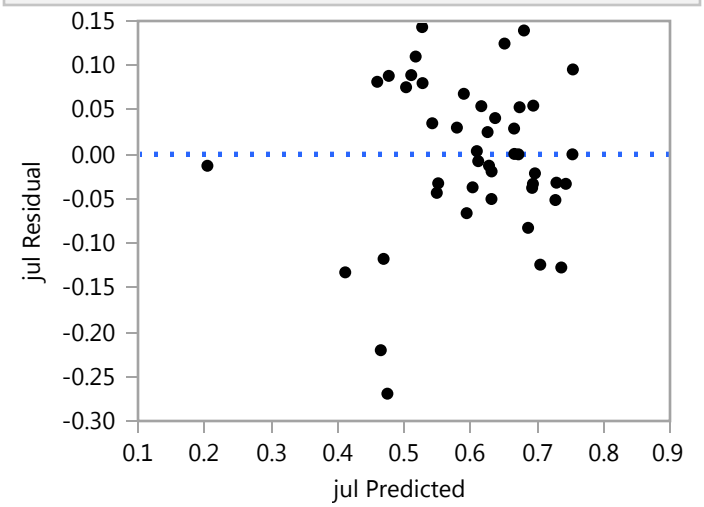

Expanded Estimates

Nominal factors expanded to all levels

Term	Estimate	Std Error	t Ratio	Prob>|t|
Intercept	0.9912191	0.507429	1.95	0.0612
Drainage Area	3.3485e-5	2.635e-5	1.27	0.2146
Average Slope (%)	0.010833	0.002612	4.15	0.0003 *
Average Elevation (m)	6.0915e-5	0.000329	0.19	0.8544
A(2250)	-0.001558	0.001518	-1.03	0.3139
Dominant Aspect[E]	-0.08135	0.080044	-1.02	0.3185
Dominant Aspect[N]	-0.082465	0.046367	-1.78	0.0866
Dominant Aspect[NE]	0.2494648	0.137697	1.81	0.0812
Dominant Aspect[NW]	-0.100382	0.053233	-1.89	0.0701
Dominant Aspect[S]	0.0422933	0.050268	0.84	0.4075
Dominant Aspect[SE]	0.0354838	0.076165	0.47	0.6450
Dominant Aspect[SW]	0.039093	0.0627	0.62	0.5382
Dominant Aspect[W]	-0.102138	0.054744	-1.87	0.0730
Rippability Index[Marginally Rippable]	0.0697537	0.033732	2.07	0.0484 *
Rippability Index[Non-Rippable]	0.0509285	0.037282	1.37	0.1832
Rippability Index[Rippable]	-0.120682	0.055335	-2.18	0.0381 *
Landcover[Alpine]	0.1028755	0.135208	0.76	0.4533
Landcover[Alpine/Forrested]	-0.073812	0.063918	-1.15	0.2583
Landcover[Forrested]	-0.029066	0.049561	-0.59	0.5624

Least Squares Fit

Response jul

Whole Model

Expanded Estimates

Term	Estimate	Std Error	t Ratio	Prob>|t|
Landcover[Scrub]	2.8486e-6	0.061649	0.00	1.0000
Average Annual Precipitaiton (mm)	-0.000949	0.000587	-1.62	0.1172

Drainage Area

Leverage Plot

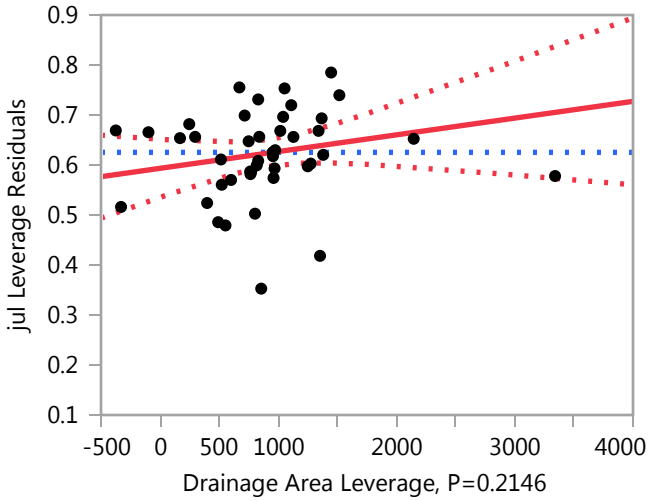

Average Slope (%)

Leverage Plot

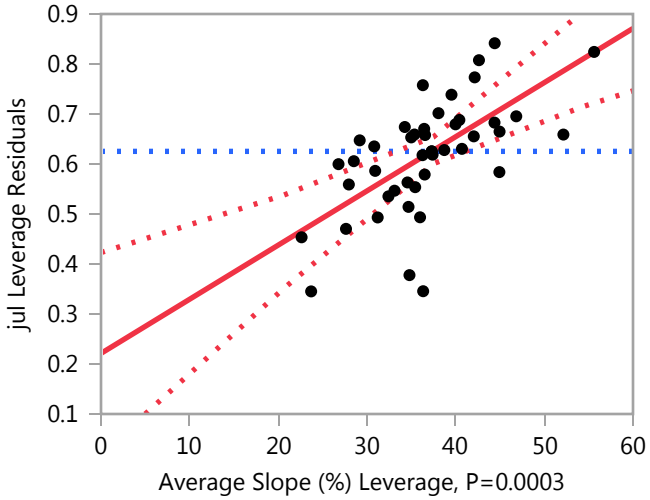

Least Squares Fit

Response jul

Average Slope (%)

Leverage Plot

Average Elevation (m)

Leverage Plot

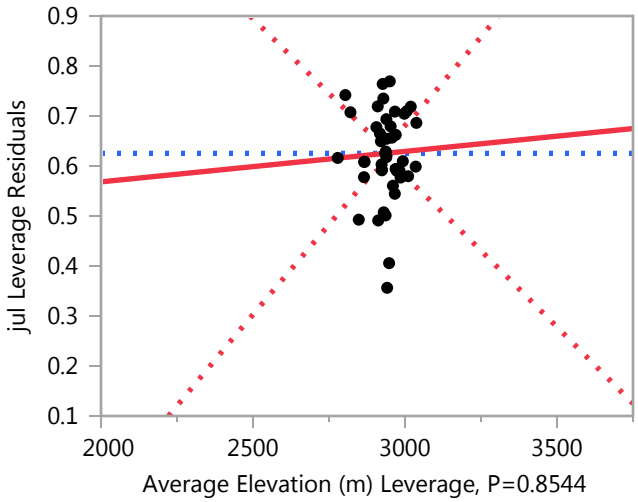

A(2250)

Leverage Plot

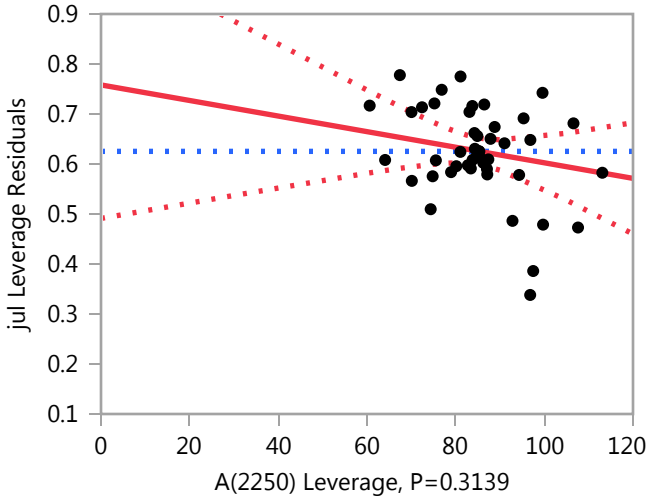

Least Squares Fit

Response jul

Dominant Aspect

Leverage Plot

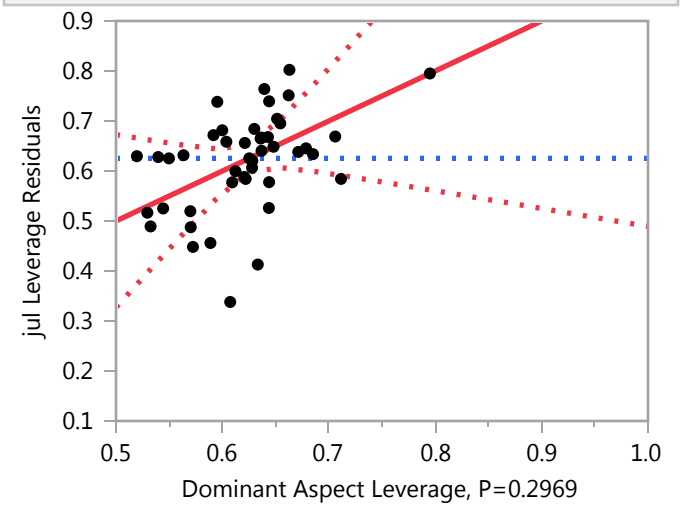

Least Squares Means Table

Level	Least Sq Mean	Std Error	Mean
E	0.65046014	0.08393992	0.572323
N	0.64934483	0.05343520	0.649820
NE	0.98127473	0.17032561	0.753298
NW	0.63142791	0.05649003	0.644478
S	0.77410324	0.07547971	0.631377
SE	0.76729372	0.10032972	0.622649
SW	0.77090290	0.09804880	0.555591
W	0.62967175	0.07562594	0.509558

Least Squares Fit

Response jul

Rippability Index

Leverage Plot

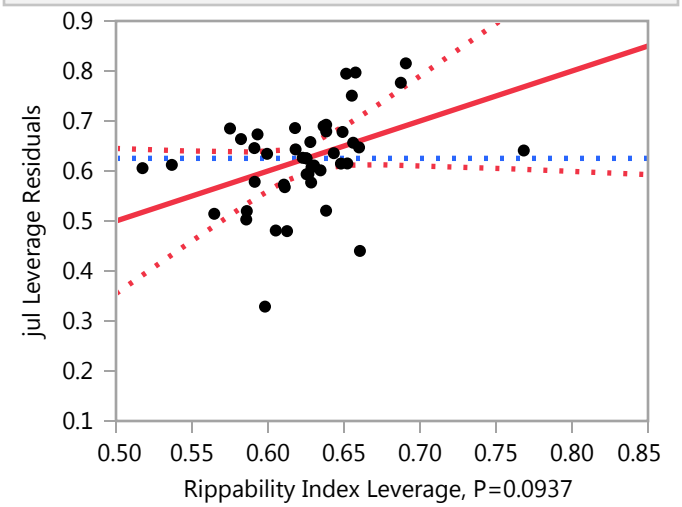

Least Squares Means Table

Level	Least Sq Mean	Std Error	Mean
Marginally Rippable	0.80156358	0.08186094	0.591388
Non-Rippable	0.78273838	0.08199379	0.678392
Rippable	0.61112774	0.05012505	0.617781

Landcover

Leverage Plot

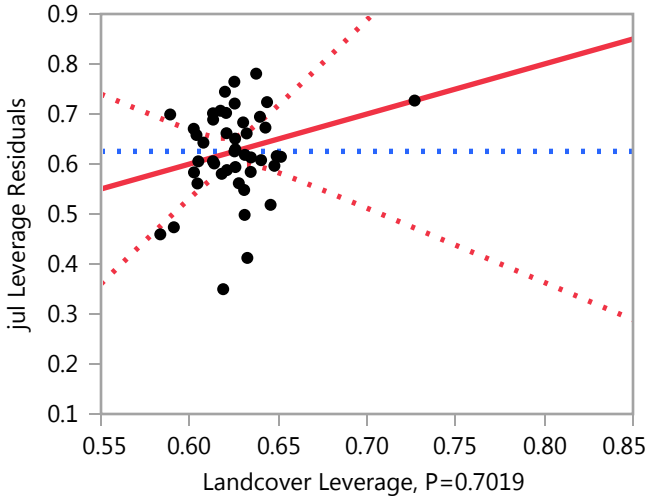

Least Squares Fit

Response jul

Landcover

Leverage Plot

Landcover Leverage, P=0.7019

Least Squares Means Table

Level	Least Sq Mean	Std Error	Mean
Alpine	0.83468537	0.17838621	0.672050
Alpine/Forrested	0.65799756	0.06503945	0.630229
Forrested	0.70274393	0.03896052	0.622425
Scrub	0.73181275	0.06964120	0.633765

Average Annual Precipitaiton (mm)

Leverage Plot

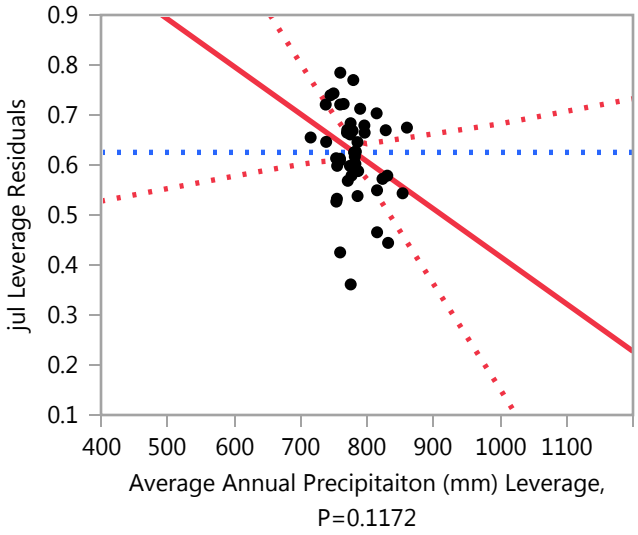

Least Squares Fit

Response jul

Average Annual Precipitaiton (mm)

Response aug

Whole Model

Actual by Predicted Plot

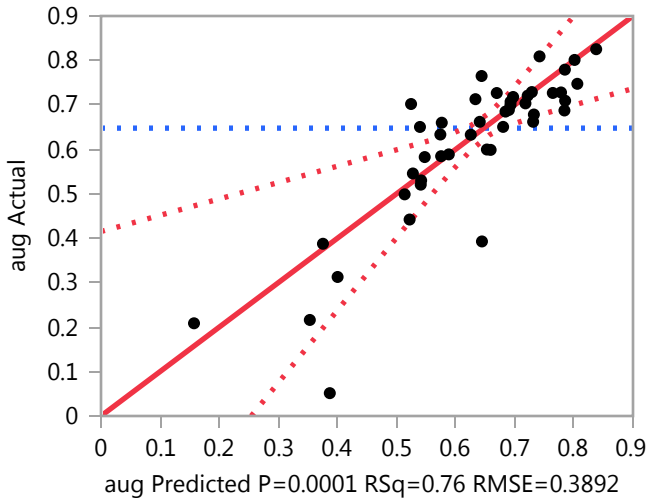

Summary of Fit

RSquare	0.756259
RSquare Adj	0.602793
Root Mean Square Error	0.389172
Mean of Response	0.647675
Observations (or Sum Wgts)	1114

Analysis of Variance

Source	DF	Sum of Squares	Mean Square	F Ratio
Model	17	12.687892	0.746347	4.9278
Error	27	4.089280	0.151455	Prob > F
C. Total	44	16.777172		0.0001 *

Least Squares Fit

Response aug

Whole Model

Parameter Estimates

Term	Estimate	Std Error	t Ratio	Prob>|t|
Intercept	0.0422897	0.454686	0.09	0.9266
Drainage Area	1.3261e-5	2.361e-5	0.56	0.5790
Average Slope (%)	0.0094512	0.002341	4.04	0.0004 *
Average Elevation (m)	0.0006148	0.000295	2.09	0.0464 *
A(2250)	-0.004012	0.00136	-2.95	0.0065 *
Dominant Aspect[E]	-0.132093	0.071724	-1.84	0.0765
Dominant Aspect[N]	-0.0762	0.041547	-1.83	0.0777
Dominant Aspect[NE]	0.1226814	0.123384	0.99	0.3289
Dominant Aspect[NW]	-0.074176	0.0477	-1.56	0.1316
Dominant Aspect[S]	0.0739129	0.045043	1.64	0.1124
Dominant Aspect[SE]	0.1255225	0.068248	1.84	0.0769
Dominant Aspect[SW]	0.0569537	0.056183	1.01	0.3197
Rippability Index[Marginally Rippable]	0.0347157	0.030226	1.15	0.2608
Rippability Index[Non-Rippable]	0.005949	0.033407	0.18	0.8600
Landcover[Alpine]	0.1884664	0.121154	1.56	0.1315
Landcover[Alpine/Forrested]	-0.127149	0.057274	-2.22	0.0350 *
Landcover[Forrested]	-0.042124	0.044409	-0.95	0.3513
Average Annual Precipitaiton (mm)	-0.00146	0.000526	-2.78	0.0098 *

Effect Tests

Source	Nparm	DF	Sum of Squares	F Ratio	Prob > F
Drainage Area	1	1	0.0477815	0.3155	0.5790
Average Slope (%)	1	1	2.4696692	16.3063	0.0004 *
Average Elevation (m)	1	1	0.6598323	4.3566	0.0464 *
A(2250)	1	1	1.3181046	8.7030	0.0065 *
Dominant Aspect	7	7	1.9025490	1.7945	0.1295
Rippability Index	2	2	0.2004810	0.6619	0.5241
Landcover	3	3	0.7473363	1.6448	0.2024
Average Annual Precipitaiton (mm)	1	1	1.1680128	7.7120	0.0098 *

Least Squares Fit

Response aug

Whole Model

Residual by Predicted Plot

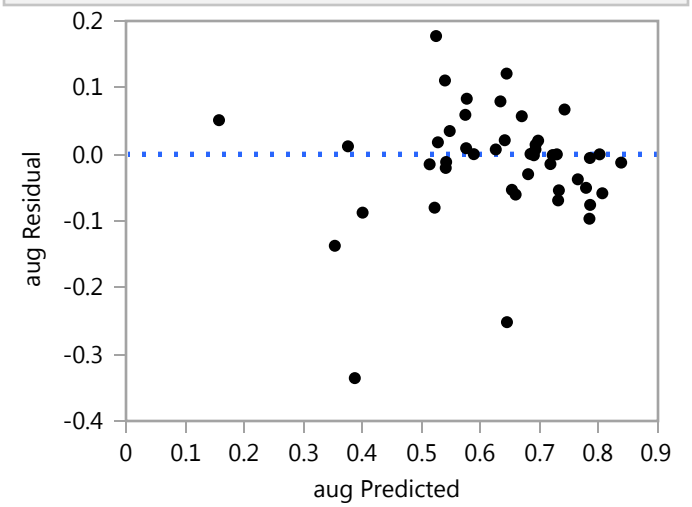

Expanded Estimates

Nominal factors expanded to all levels

Term	Estimate	Std Error	t Ratio	Prob>|t|
Intercept	0.0422897	0.454686	0.09	0.9266
Drainage Area	1.3261e-5	2.361e-5	0.56	0.5790
Average Slope (%)	0.0094512	0.002341	4.04	0.0004 *
Average Elevation (m)	0.0006148	0.000295	2.09	0.0464 *
A(2250)	-0.004012	0.00136	-2.95	0.0065 *
Dominant Aspect[E]	-0.132093	0.071724	-1.84	0.0765
Dominant Aspect[N]	-0.0762	0.041547	-1.83	0.0777
Dominant Aspect[NE]	0.1226814	0.123384	0.99	0.3289
Dominant Aspect[NW]	-0.074176	0.0477	-1.56	0.1316
Dominant Aspect[S]	0.0739129	0.045043	1.64	0.1124
Dominant Aspect[SE]	0.1255225	0.068248	1.84	0.0769
Dominant Aspect[SW]	0.0569537	0.056183	1.01	0.3197
Dominant Aspect[W]	-0.096603	0.049054	-1.97	0.0593
Rippability Index[Marginally Rippable]	0.0347157	0.030226	1.15	0.2608
Rippability Index[Non-Rippable]	0.005949	0.033407	0.18	0.8600
Rippability Index[Rippable]	-0.040665	0.049583	-0.82	0.4193
Landcover[Alpine]	0.1884664	0.121154	1.56	0.1315
Landcover[Alpine/Forrested]	-0.127149	0.057274	-2.22	0.0350 *
Landcover[Forrested]	-0.042124	0.044409	-0.95	0.3513

Least Squares Fit

Response aug

Whole Model

Expanded Estimates

Term	Estimate	Std Error	t Ratio	Prob>|t|
Landcover[Scrub]	-0.019193	0.055241	-0.35	0.7310
Average Annual Precipitaiton (mm)	-0.00146	0.000526	-2.78	0.0098 *

Drainage Area

Leverage Plot

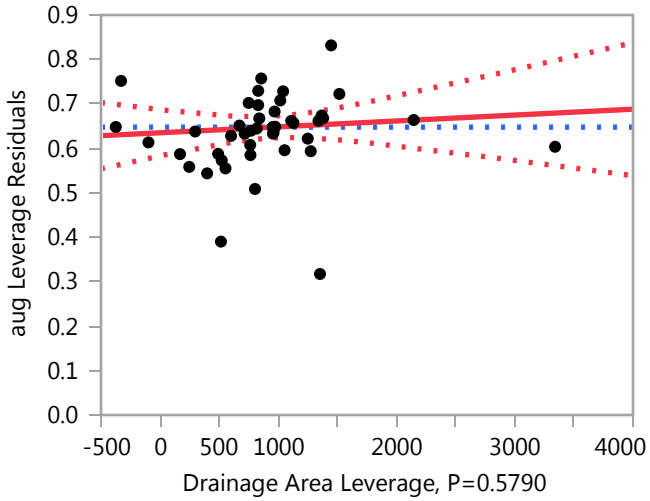

Average Slope (%)

Leverage Plot

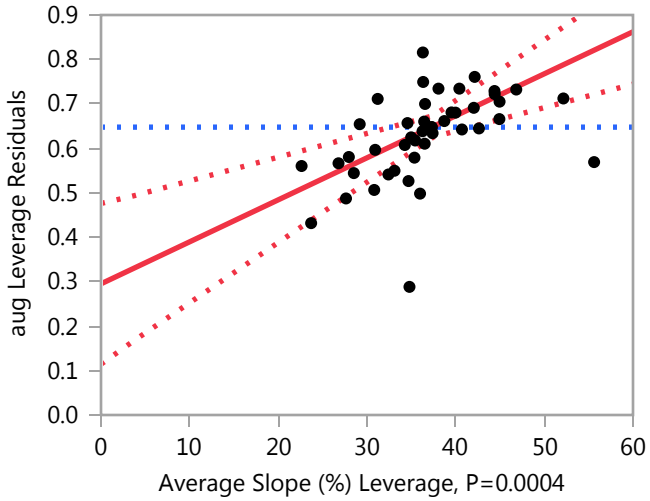

Least Squares Fit

Response aug

Average Slope (%)

Leverage Plot

Average Elevation (m)

Leverage Plot

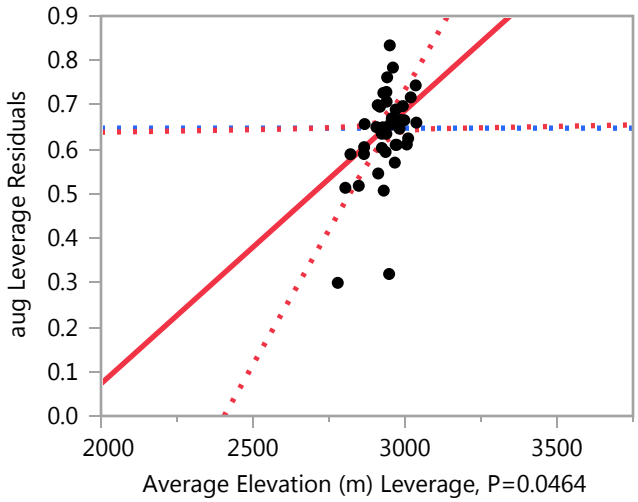

A(2250)

Leverage Plot

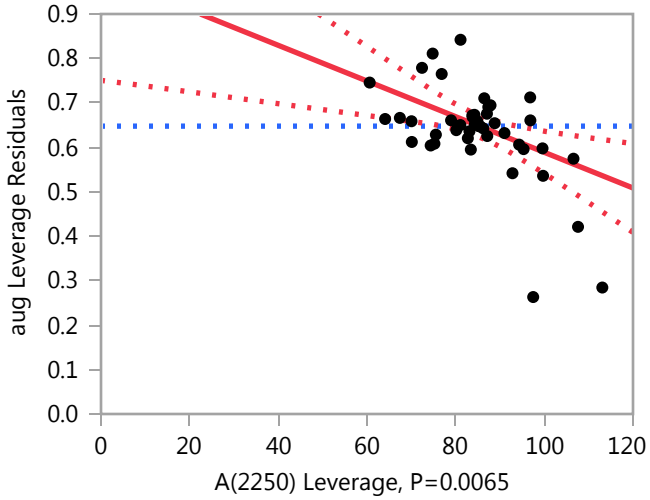

Least Squares Fit

Response aug

Dominant Aspect

Leverage Plot

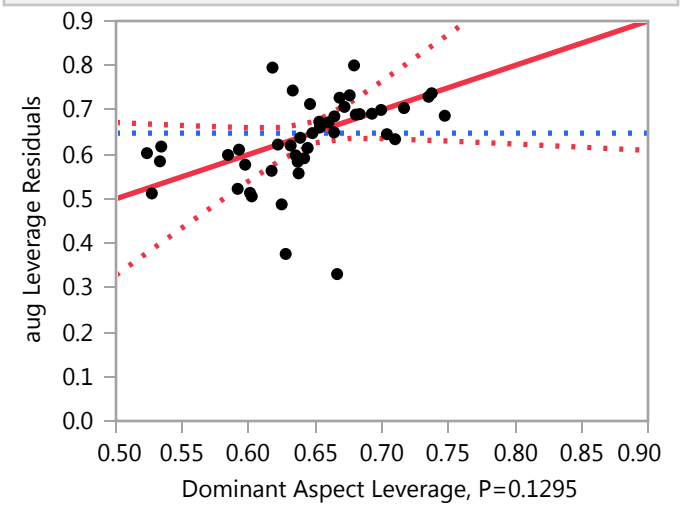

Least Squares Means Table

Level	Least Sq Mean	Std Error	Mean
E	0.59797369	0.07521502	0.587650
N	0.65386682	0.04788102	0.633437
NE	0.85274773	0.15262159	0.728858
NW	0.65589070	0.05061833	0.656395
S	0.80397925	0.06763418	0.711359
SE	0.85558886	0.08990122	0.694163
SW	0.78702002	0.08785739	0.617834
W	0.63346384	0.06776521	0.489165

Least Squares Fit

Response aug

Rippability Index

Leverage Plot

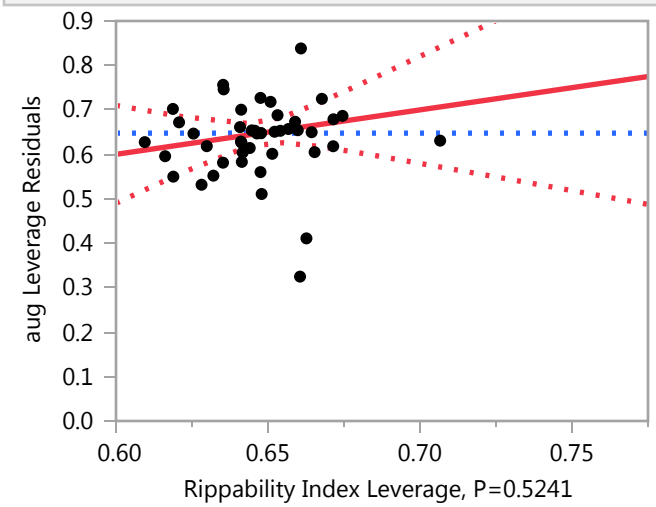

Least Squares Means Table

Level	Least Sq Mean	Std Error	Mean
Marginally Rippable	0.76478205	0.07335213	0.604593
Non-Rippable	0.73601539	0.07347117	0.714386
Rippable	0.68940166	0.04491494	0.638499

Landcover

Leverage Plot

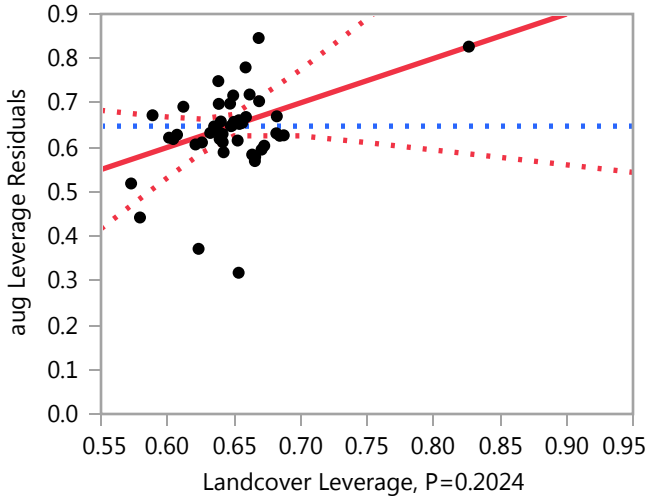

Least Squares Fit

Response aug

Landcover

Leverage Plot

Landcover Leverage, P=0.2024

Least Squares Means Table

Level	Least Sq Mean	Std Error	Mean
Alpine	0.91853278	0.15984435	0.801149
Alpine/Forrested	0.60291746	0.05827911	0.698805
Forrested	0.68794192	0.03491088	0.643027
Scrub	0.71087330	0.06240254	0.626311

Average Annual Precipitaiton (mm)

Leverage Plot

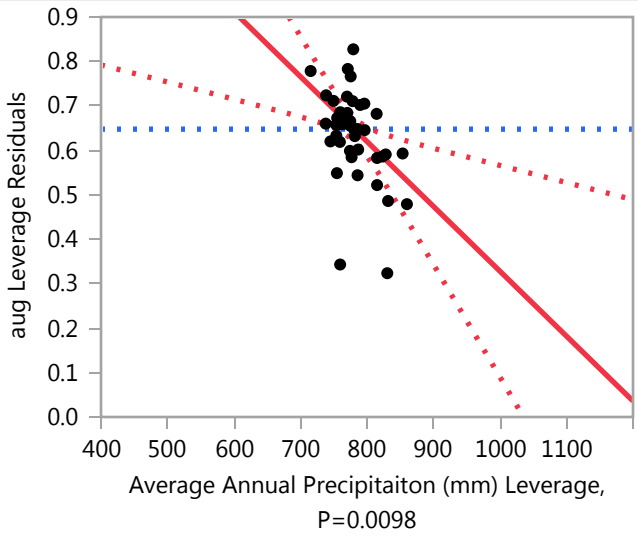

Least Squares Fit

Response aug

Average Annual Precipitaiton (mm)

Response sep

Whole Model

Actual by Predicted Plot

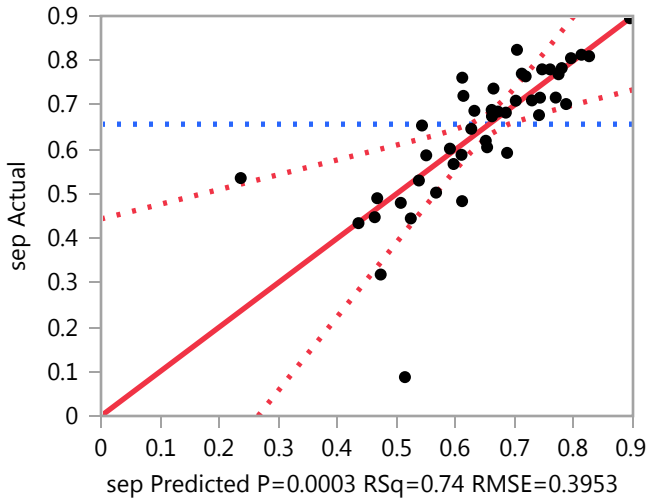

Summary of Fit

RSquare	0.736523
RSquare Adj	0.57063
Root Mean Square Error	0.395263
Mean of Response	0.656568
Observations (or Sum Wgts)	1114

Analysis of Variance

Source	DF	Sum of Squares	Mean Square	F Ratio
Model	17	11.791804	0.693636	4.4397
Error	27	4.218294	0.156233	**Prob > F**
C. Total	44	16.010098		0.0003 *

Least Squares Fit

Response sep

Whole Model

Parameter Estimates

Term	Estimate	Std Error	t Ratio	Prob>|t|
Intercept	0.4258242	0.461803	0.92	0.3646
Drainage Area	0.0000171	0.000024	0.71	0.4817
Average Slope (%)	0.0103217	0.002377	4.34	0.0002 *
Average Elevation (m)	0.0004517	0.000299	1.51	0.1427
A(2250)	-0.002868	0.001381	-2.08	0.0475 *
Dominant Aspect[E]	-0.032293	0.072846	-0.44	0.6611
Dominant Aspect[N]	-0.091686	0.042198	-2.17	0.0387 *
Dominant Aspect[NE]	0.2402267	0.125315	1.92	0.0659
Dominant Aspect[NW]	-0.096498	0.048446	-1.99	0.0566
Dominant Aspect[S]	0.0665036	0.045748	1.45	0.1576
Dominant Aspect[SE]	-0.024447	0.069317	-0.35	0.7271
Dominant Aspect[SW]	0.0059243	0.057062	0.10	0.9181
Rippability Index[Marginally Rippable]	0.0710986	0.030699	2.32	0.0284 *
Rippability Index[Non-Rippable]	0.0255195	0.03393	0.75	0.4585
Landcover[Alpine]	0.1788346	0.12305	1.45	0.1577
Landcover[Alpine/Forrested]	-0.136676	0.058171	-2.35	0.0264 *
Landcover[Forrested]	-0.053534	0.045104	-1.19	0.2456
Average Annual Precipitaiton (mm)	-0.001449	0.000534	-2.71	0.0114 *

Effect Tests

Source	Nparm	DF	Sum of Squares	F Ratio	Prob > F
Drainage Area	1	1	0.0795062	0.5089	0.4817
Average Slope (%)	1	1	2.9455306	18.8534	0.0002 *
Average Elevation (m)	1	1	0.3561311	2.2795	0.1427
A(2250)	1	1	0.6737427	4.3124	0.0475 *
Dominant Aspect	7	7	1.8823235	1.7212	0.1461
Rippability Index	2	2	0.8491016	2.7174	0.0841
Landcover	3	3	0.9805009	2.0920	0.1248
Average Annual Precipitaiton (mm)	1	1	1.1513254	7.3693	0.0114 *

Least Squares Fit

Response sep

Whole Model

Residual by Predicted Plot

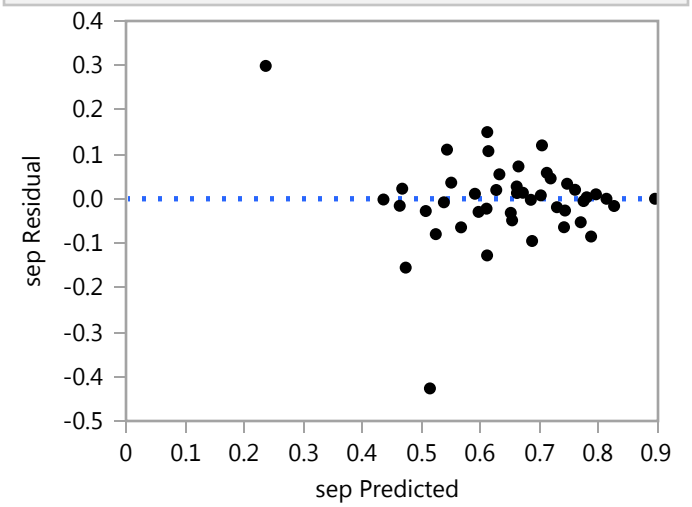

Expanded Estimates

Nominal factors expanded to all levels

Term	Estimate	Std Error	t Ratio	Prob>|t|
Intercept	0.4258242	0.461803	0.92	0.3646
Drainage Area	0.0000171	0.000024	0.71	0.4817
Average Slope (%)	0.0103217	0.002377	4.34	0.0002 *
Average Elevation (m)	0.0004517	0.000299	1.51	0.1427
A(2250)	-0.002868	0.001381	-2.08	0.0475 *
Dominant Aspect[E]	-0.032293	0.072846	-0.44	0.6611
Dominant Aspect[N]	-0.091686	0.042198	-2.17	0.0387 *
Dominant Aspect[NE]	0.2402267	0.125315	1.92	0.0659
Dominant Aspect[NW]	-0.096498	0.048446	-1.99	0.0566
Dominant Aspect[S]	0.0665036	0.045748	1.45	0.1576
Dominant Aspect[SE]	-0.024447	0.069317	-0.35	0.7271
Dominant Aspect[SW]	0.0059243	0.057062	0.10	0.9181
Dominant Aspect[W]	-0.067731	0.049822	-1.36	0.1852
Rippability Index[Marginally Rippable]	0.0710986	0.030699	2.32	0.0284 *
Rippability Index[Non-Rippable]	0.0255195	0.03393	0.75	0.4585
Rippability Index[Rippable]	-0.096618	0.050359	-1.92	0.0657
Landcover[Alpine]	0.1788346	0.12305	1.45	0.1577
Landcover[Alpine/Forrested]	-0.136676	0.058171	-2.35	0.0264 *
Landcover[Forrested]	-0.053534	0.045104	-1.19	0.2456

Least Squares Fit

Response sep

Whole Model

Expanded Estimates

Term	Estimate	Std Error	t Ratio	Prob>|t|
Landcover[Scrub]	0.0113757	0.056106	0.20	0.8408
Average Annual Precipitaiton (mm)	-0.001449	0.000534	-2.71	0.0114 *

Drainage Area

Leverage Plot

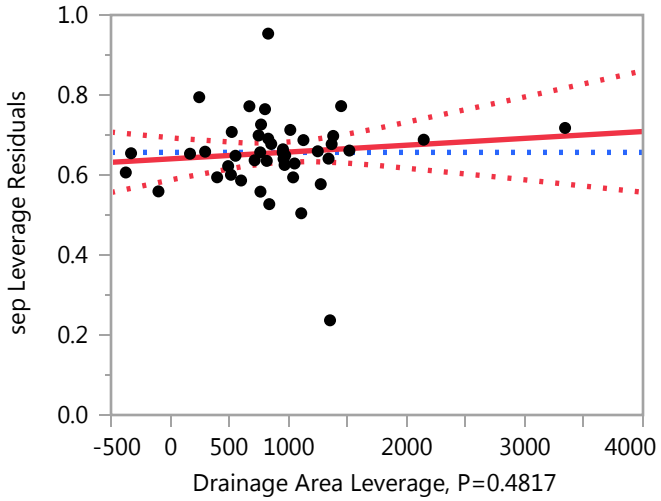

Average Slope (%)

Leverage Plot

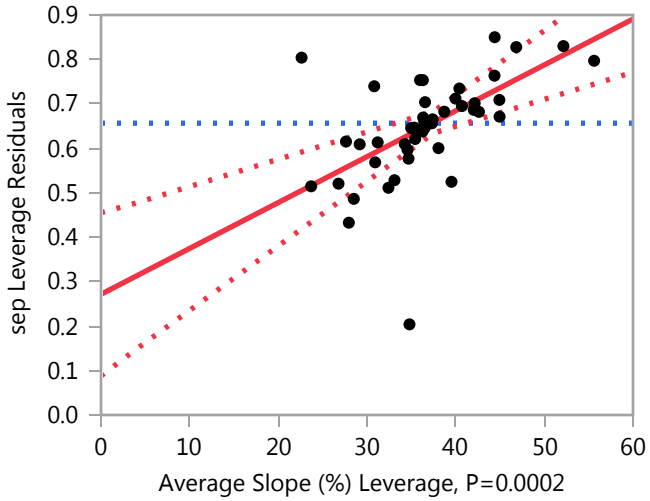

Least Squares Fit

Response sep

Average Slope (%)

Leverage Plot

Average Elevation (m)

Leverage Plot

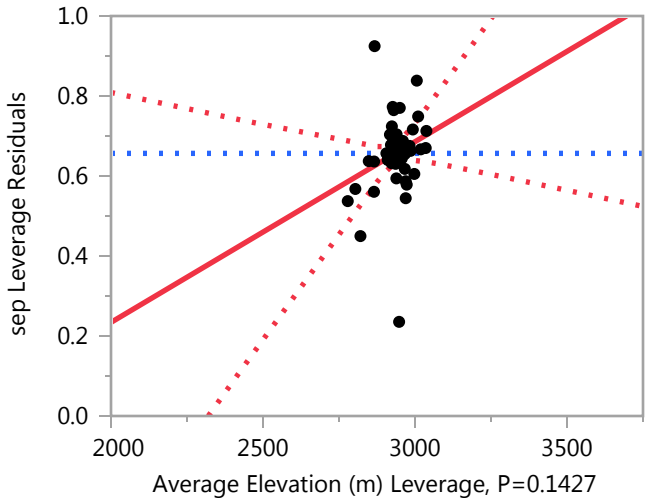

A(2250)

Leverage Plot

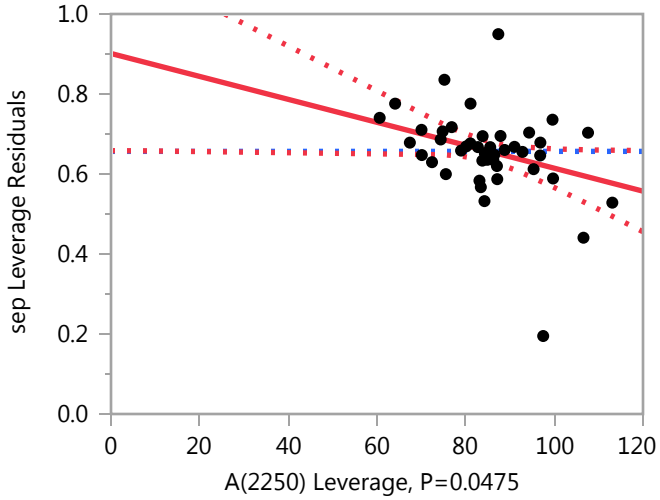

Least Squares Fit

Response sep

Dominant Aspect

Leverage Plot

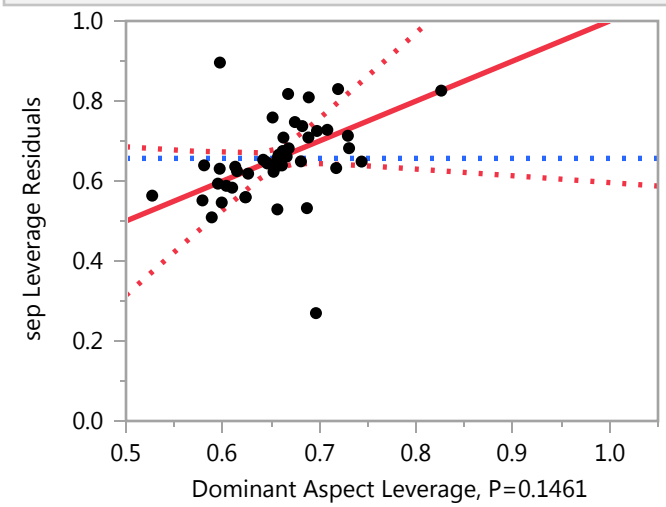

Least Squares Means Table

Level	Least Sq Mean	Std Error	Mean
E	0.7443266	0.07639229	0.716109
N	0.6849340	0.04863046	0.665921
NE	1.0168464	0.15501043	0.812797
NW	0.6801220	0.05141061	0.676958
S	0.8431233	0.06869280	0.689572
SE	0.7521723	0.09130836	0.550167
SW	0.7825440	0.08923254	0.551850
W	0.7088890	0.06882587	0.569929

Least Squares Fit

Response sep

Rippability Index

Leverage Plot

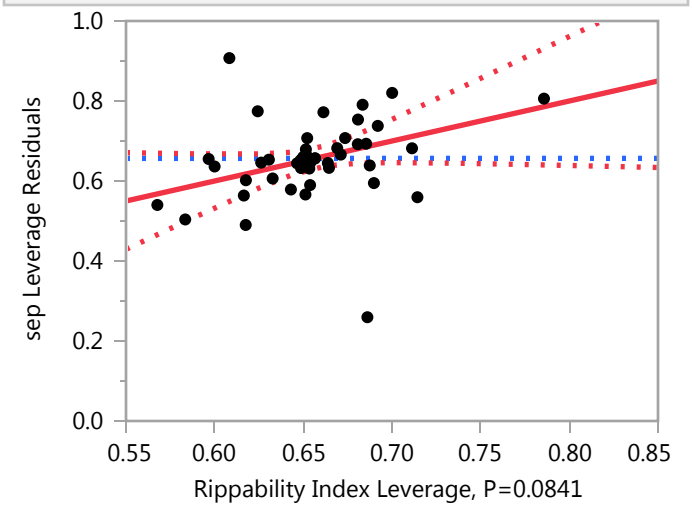

Least Squares Means Table

Level	Least Sq Mean	Std Error	Mean
Marginally Rippable	0.84771832	0.07450025	0.655839
Non-Rippable	0.80213922	0.07462114	0.728517
Rippable	0.68000160	0.04561796	0.626079

Landcover

Leverage Plot

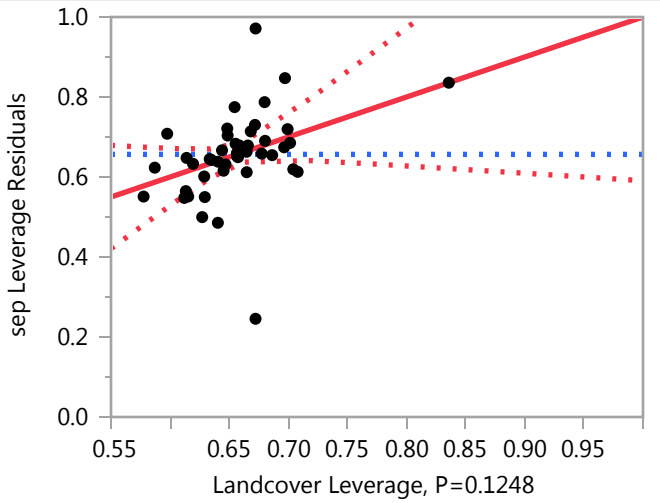

Least Squares Fit

Response sep

Landcover

Leverage Plot

Landcover Leverage, P=0.1248

Least Squares Means Table

Level	Least Sq Mean	Std Error	Mean
Alpine	0.95545434	0.16234624	0.894973
Alpine/Forrested	0.63994355	0.05919130	0.697815
Forrested	0.72308560	0.03545731	0.646068
Scrub	0.78799537	0.06337927	0.667837

Average Annual Precipitaiton (mm)

Leverage Plot